COMPUTERISED EXTRACTION AND ANALYSIS OF DATA FROM MEDICAL RECORDS :

AN EXAMINATION OF QT DISPERSION IN THE ELECTROCARDIOGRAM

Thesis submitted for the degree of

Doctor of Philosophy

at the University of Leicester

by

Harsangeet K. Bhullar

Department of Engineering

University of Leicester

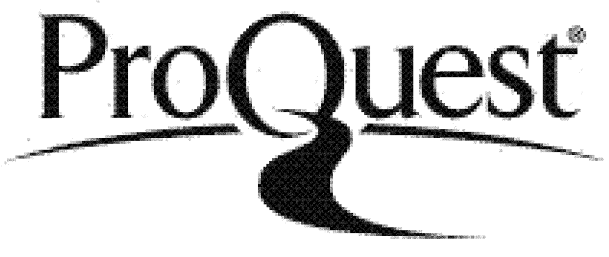

ProQuest LLC
789 East Eisenhower Parkway
P.O. Box 1346
Ann Arbor, MI 48106-1346

The direction of *progress*

lies with the conscience of man.

Computerised Extraction and Analysis of Data from Medical Records :

An Examination of QT Dispersion in the Electrocardiogram

by

Harsangeet K. Bhullar

Declaration of Originality

A thesis submitted in fulfilment of the requirements for the degree of Doctor of Philosophy in the Department of Engineering, The University of Leicester, U.K. All work recorded in this thesis is original unless otherwise acknowledged in the text or by references. No part of it has been submitted for any other degree, either to the University of Leicester or to any other University.

Harsangeet Kaur Bhullar

November 1992

Acknowledgements

There are many people who have helped me in the 3 years of my Ph.D. and who have given me their friendship and support. In the first instance, I wish to thank Mr John Hewson who recommended me to Professor de Bono to undertake a sponsored Ph.D. project, without whom I may not have been here. A very big thank you is due to my two supervisors Dr. John Fothergill and Professor David de Bono without whose encouragement, guidance and support this Ph.D would have been a much harder task.

A special thank you to John Fothergill for his moral support during the writing up of this Ph.D. The Rhino has finally won! Also, a special thanks to Professor N.B.Jones for his advice and guidance in the last 3 years. A special thank you is also reserved for Professor David de Bono who obtained funding via the British Heart Foundation to initially sponsor my Ph.D and subsequently employ me and for whom no item of equipment was too expensive!

I would also like to thank some very special friends, Cathy Au, May Awaida, Frederique, Kumaran Ambalavanar and Chris Ryan for their constant support during this Ph.D. There are also many numerous friends from the Biomedical group (some who have now left it) - Salih, Vin, Assad, George, Wang Jian Tao, Tuan Tran, S.Q. Wang, Yuehe Wang, Paul Goodyer and Kim Man Ho without whose friendship and constant ribbing sessions, life wouldn't have been as enjoyable.

I also wish to thank Mr Stephen Rawlinson who conducted all the library searches.

A very special thank you is reserved for my family, my parents and two brothers for their constant love and support without whom this Ph.D would not have been possible.

Finally I would like to thank the most important person of all, Gareth Loudon, without whose love and support life would have been very different.

I would like to dedicate this Ph.D. to my parents

CONTENTS

CHAPTER SIX

- **Clinical Investigation and Results**

Abstract

The first part of this Ph.D. thesis describes the significance and basis of QT dispersion in the light of recent clinical findings. A system is then described which was developed for the analysis of QT dispersion using standard twelve lead Electrocardiogram (ECG) paper records. In the first part of the system, ECG records are scanned and stored on computer as '.PCX' files. These files are pre-processed to remove random noise using a set of heuristic rules. An image processing technique known as 'thinning' is used to retrieve the lineal structure of the ECG waveforms. Digital data values are then extracted from these 'thinned' waveforms. The data recovery system was validated by a series of tests one of which showed that the cross-correlation coefficient between original and digitised data was greater than 0.99. A graphical interface incorporating a patient data base was designed to allow for the display and user-interactive measurement (using a cursor) of the recovered waveforms.

The next part of the thesis describes the design of an 'automatic algorithm' for the detection of characteristic points of the ECG including the QRS onset, R wave peak and T wave end positions. A transformed signal which is the three-point averaged derivative of the ECG is used to detect significant areas of QRS activity. Peaks corresponding to the R waves are detected and the ECG waveforms are then segmented as a function of heart rate. A normalised threshold is found and used to detect the QRS onset position. T wave peak and end detection is carried out by the study of "area maps" in the transformed signal. Once area maps corresponding to the T wave are determined, the T wave end is detected by using a three point moving average window and a threshold which takes into account the T wave slope.

Manual, user-interactive and automatic measurements revealed that (i) the user-interactive system measurements were easily performed by cardiologists and this technique resulted in more accurate and reproducible measurements than the standard manual method; and (ii) values of QT and RR intervals obtained by the automatic algorithm agreed well with measurements made by ten physicians. The final part of the study attempted to find a suitable parameter to characterise QT dispersion. The importance of QT dispersion was then investigated by undertaking a clinical study, whose results supported the value of QT dispersion as a risk indicator of patients prone to ventricular arrhythmias. Use of the automatic algorithm in finding QT dispersion gave the best discrimination of patient groups.

GLOSSARY OF TERMS

hypertrophy:- Excessive or increased growth of tissue by enlargement, without multiplication of its cells.

myocardial infarction (M.I.):- death and scarring of the tissue in the heart due to congestion and blockage of a blood vessel in the heart.

ischemia:- Insufficient supply of blood to a part of the body, e.g. to the heart muscle causing severe pain due to the shortage of oxygen.

autonomic nervous system:- System which regulates bodily functions other than voluntary movement and conscious sensation, by reflex action.

arrhythmias:- Any disturbance to the natural rhythm of the heart.

fibrillation:- Rapid, uncoordinated twitching of muscle fibres.

sympathetic nervous system:- Nerve system which causes the stimulation of the heart, suppression of digestive activity and enhancement of physical activity, by the release of adrenalin.

parasympathetic nervous system:- Nerve system which causes the opposite effects to that of the nervous sympathetic nervous system, by the release of acetyl choline.

vagal tone:- A state of the heart controlled by the vagus nerve i.e. a parasympathetic state.

refractory period:- that period of time in the action potential curve of a muscle cell during which no stimulus will propagate another action potential.

Chapter 1 The Significance and Basis of QT dispersion in the Electrocardiogram

1.1 Introduction

This chapter first outlines the origin and clinical significance of the electrocardiogram (ECG). It discusses conventional methods of recording the electrocardiogram. It then discusses briefly the clinical significance of the QT interval of the electrocardiogram and the factors affecting it. The concept of *QT dispersion* i.e. variation in the QT intervals measured in the different leads of the conventional 12 lead electrocardiogram is then introduced and its basis and significance is discussed in the light of recent clinical findings.

1.2 Electrophysiology of the Heart

The contraction of any muscle is associated with electrical changes called 'depolarisation'. These changes can be detected by electrodes attached to the surface of the body. The spread of electrical activation through the myocardium (muscular substance) of the heart gives rise to the electrocardiogram or ECG. To understand better the derivation of the ECG, the following section describes the electrophysiology of depolarisation and repolarisation of myocardial cells.

1.2.1 Initiation and Spread of Electrical Activation in the Heart

The myocardium of the heart is made up of millions of myocardial cells, which are however, capable of communicating electrically. In their normal resting state, myocardial cells are said to be polarised, i.e. the outside of the cell having positive charges, the inside, having an equal number of negative charges. Depolarisation implies a reversal of that charge distribution. If one electrode is placed on the surface of a resting muscle cell and a second indifferent electrode is placed in a remote location, no electrical potential will be recorded because of the high impedance of the cell

membrane. If however this membrane is penetrated by a capillary electrode, a negative potential of -90mV will be recorded. This is known as the membrane resting potential (MRP).

When an external influence like an electrical stimulus or activation wave arrives, (i.e. at the onset of depolarisation) it causes a change in permeability of the cell membrane to sodium. This causes a sudden, rapid, influx of Na+ ions from the extracellular fluid into the cell and so the inside of the cell becomes more positively charged than the outside. The transmembrane potential thus briefly becomes +20mV. This is designated as phase 0 of the entire curve of intracellular potential. Following depolarisation, there is a relatively slow and gradual return of intracellular potential to the MRP (phase 4). This is repolarisation and can be divided into three phases:-

- Phase 1:-The initial influx of Na+ rapidly ceases but is followed by a slower entry of Na+ ions.
- Phase 2:-At this stage, Ca++ ions also move into the cell. Together the Ca++ and Na+ influx causes the transmembrane potential to become even more positive. This is balanced by the outflow of K+ ions. The result is a 0V transmembrane potential existing for some 200 ms.
- Phase 3:- This represents the slow, gradual return of the intracellular potential to MRP. It results from the extrusion of potassium ions out of the cell which reestablishes the normal, negative, resting potential. However the cell is left with an excess of Na+ ions and a deficit of K+ ions. Therefore a sodium-potassium pump mechanism becomes effective.

This pump removes sodium from the cell and permits potassium influx. The entire curve of intracellular cellular potential is also called the *monophasic action potential.* Its duration is from the onset of depolarisation to the termination of repolarisation and it is different for different muscle cells in the heart. Figure 1.1 shows the monophasic action potential of a ventricular muscle cell.

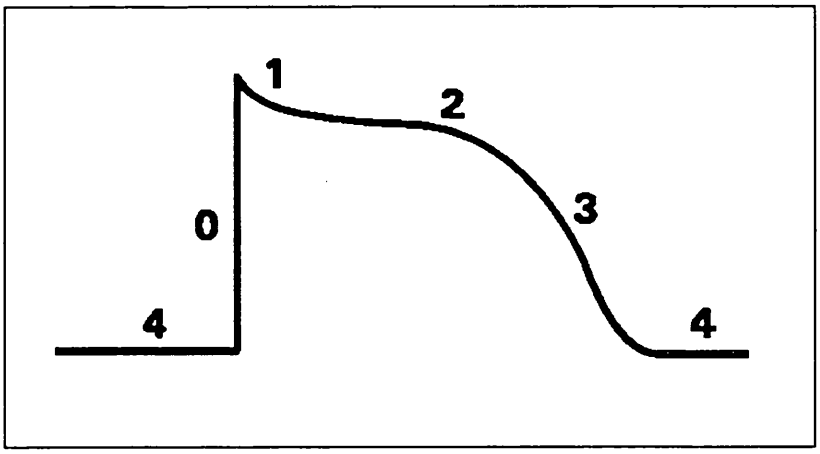

Figure [1.1] Example of a ventricular action potential (extracted from A.M.Katz, 1977)

Once depolarisation has been induced in any area of the myocardial cell membrane, it will spread spontaneously over the whole of the membrane of that cell and all other cells with which it is in electrical contact. This is because, when the surface of one myocardial cell changes its polarity from positive to negative, there will be a flux of positive ions in the extracellular fluid away from the adjacent "resting" cells towards the depolarised cells. This ionic movement triggers depolarisation in the resting cells.

Thus depolarisation spreads outwards like an advancing wave across the membrane of the myocardial cells, from the cell that was first depolarised. This activation wave has vector properties, i.e. magnitude and direction. Its magnitude depends simply on the mass of myocardium being depolarised. Its direction depends on the position on the surface membrane at which depolarisation is first induced and the anatomical distribution of myocardium available for depolarisation starting from that point.

For each cardiac cycle, the electrical discharge starts in a special area of the right atrium called the 'sinoatrial', (SA) node. See Figure 1.2a and b. Depolarisation then spreads to the adjacent atrial muscle fibres (myocardium) and all across it. Note that the predominant direction of spread is to the left and somewhat downwards. The myocardium has the ability to conduct depolarisation in any direction. The actual direction depends on the position at which activation is initiated. The predominant direction of spread will be that direction in which the greatest mass of myocardium is available from the starting point.

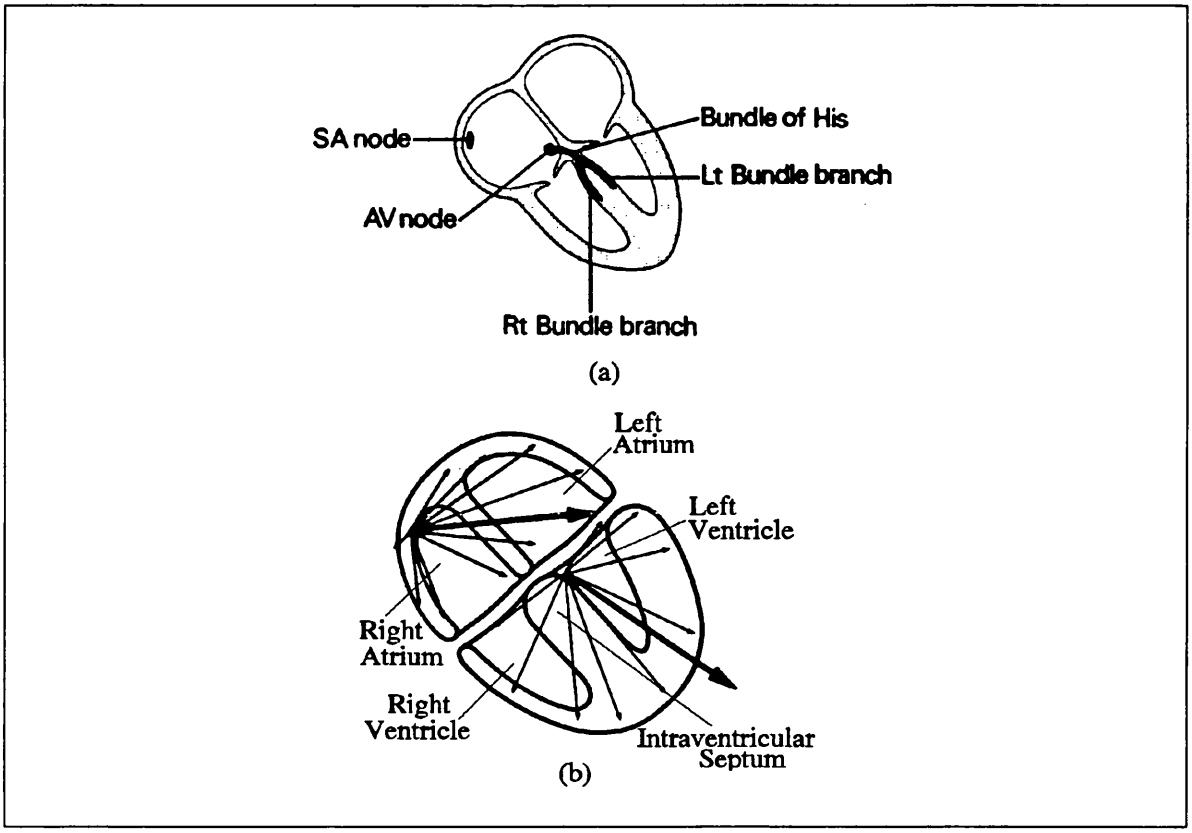

Figures [1.2a] The wiring diagram of the Heart. Figure [1.2b] The direction of the activation waves (extracted from J.R.Hampton,1986 and D.J.Rowlands,1985)

There is a delay while depolarisation spreads through another special area in the atrium, the 'atrioventricular' (AV) node. Thereafter conduction is very rapid down specialised conduction tissue: first a single pathway, the 'bundle of His' which then divides into the left and right bundle branches. The left bundle branch itself divides into two. Within the mass of ventricular muscle, conduction spreads rapidly through specialised tissue called the 'Purkinje fibres'. The multiple arrows over the atria and the ventricles in Figure 1.2b indicate the directions of the activation waves; their lengths indicating their relative magnitudes. Therefore each arrow represents an activation vector. The important thing to note about the activation wave vectors is that the apparent magnitude of the vector depends on the direction in which it is sensed (D.J.Rowlands, 1985).

1.2.2 The Basic ECG Waveform

The ECG is obtained from electrodes placed on the surface of the body. It provides a representation of the sequence of changes in electrical potential differences recorded between different regions of the body surface. Conventionally 12 leads are used in the

recording of the ECG. The word 'lead' is used in a rather confusing way in ECG recordings. Sometimes it is used to mean the pieces of wire that connect the patient to an ECG recorder. Other times and more conventionally, the term 'lead' is used to represent a set of electrodes and the waveforms recorded from them. Figure 1.3 shows the basic ECG waveform. It consists of three recognisable deflections, the 'P' wave, 'QRS' complex and 'T' wave, each of which were named by W.Einthoven (1950).

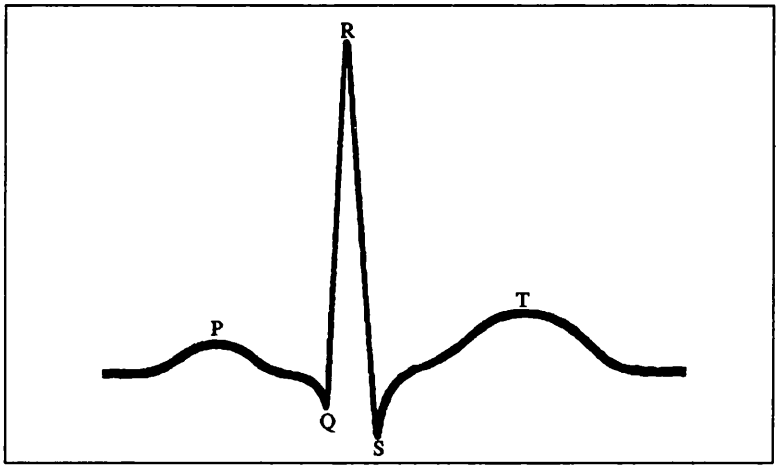

Figure [1.3] The Basic ECG waveform

The first deflection of the ECG is known as the 'P' wave. It represents the spread of electrical activation or depolarisation through the muscle substance (myocardium) of the atria and is due to the summation of all phase 0 potentials of atrial myocardial cells. Although depolarisation of the SA node precedes atrial depolarisation, no manifestation of this pacemaker activity are seen in the ECG because the SA node is too small to generate electrical potential differences great enough to be recorded from the body surface. The width of the P wave (i.e. its duration) reflects the time taken for the wave of depolarisation to spread across the atria.

Following the P wave, the ECG returns to its baseline, indicating that no changes in potential difference between various regions of the heart are apparent at the body surface. Yet during this silent interval between the P wave and the QRS complex (see Figure 1.4) the wave of electrical depolarisation is being propagated through the AV node, the AV bundle, bundle branches and the Purkinje network. The lack of influence of these important electrical events on the ECG is due to the small mass of tissue involved.

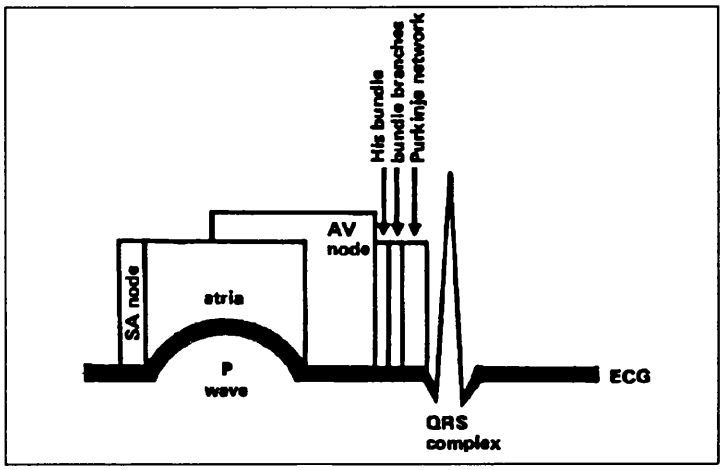

Figure [1.4] Tissues depolarised by a wave of activation commencing in the SA node are shown in a series of blocks superimposed on the initial deflections of the ECG (extracted from A.M.Katz, 1977).

The 'QRS complex' records the potentials that appear at the body surface when the wave of depolarisation spreads through the ventricular myocardium and is due to the summation of all phase 0 potentials of the ventricular muscle cells. The amplitude of the QRS complex is much higher than that of the P wave because the mass of ventricular tissue is greater than that of the atria; conversely the duration of the QRS complex is approximately the same as that of the P wave. However, the QRS complex is more spiky in shape than the P wave, a phenomena which is readily explained since the wave of depolarisation spreads through the ventricles via the rapidly conducting Purkinje network.

The rules followed in naming the presence and relative size of the 'waves' or deflections of the several possible components of the QRS complex may be indicated by a convention using combinations of the letters q,r,s,Q,R,S (Figure 1.5) :

- i) The first positive (up-going) wave is labelled r or R.
- ii) Any second positive wave is labelled r' or R'.
- iii) A negative wave (one descending below the baseline) is labelled an s or S if it follows an r or R wave.
- iv) A negative wave is labelled q or Q if it precedes r or R wave. (It must thus be the first wave to occur)
- v) Any wave which is entirely negative is labelled qs or QS.
- vi) Large deflections are labelled with an appropriate upper case (capital) letter. Small deflections are labelled with an appropriate lower case letter.

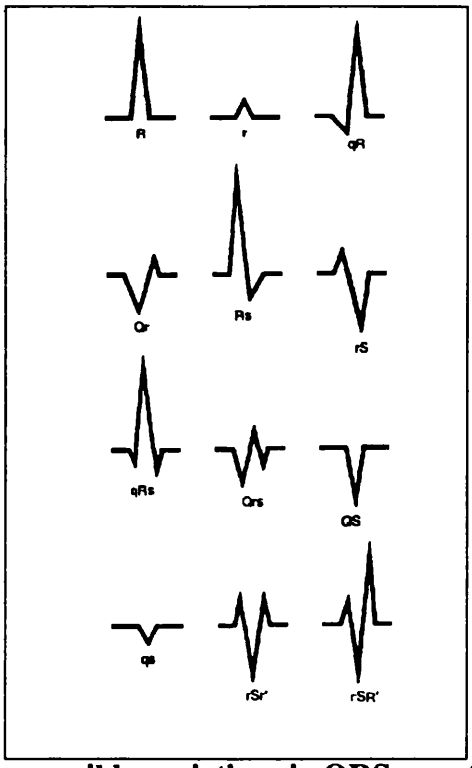

Figure [1.5] 12 of the possible variations in QRS waveform (extracted from D.J.Rowlands, 1985)

Following the QRS complex, the ECG waveform returns to, or very nearly to, its baseline, where it remains until the inscription of the T wave. This brief isoelectric phase, the S-T segment is inscribed at a time during systole when all regions of the ventricles are in a depolarised state. The long duration of the S-T segment reflects the normally prolonged plateau (phase 2) of the action potentials of ventricular muscle cells (see Figure 1.1).

Repolarisation of the ventricles generates the T wave which corresponds to the end of phase 2 and 3 of the action potentials of the ventricular muscle cells. The duration of the T wave is much longer than the QRS complex because unlike the QRS complex, the T wave is not a rapidly propagated wave. Instead the duration of the T wave is determined primarily by local factors that influence the duration of the action potentials in each region of the ventricle. Thus the narrow QRS complex arises from the rapidly conducted wave of depolarisation that passes over the ventricles whereas the broader T wave reflects the less synchronous repolarisation of the ventricles. The sequence of ventricular repolarisation also differs greatly from that during depolarisation. If the relationship between the QRS complex of Figure 1.3 and the ventricular action potential of Figure 1.1 was studied, it can be seen that the QRS complex corresponds to the

upstroke (phase 0) of the action potential. The S-T segment corresponds to the plateau (phase 2) while the T wave reflects repolarisation (phase 3). This relationship however is much more complex because the QRS and T waves represent the *sum* of the effects of all the action potentials in the millions of ventricular cells that are depolarised in different places and at different times. For this reason the rapidity of the potential changes during the QRS complex also reflect the high velocity with which the wave of depolarisation is conducted over the ventricles, whereas the more slowly inscribed T wave also reflects the greater dispersion of action potential duration in the heart during repolarisation of the ventricles. In some normal ECGs a small deflection is seen after the T wave. This is the 'U' wave whose mechanism of production is uncertain. It has been proposed that the U wave is related to the repolarisation of the Purkinje network, in which the action potential duration is greater than that of the ventricular myocardium, but this explanation has not been fully substantiated.

1.3 Recording the ECG

One of the most popular electrocardiographic systems used to record the ECG is the conventional 12 lead configuration consisting of the Einthoven limb leads (I,II,and III), the augmented leads (aVR, aVL, aVF), and the precordial leads (V1-V6). The other lead measuring system is the orthogonal 3-lead Frank system (E.Frank, 1956).

The former system records the electrical potentials (i.e. instantaneous vectors) in one single axis, whilst the latter gives a loop recording (or vectorcardiogram) representing the same electrical events but in 2 perpendicular axes. The latter has a solid biophysical background and allows more direct correlation between the ECG and the electrical activity of the heart (C.Levkov, 1987). This is because it takes into consideration contour and rotation of the vectorcardiographic loops, in addition to measurements of amplitude and duration. There is no direct counterpart in 12 lead ECG. Vectorcardiography therefore lends itself well to the diagnosis of hypertrophies, bundle branch block and myocardial infarction (M.I.) (L.Edenbrandt and O.Pahlm, 1988; M.J.Goldman, 1982). Conversely, it is of little value in the recording of arrhythmias unless moving photographic equipment is used or independent scalar X,Y and Z leads are used. Its value in clinical practice is also limited due to the following reasons:

- (i) the expense of the equipment and the time involved;
- (ii) definite standards for the normal and abnormal vectors are only now being established;
- (iii) no complete uniformity of opinion exists, as to the best lead system to be used (M.J.Goldman, 1982)

By far the most common method of measuring ECGs is by the use of the 12 lead ECG system. It is widely accepted and more than ninety percent of the world's ECG recordings are still made with this system.

1.3.1 The 12 Lead ECG

To obtain the 12 lead ECG, 5 electrodes are used altogether. 4 electrodes are fastened to a limb each whilst one is held by suction to the front of the chest and moved to different positions.

3 vertical pictures of the heart are obtained from unipolar limb leads (VR,VL,VF) and another 3 are obtained from the standard/bipolar limb leads (I,II,III). These give 6 vertical pictures of the heart. The remaining 6 horizontal pictures are obtained from the chest/precordial leads (V1,V2,V3,V4,V5,V6).

Despite the fact that all the electrodes are 'looking' at the same depolarisation wave, they each record very different things, because of their very different orientations. This is the reason for the varying ECG shapes obtained in the various leads.

Before explaining the form of the recordings of the 12 lead ECG, it is necessary to consider the difference between the behaviour of a volume conductor and that of a linear conductor. The most important difference is that a linear conductor has virtually identical voltages at all points along its length, whereas the voltage may vary appreciably at different locations within a volume conductor.

The human trunk behaves as a volume conductor and therefore electrode positioning on the trunk materially affects the record obtained and correct positioning of the chest electrodes is essential. The limbs behave like linear conductors and therefore the same record would be obtained whether the recording electrode is attached to the wrist, forearm, elbow, upper arm or shoulder.

Unipolar limb leads - R,L and F

The unipolar leads employ 4 electrodes altogether; one attached to each limb. Electrodes are positioned on the right arm (R), the left arm (L), the left leg ("foot", F), and right leg. The fourth electrode on the right leg acts as an earth to minimise interference. As the limbs act as linear conductors, their effective sensing positions are at the shoulders and the left groin. Figure 1.6a illustrates the positioning of the 3 limb electrodes and earth. Figure 1.6b shows the heart to lying at the centre of an equilateral triangle, the apices of which are the 2 shoulders and the left groin. Therefore leads R,L and F are in fact looking at the heart along the directions shown in Figure 1.6b. This is a diagrammatic representation of the *Einthoven Triangle Hypothesis.* The simplifying assumptions of the hypothesis are presented here:

- (1) The trunk is a homogeneous volume conductor. (It is obvious that the conductivities of the various body tissues differ from one another but the differences are surprisingly small).
- 2) The sum of all the electrical forces being produced at any instant or the mean of all the electrical forces generated during the cardiac cycle can be considered as originating in a dipole located in the centre of the heart. (A dipole is a positive charge and a negative charge of equal magnitude located so close to one another that they may be considered to be at the same point).

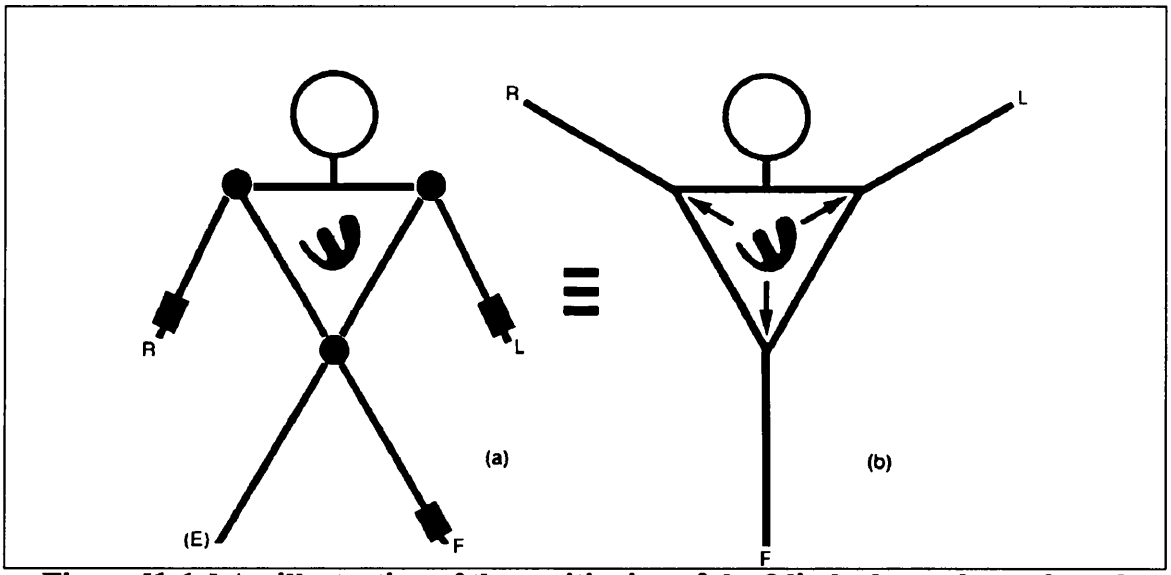

Figure [1.6a] An illustration of the positioning of the 3 limb electrodes and earth. Figure [1.6b] An illustration of the heart at the centre of an equilateral triangle, the apices of which are the 2 shoulders and the left groin (extracted from D.J.Rowlands, 1985)

- (3) The extremity leads (R,L,and F) pick up potential changes in the frontal plane only. (In general this is true).
- (4) The attachments of the three extremities used in making the limb leads (R,L and F) form the apices an equilateral triangle with reference to a dipole located at its centre. (Anatomically, of course, the roots of the right arm, left arm and left leg in no sense form an equilateral triangle). However, if the cardiac electric field is considered as originating from a dipole, the positive and negative charges are, by definition, extremely close together (i.e. the distance separating them is zero) and in relative terms the distances of each of the limb roots from this dipole are great enough to be considered infinite.

To see how depolarisation and repolarisation give rise to different deflections in the unipolar limb leads, consider the ventricles as a simple muscle strip, Figure 1.7 then shows how a depolarising wave vector travelling along this myocardial strip will give rise to deflections in R, L, F and some other lead X. Electrode X sees the full magnitude of the vector strip. Being at right angles to the depolarisation wave direction, electrode L would see no deflection. Electrode F and R record both positive and negative waves of varying magnitudes respectively.

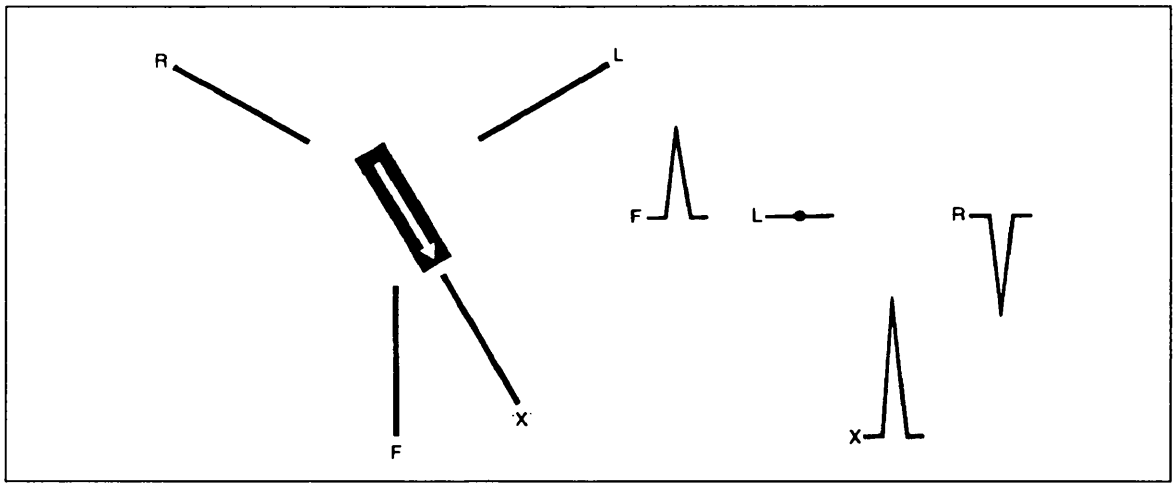

Figure [1.7] An example showing how a depolarising wave vector travelling a myocardial strip will give rise to deflections in R, L, F and some other lead X. (extracted from D.J.Rowlands,1985)

An important point to note is that although these limbs are called unipolar, they are actually measured against a reference electrode which is so arranged that its potential does not vary during the cardiac cycle. This reference electrode is formed by joining together leads R, L, and F to give a total deflection of 0V, provided the limb leads are distributed evenly across the heart. This "indifferent" connection (formed from R,L and F) is called a "V" lead. Such a connection is used for the limb leads VR,VL,VF and also the chest leads V1,V2,V3,V4,V5 and V6.

To obtain VL,VF, or VR, the exploring electrode is attached to the limb in question, and connected to the positive recording terminal whilst the indifferent "V" connection is connected to the negative terminal. Nowadays, the limb connections are slightly modified to augment the amplitude of the deflection obtained from R,L,F, to be 50% greater. These augmented leads are called aVR, aVL, and aVF. However everything that has been understood for L,F and R is equally applicable to aVL, aVF, and aVR.

Bipolar or Standard limb leads - I, II, III

Bipolar leads are formed by connecting one end of the recording galvanometer to one limb and the other end to a second limb. Since the voltage change observed could be due to either limb or both limbs, the lead is bipolar. Only 3 limbs are used - right arm, left arm and left leg. As before, the right leg is used as an earth to minimise interference.

3 combinations known as leads I,II and III are achieved and they are related to the unipolar limb leads by:

I = L-R II= F-R III = F-L

There was no logic in the choice of this arrangement, it was simply a matter of convenience (see Figure 1.8).

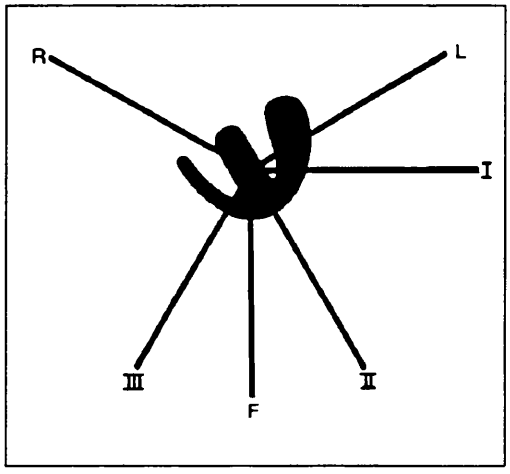

Figure 1.8 An illustration of how the effective positions of the bipolar leads I, II and III are derived from the unipolar leads (extracted from D.J.Rowlands, 1985)

Figure 1.8 shows the orientation of these leads. Lead I effectively looks at the heart from a position anatomically inferior to that from which the left arm looks. Lead II looks at the heart from a position to the left of the foot lead. Lead III looks at heart from a position to the right of the foot lead.

The General Form of the QRS complexes in the Six Limb leads

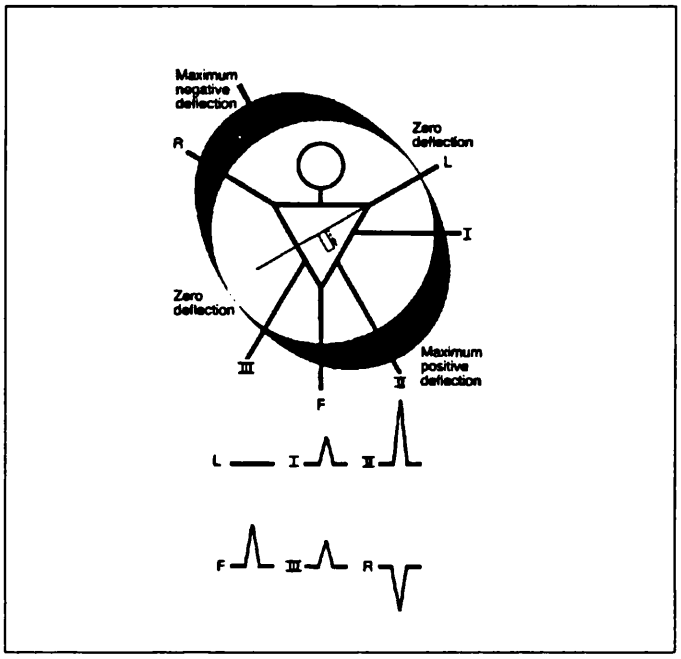

Figure [1.9] An illustration of the differing deflections recorded by the six limb leads during depolarisation using the strip of myocardium as a simple model of the ventricle (extracted from D.J.Rowlands, 1985)

Considering again the strip of myocardium as a simple model of the ventricle, the differing deflections recorded by the six limb leads, as the strip is depolarised, can be observed in Figure 1.9. Being parallel to the direction of depolarisation, lead II shows the largest, positive deflection. The deflection in F is positive, but less than that in II, since it is not placed precisely parallel to the direction of depolarisation. Similarly, I and III are oriented in front of the depolarisation wave, but less advantageously, so they see smaller positive deflections. Since the depolarisation wave approaches I and III at the same angle, these two leads show the same deflections. Being at right angles to the depolarisation wave, L shows no deflections. R lies behind the depolarisation wave and records a negative deflection.

As an example, using a more realistic model of the heart, let us consider how depolarisation of the *left ventricular myocardium,* as recorded by all the 6 limb leads, gives rise to the QRS complex (Figure 1.10).

Figure 1.10a shows the direction of left ventricular depolarisation. It can be observed as five sequential phases, represented by five arrows:

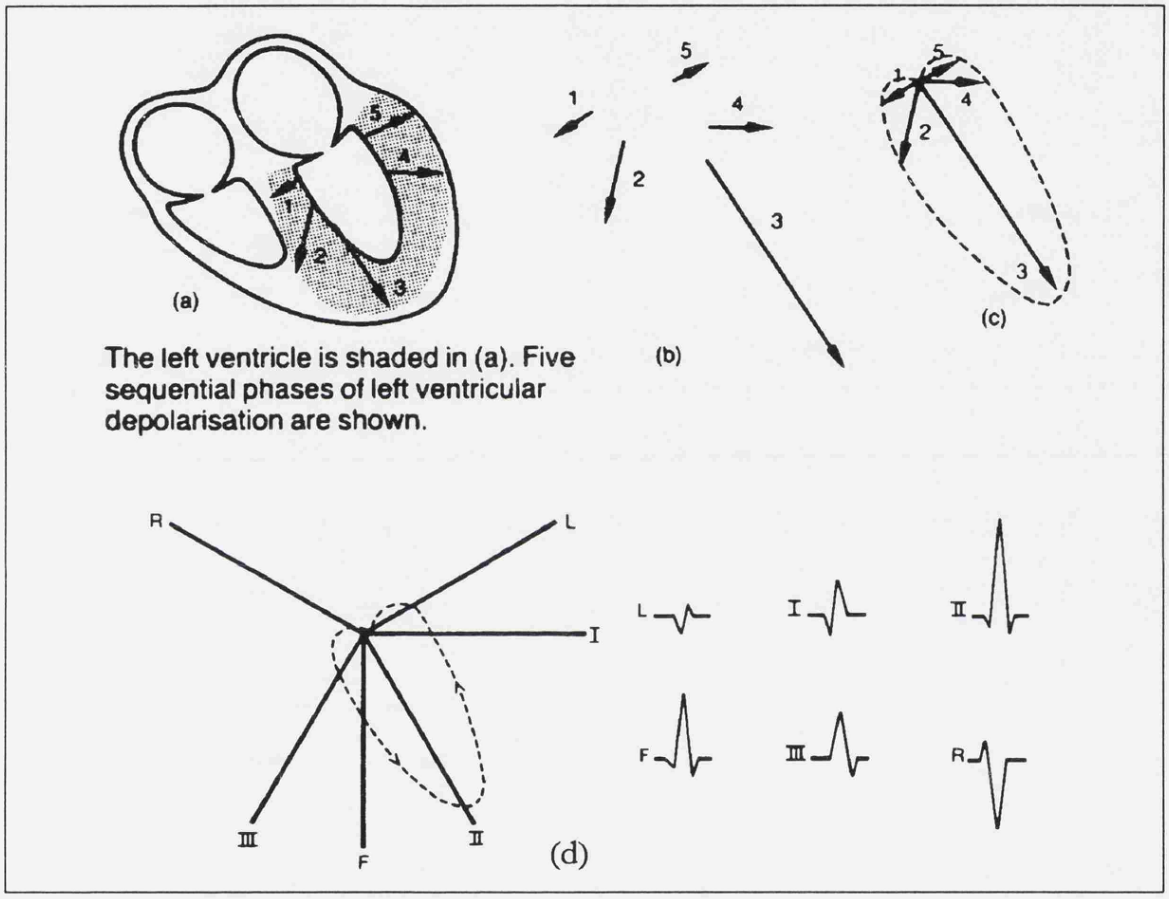

Figure [1.10 a,b,c,d] An illustration of the different phases of left ventricular myocardium depolarisation and the differing deflections recorded by the six limb leads during this period (extracted from D.J.Rowlands, 1985)

- Phase 1 The inter-ventricular septum is depolarised from left to right
- Phase 2 Depolarisation spreads down the septum, towards the apex of the heart
- Phase 3,4,5 Depolarisation spreads progressively along the free wall of the left ventricle, always from endocardium to pericardium

Figure 1.10b and 1.10c show their direction and magnitude. Note that the divisions into the five phases are completely arbitrary and were chosen to promote understanding. In reality, there are an infinite number of instantaneous arrows as the direction of

ventricular depolarisation is constantly changing. Because of this as well as their varying magnitudes, the arrangement of these vectors can be illustrated by the vector loop (interrupted line) shown in Figure 1.10(c). An illustration of the differing deflections recorded by the six limb electrodes during the different phases of left ventricular myocardium depolarisation is given Figure 1.10d.

Precordial/Chest leads - V1, V2, V3, V4, V5, V6

In the case of the precordial leads, the positive recording terminal of the galvanometer is connected to an electrode at 6 agreed sites on the chest wall. The negative terminal is the 'indifferent' connection. Hence the chest leads are "V" leads- in this case, not augmented. The standard anatomical positioning of the precordial electrodes as agreed between the British Cardiac Society and the American Heart Association is shown in Figure 1.11a. The relationship of the precordial leads to the heart chambers is shown in Figure 1.11b.

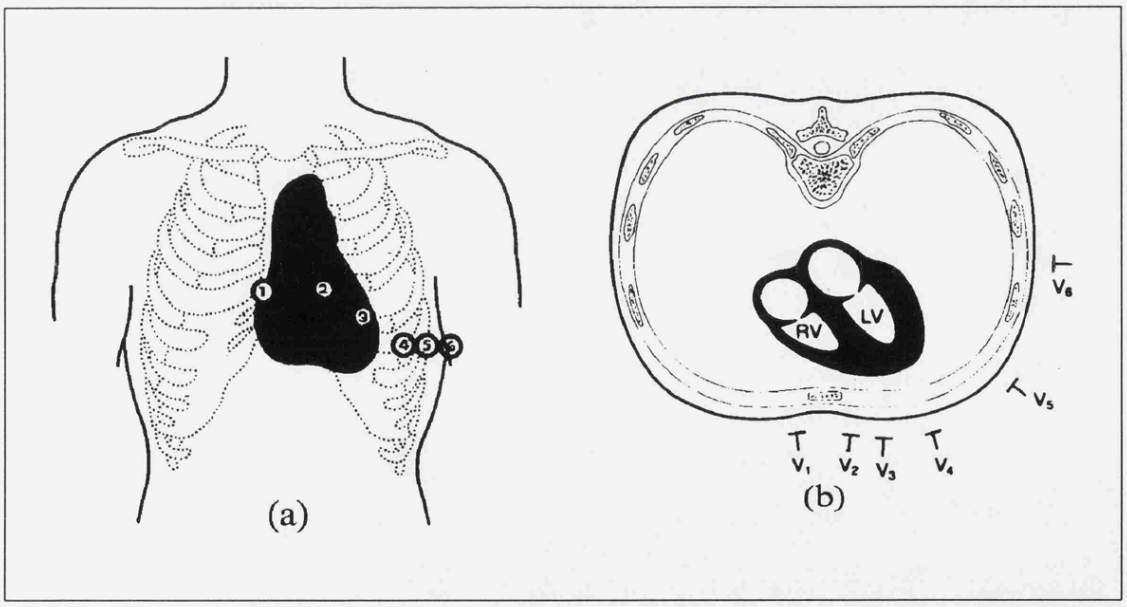

Figure [1.11a] The standard anatomical positioningof the precordial electrodes.
Figure [1.11b] Relationship of the precordial leads to the heart chambers (extracted from D.J.Rowlands,1985)

The General form of the QRS Complexes in the Six Precordial leads

Although the full sequence of ventricular depolarisation is an extremely complex process, to facilitate understanding the QRS form in the precordial leads, it is convenient to simplify it arbitrarily into three stages, as shown in Figure 1.12.

The interventricular septum is depolarised first. Depolarisation of the right and left ventricular free walls then follows. Therefore, Phase 1 occurs initially, alone, and phase 2 and 3 occur simultaneously after. The result of these three waves of depolarisation can

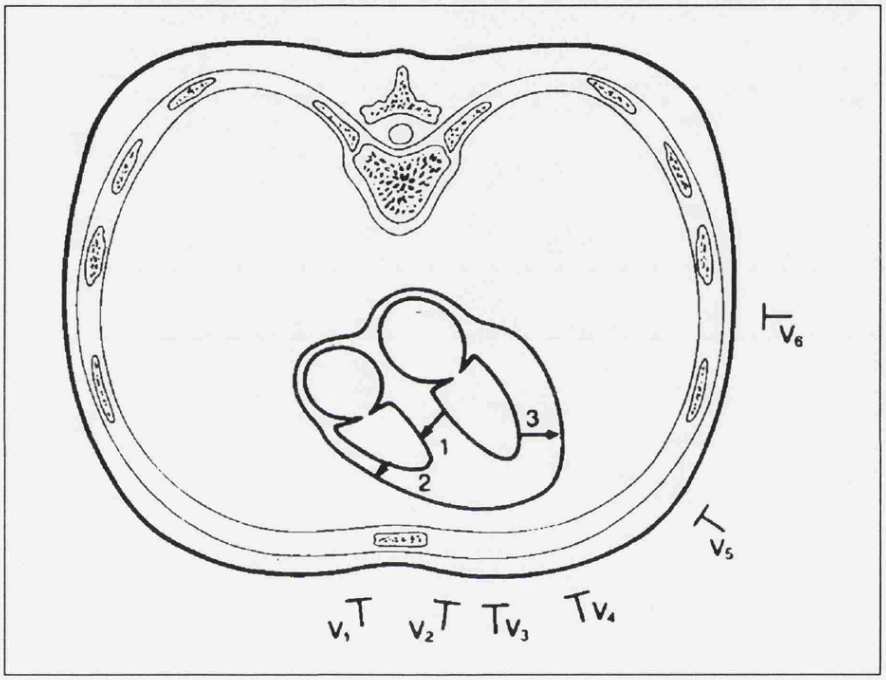

Figure [1.12] A simplification of the 3 phases of ventricular depolarisation as seen by the precordial leads (extracted from D.J.Rowlands,1985)

be observed in two leads; V1 (facing right ventricle) and V6 (facing left ventricle), as shown in Figure 1.13 and Figure 1.14.

As can be seen, the QRS complex in V1 typically shows an rS pattern whilst that in V6 shows a qR pattern. The form of the QRS complexes in the remaining precordial leads are shown in Figure 1.15.

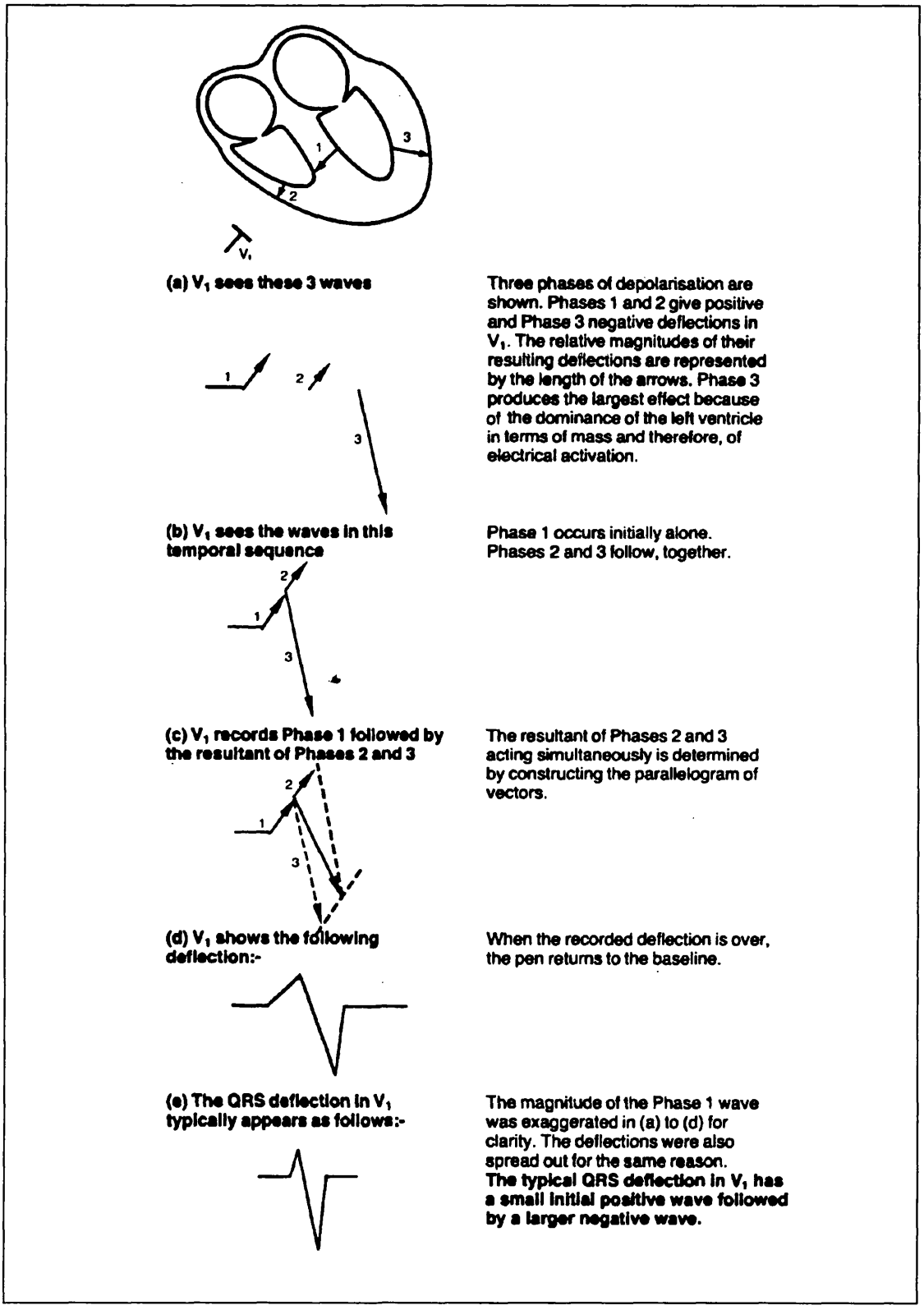

Figure [1.13] The result of ventricular depolarisation as seen by leads V1 (extracted from D.J.Rowlands,1985)

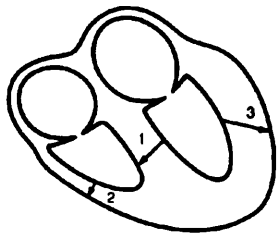

(a) V_6 sees these 3 waves

Three phases of depolarisation are shown. Phases 1 and 2 give negative and Phase 3 positive deflections in V_6. Phase 3 gives a larger deflection (positively) in V_6 than it gave (negatively) in V_1 since the left ventricular free wall is closer to V_6 than to V_1. Conversely Phases 1 and 2 give smaller deflections in V_6 than they did in V_1.

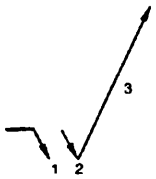

(b) V_6 sees these waves in this temporal sequence

Phase 1 occurs initially, alone, then 2 and 3 follow together.

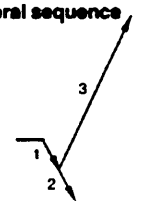

(c) V_6 records Phase 1 followed by the resultant of Phases 2 and 3

The resultant of Phases 2 and 3 acting simultaneously may be determined by constructing a parallelogram of forces.

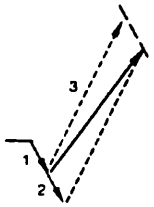

(d) V_6 shows the following deflections:-

When the recorded deflection is over, the pen returns to the baseline.

(e) The QRS deflection in V_6 typically appears as follows:-

In (a) to (d) the deflections were spread out for greater clarity. Here it is shown in its normal perspective. The typical QRS deflection in V_6 has a small initial negative wave followed by a large positive wave.

Figure [1.14] The result of ventricular depolarisation as seen by leads V6 (extracted from D.J.Rowlands,1985)

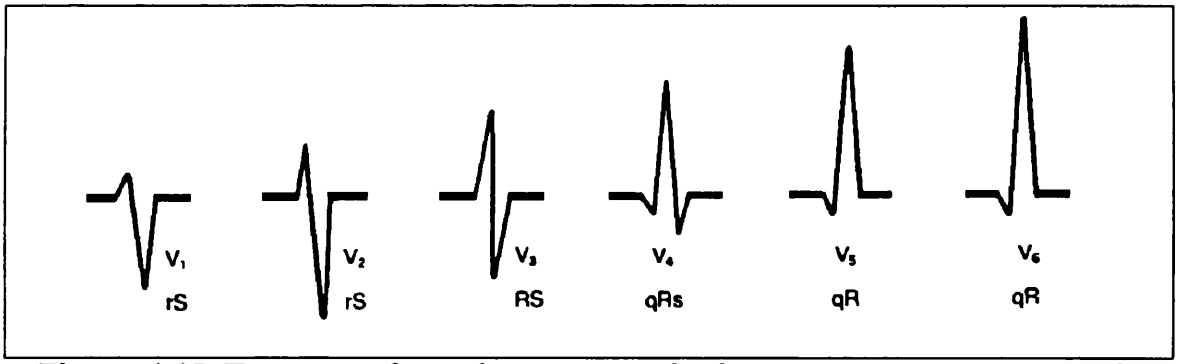

Figure [1.15] The result of ventricular depolarisation as seen by all the precordial leads (extracted from D.J.Rowlands,1985)

1.4 QT Interval Research

From the first few sections it will be clear that the QT interval represents the time it takes the ventricular myocardium to depolarise and repolarise. It results from the sum of the action potentials of both ventricles. The QT intervals as sensed by the different leads of the 12 lead ECG often vary in duration. This has been thought to be due to the orientation of the repolarisation wavefronts being perpendicular to the sensing direction of the lead. Conventional research into the significance of the QT interval normally employs a single lead measurement of the QT interval. If the 12 leads are measured synchronously, then the QT interval is normally derived from the earliest onset point of the Q wave in all the leads and the T wave end is taken as the latest offset point of the T wave in all the leads. If the 12 leads are not recorded simultaneously, the lead reflecting the longest QT interval is selected.

The significance and prognostic value of this single QT interval measurement has long been the subject of research and discussion. The following sections discuss some of the research relating to the QT interval.

1.4.1 QT Interval Prolongation,Ventricular Arrhythmias and Sudden Death

Clinically there are a group of patients who have a *prolonged QT interval* (>440 ms) and who are subject to cardiac arrhythmias and sudden death (M.Moller, 1981; K.F.Browne et al., 1983; S.Ahnve, C.Helmers, T.Lundman et al., 1980; P.Scharwtz and S.Wolf, 1978; R.Haynes et al., 1978; M.Shoaleh-var et al., 1978; P.J.Bourdillion, 1979). Amongst those most vulnerable to sudden death are individuals who have sustained a myocardial infarction (M.I.) and who are either in the acute, early or late stages of

recovery (M.Moller, 1981; P.Scharwtz and S.Wolf, 1978; S.Ahnve, C.Helmers et al., 1980). The main cause of sudden cardiac death is ventricular fibrillation whether in the presence of myocardial infarction or not.

It has been suggested that the *prolonged QT interval* may be an indicator of delayed or asynchronous ventricular repolarisation (M.Moller, 1981; K.F.Browne et al., 1983). It may correspond to an abnormally long action potential for the heart as a whole, but it may also reflect the dispersion of action potentials, long in some zones and normal in others. This increase in the degree of temporal dispersion of refractory periods could constitute a propitious substrate for the appearance of ventricular arrhythmias (V.Marti et al., 1988; P.Schwartz and S.Wolf, 1978; J.Han G.K.Moe, 1964, C.S.Kuo et al., 1983) and sudden death.

Abnormal repolarisation, as reflected by a *prolonged QT interval,* has been found to be common in the early stages of acute myocardial infarction (M.I.). This may predispose a patient to the occurrence of malignant ventricular arrhythmias in the acute as well as the post M.I. period (S.Ahnve et al., 1978; G.J.Taylor et al., 1981; S.Ahnve, L.Erhardt, et al., 1980; P.E.Puddu et al., 1981; G.Forsell and E.Orinius, 1981; M.Moller, 1981; R.E.Haynes et al., 1978). In the group of patients who show the *hereditary* long QT syndrome, these repolarisation abnormalities are known to increase the risk of ventricular fibrillation and sudden cardiac death (S.Ahnve, 1985). These repolarisation abnormalities have also been discussed as potential risk factors in the sudden infant death syndrome (W.G.Guntheroth, 1982; P.J.Schwartz et al., 1982).

The interactions of the mechanisms implied in the appearance of lethal arrhythmias that lead to sudden cardiac death are not well known. There are probably several variables that condition the appearance of these arrhythmias, as well as other mechanisms that act more or less directly on the sequence of events that lead to sudden death, such as the state of ventricular function. It seems clear that in post-infarction patients, malignant ventricular arrhythmias, which can result in sudden death, can be explained as being due to the combined factors of ischaemia-induced anatomic alterations (anatomic substrate), the presence of frequent electrical instability, poor ventricular function and/or autonomous nervous system anomalies (V.Marti et al., 1988). Some authors believe the autonomic nervous system plays an important role in the

genesis of arrhythmias that precede sudden death (P.H.Coumel et al., 1982). The alterations of the autonomic nervous system alter the balance between sympathetic and vagal tone, decrease heart-rate variability and prolong the duration of QT interval. These factors have all been related to an increased incidence of malignant ventricular arrhythmias (W.W.Brooks et al., 1978; K.F.Browne et al., 1982; R.E.Kleiger et al., 1987; P.Scharwtz and S.Wolf, 1978).

Although the QT interval has been shown to predict severe ventricular arrhythmias in the acute stage of an M.I., research into the long term prognostic implications of QT interval has yielded diverging results (M.Moller, 1981; P.Scharwtz and S.Wolf, 1978; S.Ahnve, C.Helmers, T.Lundman, 1980). Some researches found a shorter QT interval in patients who subsequently suffered from sudden death (M.Moller, 1981; S.Ahnve, C.Helmers, T.Lundman, 1980). In this instance, the effect of QT interval shortening was attributed to the effect of the drug digitalis.

R.E.Haynes et al., (1978) found that post-infarction patients who presented ventricular fibrillation and who were resuscitated had, compared to a control group of the same clinical characteristics, greater ST depression (46% vs 10%), more flattened T waves (52% vs 26%) and a more prolonged QT interval (35% vs 18%). The studies by P.Scharwtz and S.Wolf (1978) and S.Ahnve, C.Helmers, T. Lundman et al., (1980) support the prognostic value of QT measurement after infarction, while other authors (S.Pohjola-Sintonen et al., 1986; P.E.Puddu and M.G.Bourassa, 1986, K.Wheelan et al., 1986) do not find this relationship.

Tests studying the relationship between QT interval and exercise induced ventricular arrhythmias (EIVA) showed that only subjects with coronary artery diseases who developed EIVA showed significantly longer QT intervals than the control subjects at rest and during exercise (J.Han and B.G. Goel, 1972).

1.4.2 Factors affecting the QT Interval

As early as 1920, it was noticed that the QT interval varied with heart rate in a definite manner (on the standard 12 lead ECG, the heart rate is given by the inverse of the RR interval). Studies demonstrated that the QT interval shortened with increasing heart rate and lengthened with decreasing heart rate. Thus in order to meaningfully

compare one QT interval with another, it was realized that some account must be taken of heart rate. Many formulas have since been proposed to describe this relationship i.e. linear, logarithmic, square root and cube root (H.Bazett, 1920; R.Ashman, 1942; I.Schlamowitz, 1946; E.Simonson et al., 1962; S.Ahnve, 1985; G.R.Pai and J.M.Rawles, 1989). Bazett's formula which is the most commonly used formula today, proposed that the relationship between the QT interval and the heart rate is as follows: the QT interval expressed in seconds divided by the square root of the RR interval expressed in seconds is a constant. This value is the so called rate-corrected QT interval, QT_C.

The various formulae were developed to ascertain their value in detecting and measuring abnormalities in the physiological state of the cardiac conducting system as well as organic changes in the heart muscle itself, by eliminating the effect of heart rate changes (I.Schlamowitz, 1946; K.F.Browne et al., 1983). Also, because a great number of other factors affect the QT interval, it was important to establish accurately the relationship between the QT interval and heart rate and to know the normal range of variation (R.Ashman, 1942). The differences in the various equations obtained by these authors and in the constants obtained in their equations is largely due to chance variations in sampling and different compositions of samples (E.Simonson et al., 1962). The considerable error in measurement of the QT interval contributes to this variability.

Recent studies conducted on patients who were steadily paced at different frequencies and on patients with atrial fibrillation (W.A.Seed et al., 1987; G.R.Pai and J.M.Rawles, 1989) suggest that simple correction of QT interval for heart rate is inadequate as it does not take into account instantaneous changes in heart rate. QT rate correction may also lead to erroneous results in instances where QT duration changes whilst the heart rate is constant.

Many other factors affect the QT interval. Drugs like digitalis (S.Ahnve, C.Helmers et al., 1980) have the effect of shortening the QT (corrected) interval. The rate-corrected QT interval was also found to decrease in severely diseased patients treated with alprenelol (G.Nyberg et al., 1979) and in survivors of acute M.I. who were on metoprolol (S.Ahnve, L.Erhardt et al., 1980). Local cellular changes also affect the duration of the QT interval (S.Ahnve, C.Helmers et al., 1980; S.Ahnve, 1985). One example of this is blood calcium level (R.Ashman, 1942). As the ionised calcium level

rises, the QT interval shortens and vice-versa. Intravenous injection of metaphosphate, which prevents the ionisation of calcium salts, have shown to markedly lengthen the QT interval in tests done on dogs.

Other factors that can affect the QT interval are imbalances of the sympathetic nervous system, cardiac or heart disease, (S.Ahnve, T.Lundman, 1980; R.Ashman, 1942; I.Schlamowitz, 1946), as discussed earlier, and even sleep. During sleep, QT prolongation is observed independently of the change in heart rate (K.F.Browne et al., 1983). In the awake state the QT interval is affected by physical activity, meals and activities like smoking (K.F.Browne, 1983). Factors like age and sex of the patient also have an effect on the QT interval. In general, longer QT intervals are observed in men compared with women and to a very small extent, in older patients compared with younger patients (R.Ashman, 1942).

1.5 Clinical Significance and Basis of QT dispersion

QT prolongation has been seen to be useful in identifying patients prone to ventricular arrhythmias and sudden cardiac death, and high risk survivors of acute M.I.. The single value of QT interval used embodies the concept of a global value for cardiac repolarisation time. This may not however be the best measure by which to study heterogeneity of ventricular repolarisation times.

Recent work done by D.Mirvis et al. (1985) which involved the study of the *spatial or regional* variation in QT intervals on the body surface of normal subjects and patients with acute M.I. using 150 electrodes showed that the QT interval distributions in normal and abnormal states showed distinctive spatial distributions that were consistent with known electrophysiology. In normal subjects, the difference between the longest and shortest interval in each case was 59.4 ± 12.9 ms. Thus, there was a significant range of QT intervals when measured from different torso sites in any one subject. The long QT intervals were spatially located over the left lateral torso and short QT intervals were found over the right inferior chest.

Mirvis believed that the spatial distribution of QT intervals may have had two components, namely the differences in onset of the QRS complex and differences in the end of the T wave. To determine which was the major factor resulting in QT interval

variations, the variances in the timing of the two instants were computed and studied in 50 normal subjects each using 150 electrodes. Variances in onset of the Q wave ranged from 9.3 to 43.4 ms^2 whilst variances in the T wave end varied from 39.9 to 254.4 ms^2. Thus variation in T wave termination rather than in QRS complex onset was found to be the major determinant of the QT interval range.

The reason that QRS onset time does not show great variation is thought to be because it reflects global or distant as well as local cardiac forces. For example, in the surface ECG any QRS complexes with initial negative Q waves reflect the relatively strong activation force in opposite cardiac structures. Thus, the onset of the QT interval is dependent on global effects and is thereby less sensitive to regional events. The end of the T wave on the other hand, was found to vary quite significantly. This was thought to reflect the regional differences in refractory and recovery times as confirmed by studies on refractory periods and monophasic action potentials by M.Burgess et al. (1972), J.Abildskov (1975) and H.Toyoshima et al. (1981). They reported different functional refractory periods in different parts of the ventricle. Studies by body surface mapping also confirm this (J.A.Abildskov et al., 1981).

In 15 patients who were studied within 72 hours of *anterior myocardial infarction*, Mirvis found that the longest interval recorded was significantly longer than the normal group. In addition, the zone with the longest QT intervals was located centrally rather than laterally. This pattern was observed in all patients with acute anterior infarction.

For the 15 subjects who were studied within 72 hours of acute *inferior infarction* the longest QT intervals recorded were, as for the previous group, much longer than the normal group. This time the longest QT intervals were located inferiorly on the anterior torso along the horizontal axis.

It can be seen therefore that acute M.I. has *modified* the distribution of QT intervals in relation to the *lesion location* in both groups of patients; the longest QT intervals were centrally positioned in anterior infarction and caudally located in inferior infarction. Even though the mean value of the QT interval was not shown to be significantly different from the normal group after infarction, the spatial distribution of QT intervals was clearly abnormal. The shift in sites of the longest intervals to regions approximating

the surface projection of the cardiac damage is consistent with the experimentally defined regional prolongation of action potential durations. The QT interval at these sites may be further prolonged by an increased activation time.

Other work also lends support to the fact that the surface ECG variations of measured rate-corrected QT intervals correspond to the established pattern of ventricular recovery: the QT interval has been found to be longest in the anteroseptal leads (R.W.F. Campbell et al., 1985) and septal leads have the longest recovery time (J.C.Cowan, H.C.Hilton et al., 1988; M.R.Franz et al., 1987). The right ventricle has also been found to show the shortest recovery time (H.Toyoshima et al., 1981).

These results are important because they show the ability of potentials recorded on the surface of the body to depict normal and abnormal regional deviations in ventricular recovery time. This being the case, the concept of a global value for cardiac repolarisation becomes less important and significant when compared to the regional information that might be gained from the study of QT intervals in more than 1 body surface lead.

In line with this, R.W.F.Campbell's group (C.Day et al., 1990) in Newcastle put forward the suggestion that the *apparent inter-lead variation in QT interval duration in all of the 12 leads of the surface ECG reflects regional repolarisation differences.* This inter-lead variation of QT intervals is termed *QT dispersion.* In cardiologically normal individuals this variation is thought to be smaller than for example, in patients who are prone to ventricular arrhythmias for whom the temporal dispersion of ventricular recovery time is greater.

In the first study carried out by the group, the differences between the maximum and minimum body surface QT intervals (the *QT dispersion* measure) were studied in 10 patients with an arrhythmogenic long QT interval (Romano Ward and Jervell and Lange-Nielsen syndromes or drug arrhythmogenicity) and in 14 patients in whom the QT interval was prolonged by the drug sotalol.

It was found that in patients with prolonged QT intervals, *QT dispersion* distinguished between those with ventricular arrhythmias and those without. Increased time dispersion of ventricular recovery time has been strongly linked with serious

ventricular arrhythmias and as *QT dispersion* has detected the arrhythmogenic group, this lends support to the hypothesis that *QT dispersion* reflects spatial or regional variation in myocardial recovery time.

In the second study carried out by the group (C.Day et al., 1991), the effect of the class III anti-arrhythmic drug sotalol on *QT dispersion* was studied in 67 patients who post-myocardial infarction were randomized to treatment with either sotalol or placebo. The action of sotalol like other class III anti-arrhythmic drugs is thought to operate by decreasing dispersion through homogeneous prolongation of recovery time. The value of the maximum rate-corrected QT interval for each patient was also studied. *QT dispersion* was calculated as before by using the difference between the maximum and minimum rate-corrected QT interval in any surface ECG lead. However, in this study, *QT dispersion* was found to be significantly affected according to the number of leads in which QT intervals were measurable; it was found to increase in proportion to the square root of the number of leads. Therefore, for *QT dispersion* analysis, the group adopted a measurement parameter: the *adjusted QT dispersion* which is calculated as the difference between the maximum and minimum rate-corrected QT interval in any surface ECG lead divided by the square root of the number of leads in which QT intervals are measurable.

Prior to randomization both the maximum rate-corrected QT interval and *QT dispersion* calculated as above were not found to be significantly different in the sotalol and placebo groups. However, both the maximum rate-corrected QT interval and *QT dispersion* varied considerably following the infarction. During the six month follow up period, the maximum rate-corrected QT interval was found to have increased significantly in patients on sotalol compared to placebo, whilst *QT dispersion* was found to decrease in patients on sotalol compared to placebo.

In order to understand the result above, let us consider the rate-corrected *prolonged QT interval* as recorded on the surface. Prolongation of the rate-corrected QT interval on the surface ECG may indicate either arrhythmia risk or an anti-arrhythmic drug effect. This apparent paradox may be explained by the differences in dispersion of ventricular recovery time (E.M. Vaughan Williams, 1980). A long QT interval associated with ventricular arrhythmias may reflect increased dispersion of recovery time, which is

known from experimental studies to be an important substrate for the development of ventricular tachycardia and ventricular fibrillation. Vaughan Williams Class III drugs however, probably decrease dispersion of recovery time despite an increase in QT interval. Support for this comes from a canine experiment in which bretylium reversed the effects of quinidine-induced increased temporal dispersion of effective refractory periods, and decreased ventricular fibrillation threshold. (H.Inoue et al., 1985).

Clearly, the maximum rate-corrected QT interval is unreliable as a non-invasive measure of ventricular recovery time dispersion. Earlier work done by the group on epicardial monophasic and QT inter-lead variability (J.C.Cowan, C.J.Hilton et al., 1988; J.C.Cowan, K.Yusoff et al., 1988) suggests that just as regional ischaemia and infarction are reflected via morphological differences in the surface ECG, so too might be regional variation in repolarisation via *QT interval dispersion.*

The result obtained showing smaller *QT dispersion* but greater maximum rate-corrected QT intervals were in accordance with the expected changes in ventricular recovery times. This finding therefore added support to the hypothesis that *QT dispersion* is a measure which reflects the regional differences in ventricular recovery time. The group have since carried out further studies on various patient groups. The results of these studies confirm the result of *QT dispersion* as a measure which reflects the regional differences in ventricular recovery time (C.Day et al., 1992; P.D.Higham et al., 1991,1992, P.D.Higham and R.W.F.Campbell, 1992).

1.6 Discussion

The previous sections have confirmed the importance of *QT dispersion* as a measure of regional variation in ventricular repolarisation. If further substantiated the concept of *QT dispersion* has very strong potential as a method of examining the anti-arrhythmic effects of drugs, arrhythmogenic tendencies in patients, as well as in establishing the prognostic value of QT measurement in post myocardial infarction patients.

The aim of the Ph.D was to develop an engineering based system which would allow the study of *QT dispersion.* As most of the conventional 12 lead ECGs are still recorded on paper, such a system would have to firstly allow the digitisation and recovery of such waveforms recorded on paper. Algorithms could then be developed to automate the

measurement of the parameters used to study *QT dispersion*. Such a system would have to be accurate, reliable and easy to use. The following chapters trace the development of such a system and its validation. A clinical study using the system developed is also presented in the final part of the thesis.

Chapter 2 Top Level System Design

2.1 Introduction

Chapter 2 describes the top level design for a system which will enable the validation of *QT dispersion* as an potentially useful risk predictor of patients susceptible to ventricular arrhythmias or sudden death using the standard 12 lead hard copy electrocardiograms (ECGs). The role and function of each component of the system is presented briefly in Figure 2.1. The chapter describes each component in greater detail.

2.2 Components of the System

The components of the system comprise *objects*:

- the standard hard-copy 12 lead ECG
- optical flatbed scanner

different algorithms for *measurement:*

- digitising algorithms
- manual measurements
- user-interactive measurements
- automatic measurements

and a series of assessments, studies, comparisons and validation procedures.

The following sections describe how each of these is related to the other in the overall system and the reasons for their relationship. Note that in all the following sections the terms *QT dispersion* will be used to refer to the general concept of *QT dispersion* and not to refer to a particular parameter representing dispersion.

2.2.1 Optical Flatbed Scanner and Digitising Algorithms

As the ECGs of interest are the hard copy standard 12 lead electrocardiograms, a method to digitise these hard-copy waveforms stored on paper so they resemble directly sampled data is required. It was decided to use an optical flatbed commercial scanner for

Figure [2.1] Top level System Diagram

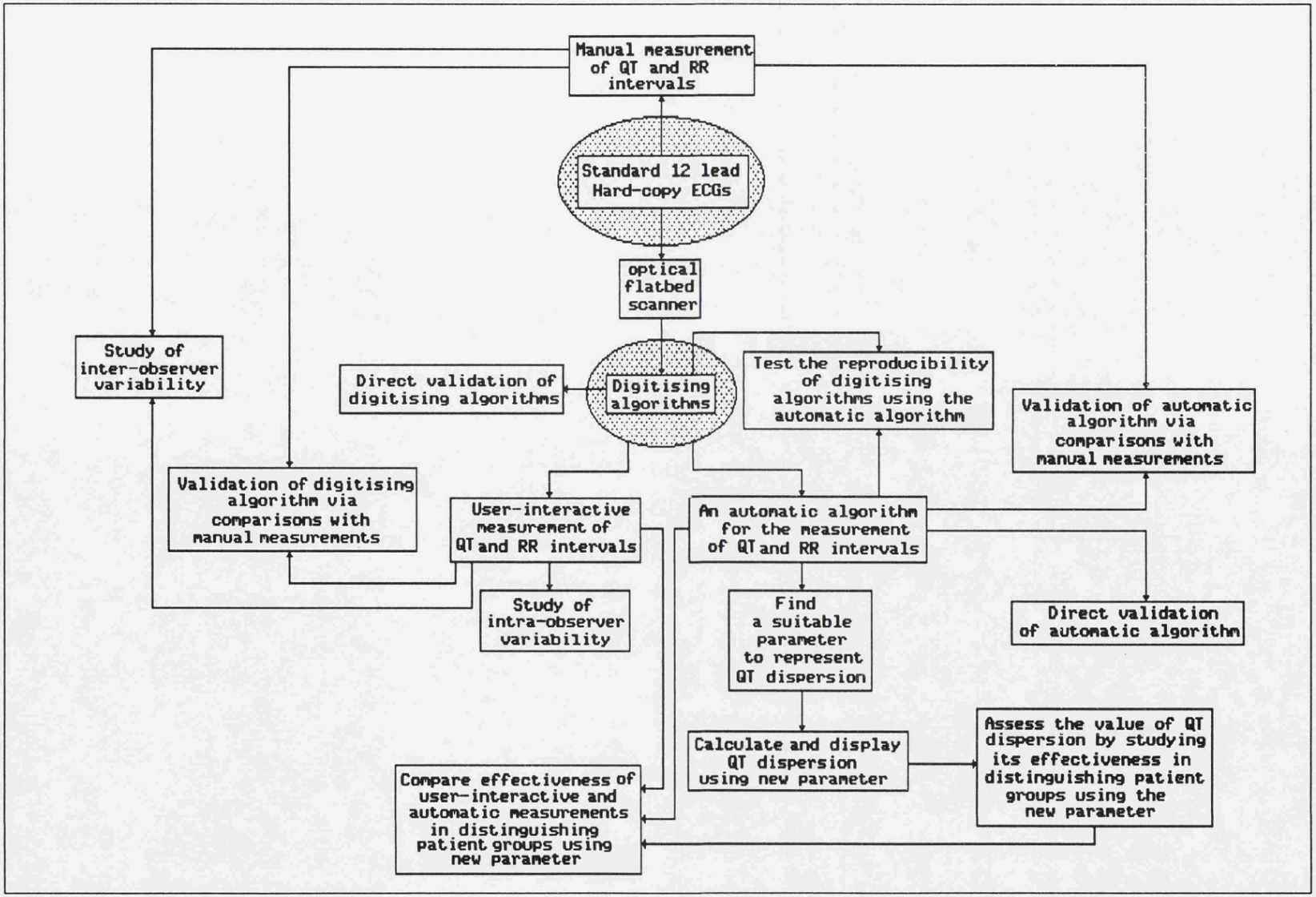

this purpose. However the optical scanner only produces image files; hence a series of digitising algorithms whose function is to interpret these files and recover the digital waveforms for each lead was required. This will provide, in permanent digital form, data that is conventionally available on paper. Therefore, large archives of data, for example, from patients who have undergone clinical trials and for whom the subsequent outcomes have become known, can be studied. Furthermore, digital procedural algorithms that can only be applied to digital data can also be implemented. Parameters of importance in the digitised waveforms can be automatically analysed hence overcoming problems due to user-bias.

These digitising algorithms can be validated directly. For example a waveform whose digital values are known, can be plotted onto paper. This waveform can then be scanned using the optical flatbed scanner. Digitising algorithms can be applied to this image of a waveform and its digital values can then be recovered. These values can be compared against the original digital values used to plot the waveforms and some inferences can be made of the likely accuracy of the scanner and digitising algorithms.

2.2.2 User-Interactive measurements

The second component of the system is software for the observer to use which will enable the display and storage of the digitised hard copy waveforms of each patient. The software should allow *user-interactive* measurements using a cursor, to enable the observer to perform QT and RR interval measurements. The software should also incorporate graphics capabilities which will enable the observer to adjust the effective resolution of the display and therefore allow features of the waveform to be accentuated if necessary. The software should incorporate the storage and display of each patient's bio-data. Finally, it should be user-friendly, with help menus etc..

Such software, which allows user-interactive measurements on waveforms recovered using the digitising algorithms, can also show the effectiveness of the digitising algorithms. This can be achieved via the comparison of common parameters such as the QT and RR intervals of the ECG measured manually and using the user-interactive system. Since it will be easy to use, the user-interactive software can be used by several observers for example, to study a particular set of ECGs. Therefore inter-observer

variability can be assessed and compared with results using the manual method of measurement. Intra-observer variability, where a single observer is asked to perform measurements on a random set of repeated waveforms, can also be assessed easily.

2.2.3 Automatic measurements

The third component of the system is an algorithm which will *automatically* detect characteristic points of the ECG like the QRS onset, R wave position and T wave end, thereby allowing the automatic derivation of QT and RR intervals. Such an algorithm if effective, will overcome the need for interactive measurements. This being the case, any elements of bias due to intra-observer and inter-observer variability would be removed (although the automatic algorithm may reflect a bias due to the person who developed it, at least it would be consistent).

The automatic algorithm would also allow the reproducibility of the digitising algorithms to be tested. For example if the same waveform were to be repeatedly measured for its QT and RR intervals using the automatic algorithm, it should always give the same results as the same criteria will be met each time. Since on its own the automatic algorithm will always give the same set of results for a particular waveform, if a waveform is repeatedly digitised and analysed from an original hard copy, any differences in the results obtained by the automatic algorithm would give an indication of the reproducibility of the digitising algorithms.

Results obtained using the automatic measurement method can also be compared against the conventional method of manual measurement. However since the automatic algorithm uses output from the digitising algorithms, such a comparison will give information on the effectiveness of *both* the digitising algorithms and the automatic algorithm. If the effectiveness of the digitising algorithms has already been assessed from Section 2.2.2, then some inferences on the compatibility of the manual and automatic methods of measurement can be made.

The automatic algorithm may not be able to recognise all the characteristic points in some of the ECGs. The performance of the automatic algorithm can therefore also be directly validated by the study of its success rate in detecting the different ECG characteristic points, using a set number of ECGs.

2.2.4 Finding a risk parameter for *QT dispersion*

In the next part of the system, a suitable risk parameter to represent *QT dispersion* should be found. This can be performed by statistically analysing the distribution of rate-corrected QT intervals from cardiologically healthy patients and patients prone to ventricular arrhythmias for example. The parameter chosen to represent *QT dispersion* in these patient groups can then be derived from *characteristic parameters* of the distribution of the rate-corrected QT intervals they follow. If the automatic algorithm is proven to be effective, then QT interval data derived using the algorithm can be used in the statistical analysis, as it should be less prone to user-bias.

2.2.5 Calculating and displaying *QT dispersion* using the new risk parameter

In the next part of the system, an algorithm which will take in QT and RR interval measurements from manual, user-interactive and the automatic methods of measurement and calculate *QT dispersion* for each patient (using the new risk parameter), should be developed. A graphical display of *QT dispersion* i.e. the differences in the QT intervals measured in the different leads of a patient, should be incorporated. This will allow observers quick visual assessment of the each patients QT interval dispersion, using all the leads in which QT intervals are measurable.

2.2.6 Assessing the value of *QT dispersion*

After a suitable risk parameter to represent *QT dispersion* has been found, and after algorithms and software have been developed to calculate the risk parameter for each patient and display their *QT dispersion*, the *value* of *QT dispersion* should be assessed. This can be performed by using statistical methods to test how effectively the risk parameter representing *QT dispersion* distinguishes different patient groups.

2.2.7 Comparing the effectiveness of User-interactive and Automatic measurements in distinguishing patient groups using the new risk parameter.

In the final part of the system, if *QT dispersion* as measured by both the user-interactive and automatic algorithms was found to distinguish patient groups, then comparisons of the relative effectiveness of each measurement method in deriving the risk parameter for *QT dispersion* can be assessed.

2.3 Discussion

The components of the overall system to be designed and implemented, their roles and functions, and how they relate to each other has been described above. The following chapters trace the development of each of these components in greater detail.

Chapter 3 Computer-based techniques for the Digitisation of Hard-Copy Waveforms

3.1 Introduction

The analysis of waveforms representing electrical or mechanical activity is important in many fields of medical investigation, including electrocardiography, electromyography (EMG) and electroencephalography (EEG). Conventionally, the waveforms have been recorded photographically or using a chart recorder, and analysed by a combination of pattern recognition by experts and manual measurement. As a result of advances in digital technology, modern equipment utilises computers to record waveform data on line via an A-to-D card, or onto magnetic tape, which can then be played back and digitised. There are many advantages to analysing data digitally. Useful transformations can be applied to the data and measurement of important parameters can be automated, thus reducing overall errors in data analysis.

Recent research has shown that quantitative digital analysis of medical waveform records can reveal clinically important information not apparent by qualitative inspection. Non-digital equipment is still however in widespread use, particularly for electrocardiography, where the standard 12 lead hard-copy electrocardiogram is still by far the most common mode of recording patient ECGs and ascertaining patient health for example after complaint of chest pain. It is also used when monitoring progress of patients undergoing clinical trials, for example before and after the administration of corrective drug therapy. Many such paper records exist in hospital archives and are potentially useful for retrospective studies of patients where the eventual outcomes are known. Figure 3.1 shows an example of a hard-copy standard 12 lead electrocardiogram.

In the analysis of *QT dispersion* that has been carried out to date, the 12 lead electrocardiogram with a digitising tablet was used to facilitate the measurement of QT and RR intervals (C.Day et al., 1990). This is time consuming and potentially prone to user-bias. In order to undertake large studies on the standard 12 lead electrocardiograms, to ascertain the value of QT dispersion, algorithms are required which will convert these

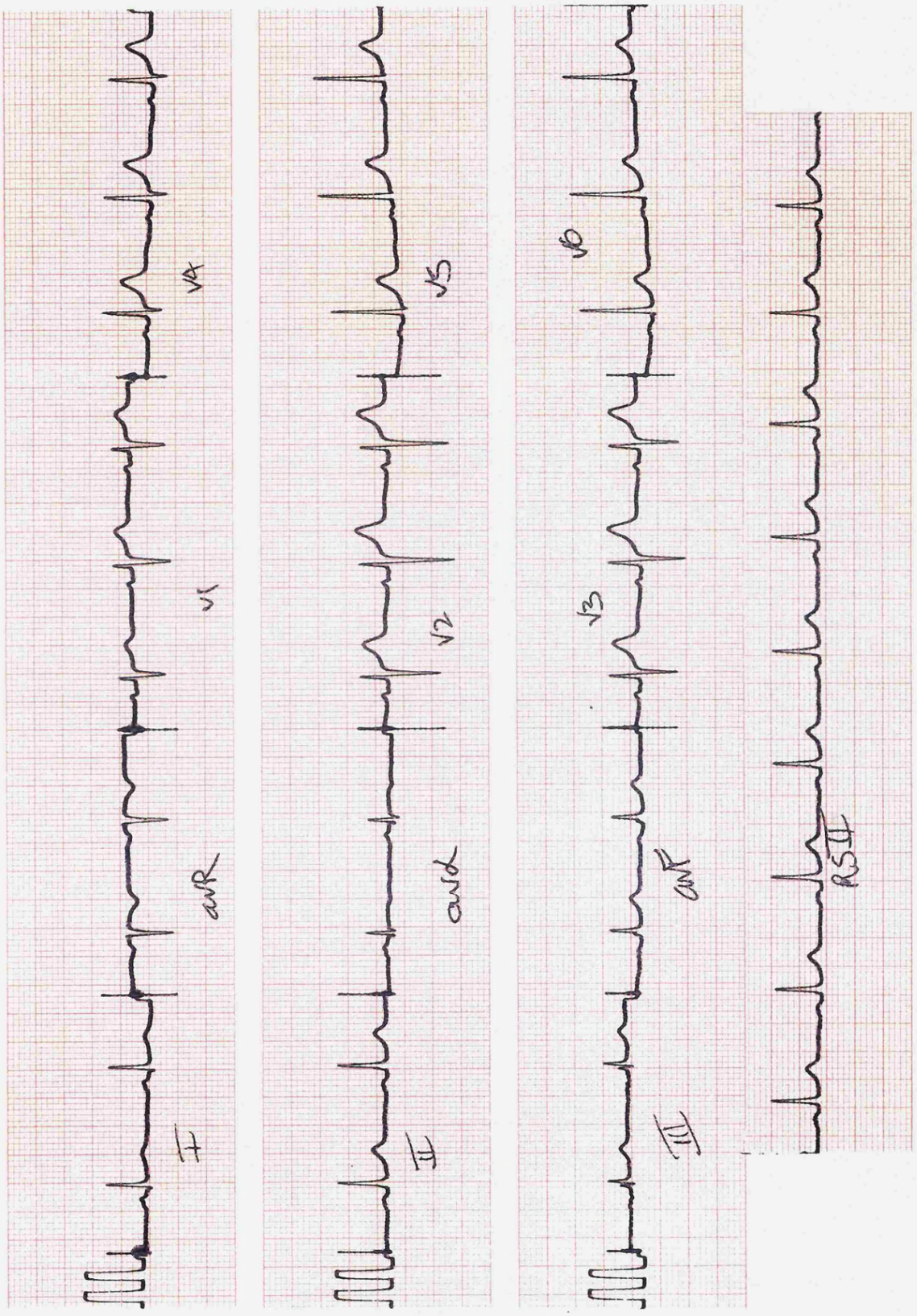

Figure [3.1] Example of a standard
hard-copy 12 Lead electrocardiogram

waveforms stored on paper to their digital values stored on computer, so they resemble directly sampled data. This must be performed in such a way that problems such as random noise and thick line widths on the original records are overcome.

In the first part of the chapter, the development of a system named DISPERSE (Digitisation and Scalarisation of Paper Electrocardiogram Recordings for Signal Evaluation) is described which uses new techniques for the digitisation of these hard-copy waveforms. The system comprises a number of processes: optical-scanning, segmentation, pre-processing, thinning (or skeletonising), extraction of digital values and filtering to remove quantisation errors and relative offset. The development of a graphical interface hence referred to as *user-interactive system* or *user-interactive algorithm* for the display and user-interactive analysis of each patient's standard 12 lead ECG waveforms is also described briefly. The chapter then presents a short review and discussion based on a comparison of these techniques and other methods that have been described for the recovery of waveforms stored on paper.

3.2 Scanning Hard-Copy Waveforms

The hard-copy standard 12 lead electrocardiograms analysed in this thesis were recorded by the Nihon Kohden Model ECG-6353/D/F/L Electrocardiograph machine, which records on paper, 3 channels simultaneously by heat writing with a tipped thermo-pen. This recording method has a frequency response 0.05Hz - 75Hz.

A flatbed black and white Hewlett Packard *ScanJet Plus* scanner connected to an IBM compatible AT machine, via an interface card is used to scan these standard 12 lead electrocardiograms using standard software provided by the manufacturer. The basic technology of a flatbed scanner comprises a fluorescent or incandescent light bulb which illuminates the image to be scanned. The scanner produces a voltage level in proportion to the amount of light reflected by the image. An analogue to digital converter processes these voltages into digital values, whose precision is based on the number of bits per pixel supported by the scanner. For the Hewlett Packard *ScanJet Plus* scanner, the number of bits per pixel is 8. Once the scanner has created an image, a high-speed direct-interface card transmits that image to the PC.

The choice of scanner sampling rate employed is 300 dots per inch (d.p.i.). This is an equivalent sampling rate of 295 Hz (3.4ms/pixel) for original hard-copy waveforms recorded at 25mm/sec. Using the scanner software provided and setting the scanner to a two level black and white mode, called the line-art mode, these 12 lead waveform images (example, Figure 3.1) are scanned and stored on the computer hard disk as a single image file in the '.PCX' format. The time it takes to scan and store these to hard-disk is approximately 12-15 seconds. A typical 12 lead waveforms image file in the '.PCX' format of size 5.5 by 10.5inches is 50Kbytes.

'.PCX' format is the native file format of the Z-Soft Paintbrush packages. It was chosen for a number of reasons. This file format is compatible with most software programs and the documentation revealing the manner in which the data representing the image is organised is readily available and easily understood. Furthermore data storage with the '.PCX' format is quicker than for most other formats (example the Tagged Image File Format; TIFF) and occupies less space. The typical time it takes to store a non-detailed image of size 8.5 inches by 11 inches in the TIFF format is 2.5 minutes if the image is uncompressed and 1.3 minutes if the image is compressed. Uncompressed this file would occupy 1.06 Megabytes, whilst its compressed counterpart would occupy 25 Kilobytes. In the '.PCX' format, the file would occupy 40 Kilobytes and take 10 seconds to store to hard-disk. The TIFF file format is non-propriety and independently documented, causing it to be open-ended to a fault. The method that is proposed in this chapter employs the '.PCX' format.

3.3 Error Considerations

Many error considerations must be made when waveforms are optically scanned. First, it must be ensured that the paper on which the waveforms are recorded be oriented in a straight line relative to the scanner body edge to ensure that no rotation and hence offset or tilt of the waveforms is introduced in the sampling process. The cover of the scanner must be held down firmly to ensure that no background light interferes with the image to be scanned. The paper on which these waveforms are recorded often have a

coloured grid in the background. This should be removed by using appropriate coloured optical filter paper which only allows the dominant pen colour (corresponding to the waveform) through.

Secondly, the scanner software allows the setting of a manual detection threshold to control the scanner image detection sensitivity. If this setting is too low, excess random noise is detected in the image (Figure 3.2a) and if too high, it can cause the image waveform detected to appear disconnected (Figure 3.2b). A threshold with the optimum level of sensitivity should be found which does not allow random noise to be detected or the image to be disconnected. Figure 3.2c shows the image detected at an optimum detection sensitivity threshold.

It can still be seen however that the square sampling grid used by the scanner has introduced sharp edges in the waveform image. These correspond to the introduction of high frequencies in the image. Such 'aliasing' problems can cause the loss of gaps (not necessarily disconnectedness) and random scatter of pixels on the actual waveform image, resulting in shape distortion. These problems may also arise due to the different scanner sensitivity to different pen recordings. These factors would be encountered even at high sampling frequencies. Different paper granularities, different recording pen thicknessess and irregularities of the pen tracing also contribute to this problem. In the system developed, pre-processing of the entire data array is carried out before any digital values are extracted.

3.4 Segmentation of the scanned 12 lead Electrocardiogram and Interpretation of PCX files

The scanner scans the standard 12 lead Electrocardiogram as a single image '.PCX' file. However this image comprises 12 separate recordings of electrocardiogram data from different electrode positions. A graphics editor is used to segment the '.PCX' image containing all 12 waveform recordings into separate rectangles of waveform data, each containing a single recording, and each stored as a smaller '.PCX' file.

The format of a '.PCX' file is described below. The explanation is derived from the ".EXE" Magazine, 1989. Each PCX file comprises two parts. The first part is a 128 byte header, which describes the resolution of the picture and the number of colours.

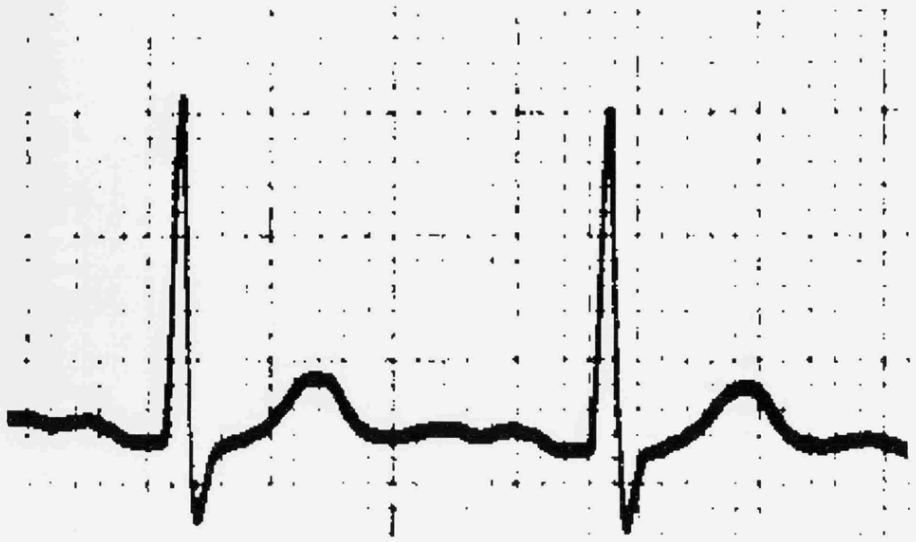

Figure [3.2a] Image waveform when scanner detection threshold is too low

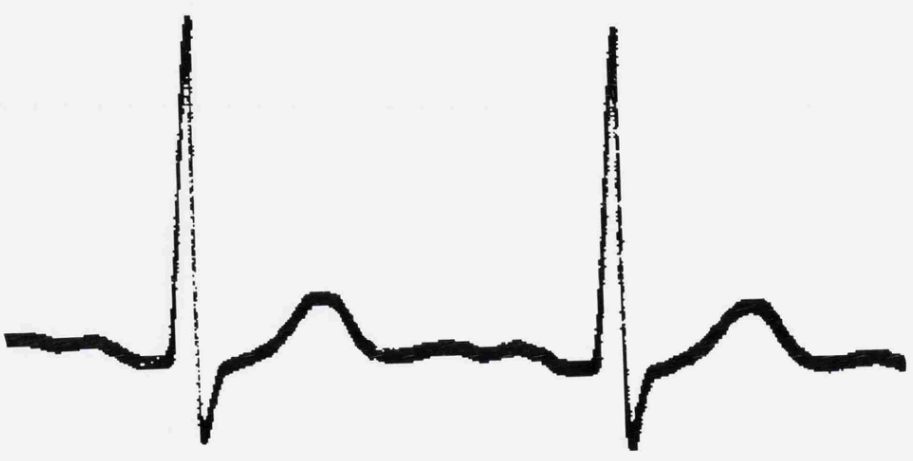

Figure [3.2b] Image waveform when scanner detection threshold is too high

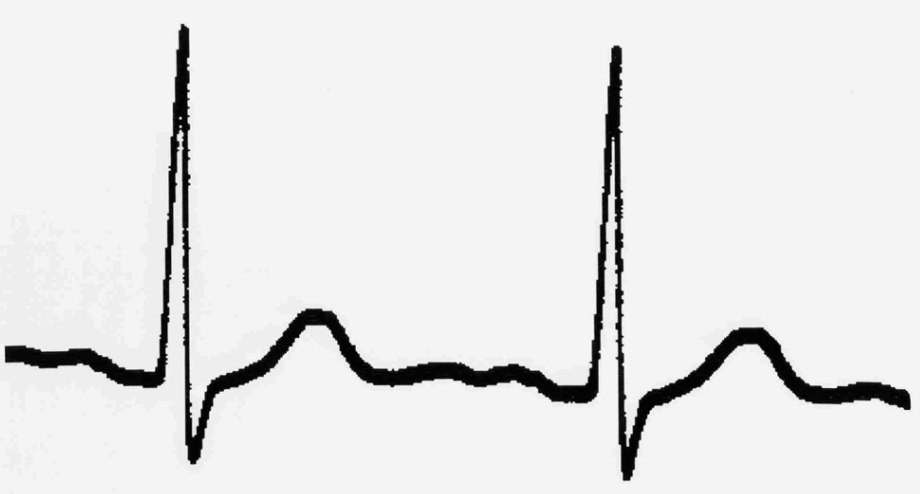

Figure [3.2c] Image waveform when scanner detection threshold is optimum

For black and white images, the graphics data is simply a stream of bits. Each bit represents one pixel. To decode the data:

- 1) Read the first byte after the header.
- 2)If the two most significant bits are set i.e. have values of 1, the byte is a counter. Strip the most significant two bits (by subtracting the value c0), to find the count value. For example:-

If you read a c7 byte:

1 1 0 0 / 0 1 1 1,

stripping the most significant two bits i.e. subtracting c0

1 1 0 0 / 0 0 0 0,

leaves 7:

0 0 0 0 / 0 1 1 1

This is a count, so read the following byte to obtain the image pattern (for example, a byte value of 255 or hexadecimal ff has a pattern 1111 1111) and duplicate it six times (count-1) to make it a total of 7 of them.

- 3) If the byte does not have the most significant two bits set, it is not a count but is an actual data byte that is not repeated. Its value expressed in 8 bits represents an image pattern.

Each byte is read in turn and interpreted until all the bytes in the file are analysed. The picture dimensions are stored in the 4th, 6th, 8th and 10th offset bytes of the header (see below). X1,Y1 is the top left corner, and is normally zero for '.PCX files'. X2,Y2 is the bottom right hand corner. The picture dimensions are X2-X1+1 and Y2-Y1+1.

Offset	Name	Length	Comments
4	d_X1	Word	Picture dimensions inclusive
6	d_Y1	Word	Picture dimensions inclusive
8	d_X2	Word	Picture dimensions inclusive
10	d_Y2	Word	Picture dimensions inclusive

The actual image is represented as 0s and the background as 1's. As a matter of preference, we wished the image to be represented by 1s and the background as 0s. Therefore, the image was inverted by subtracting 255 or the hexadecimal value of 'ff'

from all the bytes representing the image. A two-dimensional data array is then formed with each black pixel represented by a 1 and each white pixel (background) represented by a 0.

3.5 Pre-processing Waveforms

Pre-processing each individual recording of ECG waveform image is performed by two successive passes of an algorithm: the first uses a 5x5 window to recognise small groups of noise patterns (pixels distributed randomly) on the waveform image and flag these points for deletion; the second uses the same 5x5 window to recognise small gap patterns in the waveform image and flag these points for filling.

After a careful study of the nature of noise distribution and gaps on the waveform, a set of heuristic rules describing noise and gap patterns was developed. Figure 3.3 shows the 5x5 window or mask that is used for both passes of the pre-processing algorithm. In the first pass of the algorithm, it is used to traverse all the waveform points (or black pixels) column by column, and row by row, in the two-dimensional data array. As this window traverses the array, each element of the array is in turn assigned to be 'p1' and

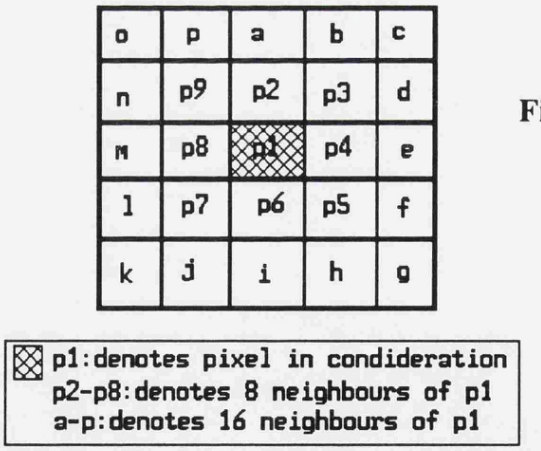

Figure [3.3]

the relationship between itself and its 8 neighbours (p2,p3,p4,p5,p6,p7,p8,p9) and 16 neighbours (a,b,c,d,e,f,g,h,i,j,k,l,m,n,o,p) is studied. Based on these relationships, the heuristic rules describing random noise distribution are then used to make a decision on where random noise exists in the image. Once the entire array has been traversed, these points are deleted (changed from 1 to 0).

In the second pass of the algorithm, the 5x5 window is used to traverse all the white pixels that are embedded between the respective end black pixels on each row, column by column, and row by row, in the two-dimensional data array. In this way redundant processing of non-relevant pixels is avoided. As above, when this window traverses the array, each element of the array is in turn assigned to be 'p1' and the relationship between itself and its 8 and 16 neighbours is studied. Based on these relationships, the heuristic rules describing gaps that occur on a waveform are then used to make a decision on where gaps exist in the waveform image. Once the entire array has been traversed, these points are filled. (changed from 0 to 1). It is important that these points are only changed after each successive pass of the algorithm to prevent the waveform image from changing during the program execution.

Figure 3.4a shows an unthinned and unprocessed image of a typical ECG waveform. The point marked (a)* is described by rule (a) illustrated visually by Figure 3.5a and given below. It gives an example of a point that has been detected as random noise and which should be deleted. Points (b)*,(c)*,(d)*,(e)* and (f)* on Figure 3.4a (illustrated by their corresponding rule diagrams Figures 3.5b to f and described by their corresponding rules below) have been tagged as gaps in the image waveform that need to be filled.

Examples of some of the rules that describe the orientation of the pixels in the 8 and 16 neighbourhood, which decide whether the pixel point under consideration should be removed or filled are given below:

An example of heuristic rules for the removal of randomly distributed pixels

Rule (a)
If:
i) p1 is 1
ii) the logical *'or'* of p4,p5,p6,p7,p8,e,f,g,h,i,j,k,l,m is 0
iii) the logical *'and'* of p9,p2,p3,n,d is 1
then store the coordinates of p1 in a file for later removal

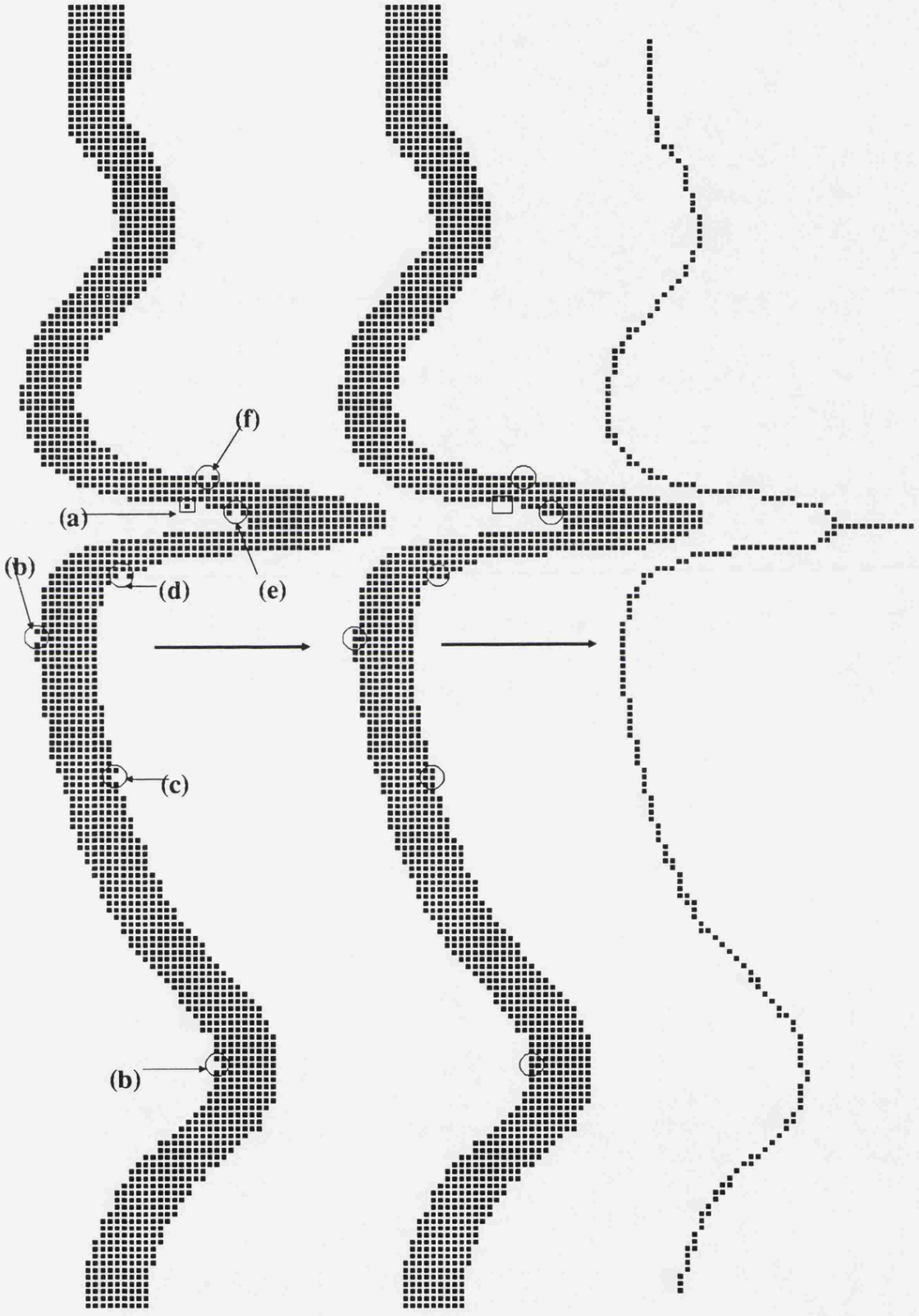

Figure [3.4a] Unthinned and Unprocessed Image

Figure [3.4b] Pre-processed Image

Figure [3.4c] Skeleton of an ECG Waveform

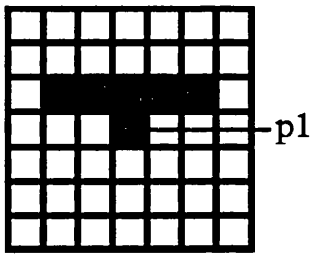

Figure [3.5a] Rule (a)

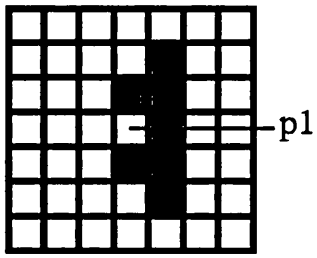

Figure [3.5b] Rule (b)

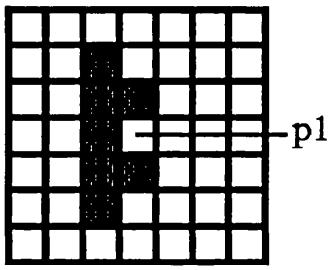

Figure [3.5c] Rule (c)

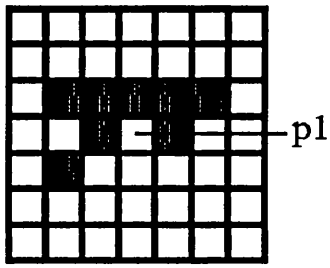

Figure [3.5d] Rule (d)

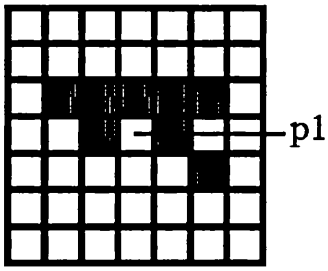

Figure [3.5e] Rule (e)

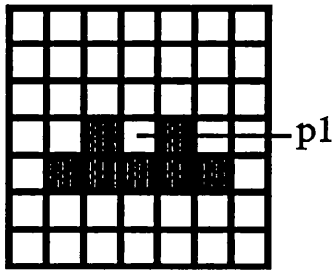

Figure [3.5f] Rule (f)

Some examples of heuristic rules for the filling in of gaps and removal of disconnectedness

Rule (b)
If:
i) p1 is 0
ii) the logical *'or'* of p7,p8,p9,j,p is 0
iii) the logical *'and'* of p3,p4,p5,b,h is 1
iv) the logical *'and'* of p6,p2 is 1
then store the coordinates of p1 in a file for later conversion to a value of 1

Rule (c)
If:
i) p1 is 0
ii) the logical *'or'* of p3,p4,p5,b,h is 0
iii) the logical *'and'* of p7,p8,p9,j,p is 1
iv) the logical *'and'* of p2,p6 is 1
then store the coordinates of p1 in a file for later conversion to a value of 1

Rule (d)
If:
i) p1 is 0
ii) the logical *'or'* of l,p7 is 1 and the logical *'or'* of p5,p6,f is 0
iii) the logical *'and'* of p9,p2,p3,n,d is 1
iv) the logical *'and'* of p4,p8 is 1
then store the coordinates of p1 in a file for later conversion to a value of 1

Rule (e)
If:
i) p1 is 0
ii) the logical *'or'* of f,p5 is 1 and the logical *'or'* of p6,p7,l is 0
iii) the logical *'and'* of p9,p2,p3,n,d is 1
iv) the logical *'and'* of p4,p8 is 1
then store the coordinates of p1 in a file for later conversion to a value of 1

Rule (f)
If:
i) p1 is 0
ii) the logical *'or'* of p9,p2,p3,n,d is 0
iii) the logical *'and'* of p5,p6,p7,f,l is 1
iv) the logical *'and'* of p8,p4 is 1
then store the coordinates of p1 in a file for later conversion to a value of 1

These rules are implemented taking into account that the data can be oriented in any four directions (right, left, up or down). Compare points b* and c* in Figure 3.4a. The reason for selecting a 5x5 window is because random noise distributes itself in small areas; similarly most missing pixels causing gaps in the image occur within such an area. If large gaps exceeding the relationships expressed in the 5x5 window are observed,

these are taken into account at a later stage, when digital data points are to be extracted. It was not thought computationally wise to use masks larger than 5x5 as the computational complexity and time involved far outweigh any benefits that might be gained.

Figure 3.4b shows the elimination of random noise and the filling in of gaps of the ECG waveform as performed by the heuristic rules (a) to (f) in the pre-processing stage. A full list of all the rules developed for the removal of random noise and the filling in of gaps is given in Appendix E.

3.6 Skeletonising Scanned Waveforms

The main consideration in the reconstruction of medical waveforms is the preservation of shape information i.e. the waveforms should not be distorted in the amplitude or time axis, so that digital data can be recovered accurately. Because of this consideration, a scanner sampling rate of 300 dots per inch was used. This would further ensure that no lines would be broken in the reconstructed image. As can be seen in Figure 3.4a however, this causes a width of more than 2 pixels to be used to form the scanned image. This represents the spread of the recording pen ink (due to the pen thickness) when the line was drawn on the original hard-copy graph. The problem here is to estimate from the thick line image the most likely line of curve the pen would have followed, i.e. the lineal structure of the wave shapes should be recovered, before any digital values can be extracted. An important approach for recapturing the lineal structure of data without destroying its connectivity is a procedure called 'thinning' (T.Y.Zhang and C.Y.Suen, 1984; T.Pavlidis 1990; R.C.Gonzalez and P.Wintz, 1987).

Thinning is often used on binary images to obtain their skeleton, where the skeleton of a region may be defined by the medial axis transform (MAT) proposed by H.Blum (1967). The MAT of a region R with border B is defined as follows. *For each point p in R, its closest neighbour in B is found. If more than one such neighbour exists for p, it is said to belong to the medial axis* (skeleton) of R. The concept of 'closest' depends on the definition of a distance and therefore the MAT will be influenced by the choice of a given distance measure.

Although the MAT of a region yields an intuitively pleasing skeleton, a direct implementation of the idea is computationally prohibitive as it potentially involves calculating the distance from every interior point to every point in the boundary of a region. A number of algorithms have been proposed for improving computational efficiency while at the same time attempting to produce a medial axis representation of the given region. Typically these are thinning algorithms that iteratively delete edge points of a region subject to the constraints that the deletion of these points does not remove end points, break connectedness or cause excessive erosion of the region.

Skeleton derivation is usually associated with binary data. Because of its ability in retrieving the lineal structure of waveforms without destroying connectivity, it was decided to use 'thinning' on the scanned waveforms. An elegant algorithm developed by T.Y.Zhang and C.Y.Suen (1984) for thinning digital patterns in binary regions has been adopted for this procedure. For this analysis, region points (in our case representing the waveform images) have a value of 1 and background points have a value of 0. The method consists of separate passes of two basic steps applied to contour steps of a region where a *contour point is any pixel with a value 1 and having at least one of its 8 neighbours valued 0*. Using the 8-neighbour definition shown in Figure 3.3, the first step flags a point p1 for deletion if all the following conditions are satisfied:

(a) $2 \leq B[p1] \leq 6$

(b) $A[p1] = 1$

(c) $p2 \cdot p4 \cdot p6 = 0$

(d) $p4 \cdot p6 \cdot p8 = 0$

where A[p1] is the number of 01 patterns in the ordered sequence p2,p3,...p7,p8,p9 that are the eight neighbours of p1, and

B[p1] is the number of nonzero neighbours of p1; that is,

$B[p1] = p2 + p3 + p4 + p5 + p6 + p7 + p8 + p9.$

In the second step, conditions a) and b) remain the same but conditions c and d are changed to:

(c') $p2 \cdot p4 \cdot p8 = 0$

(d') $p2 \cdot p6 \cdot p8 = 0$

Step one is applied to every border pixel in the binary region under consideration. If one or more of the conditions (a) through to (d) are violated, the value of the point in question is not changed. If all the conditions are satisfied, the point is flagged for deletion. It is important to note however that the point is not deleted until all border points have been processed. This prevents changing the structure of the data during the execution of the algorithm. After step 1 has been applied to all the border points, those that were flagged are deleted (i.e., changed to 0). Then, Step 2 is applied to the resulting data in exactly the same manner as step 1. This basic procedure is applied iteratively until all no further points are deleted, at which time the algorithm terminates, yielding the skeleton of the region.

The justification for the rules (a), (b), (c), (d), (c'), (d') is as follows. Condition (a) is violated when the contour point p1 has only one or seven neighbours valued 1. Having one such neighbour implies that p1 is the end point of a skeleton stroke and obviously should not be deleted. If conversely, p1 had seven neighbours and it was deleted, this would cause erosion of the region. Condition (b) is violated when it is applied to points on a stroke one pixel thick, and hence prevents the disconnection of segments of a skeleton during the thinning operation. Conditions (c) and (d) are satisfied by the following minimum set of values: p4 = 0, or p6 = 0, or (p2 = 0 and p8 = 0). From the 8-neighbourhood arrangement, a point that satisfies this condition as well as conditions (a) and (b) is an east or south boundary point, or a northwest corner point in the boundary. In either case, p1 is not part of the skeleton and should be removed. Similarly conditions (c') and (d') are satisfied simultaneously by the following minimum set of values: p2 = 0 or p8 = 0, or (p4 = 0 and p6 = 0). These correspond to north or west boundary points, or a southeast corner point. Note that northeast corner points have p2 = 0 and p4 = 0 and thus satisfy conditions (c) and (d), as well as (c') and (d'). This is also true of southwest corner points, which have p6 = 0 and p8 = 0.

To illustrate the results obtained with our algorithm for each stage of the thinning, the following iterations using a Figure H is shown (Figure 3.6a-f):

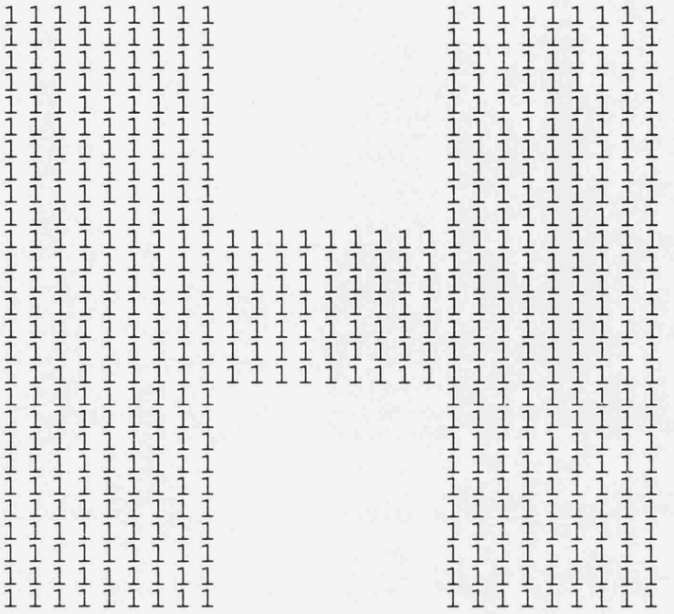

Figure [3.6a] The image before any 'thinning' operation

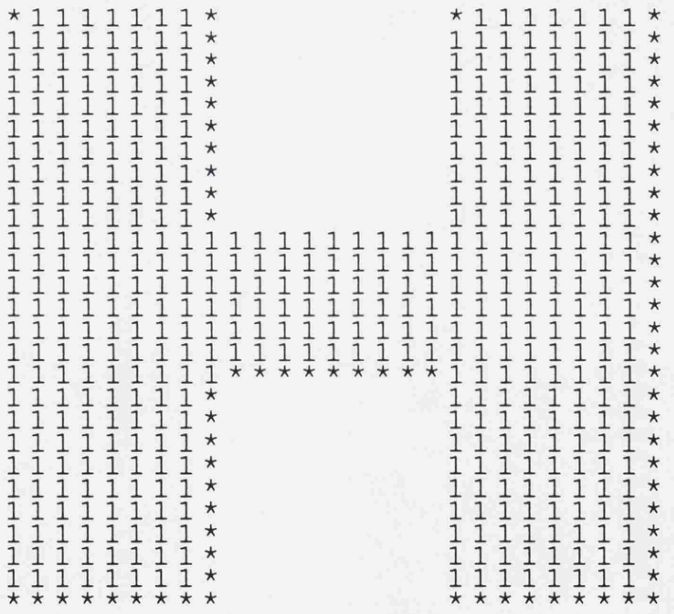

Figure [3.6b] Result of step 1 of the 'thinning' algorithm during the first iteration through a region; the * denote the points flagged for deletion

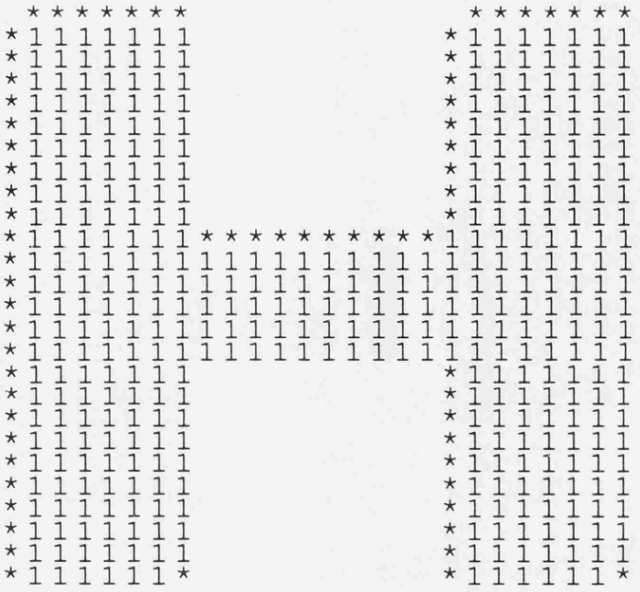

Figure [3.6c] Result of step 2 during the second iteration through a region

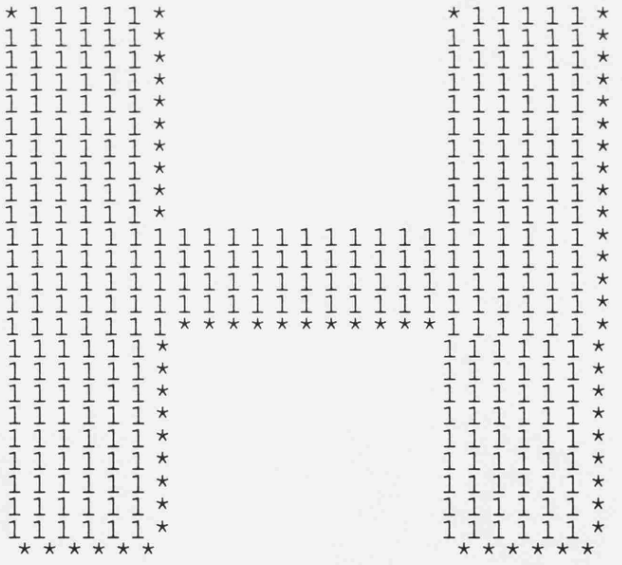

Figure [3.6d] Result of step 1 during the third iteration through a region

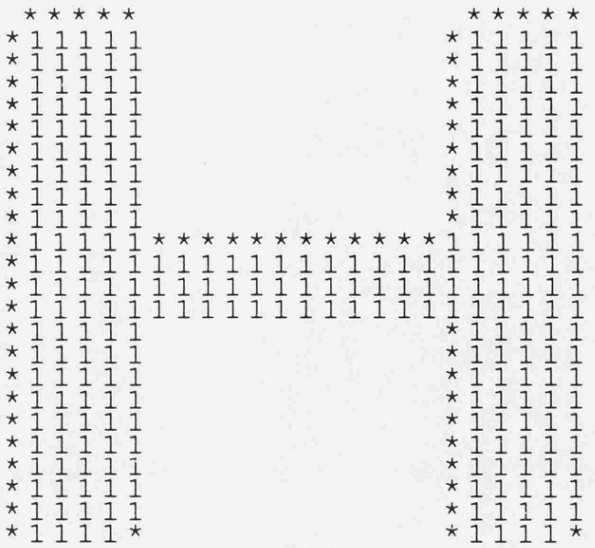

Figure [3.6e] Result of step 2 during the fourth iteration through a region

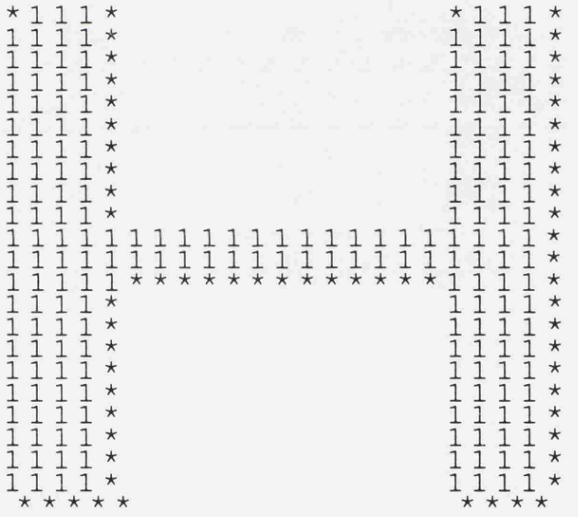

Figure [3.6f] Result of step 1 during the fifth iteration through a region

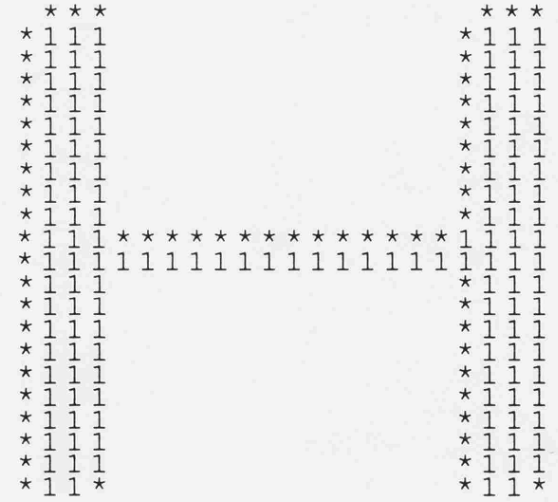

Figure [3.6g] Result of step 2 during the sixth iteration through a region

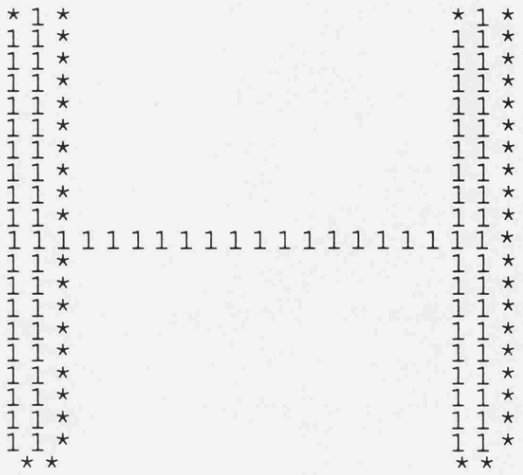

Figure [3.6h] Result of step 1 during the seventh iteration through a region

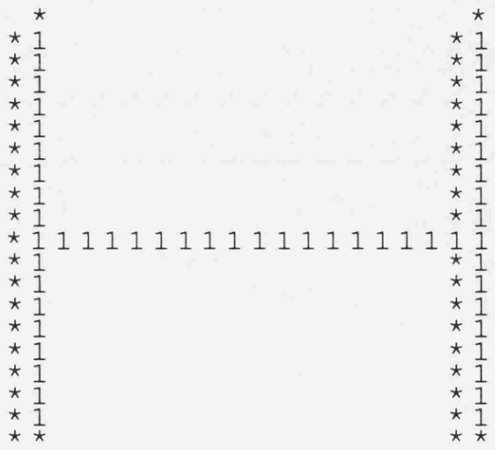

Figure [3.6i] Result of step 2 during the eighth iteration through a region

Figure [3.6j] Final thinned image after the ninth iteration

Figure 3.4c shows the thinned image or skeleton of the ECG waveform obtained using the algorithm. As can be seen thinning has yielded the lineal structure of the ECG waveform. However the lineal structure alone does not correspond to the path or line of curve the original pen recording would have followed. Data values that correspond to the line of path of the original pen recording still need to be extracted from the skeleton and filtered to remove high frequency noise components introduced by the scanning, thinning and extraction processes.

3.7 Extraction of digital values from the Skeleton

Digital data values are extracted from each row of the *skeleton* of the waveform stored in a two-dimensional array, by moving across from left to right of each row of the array (See Figure 3.7b). Two different rules apply for the extraction of digital values depending on whether the row in question corresponds to a sharp peak in the skeleton waveform or not:

If a particular row corresponds to a sharp peak, then the position of the pixel point corresponding to the peak (and counted as an offset from the left-most column of the row) is the digital value extracted from that row. It may be the first or last black pixel in the row depending on the orientation of the peak.

If the row does not correspond to a sharp peak, then for each row of the two-dimensional array containing the skeleton, the start and end black pixel is determined. The mid-point of the position of the start and end black pixel points for each row of the skeleton (counted as an offset from the left-most column of the row) then gives the digital value expressed to the nearest half pixel. By taking the mid-point of the first and last occurrence of black pixels in a row, any problem pertaining to larger gaps between black pixels than that accounted for by the 5x5 window of the pre-processing stage is overcome.

The reason for selecting the end point of peaks of the skeleton and not the mid-point is that when the recording pen attempts to plot a peak point, its dynamics change and instead of moving horizontally across the sheet of paper with a steady velocity, it moves upwards and downwards (or vice versa) very quickly. This causes a smearing or merging of the upward and downward limbs of the peak for a short time before they

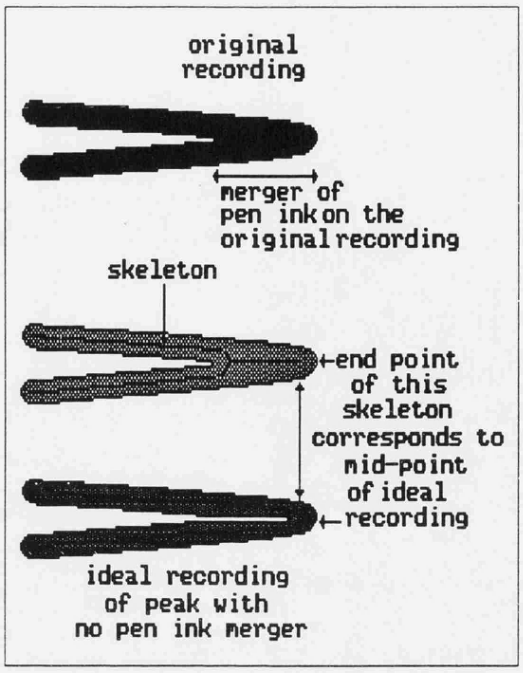

Figure [3.7a]

separate again. This is clearly an artefact of the recording pen mechanism. The skeleton however simply retrieves the lineal structure of this merged section and therefore the true peak point can not lie in the middle of the skeleton but must lie instead beyond it. The end-point of the skeleton peak is a better estimate of where the true peak of the waveform lies as it has already taken into account pen thickness.

Figure 3.7a clearly illustrates the problem above. The top figure shows the merging of the pen ink that occurs at a peak. The bottom figure shows the ideal pen recording of a peak if no merging of the limb slopes at the peak occurred. For such an ideal pen recording, the mid-point might give a true estimate of the peak position and hence its digital value. The middle figure shows the skeleton inside of the peak. It can be seen that the end point of this skeleton corresponds quite well to the mid-point of the ideal recording of the peak.

Figure 3.7b shows the two-dimensional array from which data points are extracted. The column of data below Figure 3.7b gives the digital values extracted for each row in the array alongside the arrow. These values are then scaled by a constant factor and a data file with amplitude values for each data point is then obtained. Based on the relationship between the scanner sampling rate used and the time and amplitude relationships of the actual waveforms recorded on paper, correct time and amplitude values can be assigned to each data point.

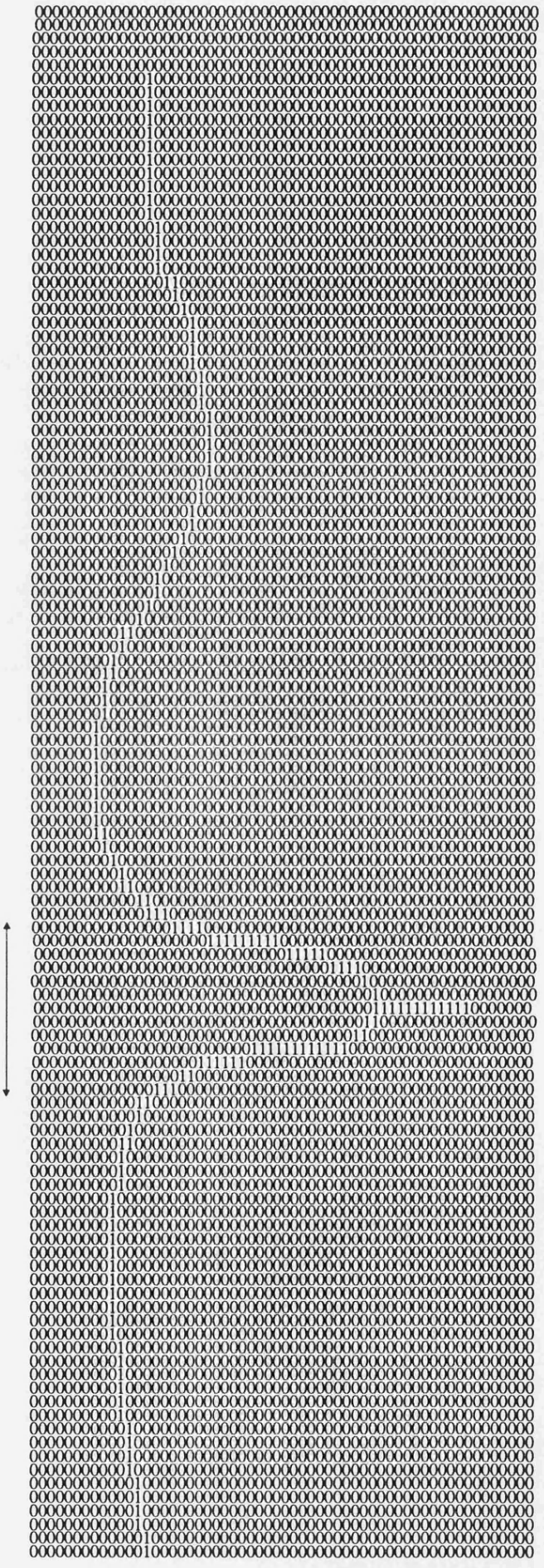

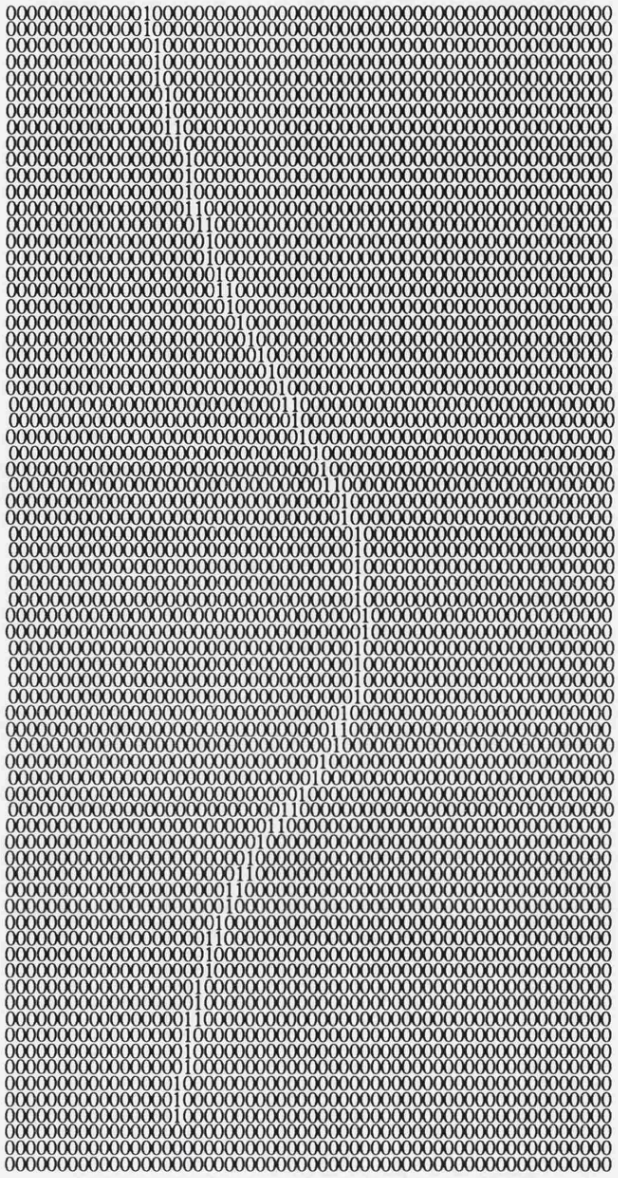

Figure [3.7b] Example of a 2-Dimensional Array containing the Skeleton of an ECG waveform

The digital values extracted corresponding to the arrow on the previous page:

18.5
25
32
36.5
39
40
51
39.5
38.5
31.5
22.5
18.5
16

3.8 Filtering the Extracted Values

As the extraction procedure introduces a fixed offset into the digital values extracted and because the scanner sampling process has also introduced high frequency components, the extracted digital values must be high-pass filtered to remove any d.c. offset and then smoothed using a low-pass filter to eliminate the effects of quantisation introduced in the scanning, thinning and extracting process.

The high-pass filter is described first. The filter, known as a low pass differentiator (S.Usui and I.Amidror, 1982) uses an infinite impulse response to enable a fast implementation of the high pass filtering. The transfer function of the filter is:-

$$H(z) = \frac{1 - z^{-1}}{1 - z^{-1} e^{-\sigma\tau}} \quad \ldots\ldots\ldots\ldots\ldots\ldots\ldots (3.1)$$

where σ = 3dB cut-off frequency value, τ = sampling interval and z^{-1} is the backward shift operator.

A high cut off frequency setting on the high pass filter can distort the ECG signal, so a trade off is required between noise suppression and signal distortion. As the filter was only required to remove dc offset, the cut-off frequency of the filter for ECG waveforms was set at 0.01Hz (the 3dB point). Figures 3.8a and b show the gain and phase characteristics of the low pass differentiator. The filter was designed with very small phase distortion within the passband.

The second step is a low pass filtering of the signal to eliminate the effects of quantisation introduced in the scanning process. A finite impulse response filter was designed for this purpose. A frequency-domain design was used with a Hamming window function.

For an ECG signal that is recovered from paper, the maximum frequency of waveform that can be recorded is estimated at 75Hz based on the maximum frequency response of the recording thermal pen. However the peaks in the skeleton contain higher frequencies which would be attenuated if the cut-off frequency was set at 75Hz. A compromise between smoothing and attenuation of the skeleton peaks is required. A cut-off frequency of 100Hz was chosen for the low-pass filter. The equivalent sampling

rate used by the scanner corresponds to 295.3 Hz, which is greater than four times the maximum frequency components of the signal and hence should allow the complete description of the signal in the time domain. The specified amplitude/frequency and phase/frequency characteristics of the filter were used to compute the impulse response weighting sequence. The impulse response weighting sequence, g(i)T, was then multiplied by a Hamming window function W_r (see equation 3.2). The Hamming window function reduces the oscillations in the amplitude/frequency characteristics, (known as Gibbs phenomenon) which are caused by the truncation of the Fourier series to N values. N was set at six.

$$W_r = 0.54 + 0.46 \times \cos(r\pi / I) \quad \ldots\ldots\ldots\ldots (3.2)$$

r is the coefficient number of W_r and I (= 2) the number of terms either side of g(0)T.

The resulting filter coefficients g(i)TWr are shown below :-

g(0)T = 0.66667 W0 = 1.000 g(0)TW0 = 0.66667

g(1)T = 0.25 W1 = 0.54 g(1)TW1 = 0.135

g(2)T = -0.08333 W2 = 0.08 g(2)TW2 = -0.006667

Therefore :

$$G(z) = -0.006667 \times z^{-2} + 0.135 \times z^{-1} + 0.66667 \times z^{0}$$

$$+ 0.135 \times z^{1} - 0.006667 \times z^{2} \quad \ldots\ldots\ldots\ldots (3.3)$$

z raised to a positive power represents a time advance and requires sampled data for t < 0. This can be avoided by introducing a time shift so that the transfer function G(z) contains no terms having z raised to a positive power. However it was not desirable to introduce any time shift in the filtering process. This was overcome by keeping the first two and last two terms in the filtered signal at their original values. These normally correspond to the baseline, and therefore does not distort the ECG signal. The gain and phase characteristics of the filter are shown in Figure 3.9a and b.

Figure 3.10a shows an ECG signal just extracted from the skeleton and Figure 3.10b and c show the same waveform after high-pass and low-pass filtering respectively using a filter with cut-off frequency at 100Hz (-3dB point.) The filtered signals shows the removal of d.c. offset and reduction in high frequency noise. Figure 3.10d shows the attenuation of the skeleton peaks that occurs if a lower cut-off frequency is chosen.

Figure [3.8a] Plot of gain versus frequency characteristics for the high-pass filter to remove d.c. offset

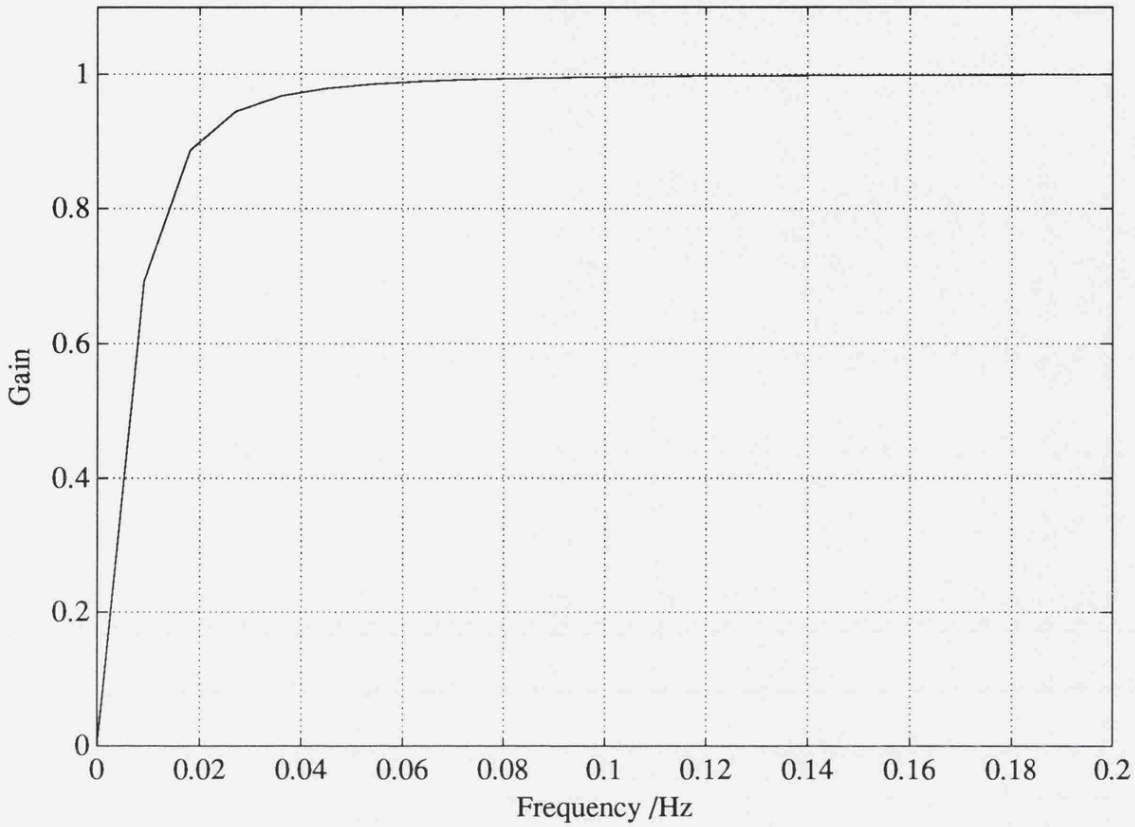

Figure [3.8b] Plot of phase versus frequency characteristics for the high-pass filter to remove d.c. offset

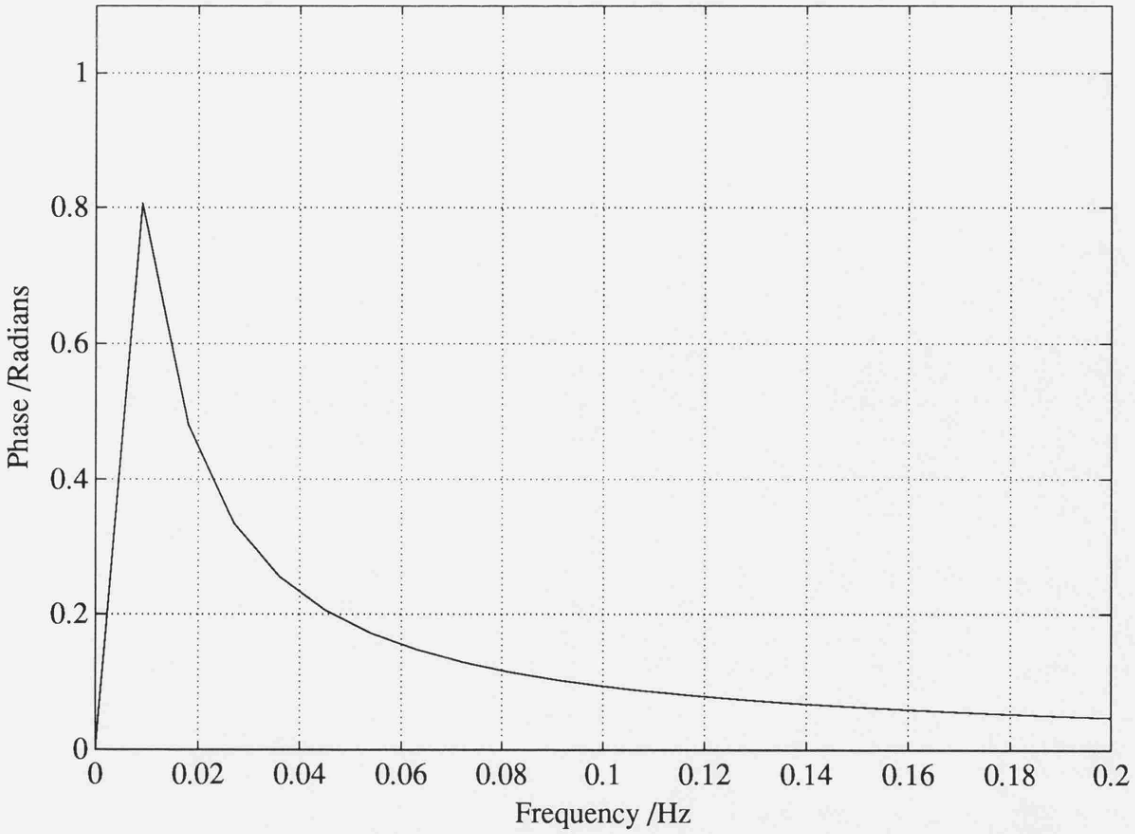

Figure [3.9a] Plot of gain versus frequency characteristics for the low-pass smoothing filter

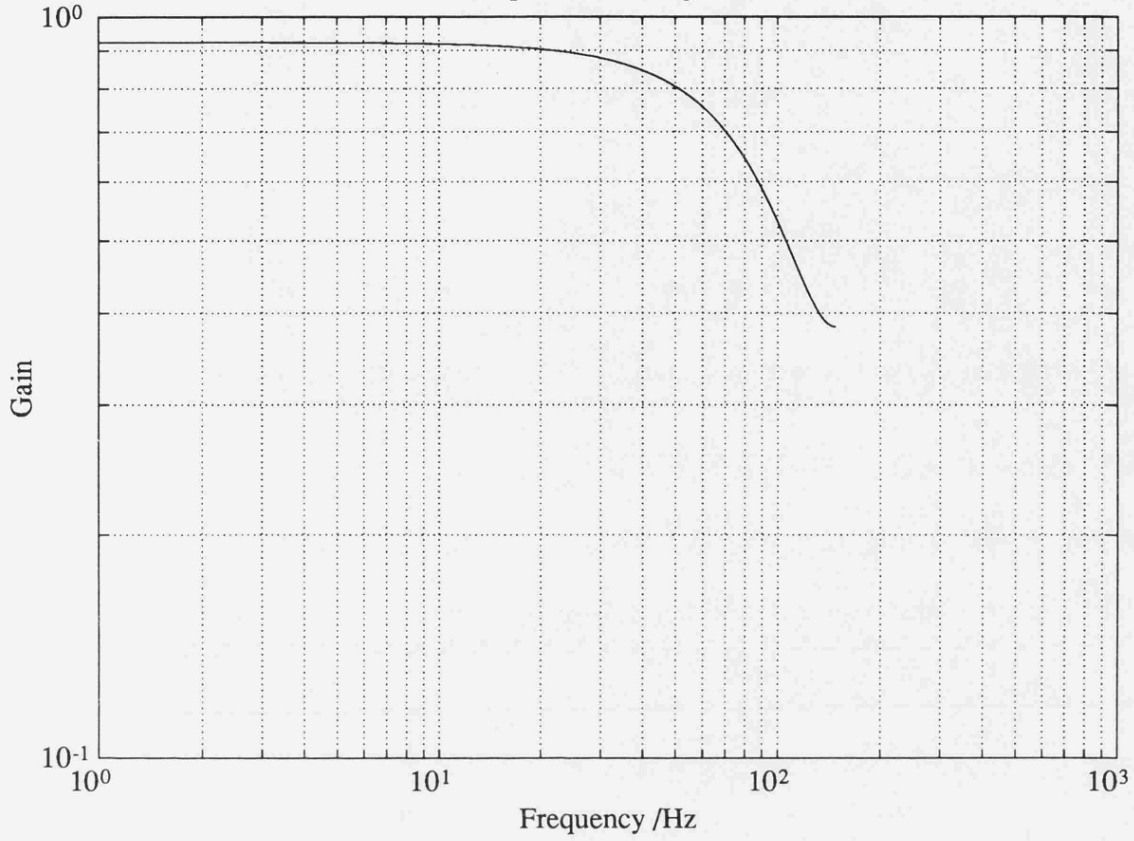

Figure [3.9b] Plot of phase versus frequency characteristics for the low-pass smoothing filter

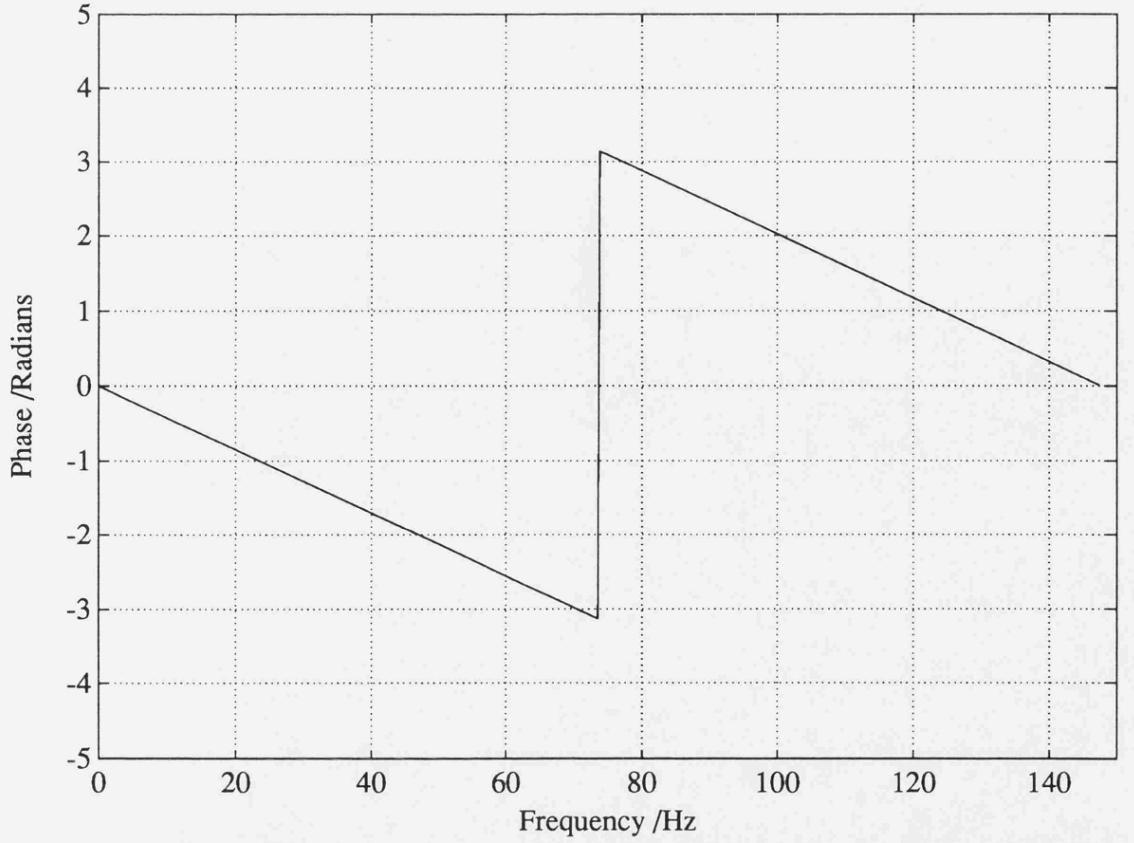

Figure [3.10a] An ECG Waveform using plain values extracted

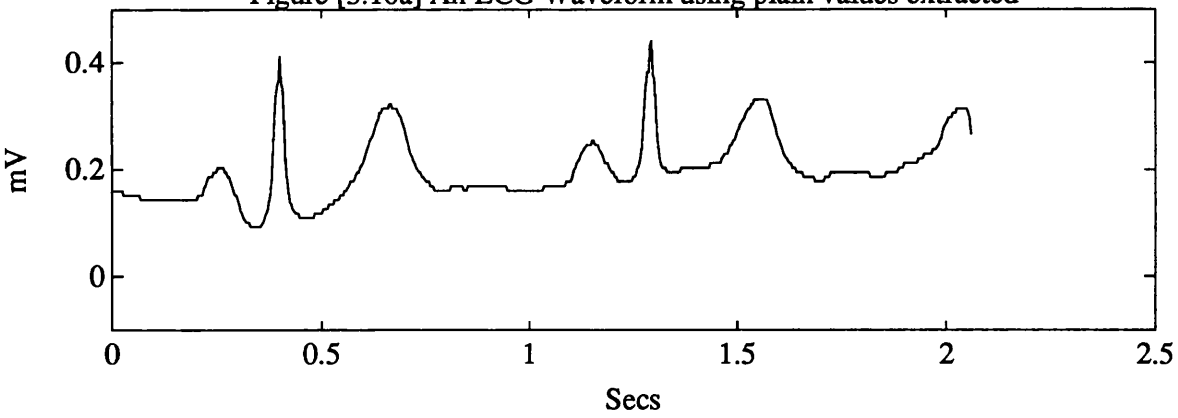

Figure [3.10b] The ECG Waveform after high-pass filtering

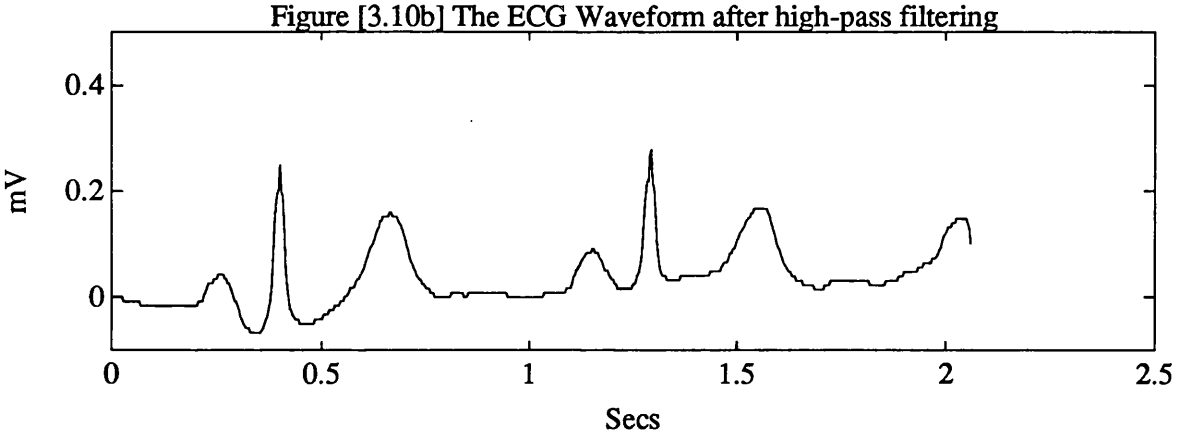

Figure [3.10c] The ECG Waveform after low-pass filtering with a filter whose cut-off frequency is 100Hz

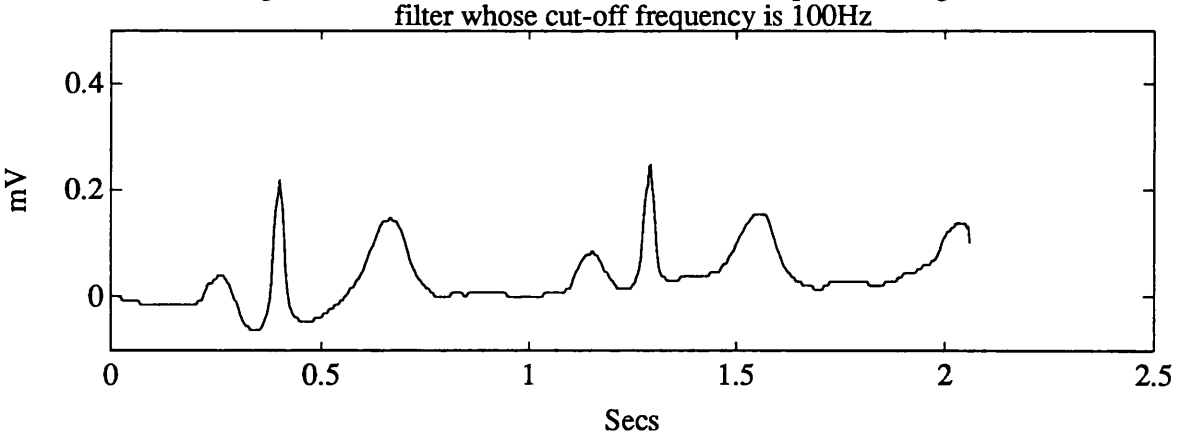

Figure [3.10d] The ECG Waveform after low-pass filtering with a filter whose cut-off frequency is 50Hz

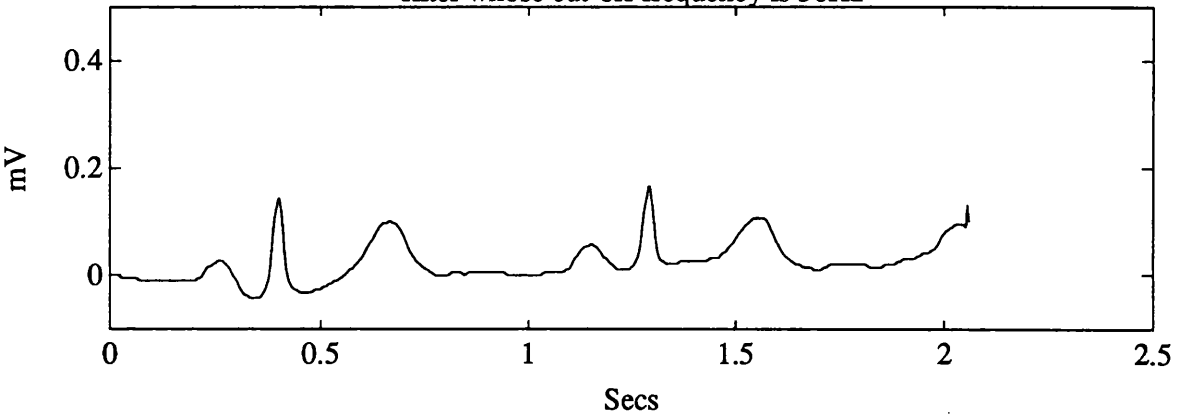

3.9 User-Interactive System

The *user-interactive system* was designed to display all 12 lead ECG signals of a patient, and allow user-interactive measurements on these waveforms using arrows or cursors to make measurements of interest, in our case QT and RR measurements. A custom built database was incorporated which keeps such information as:

- Patient Name
- Date of Birth
- Sex
- Centre ID
- Date of ECG
- Previous History
- Drugs Administered
- Diagnosis

Normal graphical function like zooming into a waveform or zooming out are included. Any measurements made on the waveform can be directly saved to a file. An advantage of the system is that the 'arrow' cursor used to make user-interactive measurements is made to follow the data values in the signal, and this allows for greater sensitivity in measurements as random human error associated with positioning of the cursor is reduced. Figure 3.11 shows a photograph of the screen when using the *user-interactive system.*

3.10 Comparison of other techniques for the recording and digitisation of hard-copy electrocardiograms

There are three popular techniques that are used in the extraction of data values from graphical records. One such technique makes use of digitising pads. Because it depends on the user for the selection of points, only certain points of interest in a signal are generally recorded. Digitising whole sets of signals is time consuming, and prone to errors due to user selection of data points.

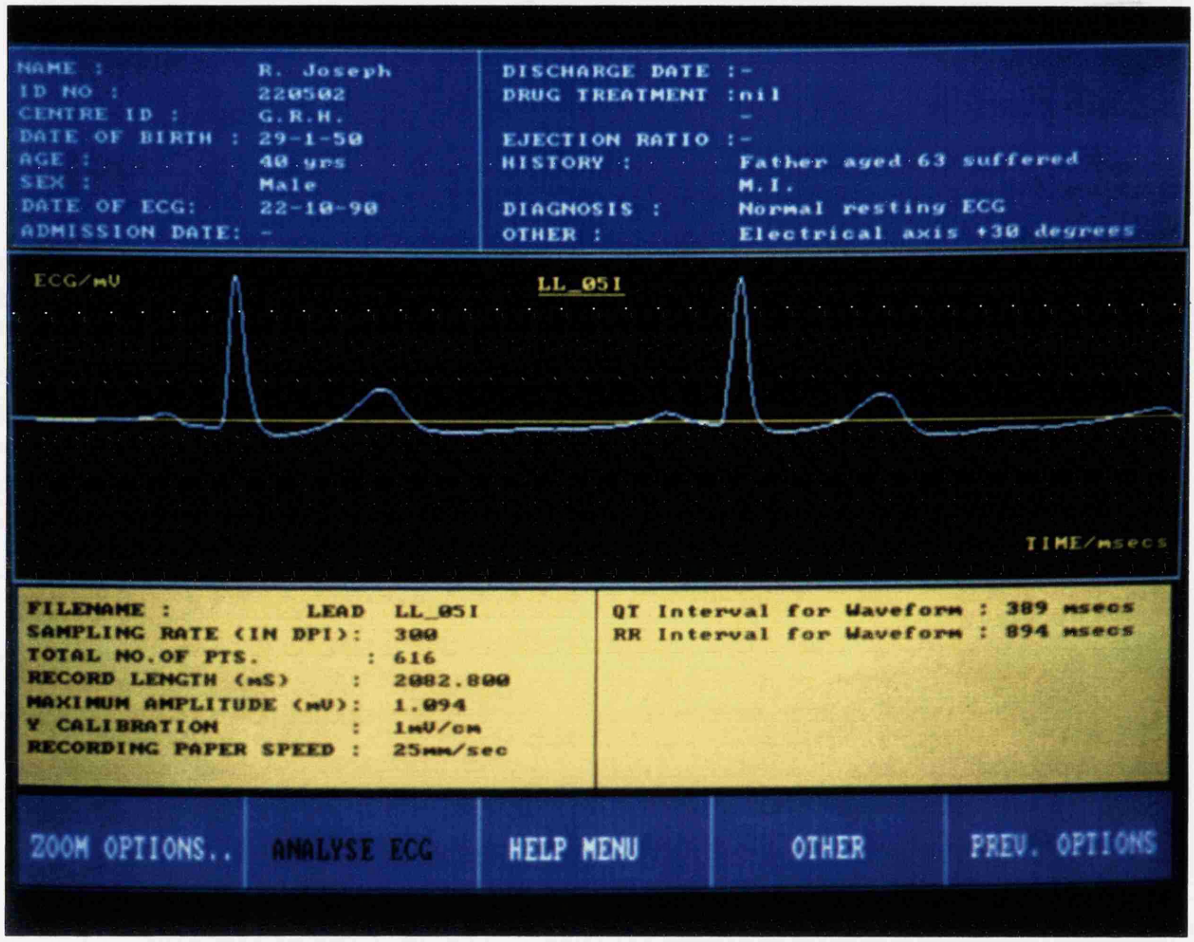

Figure [3.11] A typical computer screen display when using the *user-interactive system*

Another technique employed by S.Haenel (1982) involves the use of a high resolution TV camera to scan ECG records. The experimental resolution achieved by Haenel was 260 dots per inch (d.p.i.) and full chart length was processed by ten frames scanned in particular overlay and connected after curve extraction by a fast correlation method. Again, this is time consuming and the choice of a high resolution TV camera should be balanced against the hardware costs and the quality of the original recording. The main advantage of cameras compared to expensive optical scanners is that they can be used directly with non-printed images.

The third technique that has been proposed for the recovery of digital data from graphical records is by the use of a flatbed optical scanner. L.E.Widman and G.L.Freeman (1989) have developed a computer program that stores and processes image data stored in the Tagged Image File Format (TIFF). Their method firstly identifies the line representing the signal in the image using a line following algorithm. As the line representing the signal is a few pixels in width, two methods are then proposed for the extraction of data values relating to the value of the signal: the mid-point method and the slope following method. The first method, as mentioned by the authors, filters high frequencies in the signal which may be significant. Taking the mid-point of a segment to represent the true data point also distorts rapidly changing signals, and makes it more prone to noise artefacts.

The second method accepts the data point at the top of the line segment if the signal line is rising rapidly and at the bottom of the line segment when the line is falling rapidly, and in regions of the image where the slope is not above or below the established threshold, the value of the line is considered to be the mid-point of the segment. Whilst this method is intuitively pleasing, taking the mid-point alone does not always ensure that connectedness in the original image is maintained, especially if the region is prone to noise. At peak values, taking the end points seems sensible; however there should still be some consideration of the pen spread effect on the original recording.

3.11 Discussion

The technique proposed in this chapter does not require a search for the line representing the signal. Like Widman and Freeman, only one signal waveform is stored per file to be interpreted. A pre-processing stage has been incorporated to eliminate random noise and fill in the gaps in the image. Unlike Widman and Freeman, the new method proposes 'thinning' as a means of recovering the lineal structure of the waveforms recorded, before data values are extracted. The extraction of data values is performed by studying the two dimensional array containing the skeleton of the waveform. For relatively flat segments of the skeleton of the waveform the mid-point of the start and end value of the pixels is found for each row and this offset is assigned to be the digital value. For segments containing peaks the mid-point of the segment is not chosen: instead the pixel corresponding to the peak of the skeleton is chosen. Using the skeleton rather than the original image takes into account the spread of the pen on the original recording. The extraction and filtering procedures attempt to estimate the single best line that the pen would have followed in the original recording.

The algorithm converts '.PCX' files quickly and efficiently. Using a 286 AT machine a typical '.PCX' file of size 6.8KBytes takes 2 minutes and 22 seconds to pre-process for noise removal and skeletonising. This includes the time it takes to write the thinned image file comprising 1s and 0s to hard-disk. It takes a further 10 seconds for digital values to be extracted and filtered. Overall, if an experienced operator were to use the DISPERSE system on a single patient's 12 lead hard-copy ECG of reasonable quality, it would take approximately 1 hour to process completely starting from scanning. The time required increases if the original image quality is poor as additional manual editing using a graphics editor would be required.

3.12 Conclusions

The new method for the recovery of hard-copy waveform data, which encompasses pre-processing and thinning, has been implemented successfully. A full validation of the accuracy of the DISPERSE system is presented in Chapter 5. These techniques can be used to recover any waveforms recorded on paper. In the area of geology research,

seismological data is often stored on paper; similarly, in the monitoring of geographical data, graphs are maintained of rainfall etc. These techniques can also be used in an industrial environment where processes are monitored and signals are stored on paper. This system is already being used at the Leicester University Cardiology Department at Glenfield Hospital, in the recovery of the standard 12 lead ECG waveforms stored on paper.

Chapter 4 An algorithm which automatically determines characteristic points of the Electrocardiogram for the measurement of QT and RR intervals

4.1 Introduction

This chapter describes a new method for automatically determining the onset of the Q wave, the positions of the R and T wave peaks and T wave end of the electrocardiogram (ECG). It uses this information to calculate the QT and RR intervals. The method (henceforth known as the *automatic algorithm*) was applied to 337 electrocardiogram waveforms converted from standard 12 lead hard-copy electrocardiograms of 30 patients using the DISPERSE system. The chapter first outlines some of the common problems faced in the measurement of the QT interval of the electrocardiogram, and their solutions. Common methods for the determination of QRS onset, R wave peak, T wave peak and T wave end and some QT interval measurement algorithms are also reviewed briefly. The chapter then goes on to describe the new *automatic algorithm* and discusses the results obtained.

4.2 Common problems in the measurement of the QT interval

There are many forms of noise or interference which can contaminate the common electrocardiogram and render its interpretation difficult. The removal of these disturbances is one of the first steps before automatic processing or visual diagnosis can be carried out. Baseline wander (Figure 4.1a and c) for example is caused by respiration and movement of the body, and can seriously interfere with interpretation of the T wave and ST segment changes (D.J.Rowlands,1985). Other forms of interference are power-line interference and muscular activity. Baseline wander is of low frequency whilst the latter are of the mains or higher frequencies. There are many established filtering algorithms that can remove these sources of noise in real time or otherwise (P.Lynn 1970,1977; J.P. Marques de Sa, 1982; J.A.van Alste and T.Schilder, 1985;

Figure [4.1a] ECG signal 1 before the removal of baseline wander

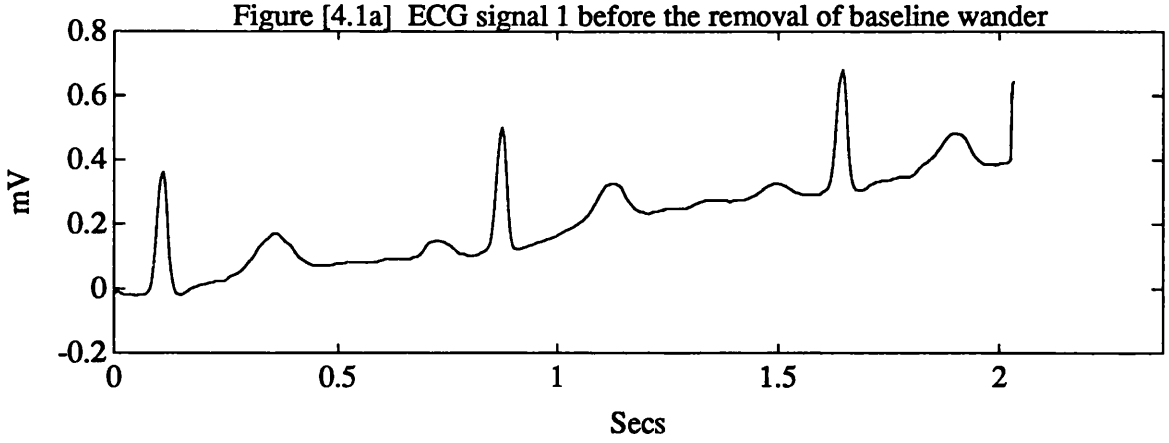

Figure [4.1b] ECG signal 1 after the removal of baseline wander

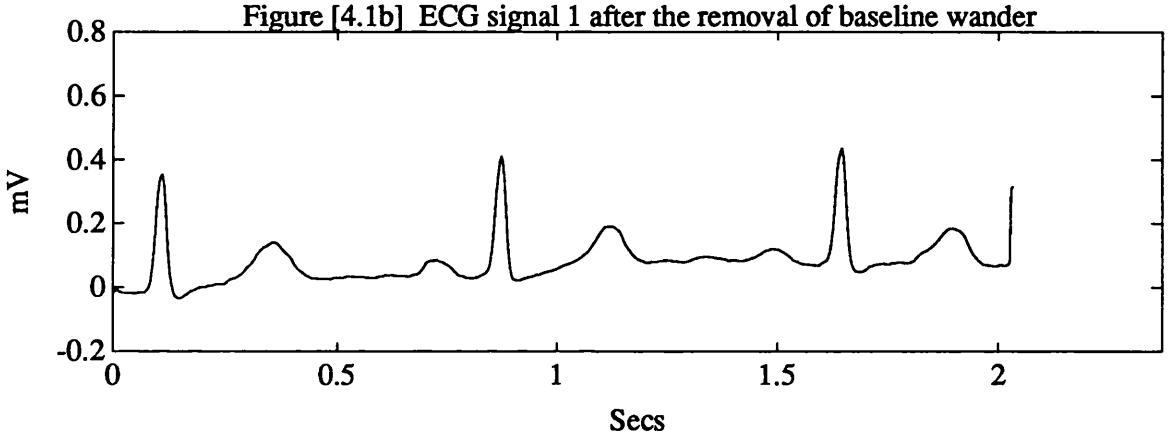

Figure [4.1c] ECG signal 2 before the removal of baseline wander

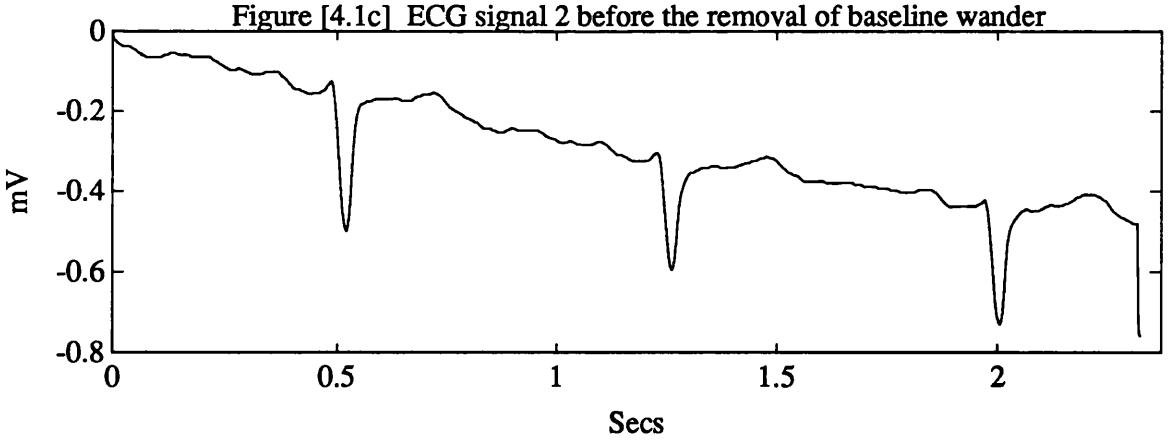

Figure [4.1d] ECG signal 2 after the removal of baseline wander

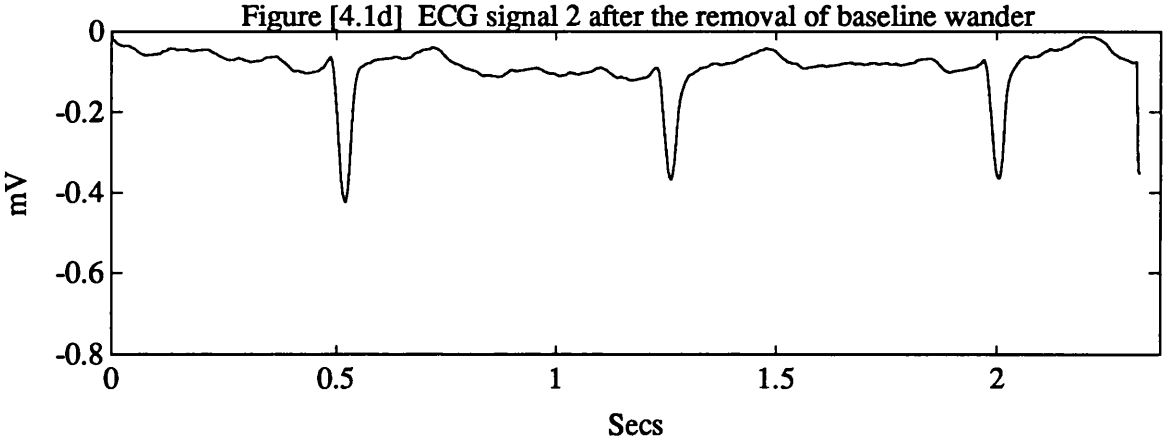

C.Cabo et al., 1988; R.Wariar, C.Eswaran, 1991). An important factor to maintain in the analysis of any time interval of the ECG, is the time relationship of the various waveforms in the ECG. This is achieved by using a linear phase filter.

The correct delineation of the QRS and T waves is also of prime importance in automated ECG analysis of the QT interval. The main problem in the measurement of the QT interval is the determination of the T wave end, due to its low frequency content (P.Laguna et al.,1990). Also, the many different morphologies of the T wave cause difficulty in defining standard criterion for the recognition of the T wave end. In many leads the T wave may not even present itself or if it does, presents itself as an indistinct blip (Figures 4.2a and 4.2b respectively). One main source of interference with the determination of the T wave end is the presence of the U wave (E.Lepeschkin and B.Surawitz, 1952). If the U wave is separated from the T wave by a distinct isoelectric interval, the two waves can be easily differentiated. If this is not the case, the U wave can be confused with the terminal portion of a notched or diphasic T wave.

Figures 4.3a, 4.3b and 4.3c show three examples of waveforms derived from our patient data set; the first is a biphasic T wave, the second is one of a U wave separated from a T wave and the third shows a T and U wave partially merged. Figure 4.4 (extracted from the paper by E.Lepeschkin and B.Surawitz, 1952) shows 16 different combinations of a positive, diphasic or negative T wave with a positive, diphasic or negative U wave. Whilst not being thoroughly understood, the U wave is thought to be the result of slow repolarisation of the intraventricular Purkinje conduction system.

4.3 Past methods for delineation of wave boundaries of the ECG and measurement of the QT interval

A few methods have been described in the literature for the delineation of wave boundaries. One of these methods uses templates with amplitude-time properties formed by a learning population of waveforms recognised beforehand by human observers (J.H.van Bemmel et al.,1973; J.L.Talmon and J.H.van Bemmel, 1983). Another method, called the maximum curvature criterion (MCC) method and based on the assumption that the curvature becomes locally maximum at the ECG complex boundaries, has been described by P.Trahanias and E.Skordalakis (1988) for the delineation of P, QRS and T

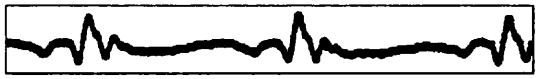

Figure [4.2a] An apparently non-existent T wave

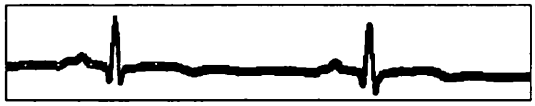

Figure [4.2b] A T wave presented as a poor blip

Figure [4.3a] A biphasic T wave

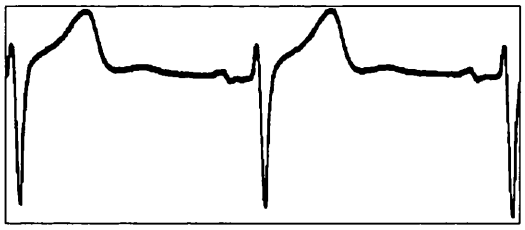

Figure [4.3b] A separate T and U wave

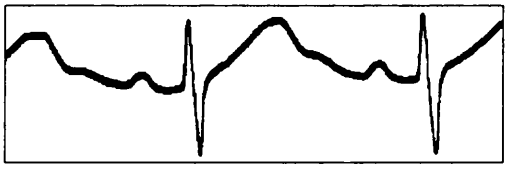

Figure [4.3c] A merged T and U wave

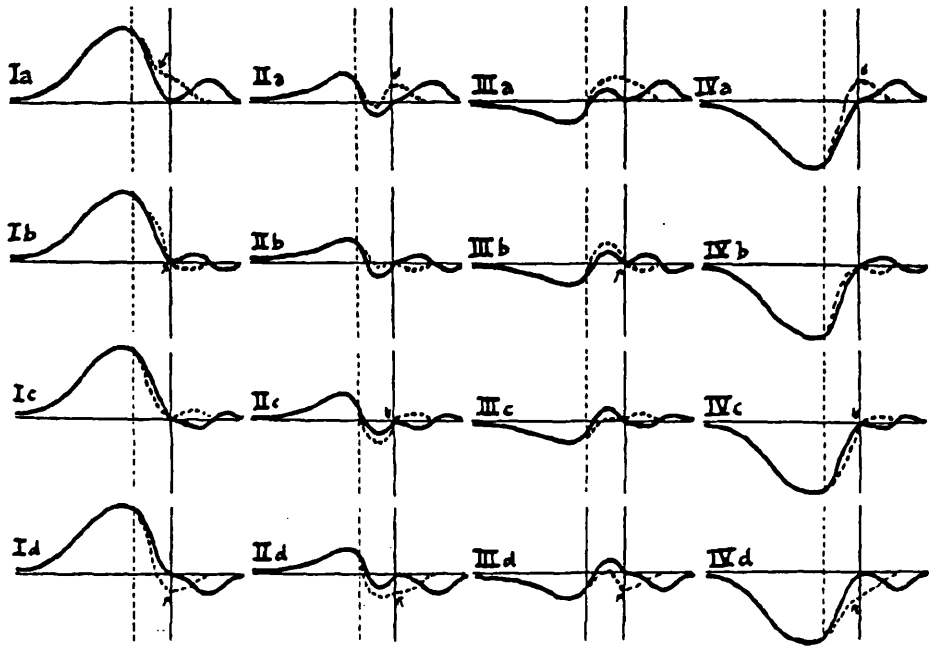

Figure [4.4] (extracted from E.Lepeschkin and B.Surawicz, 1952)

Schematic representation of the sixteen possible combinations between the T and U waves. Full curves: T and U separate. Dotted Curves: T and U waves partially merged. The vertical lines indicate the end of the T wave. The arrows point to the notch or kink between the T and U.

complexes; however the results were found not to be acceptable in all cases. F.Gritzali et al. (1988) proposed a method based on the 'length transformation' for the definition of onsets and offsets of P and T waves. This method employed suitable 'windows' and thresholds to delimit boundaries. However the authors were not satisfied that the best threshold parameter had been achieved.

Other methods for QRS and R wave detection involve the use of adaptive or variable thresholds. These are either compiled from different points of the whole ECG or determined from the first 2.5 seconds of ECG registration. P.Hamilton and W.Tompkins (1986) describe a method for QRS and R wave detection by creating a transformed signal. Their method attenuates noise using a bandpass filter and emphasises the QRS complex by differentiation, squaring and time averaging of the ECG. The location of the R point is obtained by detecting the location of the largest peak of the time averaged ECG.

Another common approach for accentuating the QRS complex and delimiting wave boundaries is to differentiate the ECG (S.J.Poppl, 1979; J.Wartak, 1970). One method of determination of the T wave end as described by J.O'Donnell et al., 1981 was to draw least square lines beginning beyond the peak of the T wave using a moving average method over 20 ms intervals, until the maximum negative slope (or positive slope for an inverted T wave) of the T wave was found. This least squares line was extrapolated to the iso-electric line and the intersect marked as the end of the T wave. This method was adapted from E.Lepeschkin and B.Surawitz, 1952.

Other algorithms have also been published which deal specifically with the problem of QT interval measurement in long term recordings. In 1982, Critelli et al. developed an algorithm which used a search window and detection threshold to define the end of the T wave. A database of $R\text{-}T_{peak}$ and $R\text{-}T_{end}$ intervals for different heart rates was used to position the search window for the detection of the T wave peak and estimate a starting point t_j for the search of the end of the T wave. Including t_j, four consecutive points were used to calculate the following expressions:

$$\sum_{i=j}^{j+3} t_j = S_j \quad \ldots\ldots\ldots\ldots\ldots\ldots\ldots\ldots\ldots\ldots \quad (4.1)$$

$$\sum_{i=j}^{j+3} | S_j - t_j | = S_j \quad \ldots\ldots\ldots\ldots\ldots\ldots\ldots\ldots\ldots\ldots \quad (4.2)$$

j=1,2,....N. N depends on the heart rate and is sufficiently large to include any possible pathological condition. This process was carried out using the first derivation (equation 4.1) until either an S_j was found with a value less than a given threshold or N was reached. If N was reached without finding the end of the T wave, the same search was performed using the second derivation (equation 4.2). If the search failed again, a value of T_{peak} - T_{end} was taken as the average of the last eight T_{peak} - T_{end} values calculated.

Algra et al., 1987 let the human interpreter serve as a model for the determination of the T wave end. He defined four requirements which were then translated to a computer algorithm. First, the end of the T wave was looked for within a narrow window after the QRS complex. An upper and lower limit of 0.36 and 0.55 times the previous RR interval were the limits of the search window. If no suitable previous RR interval was present (for example because the previous beat was labelled a premature ventricular complex (PVC) or noisy), the running RR average was used. Secondly, there had to be a transition of the terminating slope limb of the T wave to a flat segment. Therefore within the "end of T measurement window", a search was done for a flat segment of at least 40 ms duration. If such an interval was found, its beginning was used to mark the end of the T wave. Thirdly, noise should not interfere with interpretation; hence during noisy episodes with either baseline shift or high frequency noise, no flat segment would be found. Therefore the end of T measurement was suppressed. Fourthly, no end of T was to be determined in PVCs. Hence QRS complexes labelled PVC or noisy would be skipped during the end of T analysis.

In 1985 Pisani et al. developed two different algorithms for automatic determination of the end of the T wave which were based on four different morphologies of the 'normal' T wave. The first performed a 40 ms segment search from the end of the QRS complex for a signal with the same polarity with respect to the baseline. If such a segment existed, the first deflection or polarity change with respect to the baseline was denoted the T wave end. Conversely, if such a segment did not exist, the T wave end

definition was not performed. If the segment existed but no deflection was found, the end of the T wave would be taken as the theoretical end of the T wave, computed using the heart rate. The authors have not made clear which formula (for example, Bazett's or others) was used to calculate the theoretical T wave end. A second 40 ms segment search of signal at the same polarity, after the first deflection was then carried out; if it was not found, the end of the T wave would be fixed as before. If found, the point at which the signal changed polarity for the second time would denote the end of the T wave; else the end of the T wave remained fixed as before.

The second algorithm developed by Pisani was based on the assumption that the T wave, regardless of its morphology, must show a segment which leaves the baseline, reach a maximum or minimum, then return to the baseline. Starting from these considerations, the algorithm analysed the *absolute value of the derivative of the signal* in the segment starting from the S wave point to the theoretical T wave end, using a specified threshold.

If a time interval existed in this segment and if it was divided into 3 sections with the following properties:

- (i) a first section whose absolute derivative values were greater than or equal to the threshold
- (ii) a middle section whose absolute derivative values were less than or equal to the threshold
- (iii) a final section whose absolute derivative values were greater than or equal to the threshold

and in addition, if the time durations of the first two sections was greater than the last and if the duration of the three sections was greater than 50 ms, then the end of the T wave would be fixed as the last point in the final section.

A new threshold would then be calculated which followed the average value of the derivative in the segment starting from the S wave point to the theoretical T wave end (so that its value followed the slope changes of the T complex during the recording). If none of the above conditions were met, the procedure was repeated using the previous threshold lowered by 25%.

If the end of the T wave could still not be found using the methods above, the end of the T wave would be fixed as the last point in the segment starting from the S wave point to the theoretical T wave end where a change in sign of the derivative occurred.

More recently, Laguna et al., 1990 also developed a method for the detection and measurement of the QT interval. His algorithm used a transformed signal based on the first derivative of the ECG and the morphology of each T wave to decide its end. To obtain the transformed/processed signal the ECG was first low-pass differentiated for QRS detection and then put through a first-order low pass filter to avoid residual noise and intrinsic differentiation noise. QRS detection was then performed based on an adaptive threshold as described in Pan and Tompkins (1985) with modifications to increase processing speed and make Q and R wave peak definition easier.

Using the differentiated plus low-pass filtered signal $f(k)$, a threshold H_n was first defined at the n^{th} beat and QRS was detected as the first maximum or minimum whose absolute value was greater than H_n. As a first step, the highest positive or negative peak in the first 2s of the signal was detected and denoted as PK_1, the absolute value of the initial peak. Then $H_1 = 0.8 \times PK_1$ (80% of the peak value). If PK_n denoted the maximum absolute value of the QRS at the n^{th} beat in the processed signal, the next threshold, H_{n+1} was calculated as:

$$H_{n+1} = 0.8H_n + 0.2(0.8PK_n)$$

The R wave point, R_p was defined as the zero-crossing point between PK_n and the highest absolute value of the nearest peak foward or backward from PK_n. Next, the Q position, Q_p (not the QRS onset), was defined as the zero-crossing preceding the R_p position in the *differentiated* signal. The reason that the filtered ECG was not used was because the Q wave has high frequencies which would be attenuated in the low-pass filtered signal.

When the R_p - Q_p exceeded 80 ms, no Q wave was considered. This occurred when the Q wave had been detected as the R wave or when no Q wave was present. To detect the QRS onset a search backward was carried out from the Q_p (or R_p) point in the differentiated signal for a point Q_i (or R_i) of maximum slope in the ECG. With this point, a threshold was defined H_q (or H_r) as the value of the differentiated signal divided

by a constant K which was different depending on whether the Q wave was present or not. The QRS onset was then defined as the backward threshold H_q (or H_r) crossing point from Q_i (or R_i).

T wave end definition was performed on the differentiated plus low-pass filtered signal, $f(k)$ by defining a search window from the R position. Four different T wave morphologies were considered:- normal T wave (upwards-downwards), inverted T wave (downwards-upwards), only downwards T wave and only upwards T wave. The maximum and minimum values of the processed signal $f(k)$ were searched for in the defined window and depending on their amplitude and which order they appeared in, the four defined T wave morphologies were classified.

Once the highest slope point of the T wave (downwards or upwards) T_i was defined, a search for the T end point was conducted as follows:-

Let $f(T_i)$ denote the value of the processed signal at this point. This value has information on the T wave decay rate. The T wave end point was defined as a forward point from T_i where the downward (or upward in T-inverted) processed signal reached a threshold value H_t where

$$H_t = f(T_i)/K_t \quad . . . . . (4.3)$$

and K_t is an experimental value that has its best performance for $K_t = 2$.

The T wave-peak was defined as the first zero-crossing backwards from the T_i position in the processed signal $f(k)$.

4.3 Discussion

For QRS onset detection, Laguna et al. describe a good method adapted partly from Pan and Tompkins, 1985. It was thought to be efficient in calculation time and supposed to aid in baseline suppression.

For the detection of the T wave end, Critelli's method incorporates a useful feature in that the search area for the T wave end is dependent on the heart rate and this therefore takes into account possible pathologies. The first algorithm from Pisani analyses simple signal deflections from the baseline. However all the three algorithms of Pisani, Algra and Critelli do not take into account baseline drift, or other sources of interference. Pisani's second algorithm whilst giving better results than the first, still does not employ

thresholds that are related to the T wave morphology or decay rate. This is true of Critelli's and Algra's methods too. This is important as the decay rate is probably the single most important factor for deciding when the T wave returns to the baseline.

The approach adopted by Laguna which takes into account T wave decay rate is an important one. When the T wave has a higher or lower slope, H_t also has a higher or lower value to reach the end point. However Laguna still reported problems in wrong T-end definition due fundamentally to changes in the end of the T wave. Sequences with very low signal-to- noise ratios and where abnormal beats or ectopic beats were present also caused errors in the measurement of the QT interval.

This could be overcome to some extent if the algorithm incorporated some form of noise suppression. For example, when using a threshold method to detect the T wave end point, the method should not rely on just a single point crossing the threshold; the sum of a number of points may be better at suppressing false detections of T wave end caused by noise.

To avoid these problems, Laguna ensured that the highest and lowest QT intervals in each set of five beats were rejected as outliers and only three measurements were maintained. Also, if the QT value was higher or lower than 15% of the current average at the time, it was rejected. In Algra's analysis, from a total of 1587 QRST complexes, only approximately 836 QT measurements were obtained. This was because segments containing premature ventricular complexes were rejected and, in other cases, because the low amplitude of the terminal negative part of the T wave made it impossible to detect a sufficiently long, flat segment within the measurement window.

It is not clear whether validation or comparisons with manual measurement methods were made with Critelli's algorithm. Pisani, Algra and Laguna all performed comparisons with manual measurement and found their methods to compare well.

From these points, some ideas emerge about what is required of an algorithm to measure QT and RR intervals:

- It should be able to remove baseline wander.
- It should use information related to the heart rate.
- It should be simple and robust, differentiating between the lower frequency activity of the T wave and the higher frequency activity of the QRS complex easily.

- Any thresholds used for the detection of the T wave end should incorporate information about the T wave decay-rate as well as be insensitive to baseline fluctuations and other forms of noise.
- Clinical information pertaining to the time relationship of each wave in the ECG to the others should be incorporated and implemented as constraints of the algorithm.
- The use of threshold crossings using single points of the waveform should be avoided. The sum of a number of points should be used instead, to overcome noise artefacts being detected as significant points.

4.4 Development of the *automatic algorithm*

The *automatic algorithm* incorporates many stages. The first stage is the filtering of the ECG waveform for baseline removal. These ECG waveforms are then normalised and a transformed signal formed. The transformed signal is then studied to determine significant peaks that correspond to the QRS complex. This information is then used in the determination of the R wave peak, QRS onset, and T wave peak and end.

4.4.1 Filtering the ECG for base-line removal

The first step in the *automatic algorithm* is the removal of any baseline wander that might be present in the ECG signals recovered using the DISPERSE system. The filter used for this purpose has already been described in Chapter 3 where it was used to remove d.c. offset. It is known as a low pass differentiator (S.Usui and I.Amidror, 1982). In this case a cut off frequency was selected which would suppress low frequency noise caused by the electrode or body movement during recording. Too high a cut off frequency setting on the high pass filter can remove components of the ECG signal, so a trade off is required between noise suppression and signal distortion. The commonly used cut-off frequencies for baseline suppression are below 1 Hz at 0.7Hz or 0.65Hz. Frequencies above these will cause attenuation of the ECG waveform (Van Alste and T.Schilder, 1985; J.P.Marques de Sa, 1982). Figures 4.5a and b show the frequency characteristics of the low pass differentiator. A few different cut-off frequencies were experimented with. The cut-off frequency selected for the filter (the 3db point) was set at 0.3 Hz. The cut-off frequency was high enough to remove baseline wander effectively,

Figure [4.5a] Plot of gain versus frequency characteristics for the high-pass filter to remove baseline wander

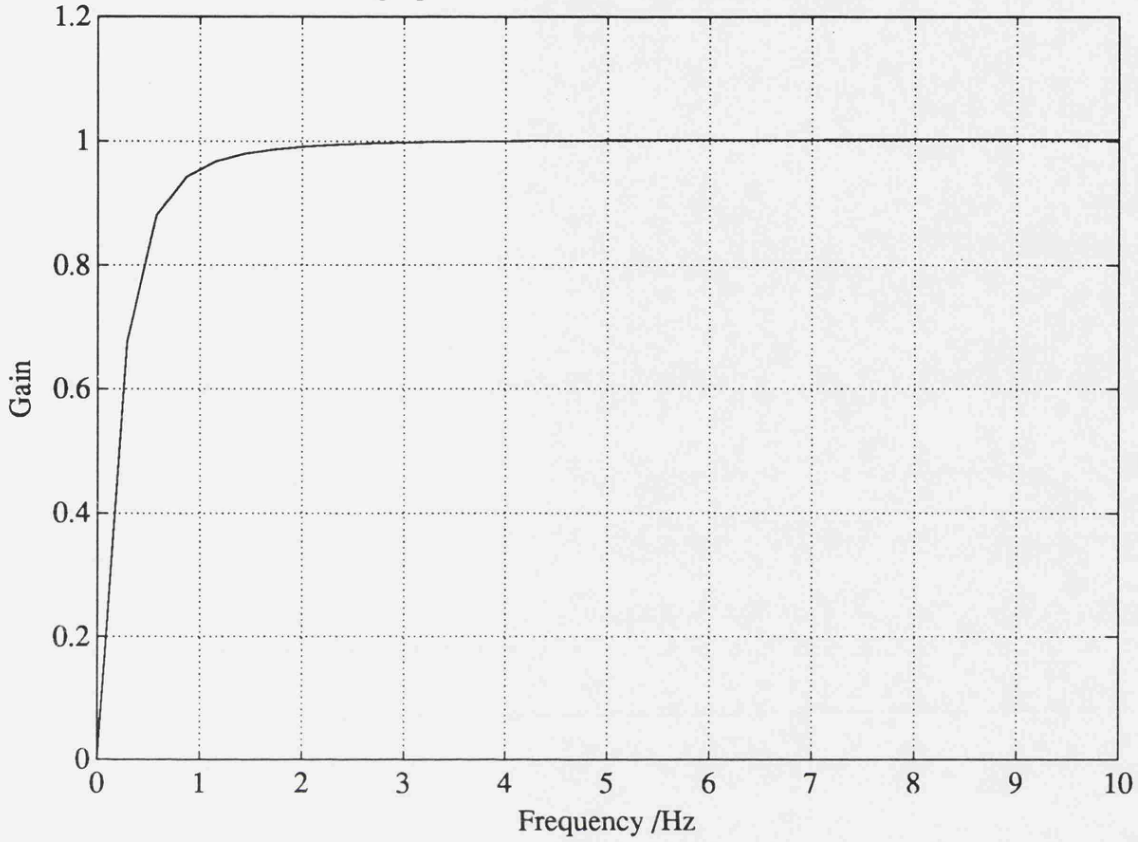

Figure [4.5b] Plot of phase versus frequency characteristics for the high-pass filter to remove baseline wander

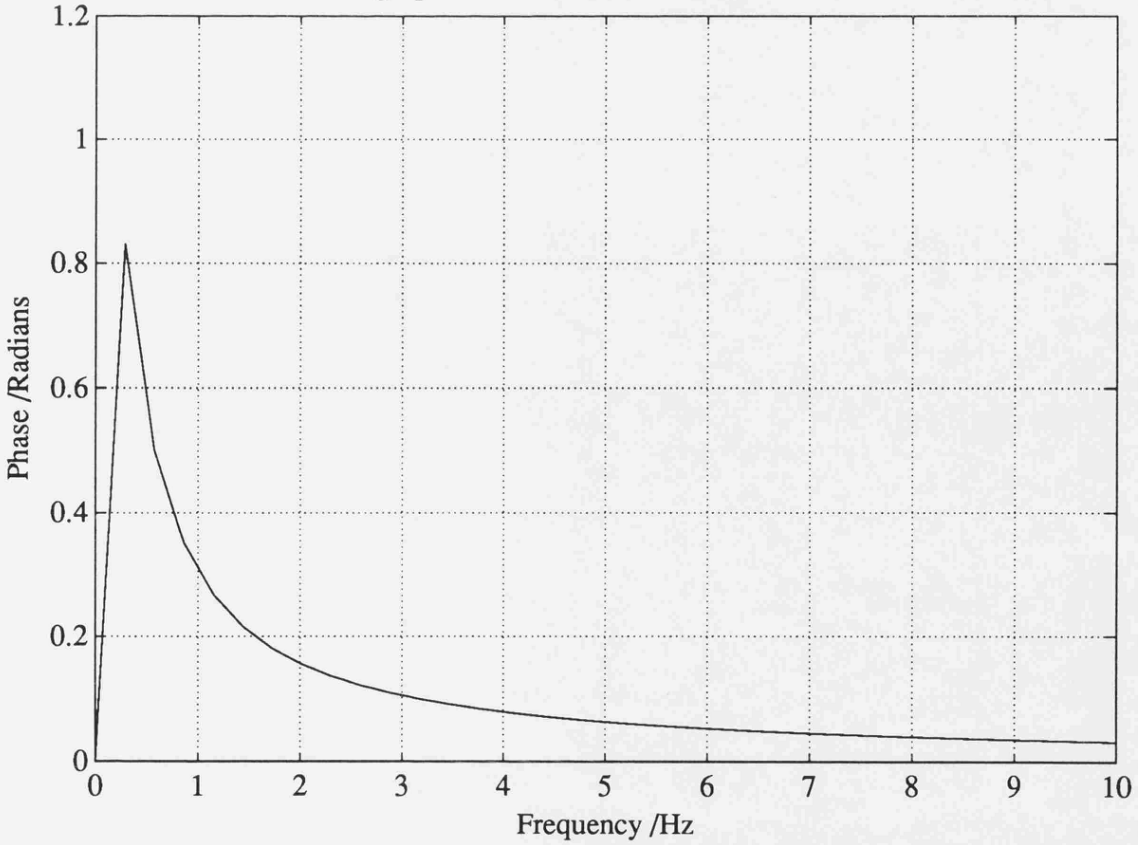

Figure [4.6a] Example of two ECG waveforms

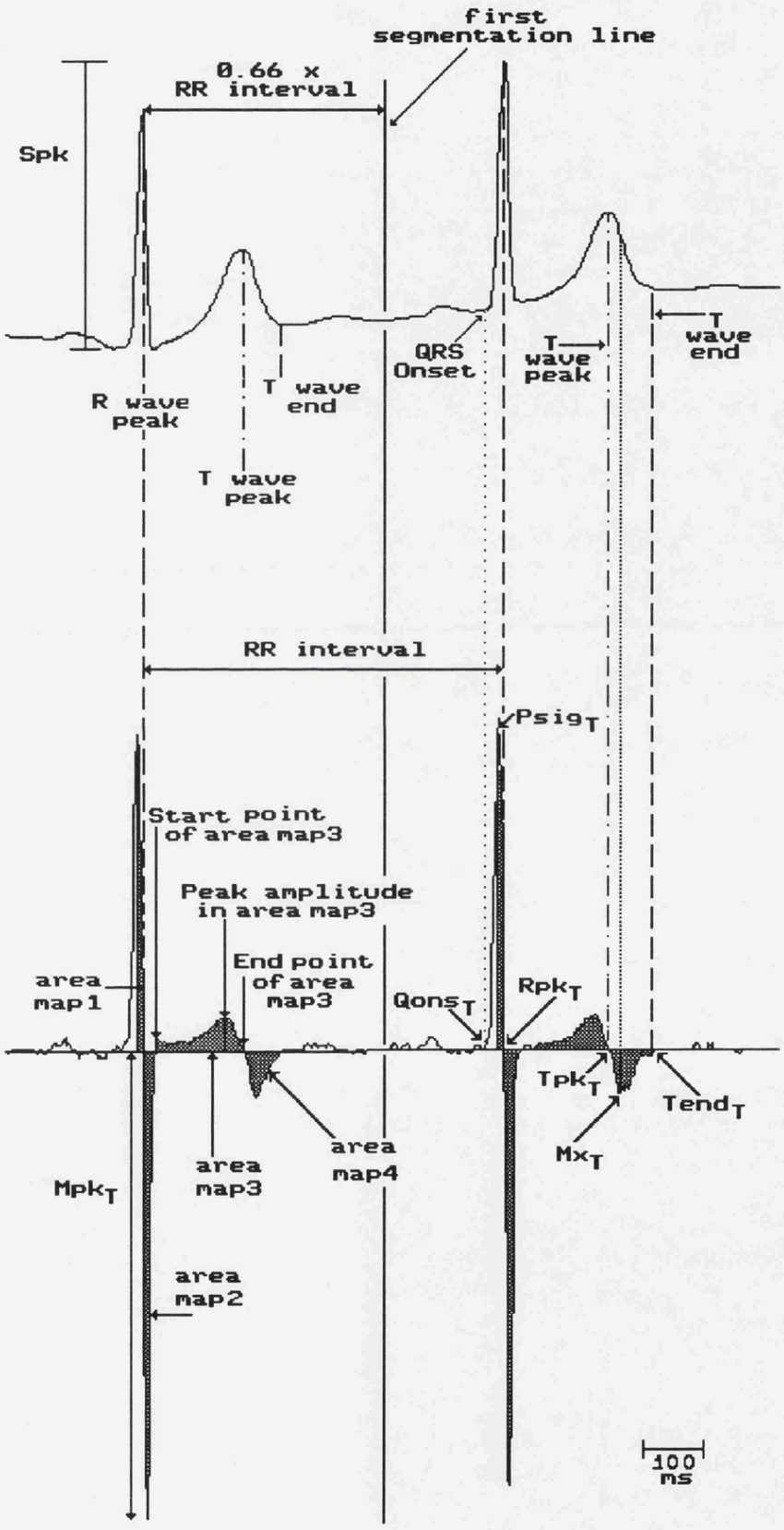

Figure [4.6b] T(n), the transformed ECG waveforms using the example above

Figure [4.7a] Plot of gain versus frequency for a 3-pt averaged differential filter

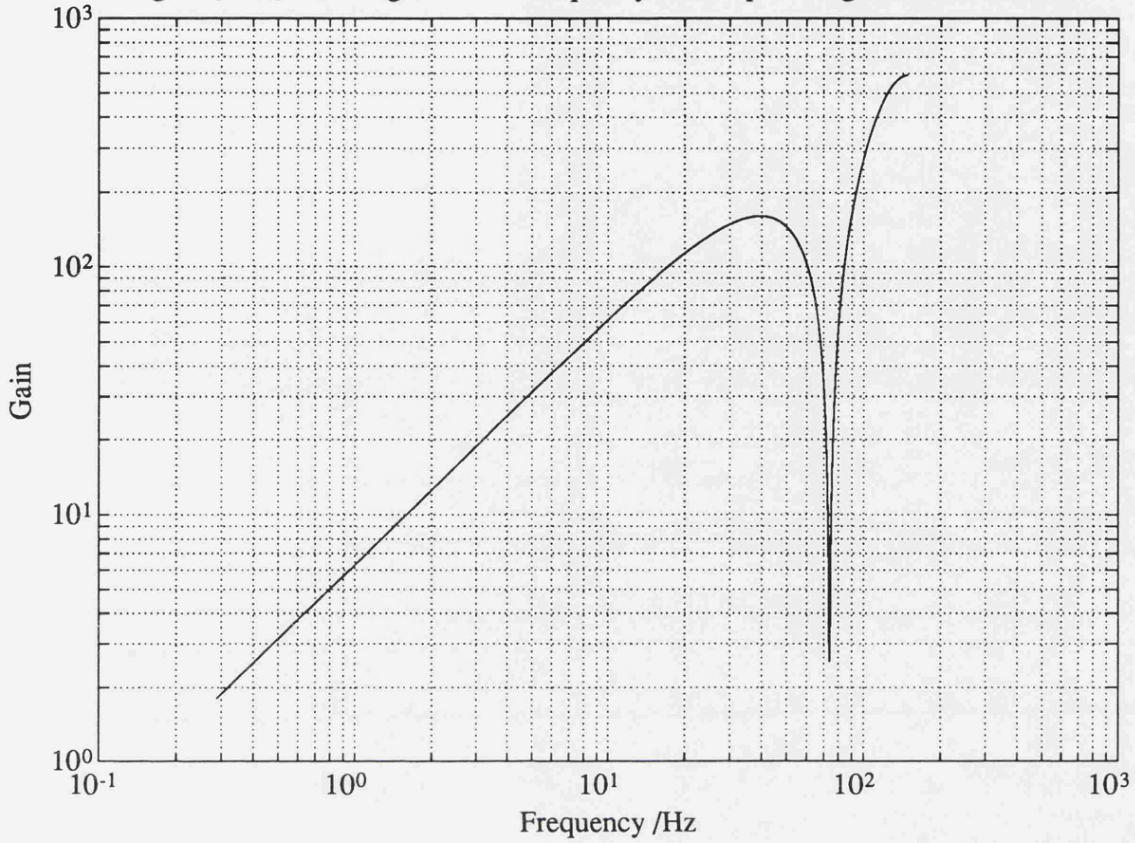

Figure [4.7b] Plot of phase versus frequency for a 3-pt averaged differential filter

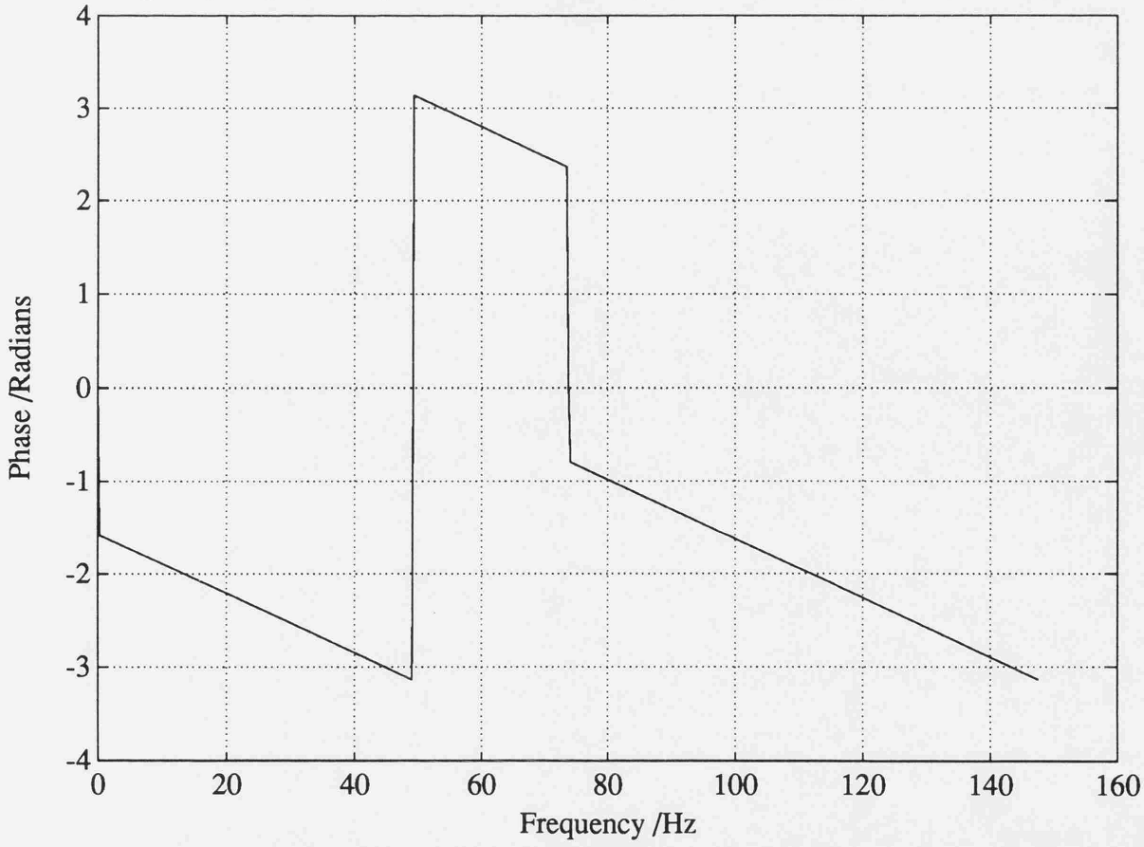

so a higher cut-off frequency was avoided. It is essential that the filter causes minimum phase distortion of the ECG signal, hence it has been designed with very small phase distortion within the passband. This is confirmed by visual inspection of Figures 4.5a and b.

4.4.2 Normalisation

The second step in the *automatic algorithm* is a normalisation of the ECG signals. The ECG amplitude and shape varies from lead to lead and from person to person. In order to use criteria which are valid for all sets of ECG data, it is necessary to normalise the magnitude of each ECG data set by the peak-to-peak variation in both positive or negative amplitudes. As a first step, S_{pk} is calculated where

$$S_{pk} = P_{pk} + N_{pk} \quad \ldots\ldots\ldots\ldots\ldots\ldots\ldots\ldots\ldots\ldots \quad (4.4)$$

and P_{pk} and N_{pk} correspond to the maximum absolute positive and negative values in an ECG signal, relative to the first point in the ECG data set which has a value of 0 (see Figure 4.6a). The ECG data set is then normalised by dividing all the data points in the set by S_{pk} and multiplying by a standard value (in this case 0.5) (Equation 4.5). This normalisation stage overcomes the need to set a threshold manually in the later stages of analysis.

$$(ECG_{normal})i = \frac{(ECG_{raw})i}{S_{pk}} \times 0.5 \quad \ldots\ldots\ldots\ldots\ldots\ldots\ldots\ldots \quad (4.5)$$

where i refers to the i^{th} sample in the data set.

4.4.3 Formation of the Transformed Signal

The next stage in the *automatic algorithm* involves the formation of a transformed signal (denoted by $T(n)$) which is used for the detection of characteristic points (R wave point, QRS onset etc.) of the ECG. The transformed signal is the 3-point averaged differential of the ECG. This is a different transformation from that used by J.Pan and W.Tompkins, or P.Laguna. The aim of this transformation is to emphasise the QRS complex of the ECG as well as to suppress very low frequency noise artefacts, whilst maintaining information on the T wave, itself a wave of low frequency. Figures 4.7a and b show clearly the frequency and phase characteristics of the 3-pt averaged differential.

filter. The transformation has the characteristics of a finite impulse response filter and has linear phase characteristics. This means that no distortion of the time relationship of the waveforms occurs.

The equation characterising the transform is given by:

$$H(z) = -\frac{0.5}{ts}z^0 + \frac{0.5}{ts}z^{-1} - \frac{0.5}{ts}z^{-2} + \frac{0.5}{ts}z^{-3} \quad \ldots\ldots\ldots\ldots\ldots\ldots \quad (4.6)$$

where *ts* is the sampling interval. Figure 4.6a and b show two ECG waveforms from a patient data set and their corresponding transformed signals.

4.4.4 Determination of QRS activity to yield search positions for R wave, QRS onset and T wave end determination.

The aim of this stage of the *automatic algorithm* is to gain information on QRS activity which can then be used for the :

- (i) detection of the R wave position
- (ii) detection of the onset position of QRS activity
- (iii) determination of the T wave end

As the QRS complex contains the high frequencies present in the ECG waveform, the transformed signal which is the 3-pt averaged differential of the original ECG signal accentuates this activity and produces peaks which correspond to the maximum slopes of the upward and downward going limbs of the QRS peaks in the original ECG waveform.

By studying all the peaks on the transformed signal *T(n)*, denoted as 'significant peaks', information can be derived about where the search for the R wave peak, QRS onset and T wave end should commence. Figure 4.6b shows two significant peaks in the transformed signal for each QRS complex. However, this is not the only combination of peaks that may occur on the transformed signal due to QRS activity on the original signal. In some instances 3 or 4 significant peaks may be recorded on the transformed signal per QRS complex.

In the first stage of the *automatic algorithm*, the significant peaks on the transformed signal *T(n)* which correspond to QRS activity on the original signal, are determined. A new approach to determining these significant peaks is proposed which initially uses a low threshold based on the maximum absolute peak value in the transformed signal. All

values of $T(n)$ that exceed this threshold are determined. These values are studied and a new higher threshold, called a *peak discrimination factor* is then used to determine values of $T(n)$ which arise from the peak regions of the transformed signal. These values (called *possible peak values*) are separated and classified into consecutive groups of single signed values. The absolute maximum or minimum value in each group then gives the absolute peak values in $T(n)$. This method does not rely on a single high value of threshold which may cause some peaks in $T(n)$ to go undetected.

The first step is to determine the maximum absolute peak value in $T(n)$ and denote this as Mpk_T (see Figure 4.6b). An uppper and lower threshold limit UL and LL are set as 1 and 0.4 and a search is then carried out in the transformed signal $T(n)$ for values of $T(n)$ which meet the following conditions:

$$LL < \left| \frac{T(n)_i}{Mpk_T} \right| < UL \quad \ldots\ldots\ldots\ldots\ldots\ldots\ldots\ldots\ldots\ldots \quad (4.7)$$

where i refers to the i^{th} point in the transformed ECG data set. This is repeated until all points in the transformed signal have been traversed. All the points meeting these conditions are used to determine the *possible peak values* that correspond to QRS activity.

An example of values that meet the conditions in (4.7) is given here:

$\frac{T(n)_i}{Mpk_T}$	*Position in T(n)*
0.448718	102
0.605128	103
0.676923	104
0.638462	105
0.525641	106
-0.515385	109
-0.874359	110
-0.823077	112
-0.420513	113
0.45641	341
0.612821	342
0.692308	343
0.664103	344
0.55641	345
0.420513	346
-0.584615	349
-0.917949	350
-0.930769	351
-0.735897	352
0.469231	584

0.587179	585
0.635897	586
0.574359	587
0.464103	588
-0.446154	591
-0.782051	592
-0.971795	593
-0.810256	594
-0.446154	595

A peak *discrimination factor* which is used to detect *possible peak values* that arise from the peak regions of $T(n)$ is then calculated by finding the *median* value of the absolute values from the first column, in this case: 0.6051. The median was selected for the following reason. The upper and lower limits of 1 and 0.4 caused $T(n)$ values of varying amplitudes to be detected in the previous stage. The median value of these amplitudes provides a peak *discrimination factor* which is based on the predominant value of the amplitudes of $T(n)$ detected. So if the values of $T(n)$ are predominantly large, the peak *discrimination factor* is large and if the values of $T(n)$ are small, the peak *discrimination factor* selected is small. The median was found to give good performance.

All values of $T(n)$ are now studied again and if the relationship:

$$\left| \frac{T(n)_i}{MpkT} \right| > discrimination\ factor \quad \ldots\ldots\ldots\ldots\ldots\ldots\ldots\ldots (4.8)$$

is satisfied then these values are stored as points coming from the peak regions of $T(n)$ and their values and positions on the transformed signal $T(n)$ noted :

possible peak values from $T(n)$: 17.3533 at position 103
possible peak values from $T(n)$: 19.4122 at position 104
possible peak values from $T(n)$: 18.3092 at position 105
possible peak values from $T(n)$: -25.074 at position 110
possible peak values from $T(n)$: -28.677 at position 111
possible peak values from $T(n)$: -23.6034 at position 112
possible peak values from $T(n)$: 17.5739 at position 342
possible peak values from $T(n)$: 19.8533 at position 343
possible peak values from $T(n)$: 19.0445 at position 344
possible peak values from $T(n)$: -26.3241 at position 350
possible peak values from $T(n)$: -26.6917 at position 351
possible peak values from $T(n)$: -21.1034 at position 352
possible peak values from $T(n)$: 18.2357 at position 586
possible peak values from $T(n)$: -22.4269 at position 592
possible peak values from $T(n)$: -27.8682 at position 593
possible peak values from $T(n)$: -23.2358 at position 594

Note that if all the *possible peak values* detected by the algorithm are positive only or negative only, (this is not correct because the transformed signal corresponding to a set of QRS peaks will always have *at least two peaks of opposite sign*) the algorithm repeats the procedure using a lower *discrimination factor* of 0.25. If the possible peaks detected are still all of a single sign the algorithm keeps repeating itself using a *discriminating factor* of 0.02 less than the previous until it detects *possible peak values* of different signs. These values are then stored and their positions on the transformed signal *T(n)* noted.

In the next stage of the processing, each of the *possible peak values* detected of *T(n)* are grouped according to their sign. For example, values from position 103-105 are classified as coming from one group and values from position 110-112 are classified as coming from another group. The absolute maximum values in each group are found and these correspond to the peaks of *T(n)*. Two conditions are used to ensure that consecutive and similarly signed values are classified as coming from the same group : they must lie within 30 ms or 10 points (for this example) of each other (this is based on the QRS morphology on the original signal) and their signs must be the same.

Peak values of *T(n)* detected are:

19.4122 -28.6770 19.8533 -26.6917 18.2357 -27.8682 . . . . . (4.9)

and their corresponding positions are:

104 111 343 351 586 593

The first two values of *T(n)* are the result of QRS activity from the first complex in the original signal, as can be seen from their close positions 104 and 111, the second two values are from the second QRS complex and the third set of two values come from the third QRS complex. Each time a positive or negative peak is detected in *T(n)*, a counter is incremented to keep a count of the number of positive and negative peaks detected. Similarly a counter is also maintained for the number of waveforms in the lead. To calculate this, the positions of the *T(n)* peaks above are used. If the difference between two consecutive peaks is greater than 170 ms, or 50 points (for this example), then it is deemed that there has been a transition from one QRS complex to another on the original waveform and the number of waveforms is incremented. The purpose in keeping a count of the number of positive and negative peaks and the number of

waveforms is so that this information can be used to check that the *discrimination factor* from the previous stage detected the correct number of *T(n)* peaks. This is studied by using the following relationship:

If

$$\frac{\textit{the number of positive peaks}}{\textit{the number of waveforms}} \quad \ldots\ldots\ldots\ldots\ldots\ldots \quad (4.10)$$

is a whole number

and

If

$$\frac{\textit{the number of negative peaks}}{\textit{the number of waveforms}} \quad \ldots\ldots\ldots\ldots\ldots\ldots \quad (4.11)$$

is a whole number

then the *discrimination factor* detected the correct number of peaks. This is based on the reasoning that the pattern of *T(n)* peaks reflecting QRS activity repeats itself and therefore, the same number of positive and negative peaks in *T(n)* should always be a multiple of the number of waveforms detected. For the numbers obtained in the example above, the number of positive and negative peaks is three and the number of waveforms detected using the conditions described is also three. Using conditions 4.10 and 4.11, whole numbers are obtained. Therefore the *discrimination factor* of 0.6051 can be said to have correctly detected the number of QRS peaks.

If a whole number was not obtained, this might be for two possible reasons. One reason is that the *discrimination factor* was too low in the presence of some high energy P or T waves on the original signal which caused spurious peaks in *T(n)* to be detected. The other reason is that the *discrimination factor*, Mpk_T, was too high because the maximum absolute peak in the lead may have been too high relative to the remaining peaks, thus causing some peaks of slightly lower magnitude to go undetected. In these cases, the user is warned and given the option of lowering or increasing the *discrimination factor*. If however, the QRS complex changed morphology from one waveform to another, the pattern of positive or negative peaks in *T(n)* will not necessarily be a multiple of the number of waveforms detected, and the algorithm may terminate there. The latter case was found to be rare: only one in the total of 337 studied.

Now that peaks in *T(n)* corresponding to QRS activity on the original signal have been determined this information can be used to determine the search positions for the detection of the R wave, QRS onset and T wave end.

For the determination of the T wave end search start position, the position of the last positive peak in *T(n)* pertaining to each QRS complex of activity on the original signal is required. Using the data from (4.9), this is given by:

The positive peak values (due to each QRS complex on the original signal) in *T(n)* are :

19.4122 19.8533 18.2357 . . . . . (4.12)

and their corresponding positions are :

104 343 586

For the determination of the R wave and the QRS onset search start position, the first significant peak of *T(n)* pertaining to each QRS complex is determined, and its position and sign noted. The first peak in *T(n)* due to the *next* QRS cluster is detected using the conditions that it must be the same sign as the first peak in *T(n)* from the first QRS cluster and that it must be at least 170 ms from the last peak in *T(n)* of the *current* QRS cluster. The result obtained from (4.9) are the same in this case as that for the positive peaks of *T(n)*:

The first significant peak values in *T(n)* are:

19.4122 19.8533 18.2357 . . . . . (4.13)

and their corresponding positions are :

104 343 586

4.4.5 R Wave Peak Detection and Data Segmentation

Using *T(n)*, the R wave position is found by searching foward from the first significant peak (see 4.12) due to each QRS cluster until a zero-crossing point Rpk_T is reached i.e. a point where the value of *T(n)* changes sign (see Figure 4.6b). This point corresponds to the R wave peak. The first significant peak in the transformed signal normally corresponds to a dominant R wave. It must be noted however that in some QRS morphologies, a dominant Q or S wave may be detected as the R-wave, especially

if the R wave is very small or non-existent. As the R wave is used in the estimation of heart rate, and as in normal beats, the Q-Q, R-R or S-S intervals have the same value, any of these intervals can be used to estimate the heart rate.

These R wave peaks are then used to calculate the RR interval and to segment the data into individual waveforms comprising P, QRS and T waves, in a manner which is dependent on heart rate. These are then referred to as *ECG data segments*. For the first ECG *segment* the starting point is the same as the overall ECG data set. The ending point of each *segment* is a function of its RR interval. For each *segment*, starting from its R peak, the segmentation position is found by:

$$(\text{Segmentation position})_i = \text{position}(\text{Rpeak})_i + 0.66 \times [\text{position}(\text{Rpeak})_{i+1} - \text{position}(\text{Rpeak})_i] \quad . \; . \; . \; . \; . \; . \; . \; . \quad (4.14)$$

where i = 1,2, 3....[number of waveforms - 1].

This is because physiologically the onset of the next wave of atrial-ventricular depolarisation-repolarisation depends on the previous heart-rate. The segmentation procedure therefore takes into account ECG data showing varying heart rates. The starting point of the second data *segment* is one point foward from the ending point of the previous data *segment*.

The approach for RR detection (which depends on the detection of QRS activity) proposed here is different from the approach by Laguna et al. who first used an adaptive threshold to detect the first absolute maximum or minimum peak in their processed signal (due to a QRS complex) greater than a specified threshold. The initial threshold they specify is 0.8 x the absolute maximum or minimum peak detected in the first 2 seconds of the signal. The peak that they first detect from a QRS complex may not be its first significant peak and hence a search foward and backward from their peak is necessary to select the correct crossing point for the detection of the R wave.

4.4.6 Determination of QRS onset

For the determination of the onset of the QRS complex, Qons$_T$ (or R wave onset if the Q wave is absent), using the first significant peak (see 4.13) in *T(n)*, Psig$_T$, (see Figure 4.6b) a threshold Hq$_{ons}$ is calculated where:

$$Hq_{ons} = 0.09 \times | Psig_T | \quad \ldots\ldots\ldots\ldots\ldots\ldots (4.15)$$

A search backwards is carried out using a three point window. The values of the transformed signal *T(n)* in the window are summed. When the sum of the three point window is less than Hq$_{ons}$, the first point in the window is selected as the Q wave onset point on the transformed signal, Qons$_T$ i.e.:

$$Qons_T = T(p\text{-}2) \text{ if } \sum_{n=p}^{n=p-2} T(n) < Hq_{ons} \quad \ldots\ldots\ldots\ldots\ldots\ldots (4.16)$$

Taking into account that the transformed signal has a filter delay of 1 point relative to the original ECG waveform, the position of the Q wave onset on the original waveform can be found easily. When very small Q waves exist or when no Q wave is present but the R wave is very small, a multiplication factor of 0.06 is used. This is because when searching backward in the presence of a small R or Q wave the change looked for is a return to baseline. A tighter transition threshold is required to ensure that the small peak values that correspond to Q waves and R waves are not detected instead, since on the transformed signal, these peaks have very low values.

4.4.7 Determination of T wave Peak and End

For each *segment* of ECG comprising a single waveform, using the transformed signal and starting from the position of the last positive peak in *T(n)* due to a QRS complex (see 4.12), a search foward is carried out for consecutive areas of significant activity known as 'area maps'. Each area map is characterised by:

- (i) consecutive values of *T(n)* of a single sign
- (ii) its *value* which is given by the sum of all the amplitudes of the *T(n)* points in the map
- (iii) the start and end position of the map on the transformed signal *T(n)*

- (iv) the position of the maximum absolute amplitude value of *T(n)* in the area map

Note that the amplitudes of *T(n)* are all relative to 0. These area maps are used to *decide the areas of activity that correspond to the T wave in the original signal.* Figure 4.6b illustrates some area maps on the transformed signal, *T(n)*. Area maps 1 and 2 correspond to the first QRS complex. Area maps 3 (whose characteristic properties are marked out) and 4 correspond to the T wave area on the original signal. The values of *T(n)* that correspond to area maps 1 and 2 are given here:

Area map 1:
T(n) value at position 104 : 19.4122
T(n) value at position 105 : 18.3092
T(n) value at position 106 : 15.0738
T(n) value at position 107 : 10.5884

Value of area map = sum of all amplitudes is: 63.3836
Start position of area map is 104
End position of area map is 107
Maximum absolute amplitude in the area map : 19.4122
Position of maximum absolute amplitude in the area map : 104

Area map 2:
T(n) value at position 108 : -0.735309
T(n) value at position 109 : -14.7797
T(n) value at position 110 : -25.074
T(n) value at position 111 : -28.677
T(n) value at position 112 : -23.6034
T(n) value at position 113 : -12.0591
T(n) value at position 114 : -4.33832
T(n) value at position 115 : -1.25002

Value of area map = sum of all amplitudes is: -110.517
Start position of area map is 108
End position of area map is 115
Maximum absolute amplitude in the area map : -28.6770
Position of maximum absolute amplitude in the area map : 111

A list is therefore built of all positive, negative and zero area maps from the position of the last positive peak (due to a QRS complex) until the end of that ECG segment. For the first transformed ECG waveform segment shown in Figure 4.6b, the list of all the area maps is as follows:

Area Map Number	Value	Start Position	End Position	Max Absolute amplitude	Position of Max Absolute amplitude
1	63.3836	104	107	19.4122	104
2	-110.517	108	115	-28.6770	111
3	49.3392	116	174	1.9118	161
4	-37.2066	175	201	-2.9412	183
5	0	202	214	---	---
6	3.82361	215	234	0.2941	217
7	0	235	244	---	---
8	-1.02943	245	249	-0.2941	247
9	0	250	252	----	---
10	-0.882371	253	257	-0.2941	256
11	0	258	264	------	---

4.4.7.1 Search for T wave areas

Starting from the last area map stored in an ECG segment and using a set of heuristic rules a search is carried out to derive *combinations of area maps which correspond to the T wave area on the original signal.* Only area maps whose *values* are greater than 1.8 are considered, as consecutive sums of *T(n)* less than 1.8 are due to small noise fluctuations and hence are non-significant. Hence area maps of zero values are not considered.

The search for the two area maps which correspond to the T wave area on the original signal is carried out as follows. Three separate lists of area maps are maintained: (i) a list of all maps whose absolute areas are greater than 1.8 called the *non-noise area maps list.*

For the first transformed ECG waveform segment shown in Figure 4.6b, the non-noise area maps list is:

Area Map Number	Value	Start Position	End Position	Max Absolute amplitude	Position of Max Absolute amplitude
1	63.3836	104	107	19.4122	104
2	-110.517	108	115	-28.6770	111
3	49.3392	116	174	1.9118	161
4	-37.2066	175	201	-2.9412	183
6	3.82361	215	234	0.2941	217

(ii) a list derived from the 'non-noise area maps list' of all maps whose absolute values are greater than 20% of the absolute value of the first area map (called the **reference area map**). This list is called the *best area maps list.*

For the first transformed ECG waveform segment shown in Figure 4.6b, the best area maps list is:

Area Map Number	Value	Start Position	End Position	Max Absolute amplitude	Position of Max Absolute amplitude
1	63.3836	104	107	19.4122	104
2	-110.517	108	115	-28.6770	111
3	49.3392	116	174	1.9118	161
4	-37.2066	175	201	-2.9412	183

(iii) a list derived from the 'non-noise area maps list' of all maps whose absolute values are less than 20% of the absolute value of the first area map (called the **reference area map**). This list is called the *remaining area maps list.*

For the first transformed ECG waveform segment shown in Figure 4.6b, the remaining area maps list is:

Area Map Number	Value	Start Position	End Position	Max Absolute amplitude	Position of Max Absolute amplitude
6	3.82361	215	234	0.2941	217

The following search is then carried out in the order shown using the three lists:

The non-noise area maps list is considered first to eliminate rare combinations of area maps:-

If there are only 3 area maps in the non-noise area maps list the second and third area maps are put forward as corresponding to the T wave area on the original signal. These are then checked against the conditions outlined in the next section for area maps to correspond to T wave activity. If no suitable area map(s) are found, the area maps on the best area maps list are then considered.

The best area maps list

The best area maps list contains area maps that are clearly not insignificant when compared to the reference area map. The two following conditions should be met when studying the best area maps list for combinations of area maps corresponding to the T wave on the original signal:

- (a) the number of area maps in the list should be greater than two.
- (b) the second and third area maps in the list should have an absolute value less than 100

Starting from the last area map in the list, a search is carried out backwards from the bottom of the list for 2 consecutive area maps that meet the conditions outlined in the section below for area maps to correspond to T wave activity. The search for consecutive

area maps in the list is known as the first neighbour search. For example, area maps 2 and 4 are the first neighbours of area map 3, whilst area map 1 is the second neighbour of area map 3. The search using the best area maps list is terminated when it encounters the second area map in the list and no suitable area maps have been found. Alternative searches are carried out.

Best area maps list and Non-noise area maps list

If no area maps have been found suitable, a different search is carried out, still using the best area maps list, but this time studying both the *first and second neighbours* (on either side) of area maps from the best area maps list, but using the non-noise area maps list. As before, the search is carried out backwards from the bottom of the list. This allows for greater flexibility and area maps of different but significant activity to be considered as coming from the T wave area. If suitable area maps are found, these are then checked against the conditions outlined in the next section for area maps to correspond to T wave activity.

Remaining area maps list

If still no area maps have been found suitable, the highest absolute value of area map in the remaining area maps list is found and its *first and second neighbours* on either side of it on the best area maps list are studied to find suitable area maps that might correspond to the T wave area. If found suitable, these are then checked against the conditions outlined in the next section for area maps to correspond to T wave activity.

Miscellaneous conditions

If still no area maps have been found suitable, this implies that the search for two area maps corresponding to T wave activity is not feasible, due to differing configurations of the T wave on the original signal. A different search is then carried out for the last possible area map in an ECG segment that could correspond to the T wave area. *As generally the T wave area should correspond to more than 1 area map, the area map selected would correspond to the later half of the T wave.* The following search is carried out.

(a) if there are only 2 area maps in the non-noise area maps list, the second area map is put foward as corresponding to the later half of the T wave area. This area map is then checked using the conditions outlined in the section below for an area map to correspond to the later half of a T wave.

(b) If the best area maps list contains more than three area maps, the last area map in the list is proposed as coming from the T wave area provided that either of these conditions are met, i.e.,

its value is greater than 8 and less than 40.0 and the second and third area maps in the list of best areas are less than 100

or

its value is greater than 8 and the second and third areas in the list of best areas are greater than 100

and

it meets the conditions outlined in the next section for a single area map to correspond to the later half of the T wave

If no area map is still found as corresponding to the later half of the T wave, the search carries on:

(c) If the best area maps list contains three area maps, the third area map in the list is proposed as coming from the T wave area subject to it meeting the conditions outlined in the next section for a single area map to correspond to the later half of the T wave.

If still no area map is found as corresponding to the later half of the T wave, the search carries on, using area maps on the non-noise areas list:

(d) Starting from the last area map in the list, a search is carried out backwards from the bottom of the list for any *single area map* that is less than 70 and that meets the conditions outlined in the next section for a single area map to correspond to the later half of the T wave.

If still no area map is found as corresponding to the later half of the T wave, the search carries on using the best area maps list:

(e) if only two area maps exist in the list of best areas and if they are the same as the first two area maps on the non-noise area maps list, and if the number of area maps in the non-noise area maps list is 3,4,5,6,7,8, or 9, then the area map selected as

corresponding to the later half of the T wave activity is the second area map, provided it meets the conditions outlined in the section for a single area map to correspond to the later half of the T wave.

4.4.7.2 Conditions for T wave area determination

The following conditions must be met for any area maps to be considered as coming from the T wave area. The first three conditions are only applied when *two area maps* are detected as coming from the T wave area. The others are applied if *two or one area map* is detected as coming from the T wave or its later half respectively.

If two area maps are detected as coming from the T wave area on the original signal:

- (i) they must have *values* of opposite signs (See area map 3 and 4 in Figure 4.6b).
- (ii) their values must be comparable to each other, i.e. even with conditions of the area maps corresponding to the Q or S waves merging with the first area map that corresponds to the T wave area. For example, if it is imagined that area map 2 on Figure 4.6b was before area map 1 which is then next to area map3, and also if the area between area map 1 and 3 never reached zero, the resultant area map of 1 and 3 which is detected as the first area map that comes from the T wave area, would be larger than area map 4. Therefore, the following relationship must be satisfied:

$$|\textit{smaller area map}| \times 2.1 > |\textit{larger area map}| \quad \ldots\ldots\ldots \quad (4.17)$$

  The factor of 2.1 was selected after studying the relationship between typical area maps corresponding to the T wave area using a training set of 50 ECG waveforms.
- (iii) the range *between* the area map positions i.e. the difference in position between the end position of the first area map and the start position of the second area map should not be greater than 90 ms. If this condition is not met it means that *both* the area maps cannot correspond to the T wave area on the original signal and other neighbouring area maps must be studied using the search rules described earlier.

If two or one maps are detected as coming from the T wave area or the later half of the T wave respectively on the original signal:

- (iv) The value of the first area map (calculated from the last positive peak onwards for each QRS cluster in *T(n)* in each ECG data segment is known as a 'reference area map', as mentioned previously. If two area maps are detected as coming from the T wave area then each of these area maps should have a value which is not insignificant to the reference area map value. The following conditions should be met:

$$\left|\frac{first\ area\ map}{reference\ area\ map}\right| > 0.1 \quad \ldots\ldots\ldots\ldots\ldots\ldots\ldots (4.18)$$

$$\left|\frac{second\ area\ map}{reference\ area\ map}\right| > 0.1 \quad \ldots\ldots\ldots\ldots\ldots\ldots\ldots (4.19)$$

  if only one of the area maps has been discriminated as coming from the T wave area then it corresponds to the later half of the T wave activity on the original signal. Similarly then,

$$\left|\frac{area\ map\ corresponding to\ the\ later\ half\ of\ the\ T\ wave}{reference\ area\ map}\right| > 0.1 \quad \ldots (4.20)$$

  Again, a factor of 0.1 was selected after studying the relationship between area maps corresponding to the T wave area and their corresponding reference area maps using a training set of 50 ECG waveforms.

- (v) the range between the start position of the reference area map and the end position of the second area map (or single area map chosen) should be less than 30 ms. This is because the range corresponds to the R-T or S-T range, which is not greater than 30 ms.

For the first transformed ECG waveform segment shown in Figure 4.6b, the area maps found to correspond to the T wave area are:

area map 4: 49.3392
area map 6: -37.2066

Both these area maps have satisfied all the threshold and range requirements as specified by the conditions (i) to (v) above.

4.4.7.3 T wave end determination

Once the appropriate area maps or map corresponding to the T wave area or later half of T wave area respectively, have been found, the T wave end can be determined.

To determine the T wave end, the maximum absolute amplitude point of the later of the 2 area maps selected, Mx_T (see Figure 4.6b) is used to calculate a threshold Ht_{end} for the determination of the T wave end point where:

$$Ht_{end} = 0.25 \times Mx_T \quad \ldots\ldots\ldots\ldots\ldots\ldots \quad (4.21)$$

(If only one area is selected, it corresponds to the later half of the T wave area and its corresponding maximum absolute amplitude point is used).

Mx_T contains information about the slope of the T wave as it corresponds to the slope of the T wave limb returning to baseline on the original signal (See Figure 4.6b). If Mx_T comes from an area map of negative value, then it corresponds to the point of maximum slope on the downward limb of an upright original ECG waveform. If instead, Mx_T comes from an area map of positive value, then it corresponds to the point of maximum slope on the upward limb of an inverted original ECG waveform.

A search foward from the position of Mx_T is carried out using a 3 point moving window. The values of the transformed signals in the window are summed and when their value falls below Ht_{end}, the last point in the window is selected as the T wave end point on the transformed signal, $Tend_T$ i.e.:

$$Tend_T = T(p+2) \quad \text{if} \quad \sum_{n=p}^{n=p+2} T(n) < Ht_{end} \quad \ldots\ldots\ldots\ldots\ldots \quad (4.22)$$

Taking into account that the transformed signal has a filter delay of 1 point relative to the original ECG waveform, the position of the T wave end on the original waveform is established easily.

For a well defined (high slope value) T wave, Mx_T is a large value. Ht_{end} will then be a larger value. Similarly for a poorer defined T wave (i.e. one of low slope), Mx_T is a small value. Ht_{end} will therefore be small too. Like Laguna et al., the threshold value is therefore adapted to take into account T waves of different slope. However unlike Laguna et al., a 3 point window was used. This suppresses false detections of T wave end due to spurious noise and provides a reliable estimate of the T wave end based on a gradual return to baseline.

4.4.7.4 T wave peak determination

The T wave peak can be found by locating the point between the two maps on the transformed signal, Tpk_T (see Figure 4.6b). However the first area map may not always show an immediate transition to the second area map; there may exist small fluctuations due to noise in between. To establish the true T wave peak then, the interval between the two area maps selected as corresponding to the T wave area is studied. The range between the end position of the first area map and the start position of the second area map is mapped back onto the original waveform and studied.

If the second area map is *positive*, it implies that the T wave is inverted and a minimum value is searched for in the range specified on the original ECG waveform. If on the other hand, the second area map is *negative*, this implies that the T wave was upright and so, a maximum value would be searched for in the range specified on the original ECG waveform. If only one area map is selected as coming from the T wave area, it corresponds to the later half of the T wave area and so the area map before this on the non-noise area maps list is used as the first area map.

4.4.7.5 Discussion

The advantage of using the maps is that all possible combinations of significant activity after the QRS complex can be studied. Map *values* also give a better idea of overall activity as their value corresponds to the sum of similar activity over a number of points. In Laguna's approach peak values of their processed signal were searched for in a specified search window to determine the maximum or minimum absolute peak value from which the T wave end search is started. This approach works well if there is little

noise and significant peaks that correspond to the T wave slope in their processed signal. If this is not the case, the area map may be better as it gives more information about the overall activity of the region of the T wave, so even if the T wave was not well defined, the area maps corresponding to it can still be found. The maximum amplitude in a map also gives information on where the search for the T wave end should begin. By using the maps, the limits of the search for the T wave peak are also easily specified.

4.5 Other features

Some other features have been incorporated into the *automatic algorithm.* An important feature of the software developed is that it allows the user to manually override the selection of any of the characteristics points described above. So for example, if the user does not think a particular T wave end definition is correct, he or she can amend the measurement by moving a cursor (using a mouse) on a graphical screen. Different limits of the original signal to be analysed can also be specified so the analysis of 1 or 2 noisy waveforms in an otherwise normal quality data set can be avoided. Direct saving of QT and RR intervals measured by the *automatic algorithm* to a file has also been incorporated. Overall, the *automatic algorithm* incorporates a user-friendly interface. Appendix F shows the overall structure diagrams for the *automatic algorithm.*

4.6 Results

The *automatic algorithm* was found to be very successful, even though in some cases, it was not able to recognise *all* the characteristic points in some of the ECGs.Table 4.1 shows the success rate for the detection of RR peaks, QRS onset, T wave peak and T wave end by the *automatic algorithm* expressed as a percentage of the 337 ECGs it analysed. As can be seen the *automatic algorithm* shows the lowest success rate (which is still greater than 90%) when measuring the T wave end at 92.9% success rate. This is particularly due to poorly defined T waves of low slope and very slow returns to baseline. R wave point detection and QRS onset detection share the highest success rate at 98.8%. The T wave peak which by nature of the method developed depended on clear definition of the T wave end area maps had a success rate similar but slightly higher than

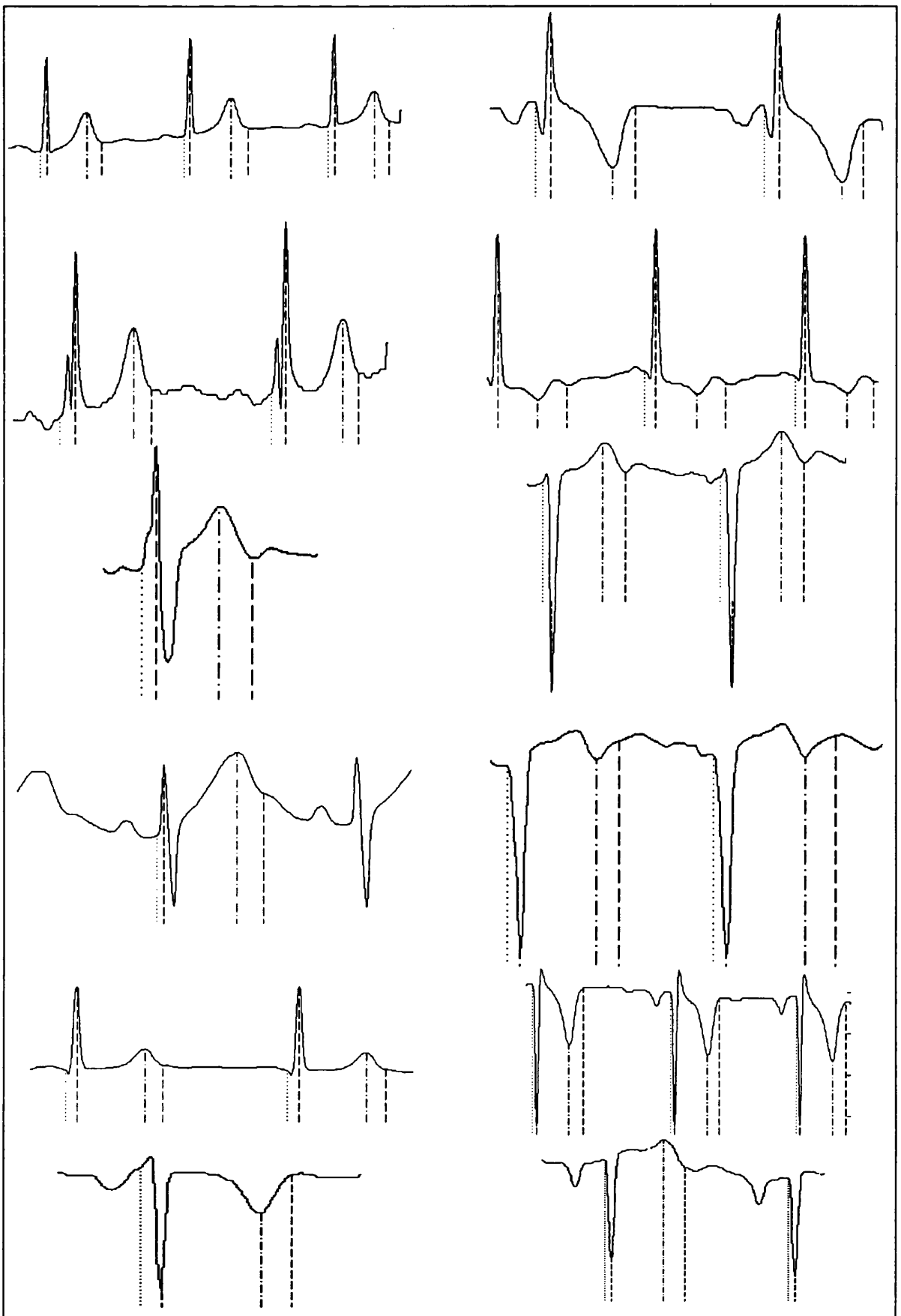

Figure 4.8 Some examples of ECGs from our data set and their characteristic points as detected by the *automatic algorithm*

the *automatic algorithm* for a variety of ECGs from our data set. The time it takes to analyse a lead of ECG which normally comprises three waveforms is approximately 2-3 minutes.

Table 4.1 Results obtained using the *automatic algorithm*

Characteristic points detected by the *automatic algorithm*	Success rate of measurement of the characteristic points of the ECGs by the *automatic algorithm*
R wave peaks	98.8%
T wave end	92.9%
T wave peak	93.2%
QRS onset	98.8%

4.7 Conclusions

The *automatic algorithm* was successful in removing baseline wander, segmenting data and determining characteristic points of the ECG. A full validation of the technique which includes comparison of measurements performed manually, using the *user-interactive algorithm* and *automatic algorithm* is presented in Chapter 5. Chapter 6 discusses the clinical results of QT dispersion obtained with the *automatic algorithm* and its effectiveness is compared to the *user-interactive algorithm.* The algorithm has been found to give comparable performance to an experienced cardiologist and is already in use at the Department of Cardiology at Glenfield General Hospital.

Chapter 5 System Validation

5.1 Introduction

This chapter describes all the different tests carried out to validate the overall system as described in Chapter 2. Validating such a system would give greater understanding of its accuracy and usefulness, by testing its different characteristics. The process of system validation can be subdivided according to the main components of the system (see Chapter 2):

a) the digitising algorithms also known as the DISPERSE system

b) the user-interactive algorithm

c) the automatic algorithm

d) the user (normally doctors)

The characteristics of such components and their relationship to each other can be determined by the development of appropriate tests. There are many questions that need to be addressed in the validation of such a system. These are addressed under the following sub-headings.

5.2 Validation of the Accuracy and Reproducibility of DISPERSE

How accurately are waveforms printed on paper recovered by the DISPERSE system? If a waveform was repeatedly scanned and processed by the DISPERSE system, and its QT and RR interval repeatedly measured by the automatic algorithm, by how much would these measurements vary?

5.2.1 Test 1

To test how accurately waveforms printed on paper are recovered by the DISPERSE system, the following test (illustrated by Figure 5.1) was devised. An ECG lead was first scanned and processed. Its digital values were extracted, smoothed to eliminate quantisation errors and baseline offset respectively. These data values were assigned to be the 'gold standard', W_GOLD. The waveforms corresponding to this data were then

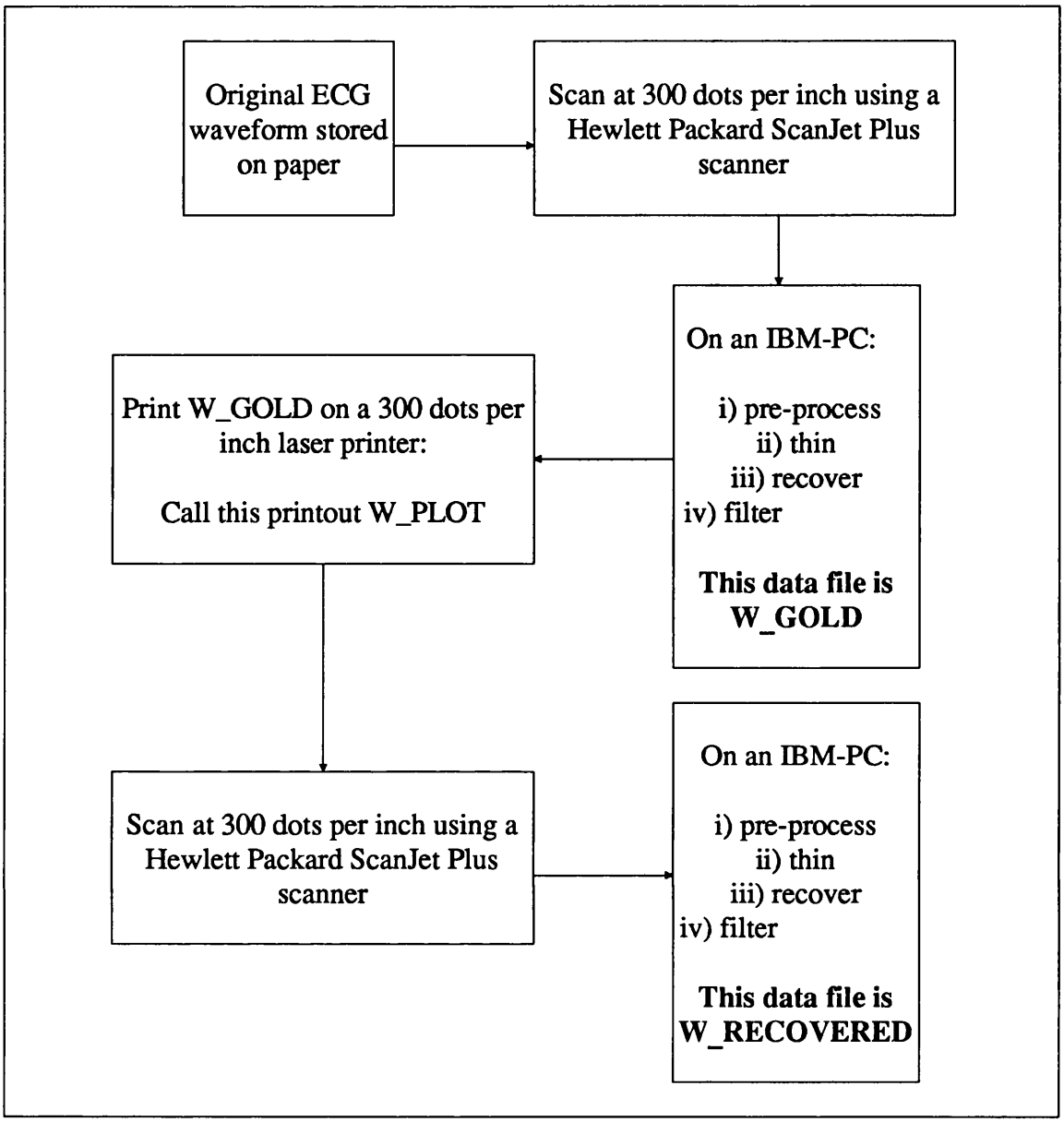

Figure [5.1] Schematic diagram of Test 1

plotted using a conventional graph plotting package, and printed using a 300 dots per inch laser printer (Model: NEC Silentwriter 2). Correct widths in inches for plotting were specified to ensure that the waveform was not distorted in any way. The waveform printed on paper can be denoted as W_PLOT. W_PLOT was scanned, processed, and as above, its digital values were extracted and smoothed. These data values can be denoted as W_RECOVERED. Figure 5.2a shows a plot of the W_GOLD (solid line) and W_RECOVERED (dashed line) waveforms. Figure 5.2b shows the difference in the amplitude in the two waveforms signals when they are perfectly aligned (W_GOLD - W_RECOVERED).

There were three main methods by which the accuracy of the digitising algorithms (DISPERSE) could be analysed:

(i) By the study of the 'root-mean-square (RMS) error' between W_GOLD and W_RECOVERED. This was calculated using the following equation:

$$\left(\frac{\sum_{i=1}^{N} \left(WG_i - WR_i \right)^2}{N} \right)^{\frac{1}{2}} \quad \ldots\ldots\ldots\ldots\ldots\ldots\ldots\ldots\ldots\ldots \quad (5.1)$$

where WGi and WR_i refer to the original and recovered data points respectively and N refers to the number of points in the data set. This was calculated to be 0.8 pixels which corresponds to 1 pixel or sampling point.

(ii) By the study of the cross-correlation function between W_GOLD and W_RECOVERED at different time shifts, and when the two waveforms were perfectly aligned. An optimal value of 0.99 was obtained when the two waveforms were perfectly aligned. This value decreased with time shifts to the right and left, of one waveform relative to the other.

(iii) By the determination of QT and RR intervals by the automatic algorithm of both W_GOLD and W_RECOVERED. Table 5.1 shows the different QT and RR intervals measured by the automatic algorithm for both W_GOLD and W_RECOVERED.

Table 5.1 QT and RR Intervals measured from W_GOLD and W_RECOVERED by the Automatic algorithm

	QT Interval 1 (ms)	QT Interval 2 (ms)	RR Interval (ms)
W_GOLD	427	420	894
W_RECOVERED	430	413	894

5.2.2 Test 2

Another manner in which the reproducibility of the data recovery system was analysed was by using the following test. Data from an ECG lead was scanned using red optical filter paper at a scanner illumination threshold of 92. As above this data was recovered using the DISPERSE system. QT and RR interval measurements were performed on this recovered ECG data, using the automatic algorithm, and tabulated. This process was repeated 8 times in all, each time, starting from the process of scanning, using the same illumination threshold. Table 5.2 shows the QT and RR intervals measured each time the lead was processed.

Table 5.2 Repeated Scanning and Processing of an ECG Lead : QT and RR Intervals measured by the Automatic algorithm

	QT Interval (ms)	RR Interval (ms)
Processed 1	467	1063
Processed 2	471	1060
Processed 3	471	1060
Processed 4	467	1060
Processed 5	467	1063
Processed 6	467	1063
Processed 7	467	1063
Processed 8	467	1063

5.2.3 Discussion

Test 1 reveals the following points: The root-mean-square error between W_GOLD and W_RECOVERED is very small: this implies that W_RECOVERED is a good representation of W_GOLD. Visual inspection of Figure 5.2a and b confirm this. The difference between signal amplitude values is very little. This is illustrated in the residual signal (Figure 5.2b). W_RECOVERED has also not been time shifted as can be

seen from the result of the cross correlation coefficient which yields an optimal value at 0.99 at zero time shift. This high value also illustrates the strong linear association between the two sets of data.

The values of the first QT interval (QT interval 1) measured by the automatic algorithm for W_GOLD and W_RECOVERED (Table 5.1) differ by 1 sampling interval, whilst that for the second QT interval (QT interval 2) differs by 2 sampling intervals. The RR interval measured for both waveforms is exactly the same. This illustrates the fact that the DISPERSE system reconstructs and extracts digital values from the scanned image waveform accurately.

Results from test 2 shown in Table 5.2 indicate that the same data processed by the DISPERSE system repeatedly and analysed by the automatic algorithm show that for the QT interval and RR interval the difference when the process was repeated 8 times was accurate to 1 sampling interval i.e approximately 3-4 ms. This must indicate a very high accuracy in the reproducibility of the system in reconstructing the digitised ECG waveform. It also shows the consistency and accuracy with which the relatively unbiased automatic algorithm predicts and calculates its intervals.

Figure [5.2a] Plot of W_GOLD (solid) and W_RECOVERED (dashed)

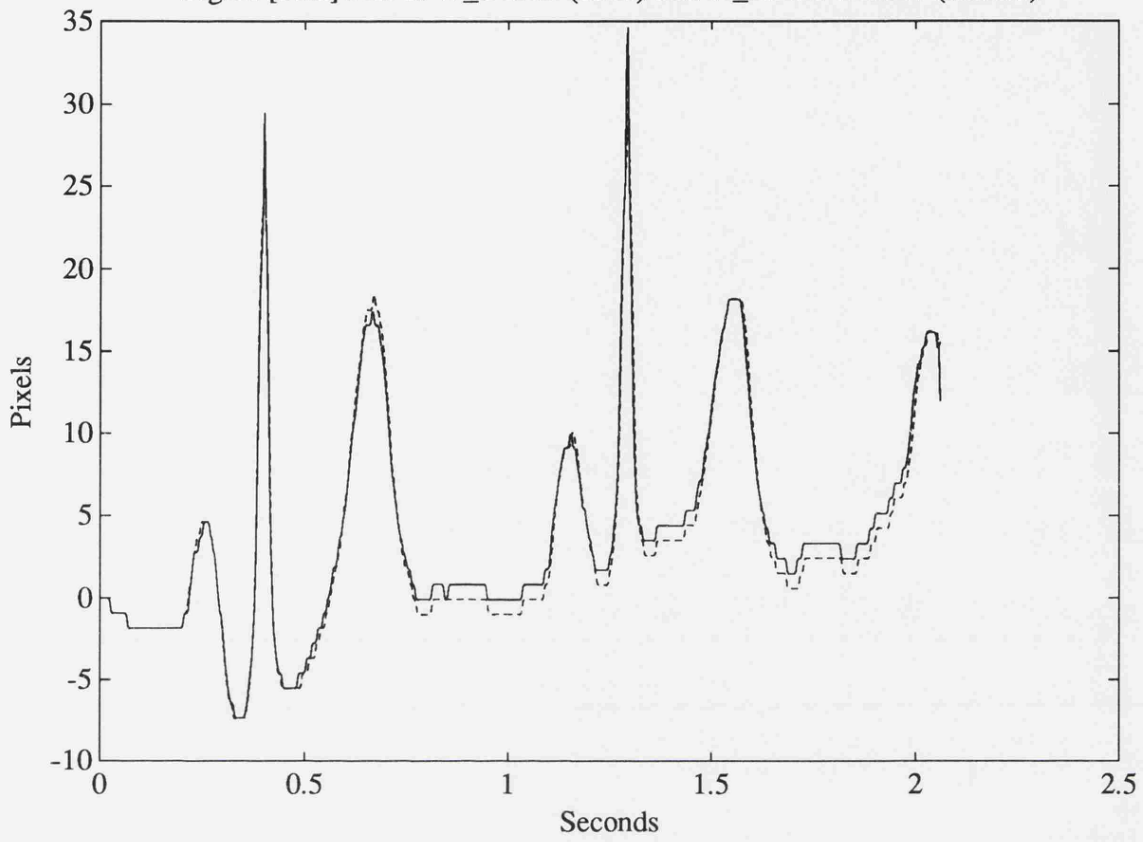

Figure [5.2b] Plot of the difference (W_GOLD - W_RECOVERED)

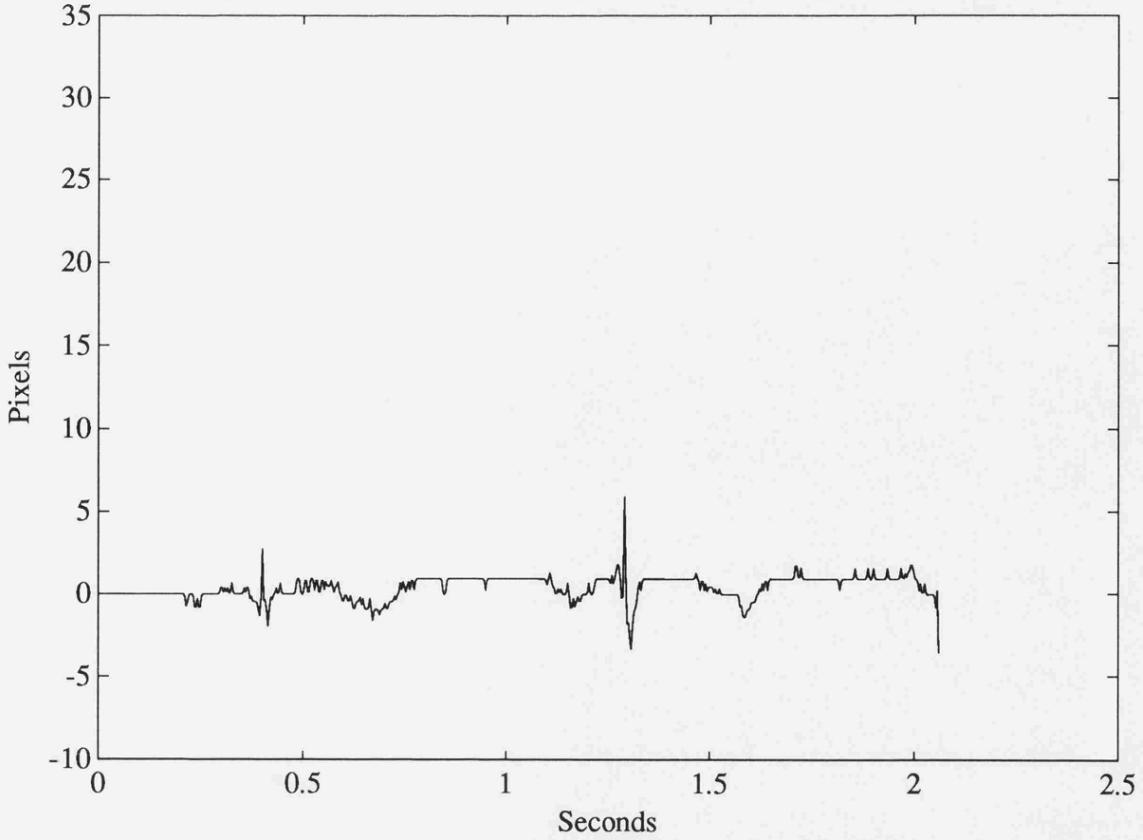

5.3 Assessment of the Characteristics of Manual and User-Interactive Methods

Do measurements obtained by the User-interactive system agree well with manual measurements? Does this depend on the type of measurement made? Is there any difference in measurements obtained by two observers who perform these measurements manually and using the user-interactive method? Is inter-observer variability in this case affected by the different types of measurement? Are measurements performed by the User-interactive system more accurate than those performed manually? Indeed, can the User-interactive system accurately replace the method of manual measurement?

5.3.1 Test 3

To test if measurements obtained by the user-interactive system compared well with manual measurement made on paper records, it was decided that 116 ECG waveforms comprising data from ten patients would be scanned and processed. The first QT and its corresponding RR interval from each of these waveforms was measured manually and by using the user-interactive system. The QT interval is not always well defined (for example the T wave end is often unclearly delimited), whilst the RR interval, delimited by peaks is a well defined interval of the ECG waveform. The measurement of this latter parameter would give an indication of the "best" performance of the DISPERSE system in comparison to the conventional manual measurements. In cases where the R wave was absent the S wave was used.

These ECG records were routine 12 lead outpatient and inpatient Electrocardiograms recorded using a Nihon-Kohden ECG Model ECG-6353/D/F/L Electrocardiograph. Since the DISPERSE system was designed by an engineer but measurements are usually made by a cardiologist, these analyses were carried out by both the system designer (observer 1) and an independent cardiologist (observer 2).

5.3.2 Measurement Protocol

For manual measurements, a stainless steel 'Mine' precision ruler was used together with a set of dividers. The dividers were used to mark the onset and offset points of these intervals, and the ruler was used to make a reading from the dividers.

Measurements were recorded in centimetres accurate to the nearest quarter of a millimetre. Examples of RR intervals are 1.950cm, 1.925cm, 1.950cm and 1.975cm. These measurements were performed only once, and the first QT and RR interval measured in each lead was recorded. These interval measurements were converted to milliseconds and stored in a file using a program written for this purpose.

Similarly only one QT interval and its corresponding RR interval was measured using the user-interactive system. These measurements were made interactively by using a cursor to define onset and offset points in the waveform, and the resulting interval measurements expressed in milliseconds, were stored in files.

Two methods have been adopted to analyse these data:

(I) The first is that developed by J.Bland and D.Altman (1986). They have discussed techniques for assessing the 'agreement' between measurement methods. Comparison of a new method of clinical measurement against an established one is required to assess if they agree sufficiently for the new to replace the old. As there does not exist a true measurement by either method, one can only test the agreement in results obtained by both methods. Many authors propose that the correlation coefficient will test agreement but this is not true. Bland and Altman have shown that the use of the Pearson's product-moment correlation coefficient ("r") may be misleading since it is an indicator of correlation and not necessarily of agreement.

Figures 5.3 a,b and c illustrate this point clearly. When two sets of data agree closely, they should lie on the line of equality. Using the example of W_GOLD and W_RECOVERED it can be seen from Figure 5.3a that most of the points in the plot of W_GOLD vs W_RECOVERED lie on this line of equality. However if a constant value was added to W_RECOVERED (Figure 5.3b) or multiplied to W_RECOVERED (Figure 5.3c) the resultant points do not lie on this line of equality any more. Therefore they do not 'agree'. As they still lie in a straight line, they would still show correlations of 0.99.

Bland and Altman suggest that whilst a plot of the two sets of data with the line of equality may be a good starting point, it would still be difficult to assess the between-method differences, as all the data points would be clustered near the line. They suggest that a plot of the difference between the methods against the mean may be more

Figure [5.3a] Plot of W_GOLD vs W_RECOVERED superimposed with the line of Equality

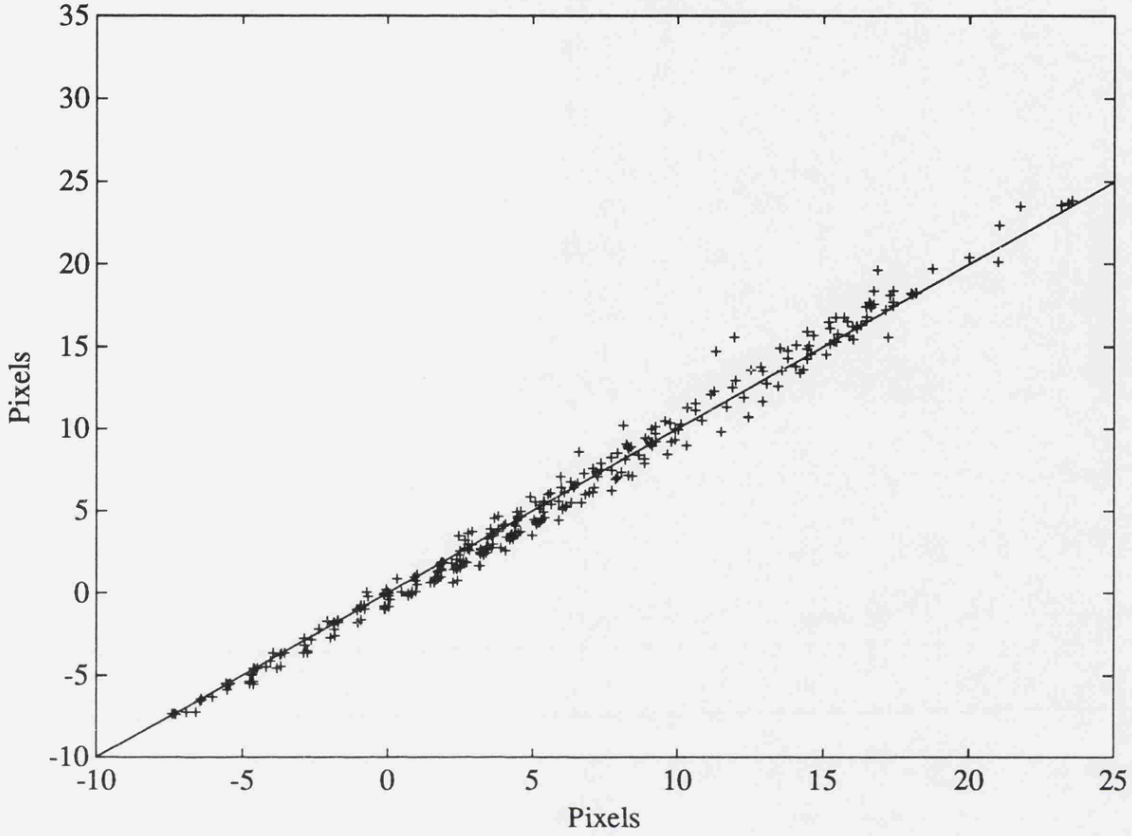

Figure [5.3b] Plot of W_GOLD plus a Constant vs W_RECOVERED compared to the line of Equality

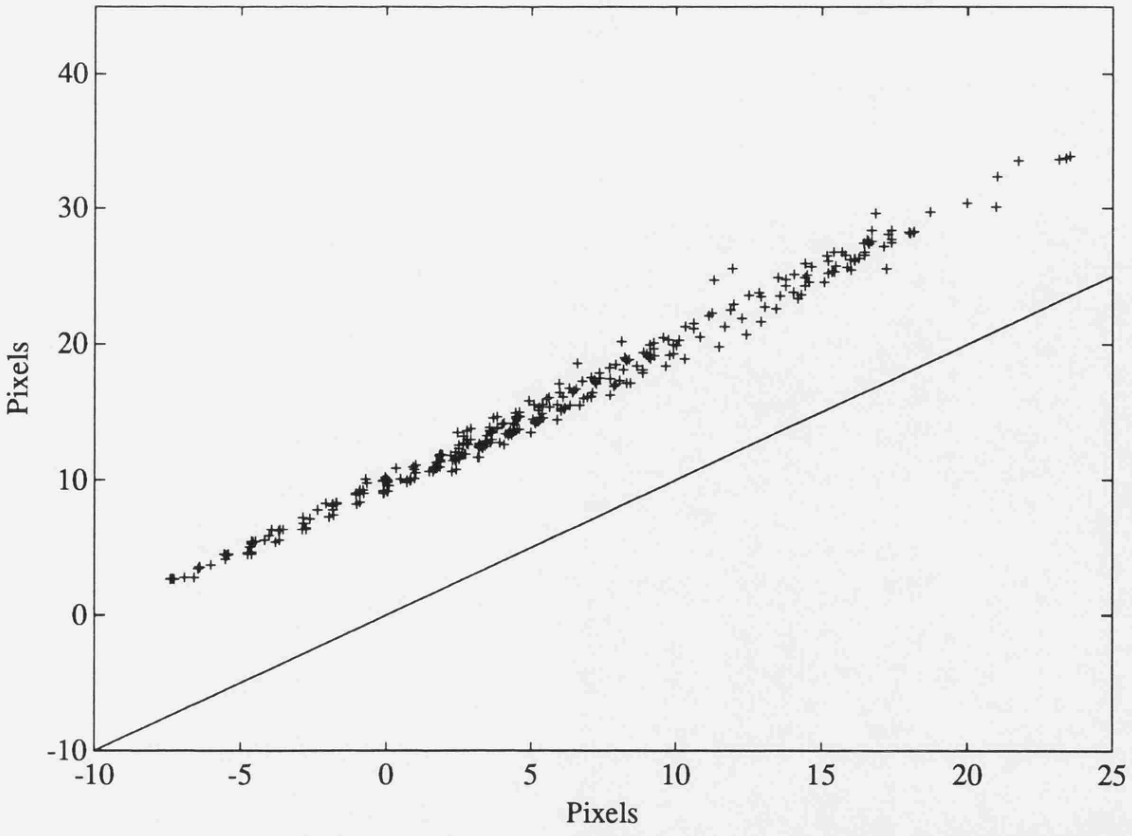

Figure [5.3c] Plot of W_GOLD multiplied by a Constant vs W_RECOVERED compared to the line of Equality

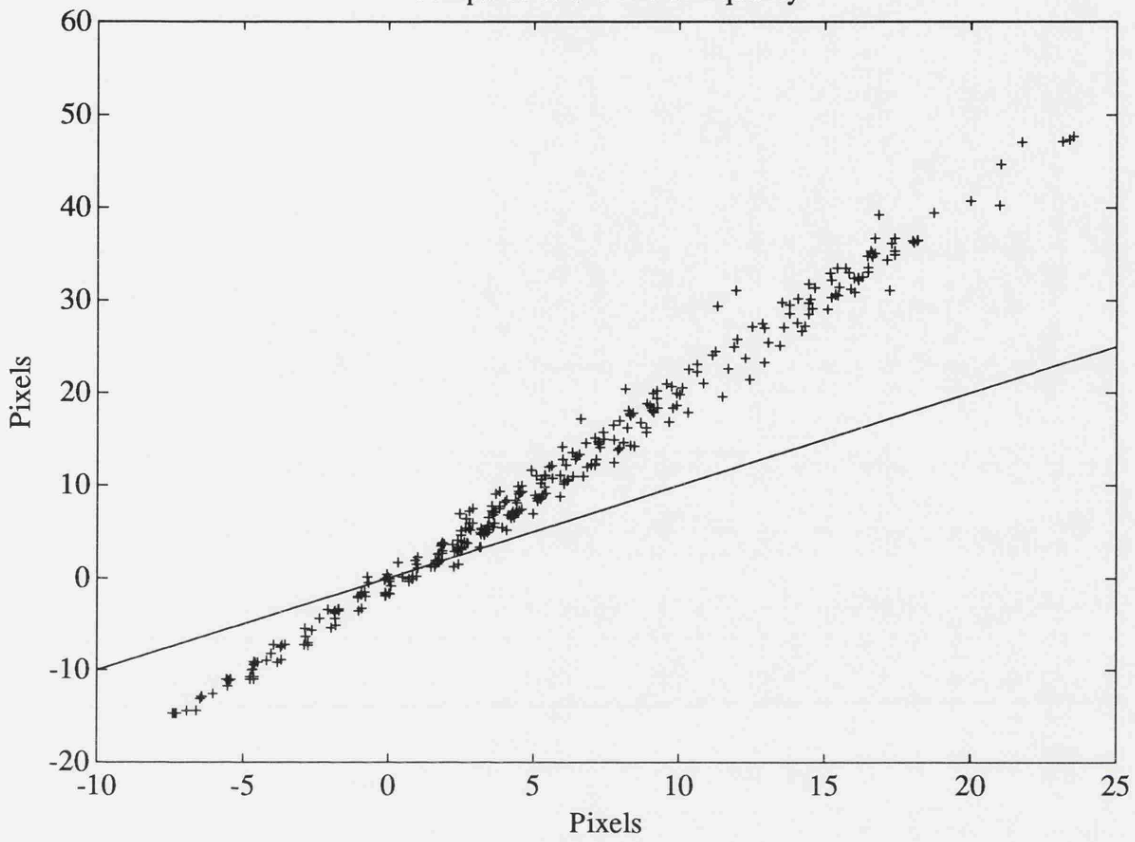

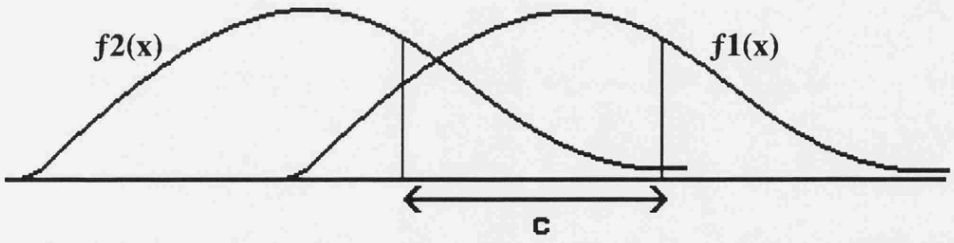

Figure [5.4] A probobility density function and its translation

informative. It would allow any possible relationship between the measurement error and the true value to be investigated where the best estimate of the true value is given by the mean of both measurements. This concept can be extended to study not only measurements derived from two methods, in this case the manual and user-interactive methods, but also to study the differences in measurements made by two observers, whether they employ the user-interactive or manual methods of measurement.

The relationships of eight different combinations of paired measurements were studied:

**(i) The difference in observer 1 measurement of RR intervals: (User-interactive measurements minus manual measurements).

**(ii) The difference in observer 2 measurement of RR intervals: (User-interactive measurements minus manual measurements).

**(iii) The difference in observer 1 measurement of QT intervals: (User-interactive measurements minus manual measurements).

**(iv) The difference in observer 2 measurement of QT intervals: (User-interactive measurements minus manual measurements).

**(v) The difference in manual measurement of RR intervals: (observer 2 minus observer 1).

**(vi) The difference in user-interactive measurement of RR intervals: (observer 2 minus observer 1).

**(vii) The difference in manual measurement of QT intervals: (observer 2 minus observer 1).

**(viii) The difference in user-interactive measurements of QT intervals: (observer 2 minus observer 1).

****Note** : the numbering from i to viii will be used to represent the paired measurements studied.

The method of analysis of Bland and Altman has been modified slightly. In their analysis the mean difference and standard deviation of these differences are employed to obtain estimates of bias. In our analysis the concept of the 'fractional difference' is used, so that each difference in measurement is normalised to its corresponding mean. The bias and confidence of agreement in the two methods or the bias and estimate of

inter-observer variability in the measurements made by two observers can be estimated from the mean fractional difference $M(d_i)$ and the standard deviation of the fractional differences $D(d_i)$ respectively. The fractional differences are likely to follow a Normal distribution because a lot variation between subjects is removed. Using measurements corresponding to vii above, Figure 5.5 shows that the fractional differences follow an approximately normal distribution.

The calculations employed in this analysis are described here:

For each paired measurement, the fractional difference:

$$d_i = \frac{x_i1 - x_i2}{(x_i1 + x_i2) \text{ X } 0.5} \qquad (5.2)$$

where x_i1 is the i^{th} measured value obtained by one method or observer, and x_i2 is the i^{th} measured value obtained by the second method or observer.

For i=1 to N where N is the total number of paired readings, the mean d_i is calculated as:

$$M(d_i) \text{ or } \bar{d_i} = \frac{\sum_{i=0}^{N} d_i}{N} \qquad (5.3)$$

The standard deviation of d_i is given as:

$$D(d_i) = \left(\frac{\sum_{i=1}^{N} \left(d_i - \bar{d_i}\right)^2}{N} \right)^{\frac{1}{2}} \qquad (5.4)$$

(II) The second method of analysing the data is known as the Sign Test. This test is often referred to as a non-parametric or distribution-free test. In distribution-free methods no underlying distribution of data is assumed and the hypotheses to be tested usually relate to the nature of the distributions as a whole rather than to a study of their parameters (eg. P.G.Hoel,1971). The only assumption is that the distributions be continuous. In our proposed analysis the sign test is used to study the difference of location of two density functions, in this case given by measurements obtained by two different methods of measurement or by two different observers. It is necessary to assume that the spread of the two distributions is the same, hence the test can be thought

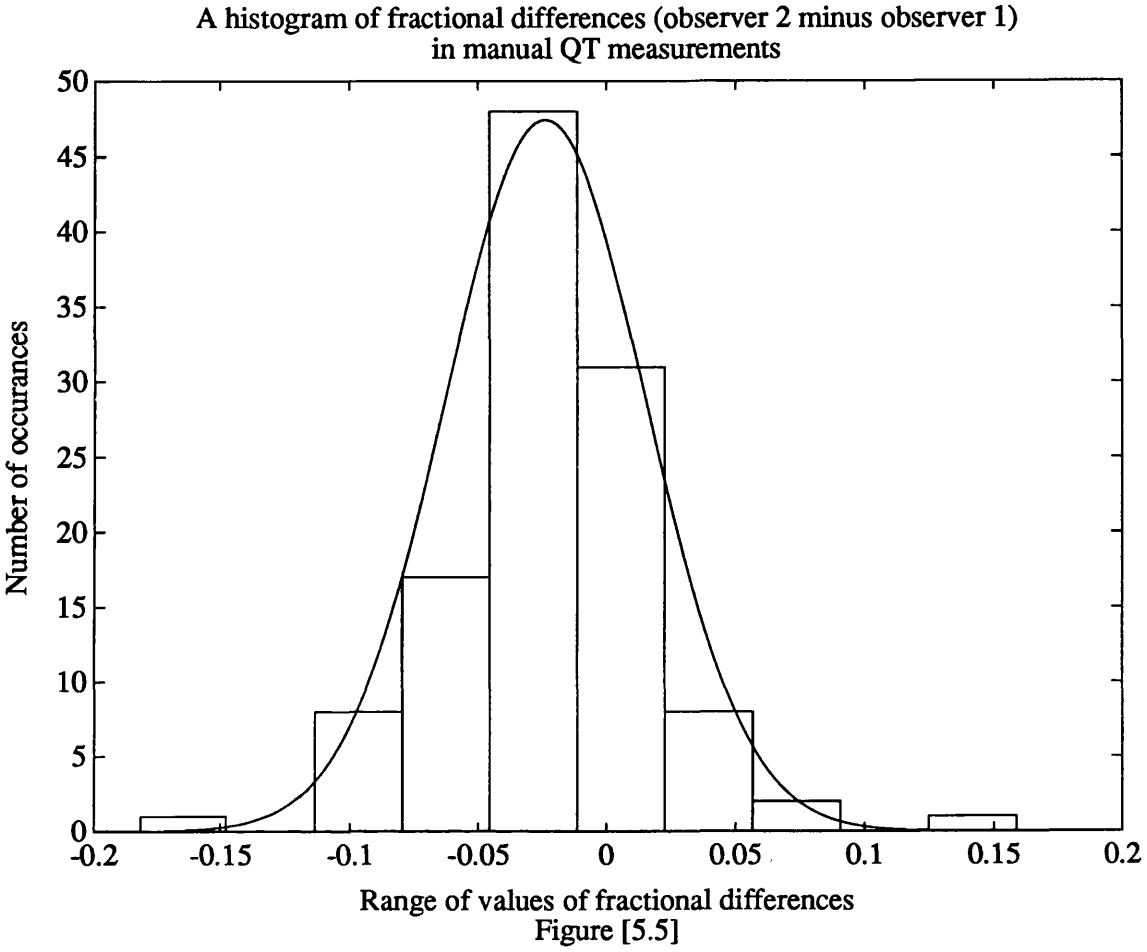
A histogram of fractional differences (observer 2 minus observer 1)
in manual QT measurements
Number of occurances
50
45
40
35
30
25
20
15
10
5
0
-0.2
-0.15
-0.1
-0.05
0
0.05
0.1
0.15
0.2
Range of values of fractional differences
Figure [5.5]

of as a *slippage* test i.e. the distribution curve of the second sample can be obtained by sliding the distribution curve of the first sample along the axis by a set quantity. In applying the sign test to the *slippage* problem, it is necessary to assume that equal size samples are taken from the two populations. The sign test is particularly useful test when observations come in related pairs, and it will therefore be described from that point of view.

Let $f1$ and $f2$ denote two continuous density functions and let (X_1,Y_1), (X_2,Y_2), ... (X_n,Y_n) denote n paired samples sample values to be drawn from the two populations. Consider the hypothesis:

$$H_0 : f_1(x) = f_2(x) \quad \ldots\ldots\ldots\ldots\ldots\ldots\ldots\ldots\ldots\ldots \quad (5.5)$$

To test this hypothesis, consider the differences X_i-Y_i $(i=1,2,3...n)$. When H_0 is true, X_i and Y_i constitute a random sample from the same population and it follows therefore that the probability that X_i-Y_i is positive is ½. Thus if the signs of the differences are now considered, a nonparametric test for H_0 can be constructed:

$$Z_i = 1, \text{ if } X_i - Y_i \geq 0 \quad \ldots\ldots\ldots\ldots\ldots\ldots\ldots\ldots\ldots\ldots \quad (5.6a)$$

$$Z_i = 0, \text{ if } X_i - Y_i < 0 \quad \ldots\ldots\ldots\ldots\ldots\ldots\ldots\ldots\ldots\ldots \quad (5.6b)$$

Then the variable Z_i is a binomial variable corresponding to a single trial of an experiment for which the probability p=½. Since the Z_i are independent, their sum:

$$U=\sum_{i=1}^{n} Z_i \quad \ldots\ldots\ldots\ldots\ldots\ldots\ldots\ldots\ldots\ldots\ldots\ldots \quad (5.7)$$

will be a binomial variable corresponding to n independent trials of an experiment where p = ½ . For p = ½ and large values of n, the binomial distribution is approximated well by the normal distribution. U can therefore be treated as a normal variable i.e. the distribution of U is normal.

Consider as an alternative to H_0 the hypothesis H_1:$f_1(x)=f_2(x-c)$ where c is some positive constant. H_1 states that the second density function is merely the first density function shifted to the left a distance of c units. Figure 5.4 illustrates the relationship between $f_1(x)$ and $f_2(x)$. Under H_1 X_i will tend to be larger than the Y_i and the variable U will tend to exceed its expected value of $n/2$. One would therefore choose as the critical

region the right tail of the binomial distribution. If c had been negative, the left tail would have been chosen. However, if a translation of unknown direction had occurred both tails would be used.

In the analysis followed here, the latter hypothesis was adopted. As before values of Z_i are summed to yield U. To account for when $(X_i\text{-}Y_i)=0$, since Xi and Yi are discreet rather than continuous values, a correction factor:

$$C.F. = 0.5 \text{ X } (\textit{Number of occurrences of } X_i = Y_i) \quad \ldots\ldots\ldots\ldots \quad (5.8)$$

is subtracted from U. Values of U are calculated for different positive values of c. Based on the number of measurements made, i.e 116 in this case, and based on the assumption that U is distributed normally, the 95% confidence intervals of U can be calculated using the equation:

$$\tau = \frac{U - \frac{n}{2}}{\left(\frac{n}{4}\right)^{\frac{1}{2}}} \quad \ldots\ldots\ldots\ldots\ldots\ldots\ldots\ldots\ldots\ldots\ldots\ldots \quad (5.9)$$

where τ is the number of standard deviations from the mean. Substituting τ=1.96 and τ= -1.96 into Eqn 5.9 will yield the 97½ and 2½ percentile values of U respectively. The median is given by $n/2$. Different positive values of the constant c are used to generate the different Us, and the values of c that generate the lower, median and upper percentiles of U are noted. If no values can be obtained i.e. if all positive values of c generate U values higher than the 3 parameters, negative values of c are used instead. If these still fail to yield appropriate U values, c must be zero and hypothesis H_0 must be true. Using the median and 95% confidence intervals, inferences can be made about the confidence in measurements made by two methods or observers.

A useful feature of the sign test is that it is applicable to situations in which the density functions $f1$ and $f2$ although identical under H_0 for each pair of samples, change from sample pair to sample pair. For example to test if 2 observers produce the same measurements of QT intervals on a given set of data using the user-interactive method, the experimenter can ask each observer to make QT interval measurements on different ECG leads. In such an experiment, it might happen that for a particular lead, both observers may record small QT intervals and that in another lead both observers may

record a larger QT interval. One would expect that the variations of QT intervals in the first lead to be considerably smaller than for the next. Such difference however do not affect the sign test because the distribution of each Z_i is binomial regardless of the nature of the density for each i.

5.3.3 Results (Test 3 : i and ii)

Figure 5.6 shows, for each lead, the difference between user-interactive and manual measurements of the RR interval as a function of the mean RR interval measured by both methods. Data is taken from both observers. The results of mean fractional difference and standard deviation of fractional differences is shown in Table 5.3 part (i) and (ii). The mean fractional difference (user-interactive minus manual) which is indicative of a consistent bias between the two methods, of observer 1 expressed as a percentage is -0.2%, whilst that of observer 2 is 0.5%. Using an average value of RR intervals of 850 ms, this corresponds to $^{-0.2}/_{100}$ X 850 = 1.7 ms and 4.3 ms respectively. As can be seen graphically in Figure 5.6, manual measurements of RR intervals are slightly greater than user-interactive ones in observer 1 '+' whilst in observer 2 'o' the reverse is true. The combined mean fractional difference of both observers given by:

$$\frac{M(d_i)1 + M(d_i)2}{2} \quad \ldots\ldots\ldots\ldots\ldots\ldots\ldots\ldots\ldots\ldots\ldots\ldots (5.10)$$

and which is indicative of an averaged bias, was 0.15% (1.3 ms). The combined standard deviation of the fractional difference of both observers was 1.2% (10 ms). This was found using the following equation:

$$\left(D(d_i)1^{\,2} + D(d_i)2^{\,2}\right)^{1/2} \quad \ldots\ldots\ldots\ldots\ldots\ldots\ldots\ldots\ldots\ldots\ldots\ldots (5.11)$$

It is an indicator of the average confidence of the agreement as it gives a measure of how dispersed the fractional differences obtained from two methods are.

Table 5.4 part i and ii give the corresponding results using the Sign Test. It shows that for observer 1 making manual and user-interactive measurements of RR intervals, the 95% confidence intervals indicate that the difference (manual-user-interactive) is most likely to be in the range of 1-3 ms. On average, manual measurements appear to be consistently 2 ms greater than user-interactive measurements (Compare with 1.7 ms obtained with Bland and Altman analysis). For observer 2 user-interactive measurements

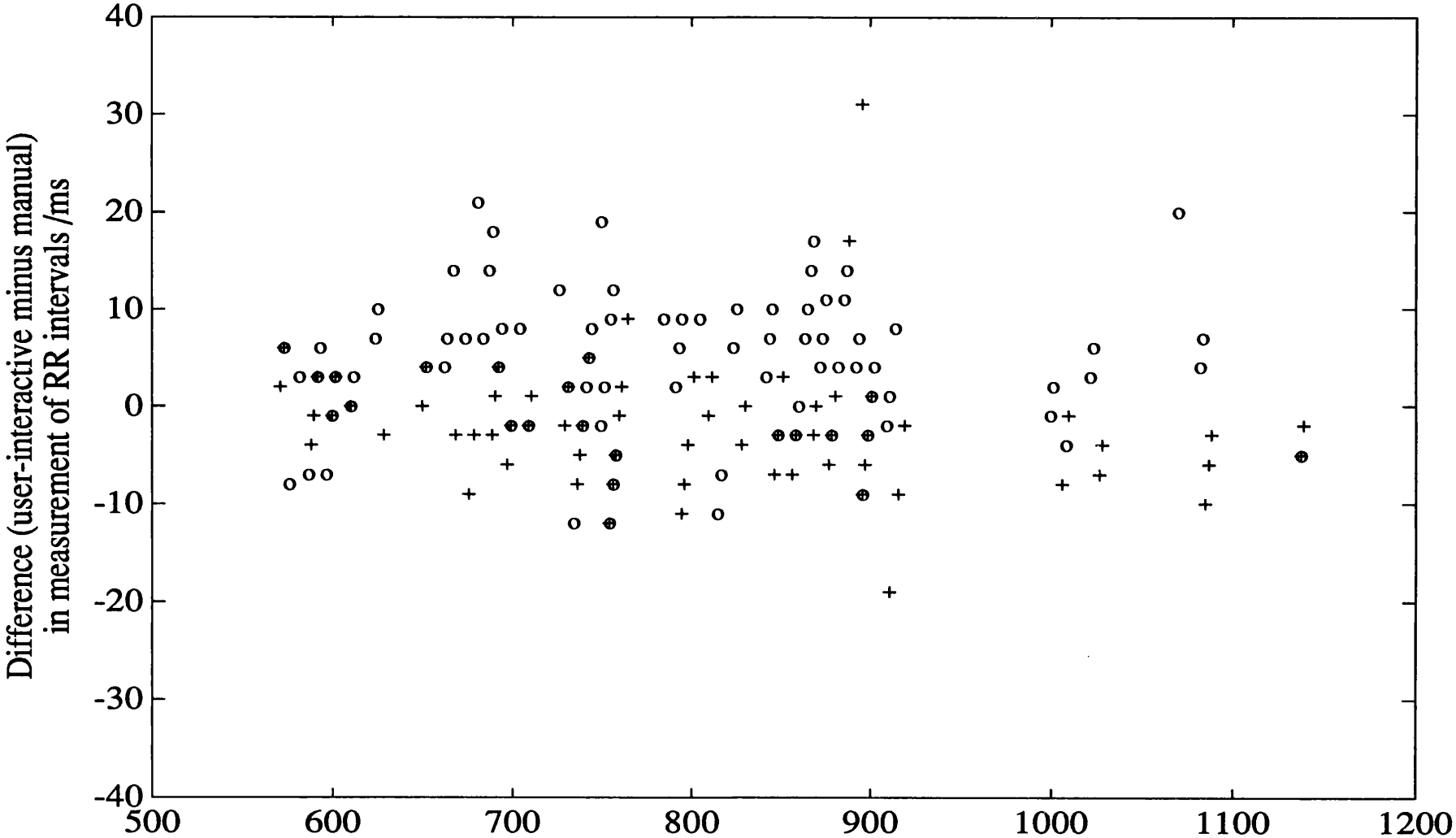
40
30
20
10
0
-10
-20
-30
-40
500
600
700
800
900
1000
1100
1200
Difference (user-interactive minus manual)
in measurement of RR intervals /ms
Mean of user-interactive and manual measurements of RR intervals /ms
+ observer 1 o observer 2

Figure [5.6]

appear to be consistently greater than manual measurements by 4 ms (compare with 4.3 ms obtained with Bland and Altman). The 95% confidence intervals indicate that the difference (user-interactive minus manual) is most likely to be in the range of 3-5 ms.

Table 5.3 Description of tests and results using the analysis of Bland and Altman

Test description	Mean Fractional Difference $M(d_i)$	Standard Deviation of Fractional Differences $D(d_i)$
(i) Manual and User-interactive measurements of RR intervals made by observer 1 (denoted by '+' in Figure 5.5)	-0.0020	-0.0078
(ii) Manual and User-interactive measurements of RR intervals made by observer 2 (denoted by 'o' in Figure 5.5)	0.0050	0.0089
(iii) Manual and User-interactive measurements of QT intervals made by observer 1 (denoted by '+' in Figure 5.6)	0.0340	0.0548
(iv) Manual and User-interactive measurements of QT intervals made by observer 2 (denoted by 'o' in Figure 5.6)	0.0479	0.0587
(v) Manual measurements of RR intervals made by observer 1 and observer 2 (denoted by 'o' in Figure 5.7)	-0.0076	0.0115
(vi) User-interactive measurements of RR intervals made by observer 1 and observer 2 (denoted by 'x' in Figure 5.7)	-0.0005	0.0040
(vii) Manual measurements of QT intervals made by observer 1 and observer 2 (denoted by 'o' in Figure 5.8)	-0.0238	0.0388
(viii) User-interactive measurements of QT intervals made by observer 1 and observer 2 (denoted by 'x' in Figure 5.8)	-0.0099	0.0638

Table 5.4 Description of tests and results using the Sign Test

Test description	Value of constant *c* for Lower 2½ Percentile Value of U (ms)	Value of constant *c* for Median 50 Percentile Value of *U* (ms)	Value of constant *c* for Upper 97½ Percentile Value of *U* (ms)
(i) Manual and User-interactive measurements of RR intervals made by observer 1	1	2	3
The probability that the difference (Manual-User-interactive) is > 3 ms or < 1 ms is less than 5 %. The most probable difference is 2 ms			
(ii) Manual and User-interactive measurements of RR intervals made by observer 2	3	4	5
The probability that the difference (User-interactive-Manual) is > 5 ms or < 3 ms is less than 5 %. The most probable difference is 4 ms			
(iii) Manual and User-interactive measurements of QT intervals made by observer 1	10	14	19
The probability that the difference (User-interactive-Manual) is > 19 ms or < 10 ms is less than 5 %. The most probable difference is 14 ms			
(iv) Manual and User-interactive measurements of QT intervals made by observer 2	12	15	16
The probability that the difference (observer 1-observer 2) is > 16 ms or < 12 ms is less than 5 %. The most probable difference is 15 ms			
(v) Manual measurements of RR intervals made by observer 1 and observer 2	9	9	9
The probability that the difference (observer 1-observer 2) is > 9 ms or < 9 ms is less than 5 %. The most probable difference is 9 ms			
(vi) User-interactive measurements of RR intervals made by observer 1 and observer 2	0	0	0
The probability that the difference (observer 1-observer 2) is > 0 ms or < 0 ms is less than 5 %. The most probable difference is 0 ms			
(vii) Manual measurements of QT intervals made by observer 1 and observer 2	9	9	10
The probability that the difference (observer 1-observer 2) is > 10 ms or < 9 ms is less than 5 %. The most probable difference is 9 ms			
(viii) User-interactive measurements of QT intervals made by observer 1 and observer 2	2	6	10
The probability that the difference (observer 1-observer 2) is > 10 ms or < 2 ms is less than 5 %. The most probable difference is 6 ms			

5.3.4 Results (Test 3 : iii and iv)

Figure 5.7 and Table 5.3 part iii and iv show the results of similar measurements but using QT intervals. The mean fractional difference (user-interactive minus manual) obtained from observer 1 and expressed as a percentage was 3.4% (11.9ms) using an average QT value of 350 ms, whilst that for observer 2 was 4.8% (16.8 ms). As can be seen in Figure 5.7 user-interactive measurements were greater than manual measurements in both observers. The combined mean fractional difference of both observers was 4.1% (14.3 ms). Similarly the combined standard deviation of the fractional differences of both observers using Eqn [5.11] was 8.0% (28 ms). Again this is reflected in Figure 5.7 where the '+' and 'o's are more dispersed than for RR intervals.

Table 5.4 part iii and iv give the corresponding results using the Sign Test. It shows that for observer 1 making manual and user-interactive measurements of QT intervals, on average, user-interactive measurements appear to be consistently 14 ms greater than manual measurements. (Compare with 11.9 ms obtained with Bland and Altman analysis). The 95% confidence intervals indicate that the difference (user-interactive minus manual) is most likely to be in the range of 10-19 ms. For observer 2 user-interactive measurements are consistently greater than manual measurements by a similar value of 15 ms. (Compare with 16.8 ms obtained with Bland and Altman analysis). The 95% confidence intervals indicate that the difference (user-interactive minus manual) is most likely to be in the range of 12-16 ms.

5.3.5 Results (Test 3 : v and vi)

Figure 5.8 shows, for each lead, the difference (observer 2 - observer 1) between the observer's measurements of the RR interval. The figure shows measurements made using both techniques. The results of mean fractional difference and standard deviation of fractional differences is shown in Table 5.3 part v and vi. The mean fractional difference (which is indicative of the bias between observers) is negligible in both cases. For manual measurements this figure is -0.76% (-6.5 ms) and for measurements made using the user-interactive method, this figure is -0.05% (-0.4 ms). The standard deviation of the fractional difference, which is indicative of inter-observer variability as it is a

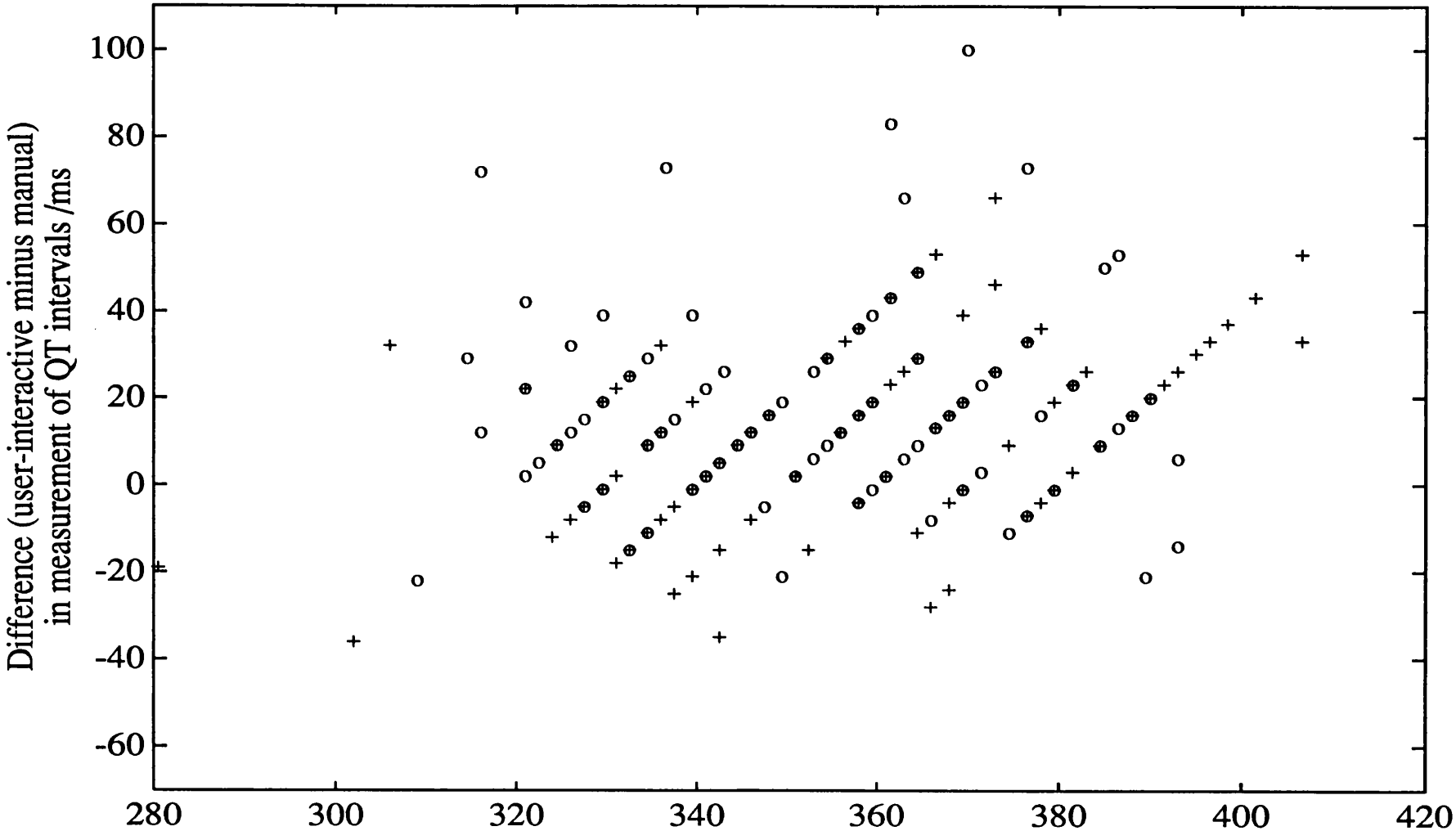
Difference (user-interactive minus manual)
in measurement of QT intervals /ms
100
80
60
40
20
0
-20
-40
-60
280
300
320
340
360
380
400
420
Mean of user-interactive and manual measurements of QT intervals /ms
+ observer 1 o observer 2

Figure [5.7]

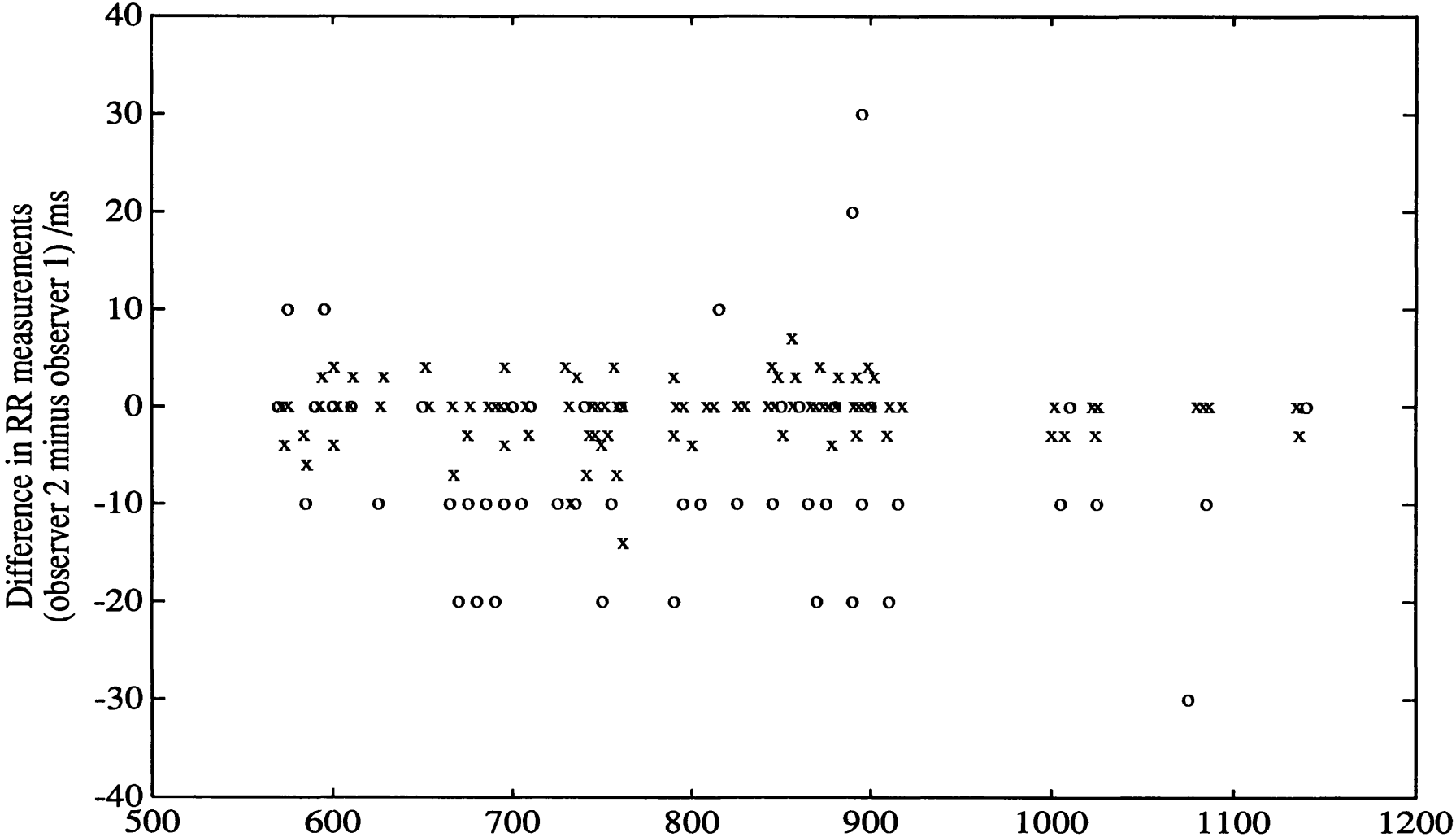
40
30
20
10
0
-10
-20
-30
-40
500
600
700
800
900
1000
1100
1200
Difference in RR measurements
(observer 2 minus observer 1) /ms
Mean of RR intervals measured by observer 1 and observer 2 /ms
x user-interactive measurements o manual measurements

Figure [5.8]

measure of the dispersion of differences between observers, is decreased from 1.1% (9.8 ms) using the manual method to 0.4% (3.4 ms) with the user interactive method. This is reflected strongly in Figure 5.8. The 'x's which correspond to the differences obtained between the two observers when using the user-interactive system are more closely clustered than the 'o's which correspond to the same measurements performed manually.

Table 5.4 part v and vi give the corresponding results using the Sign Test. It shows that for manual measurements of RR intervals made by observer 1 and observer 2, on average, observer 1 made consistently greater measurements than observer 2. The 95% confidence intervals indicate that the difference (observer 1-observer 2) is most likely to be 9 ms. (Compare with 6.5 ms obtained with Bland and Altman analysis). For user-interactive measurements of RR intervals made by observer 1 and observer 2, a difference of 0 ms (or a very small value which the resolution of 1 ms in the Sign Test does not allow us to visualise) was recorded in the measurements made. (Compare with 0.4 ms obtained with Bland and Altman analysis).

5.3.6 Results (Test 3 : vii and viii)

Figure 5.9 and Table 5.3 part vii and viii shows similar results but for QT intervals. The bias given by the mean fractional difference (bias) is again negligible in both cases. For manual measurements this figure is -2.4% (-8.3 ms) and for user-interactive measurements this figure is -0.99% (-3.5 ms). However inter-observer variability given by the standard deviation of fractional differences is increased from 3.9% (13.6 ms) using the manual method to 6.4% (22.4 ms) using the user-interactive method. Figure 5.9 reflects this difference.

Table 5.4 part vii and viii give the corresponding results using the Sign Test. It shows that for manual measurements of QT intervals made by observer 1 and observer 2, on average, observer 1 made consistently greater measurements than observer 2. The 95% confidence intervals indicate that the difference (observer 1-observer 2) is most likely to be 9 ms (same as for RR intervals) . These results also compare well with the 8.4 ms obtained with Bland and Altman analysis). For user-interactive measurements of QT intervals made by observer 1 and observer 2, on average observer 1 made consistently greater measurements than observer 2 by 6 ms. (Compare with 3.5 ms obtained with

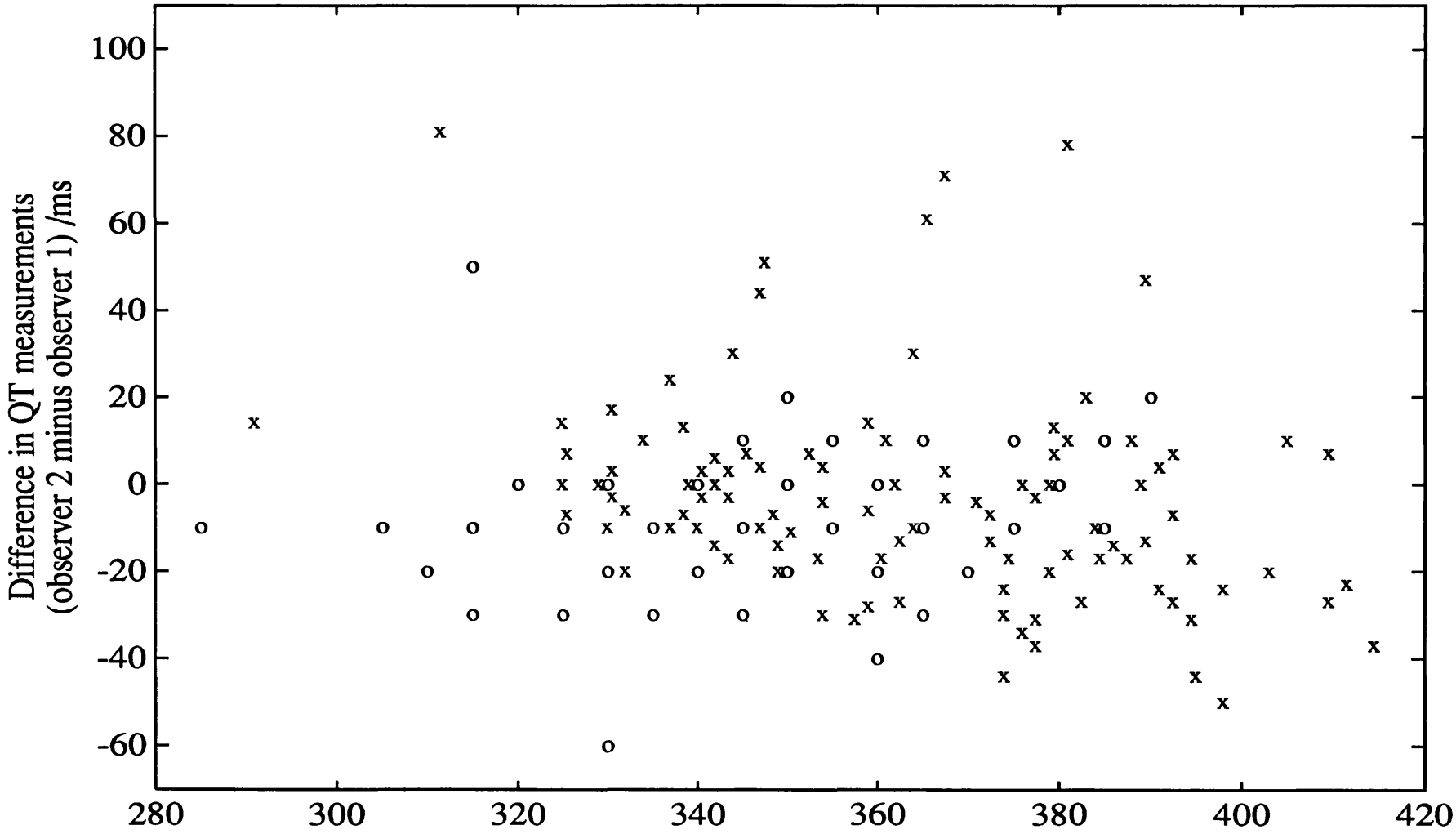
Difference in QT measurements
(observer 2 minus observer 1) /ms
100
80
60
40
20
0
-20
-40
-60
280
300
320
340
360
380
400
420
Mean of QT intervals measured by observer 1 and observer 2 /ms
x user-interactive measurements o manual measurements

Figure [5.9]

Bland and Altman analysis). The 95% confidence intervals indicate that the difference (observer 1-observer 2) is most likely to be in the range 2-10 ms. These results tie in closely with the results obtained using the Bland and Altman analysis.

5.3.7 Discussion (Test 3 : i and ii)

From table 5.3 (i) and (ii) the averaged bias between the user-interactive and manual measurements was 1.3 ms compared to the averaged confidence of agreement in the two methods which was 10 ms. The small value of averaged bias implies that the reconstruction of the waveform was accurate enough to yield measurements similar to those that would have been obtained manually. Since the RR intervals are the best defined, ± 10 ms obtained as the averaged confidence of agreement between the two methods is good representation of the likely accuracy of the system. The corresponding result of the Sign test shows that the most likely difference in the two methods when measuring RR intervals is 2 ms with observer 1 and 4 ms with observer 2. The confidence of agreement can be obtained from the 95% confidence interval which yields an average difference of 1-3 ms with observer 1 and 3-5 ms with observer 2. This is an improved estimate compared to the estimates obtained using Bland and Altman analysis. This again confirms that the two methods agree closely and therefore the user-interactive method can reliably replace the method of manual measurement.

5.3.8 Discussion (Test 3 : iii and iv)

From Table 5.3 (iii) and (iv) the averaged bias between the user-interactive and manual measurements was 14.3 ms compared to the averaged confidence of agreement in the two methods which was 28 ms. This apparent increase in bias and the decrease in agreement cannot be accounted for in terms of a malfunction of the user-interactive technique (since there was good agreement of RR intervals) but must be because the QT intervals themselves are much more subjective to define, i.e. the lack of agreement is due to inconsistencies in the way the observers have interpreted the QT intervals. The corresponding result of the Sign test reflects this result too. It shows that the most likely difference in the two methods when measuring QT intervals is 14 ms with observer 1 and 15 ms with observer 2. The confidence of agreement can be obtained from the 95%

confidence interval which yields an average difference of 10-19 ms with observer 1 and 12-16 ms with observer 2. These results show much bigger differences than for RR intervals (compare Fig 5.6 and 5.7) and suggest again that they must be due to the greater subjectivity involved when measuring QT intervals. It can be said therefore that when intervals are not clearly delimited, the element of subjectivity causes differences between two methods to be greater.

5.3.9 Discussion (v and vi)

From Table 5.3 (v) and (vi) the bias between observer 1 and observer 2 with both manual and user-interactive methods of measurement of RR intervals was 6.5 ms and 0.4 ms respectively. This lower bias with the user-interactive system indicates the better agreement obtained between two observers when using this system. The standard deviation of fractional differences, an indicator of inter-observer variability is less when using the user-interactive system (3.4 ms) compared to 9.8 ms when using the manual method. The user-interactive method allows very precise measurements of intervals delineated by peaks (RR intervals) due to the feature of cursor-tracking of the signal when making user-interactive measurements on the waveform. This gives rise to very small variations in measurements made by two observers compared to manual methods where the eye has to delimit the peaks. However because the peaks are well delineated, the effect of 'rounding off' caused by the lower resolution of manual measurements is not significant.

The results of the Sign test reflects this too. It shows that the most likely difference between two observers when measuring RR intervals is 9 ms with manual measurements and 0 ms (or a very small value which the resolution of 1 ms in the Sign Test does not allow us to visualise) with user-interactive measurements. An indication of inter-observer variability can be obtained from the 95% confidence interval which yields an average difference between observers of 9 ms with manual measurements and no difference with the user-interactive system.

This is a very interesting result as it clearly shows that there is a constant difference of 9 ms in manual measurement of RR intervals between two observers with observer 1 making consistently greater measurements than observer 2. This could reflect a

consistent bias in the manner of RR interval measurement. When the user interactive system is used, no difference in measurement is noted, i.e. inter-observer variability is 0. Hypothesis H0 is found to be true. This strongly suggests that the user-interactive system is even more accurate and reproducible than the manual method of measurement and can therefore replace it.

5.3.10 Discussion (Test 3 : vii and viii)

From Table 5.3 (vii) and (viii) the bias between observer 1 and observer 2 with both manual and user-interactive methods of measurement of QT intervals was 8.3 ms and 3.5 ms respectively. This lower bias obtained with the user-interactive system indicates the better agreement obtained between two observers when using this system. However, the standard deviation of fractional differences, an indicator of inter-observer variability increased when using the user-interactive system (22.3 ms) compared to 13.6 ms when using the manual method. As RR intervals are well defined as conventionally sharp peaks in the ECG and as inter-observer variability decreased with the user-interactive system when measuring RR intervals, the apparent increase in inter-observer variability reflected with QT interval measurements may represent the greater accuracy of the user-interactive system as well as the greater subjectivity involved in the measurements of QT intervals. The effect of 'rounding off' is also more dominant in QT intervals measured manually, as they are less well defined. This effect could contribute to the 'apparent' inter-observer variability being smaller in the manual method of measurement of QT intervals.

The results of the Sign test reflects this too. It shows that the most likely difference between two observers when measuring QT intervals is 9 ms with manual measurements and 6 ms with user-interactive measurements. As 9 ms was obtained previously with RR intervals, this confirms a consistent bias between observers using the manual method of measurement. The 6 ms difference obtained with user-interactive measurements of QT intervals must be due to the subjectivity of QT measurements, as previously with RR measurements no difference was obtained. An indication of inter-observer variability can be obtained from the 95% confidence interval which yields an average difference between observers of 9-10 ms with manual measurements and 2-10 ms with the

user-interactive system. It can be said therefore that inter-observer variability does depend on whether the intervals to be measured are clearly delineated i.e. QT or RR intervals.

Summary of Findings of Test 3

For the comparison of the user-interactive and manual methods of measurement, the small value of average bias (1.3 ms) implies that the reconstruction of the waveform by DISPERSE was accurate enough to yield measurements similar to those that would have been obtained manually. Therefore the user-interactive method can reliably replace the method of manual measurement. ± 10 ms was the estimate obtained of the likely accuracy of the system. It was also found that when intervals are not clearly delimited, the element of subjectivity caused differences between two methods to be greater.

The comparison of observer 1 and observer 2 with both manual and user-interactive methods of measurement showed that inter-observer variability decreased when using the user-interactive system compared to the manual method of measurement, especially if the intervals to be measured were clearly delineated. This was attributed to the greater resolution of the user-interactive system (4ms) compared to manual measurements (10 ms) plus the precise measurements of intervals allowed in the user-interactive system by the feature of cursor-tracking of the signal. Inter-observer variability was virtually 0 when the user interactive system was used to measure clearly delineated intervals. When the intervals were not clearly delineated, inter-observer variability increased. This increase in inter-observer variability may be a reflection of the greater accuracy of the user-interactive system as well as the greater subjectivity involved in such measurements. The effect of 'rounding off' is also dominant in such instances and could contribute to the 'apparent' inter-observer variability being smaller when manual measurements are made.

5.4 Comparison of Manual , User-interactive and Automatic Methods

How do results obtained from the automatic algorithm compare with both the method of manual measurement and the user-interactive system?

5.4.1 Test 4

To test if measurements obtained by the automatic algorithm compared well with manual measurement made on paper records and user-interactive measurements, a new set of 112 ECG waveforms comprising data from ten patients were analysed using the methods of analysis of Bland and Altman and the Sign test as above.

As before, the first QT and its corresponding RR interval from each of these waveforms was measured automatically, manually and using the user-interactive system. The latter two measurements were performed by a *cardiologist.* In cases where the R wave was absent the Q or S wave was used. The same measurement protocol was adopted as before.

The relationships of four different combinations of paired measurements were studied:

**(a) The difference in measurement of RR intervals: (Automatic measurement minus manual measurements).

**(b) The difference in measurement of QT intervals: (Automatic measurement minus manual measurements).

**(c) The difference in measurement of RR intervals: (Automatic measurement minus user-interactive measurements).

**(d) The difference in measurement of QT intervals: (Automatic measurement minus user-interactive measurements).

****Note** : the alphabets from (a) to (d) will be used to represent the paired measurements studied.

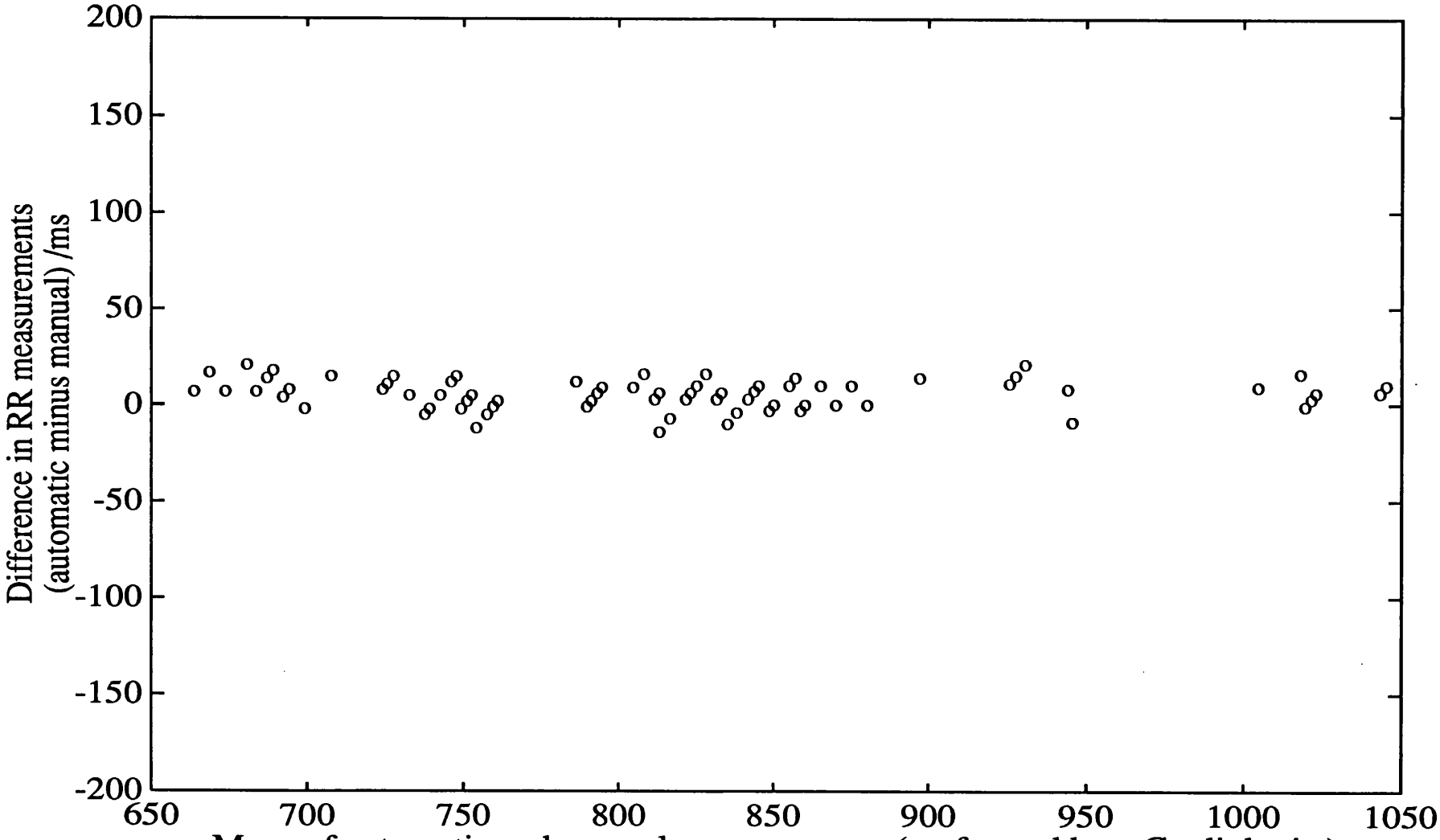
200
150
100
50
0
-50
-100
-150
-200
650
700
750
800
850
900
950
1000
1050
Difference in RR measurements
(automatic minus manual) /ms
Mean of automatic and manual measurements (performed by a Cardiologist)
of RR intervals /ms

Figure [5.10]

5.4.2 Results (Test 4 : a)

Figure 5.10 shows, for each lead, the difference between automatic and manual measurements of the RR interval as a function of the mean RR interval measured by both methods. Manual measurements were made by a cardiologist. The results of mean fractional difference and standard deviation of fractional differences of the two measurement methods is shown in Table 5.5 part (a). The mean fractional difference (automatic minus manual) which is indicative of a consistent bias between the two methods expressed as a percentage is 0.68%. Using an average value of RR intervals of 850 ms, this corresponds to 5.8 ms. From Figure 5.10, as the difference between the automatic and manual measurements are on average, positive, this means that automatic measurements are on average higher than the manual measurements. The standard deviation of the fractional difference is 0.87% which corresponds to 7.4 ms. It is an indicator of the confidence of the agreement between the two measurement methods by indicating how dispersed the fractional differences obtained from two methods.

Table 5.6 part (a) give the corresponding results using the Sign Test. The 95% confidence intervals indicate that the difference (automatic minus manual is most likely to be in the range of 5-7 ms. On average, automatic measurements appear to be consistently 6 ms greater than manual measurements (which is consistent with the value of 5.8 ms obtained from the Bland and Altman analysis).

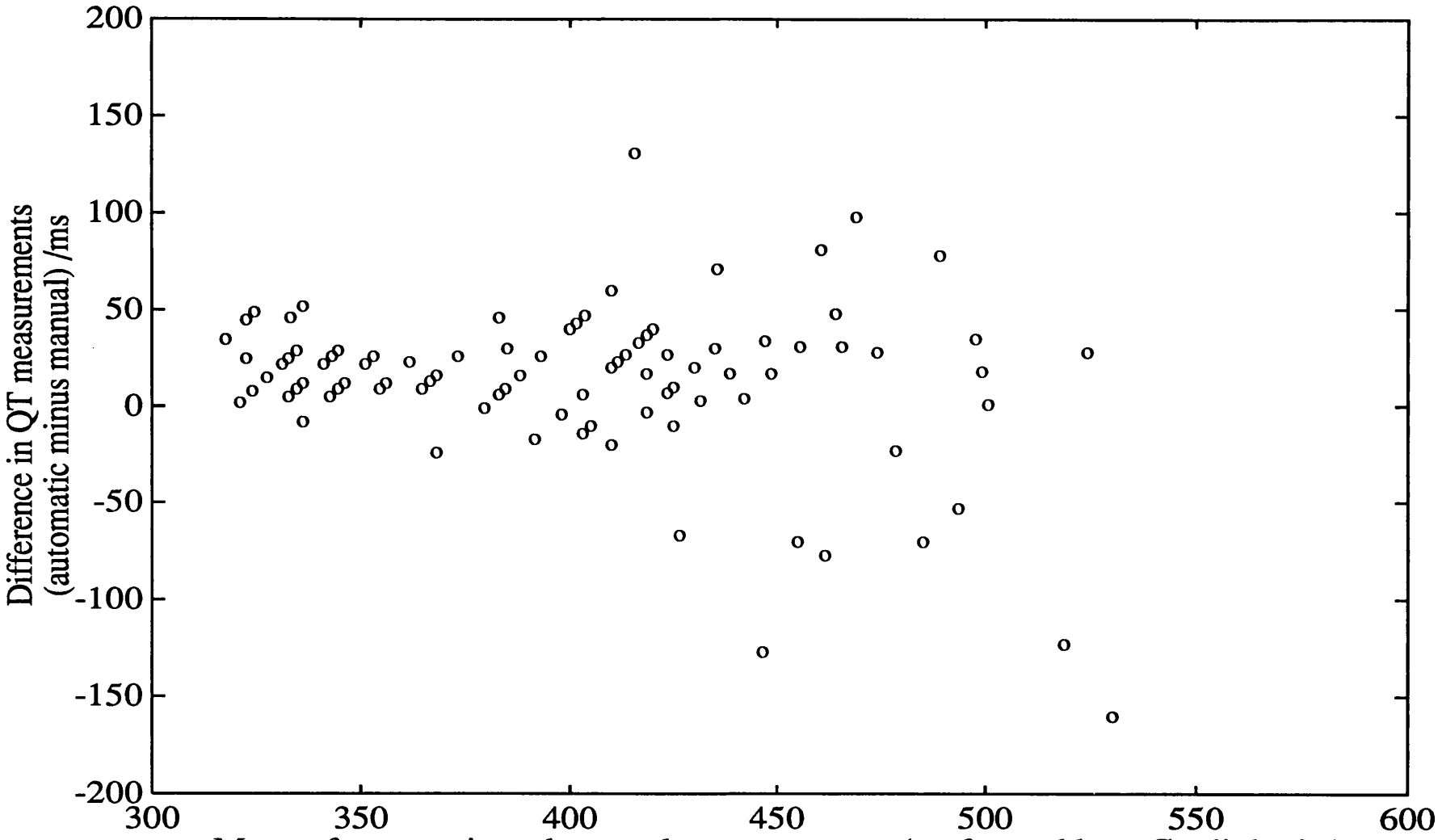
200
150
100
50
0
-50
-100
-150
-200
300
350
400
450
500
550
600
Difference in QT measurements
(automatic minus manual) /ms
Mean of automatic and manual measurements (performed by a Cardiologist)
of QT intervals /ms

Figure [5.11]

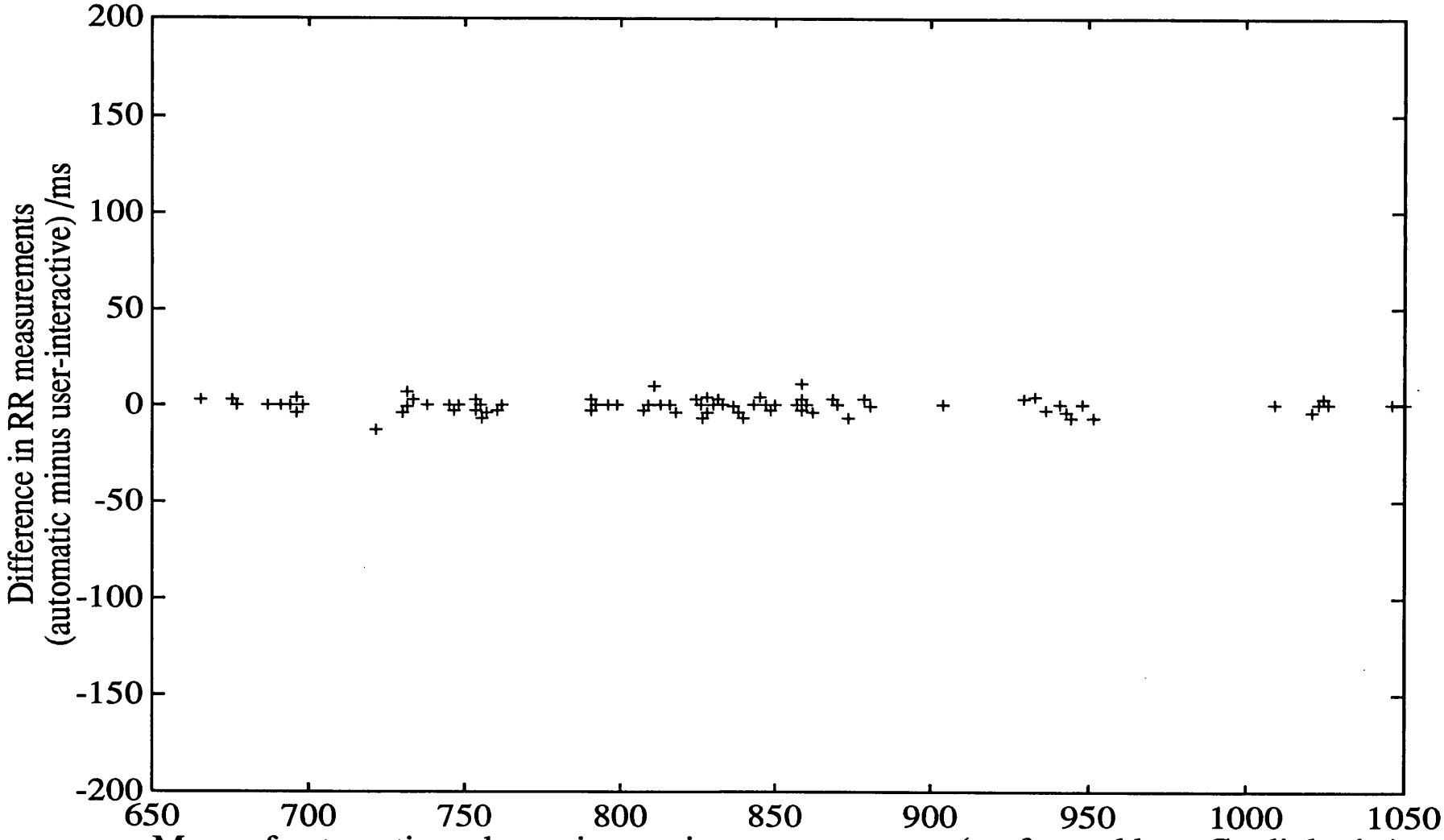
200
150
100
50
0
-50
-100
-150
-200
650
700
750
800
850
900
950
1000
1050
Difference in RR measurements
(automatic minus user-interactive) /ms
Mean of automatic and user-interactive measurements (performed by a Cardiologist)
of RR intervals /ms

Figure [5.12]

Table 5.5 A study of measurements made by a Cardiologist manually and using the user-interactive system and how they compare with automatically derived measurements (Analysis adapted from Bland and Altman)

Test description	Mean Fractional Difference $M(d_i)$	Standard Deviation of Fractional Differences $D(d_i)$
(a) Manual and Automatic measurements of RR intervals	0.0068	0.0087
(b) Manual and Automatic measurements of QT intervals	0.0375	0.0858
(c) User-interactive and Automatic measurements of RR intervals	-0.0004	0.0041
(d) User-interactive and Automatic measurements of QT intervals	0.0079	0.0854

Table 5.6 A study of measurements made by a Cardiologist manually and using the user-interactive system and how they compare with automatically derived measurements (Analysis using the Sign Test)

Test description	Value of constant *c* for Lower 2½ Percentile Value of U (ms)	Value of constant *c* for Median 50 Percentile Value of *U* (ms)	Value of constant *c* for Upper 97½ Percentile Value of *U* (ms)
(a) Manual and Automatic measurements of RR intervals	5	6	7
The probability that the difference (Automatic-Manual) is > 7 ms or < 5 ms is less than 5 %. The most probable difference is 6 ms			
(b) Manual and Automatic measurements of QT intervals	13	17	23
The probability that the difference (Automatic-Manual) is > 23 ms or < 13 ms is less than 5 %. The most probable difference is 17 ms			
(c) User-interactive and Automatic measurements of RR intervals	0	0	0
The probability that the difference (Automatic-User-interactive) is > 0 ms or < 0 ms is less than 5 %. The most probable difference is 0 ms			
(d) User-interactive and Automatic measurements of QT intervals	3	5	7
The probability that the difference (Automatic-User-interactive) is > 7 ms or < 3 ms is less than 5 %. The most probable difference is 5 ms			

5.4.3 Results (Test 4: b)

Figure 5.11 and Table 5.5 part (b) show the results of similar measurements but using QT intervals. The mean fractional difference (automatic minus manual) obtained expressed as a percentage was 3.75% (15 ms) using an average QT value of 400 ms. As can be seen in Figure 5.11 on average, automatic measurements were greater than manual measurements. Similarly the standard deviation of the fractional differences was 8.58% (34.3 ms). Again this is reflected in Figure 5.11 where the 'o's are more dispersed than for RR intervals.

Table 5.6 part (b) give the corresponding results using the Sign Test. The 95% confidence intervals indicate that the difference (automatic minus manual) is most likely to be in the range of 13-23 ms which is consistent with the value of 15.0 ms obtained with Bland and Altman analysis. The Bland and Altman standard deviation of 34.3 ms seems high in comparison to the range 13-23 ms obtained from the Sign Test. This is likely to be due to the higher weighting due to large differences by the $(x\text{-mean}(x))^2$ term in the formula for standard-deviation.

5.4.4 Results (Test 4 : c)

Figure 5.12 shows, for each lead, the difference between automatic and user-interactive measurements of the RR interval as a function of the mean RR interval measured by both methods. As before user-interactive measurements were made by a cardiologist. The results of mean fractional difference and standard deviation of fractional differences of the two measurement methods is shown in Table 5.5 part (c). The mean fractional difference (automatic minus user-interactive) which is indicative of a consistent bias between the two methods expressed as a percentage is -0.04%. Using an average value of RR intervals of 850 ms, this corresponds to -0.3 ms. From Figure 5.12, it can be seen that the difference between the automatic and user-interactive measurements are very small, clustering about 0. The standard deviation of the fractional difference is 0.41% which corresponds to 3.5 ms. It is an indicator of the confidence of the agreement between the two measurement methods by indicating how dispersed the fractional differences obtained from two methods.

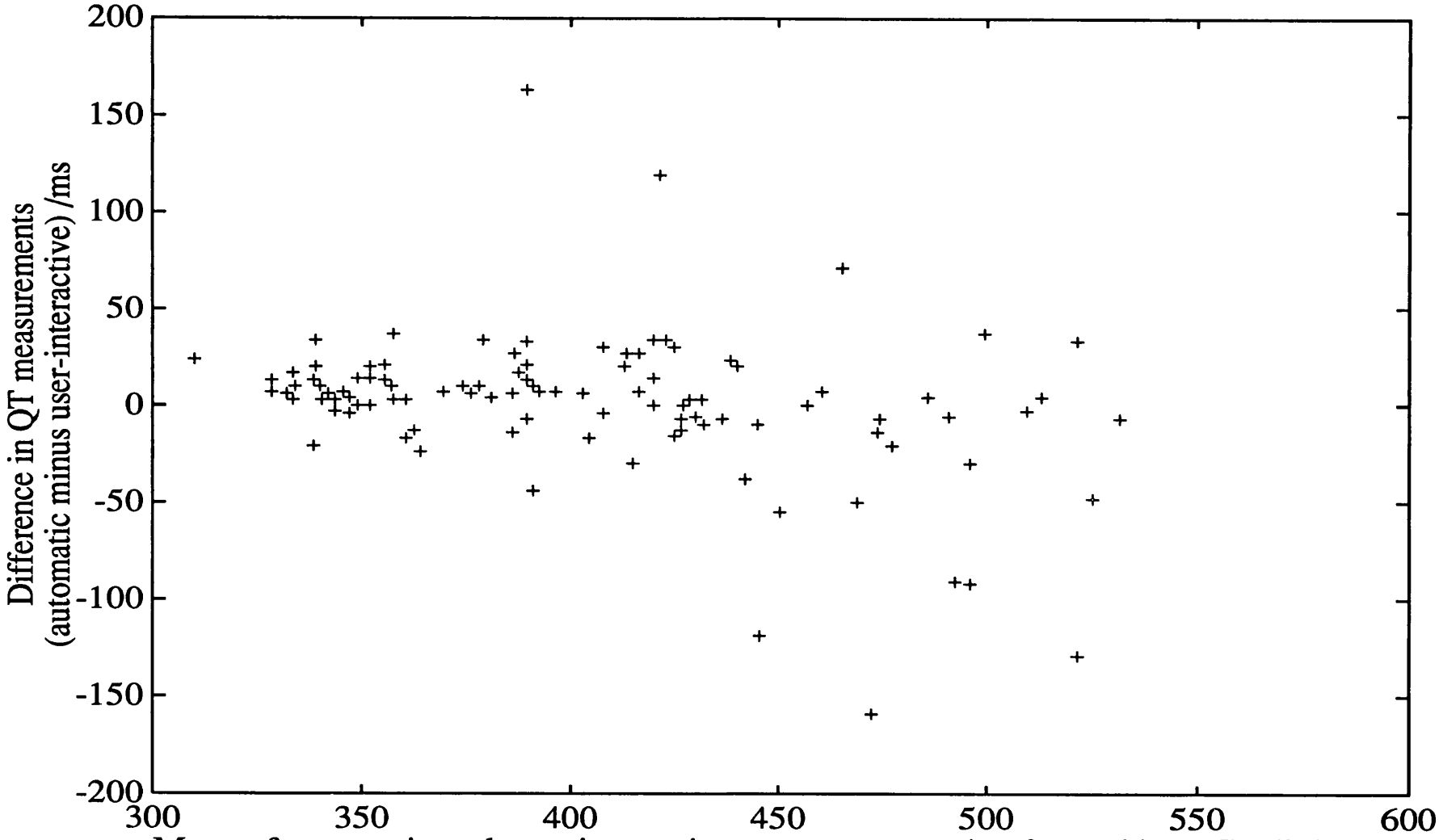
200
150
100
50
0
-50
-100
-150
-200
300
350
400
450
500
550
600
Difference in QT measurements
(automatic minus user-interactive) /ms
Mean of automatic and user-interactive measurements (performed by a Cardiologist)
of QT intervals /ms

Figure [5.13]

Table 5.6 part (c) give the corresponding results using the Sign Test. The 95% confidence intervals indicate that the difference (automatic minus user-interactive is most likely to be 0 ms, or a very small value which the resolution of 1 ms used in the Sign Test does not allow us to visualise. This is consistent with the with -0.3 ms obtained with the Bland and Altman analysis. The 95% confidence interval range shows confirms that there appears to be no difference between the automatic and user-interactive measurements.

5.4.5 Results (Test 4: d)

Figure 5.13 and Table 5.5 part (d) show the results of similar measurements but using QT intervals i.e. for each lead, the difference between automatic and user-interactive measurements of the QT interval as a function of the mean QT interval measured by both methods. The mean fractional difference (automatic minus user-interactive) obtained expressed as a percentage was 0.79% (3.2 ms) using an average QT value of 400 ms. As can be seen in Figure 5.13, on average, automatic measurements were slightly greater than user-interactive measurements when performing QT measurements compared to RR measurements. The standard deviation of the fractional differences was 8.54% (34.2 ms).

Table 5.6 part (d) give the corresponding results using the Sign Test. However the 95% confidence intervals indicate that the difference (automatic minus user-interactive) is most likely to be in the range of 3-7 ms which is consistent with the 3.2 ms obtained with Bland and Altman analysis. Again this range is a much better estimate than that obtained from the Bland and Altman analysis which gives a scatter of 34.2ms.

5.4.6 Discussion (Test 4: a)

From Table 5.5 (a) the bias between the automatic and manual method of measurement of RR intervals was 5.8 ms compared to the confidence of agreement in the two methods which was 7.4 ms. The small value of averaged bias implies that the automatic algorithm was accurate enough to yield measurements similar to those that would have been obtained manually. Since the RR intervals are the best defined, ± 7.4 ms obtained as the averaged confidence of agreement between the two methods is good

representation of the likely accuracy of the system. The corresponding result of the Sign test shows that the most likely difference in the two methods when measuring RR intervals is 6 ms. This is a very similar result with the Bland and Altman analysis. The confidence of agreement can be obtained from the 95% confidence interval which yields an average difference of 5-7 ms. These values are very similar to the estimates obtained in the comparison of the manual and user-interactive methods by each observer when measuring the RR intervals in Test 3 (i and ii). These results show that the two methods agree closely and therefore the automatic method can reliably replace the method of manual measurement.

5.4.7 Discussion (Test 4: b)

From table 5.5 (b) the bias between the automatic and manual measurements of QT intervals was 15.0 ms compared to the confidence of agreement in the two methods which was 34.3 ms. This apparent increase in bias and the decrease in agreement compared to the RR interval results cannot be accounted for in terms of a malfunction of the automatic technique (since there was good agreement of RR intervals) but must be because the QT intervals themselves are much more subjective to define, i.e. the lack of agreement is due to inconsistencies in the way the observer when making manual measurements and the automatic algorithm have interpreted the QT intervals.

The corresponding result of the Sign test reflects this result too. It shows that the most likely difference in the two methods when measuring QT intervals is 17 ms. The confidence of agreement can be obtained from the 95% confidence interval which yields an average difference of 13-23 ms. These results show much bigger differences than for RR intervals (compare Figure 5.10 and 5.11) and suggest again that they must be due to the greater subjectivity involved when measuring QT intervals. It can be said therefore that when intervals are not clearly delimited, the element of subjectivity causes differences between two methods to be greater. The value of bias and scatter obtained using this test is very similar to the estimate obtained in the comparison of the manual and user-interactive methods by observer 2 when measuring QT intervals in Test 3 (iv).

5.4.8 Discussion (Test 4: c)

From table 5.5 (c) the bias between the automatic and user-interactive method of measurement of RR intervals was -0.3 ms compared to the confidence of agreement in the two methods which was 3.5 ms. The small value of averaged bias implies that the automatic algorithm was accurate enough to yield virtually identical measurements to those that would have been obtained by using the user-interactive system. Since the RR intervals are the best defined, ± 3.5 ms obtained as the averaged confidence of agreement between the two methods is good representation of the likely accuracy of the system.

This confidence of agreement estimate is much better than that obtained in the comparisons of the automatic and manual methods of measurement (Test 4a). It can also be seen that with the user-interactive system the bias between the two methods is much less than the bias between the automatic and manual method of measurement (Test 4 a). This seems to suggest that the larger scatter obtained in (Test 4 a) is caused mainly by the inaccuracy of the manual method of measurement, since when a system of greater accuracy (the user-interactive system) is employed the bias and scatter is reduced.

The corresponding result of the Sign test confirms this result. It shows that the most likely difference between the automatic and user-interactive methods when measuring RR intervals is 0 ms (or a very small value which the resolution of 1 ms in the Sign Test does not allow us to visualise). This is a very similar result with the Bland and Altman analysis (-0.3 ms). The confidence of agreement given by the 95% confidence interval also yields an average difference of 0 ms. These values are a slight improvement on the estimates obtained in the comparison of the user-interactive and manual methods by each observer when measuring the RR intervals in Test 3 (i and ii). These results show that the two methods agree closely and therefore the automatic method can reliably replace the method of user-interactive measurement.

5.4.9 Discussion (Test 4: d)

From table 5.5 (d) the bias between the automatic and user-interactive measurements of QT intervals was 3.2 ms compared to the confidence of agreement in the two methods which was 34.2 ms. This apparent increase in bias and the decrease in agreement when compared to the results of the RR intervals cannot be accounted for in terms of a malfunction of the automatic technique (since there was good agreement of RR intervals) but must be because the QT intervals themselves are much more subjective to define, i.e. the lack of agreement is due to inconsistencies in the way the observer making user-interactive measurements and the automatic algorithm have interpreted the QT intervals.

The corresponding result of the Sign test gives a somewhat better estimate. The 95% confidence interval which corresponds to the confidence of agreement yields an average difference range of 3-7 ms. These results, whilst slightly larger than the differences for RR intervals (compare Figure 5.12 and 5.13), still give a small difference between the two methods. It suggests that when an accurate measurement method is used, the bias and scatter even when measuring intervals that are not clearly delimited can be small, hence suggesting much more accurate measurements.

Summary of Findings of Test 4

In the comparison of the automatic and manual method of measurement, the small value of bias obtained implies that the automatic algorithm was accurate enough to yield measurements similar to those that would have been obtained manually. $\pm$ 7.4 ms is the likely accuracy of the system, which corresponds to 2 pixels. These results show that the two methods agree closely and therefore the automatic method can reliably replace the method of manual measurement. It was also found that when intervals are not clearly delimited, the element of subjectivity caused differences between two methods to be greater. This is due to inconsistencies in the way the observer, when making manual measurements, and the automatic algorithm, which represents the bias of the programmer who developed it, have interpreted the intervals. The main advantage of the automatic algorithm is that it is consistent, i.e. repeated measurements on the same

waveforms will yield identical results. The results obtained here are similar to those obtained in the comparison of the manual and user-interactive methods by observer 2 using the Sign Test.

In the comparison of the automatic and user-interactive method of measurement, again the small bias shows that the automatic algorithm was accurate enough to yield measurements similar to those that would have been obtained using the user-interactive system. ± 3.5 ms is the likely accuracy of the system. Therefore the automatic method can reliably replace the method of user-interactive measurement. This bias and confidence of agreement estimates are much better than for the automatic and manual methods of measurement. This suggests that the larger scatter obtained in latter measurements were caused mainly by the inaccuracy of the manual method of measurement, since when a system of greater accuracy (the user-interactive system) was employed the bias and scatter was reduced.

As before, it was found that when intervals were not clearly delimited, the element of subjectivity caused differences between two methods to be slightly greater. This was due to inconsistencies in the way the observer, when making user-interactive measurements, and the automatic algorithm, which represents the bias of the programmer who developed it, have interpreted the intervals. These results obtained show that when an accurate measurement method is used, the bias and scatter, even when measuring intervals that are not clearly delimited, can be small. This system can thus give measurements which are more accurate.

5.5 Inter-Observer Variability Assessment; Comparisons with the Automatic Algorithm

Are there considerable differences between different users who perform the same measurements manually and using the user-interactive system? How do their results compare with results obtained from the automatic algorithm?

5.5.1 Test 5

To test if there were any differences between different users who were asked to perform the same measurements on a given set of waveforms manually and using the user-interactive system, and to compare their performance to the results from the

automatic algorithm, a set of 8 ECGs were selected, to represent a spectrum from "excellent" to "poor" in terms of waveform quality, and incorporating both mono- and biphasic T wave patterns. They are described here:

2 biphasic waveforms denoted by B1 and B2

2 waveforms with a well defined T wave end (Good) denoted by G1 and G2

2 waveforms with a very well defined T wave end (Excellent) denoted by E1 and E2

2 waveforms with a poorly defined T wave end (Poor) denoted by P1 and P2

10 clinicians were asked to analyse these waveforms. The QT and RR measurements corresponding to these waveforms were measured manually, and using the user-interactive system. In cases where the R wave was absent the Q or S wave was used. The same measurement protocol was adopted as before. The QT and RR intervals in these waveforms were also measured automatically. These were then compared to the results obtained by the clinicians.

5.5.2 Results (Test 5)

Figures 5.14 and 5.15 show graphically the results obtained. The results for the RR measurements are shown in Table 5.7 and those for QT intervals are shown in Table 5.8. The mean and standard deviation of measurements by 10 clinicians on each of these waveforms is calculated. The coefficient of variation which is a normalised value of the standard deviation is also calculated and expressed as a percentage.

5.5.3 Discussion (Test 5)

In all the waveforms, the manual measurements of RR intervals were within 2 sampling points or 20 ms of each other except for B1, G2, and P1, who all showed slightly larger standard deviations. These anomalies were generally attributed to a single doctor making measurements that deviated from the norm. For the RR intervals measured manually, the mean coefficient of variation for all eight measurements is given by 0.925%. For the user-interactive measurements this was 0.375%. The accuracy in measurements is improved when the user-interactive system was used. This is reflected

in all cases of RR measurement except P1 where similar coefficient of variation were obtained. On investigation, this was found to be due to 1 clinician making a larger or smaller measurement than normal in each case. In all the cases except B2, the automatic measurements roughly corresponded to the most popular value selected by the clinicians by both manual and user-interactive measurements. This shows that the automatic algorithm produces results that are comparable to the results produced by most experienced clinicians.

Manual measurements of QT intervals for the different waveforms showed standard deviations ranging from 6.3 to 36.5 ms. It is interesting to note that P1, a wave of poor quality T wave end showed the standard deviation of only 6 ms. Upon investigation it was found that a hole had been formed in the paper denoting the T wave end, by one of the clinicians when using the dividers. This made it difficult for the other clinicians to be unbiased. As expected waves G1, G2, E1 and E2 showed the smallest coefficients of variation for both manual and user-interactive measurements, as their T wave end was clearly delimited.

The worst inter-observer variability was observed in P2 when measurements were made user-interactively. This was expected since the user-interactive system gives more sensitive measurements and therefore would be more likely to display the difficulty in determining the T wave end.

In the biphasic waveforms the values measured manually for B1 ranged from 460 ms to 550 ms. Using the user-interactive system, this range is maintained at 464ms to 552 ms. The problem here is essentially one of definition, i.e some clinicians regarded the waveform to be biphasic, others did not. It is interesting to observe that in the biphasic waveforms, the same clinicians often present totally different values when the measurement were made manually and when using the user-interactive system. Only 3 of the doctors were consistent for B1. More were consistent in B2.

For the QT intervals measured manually, the mean coefficient of variation for all eight measurements is given by 4.5%. For the user-interactive measurements of QT intervals this value increased to 4.85%. In some cases like G2, E1 and E2, this result is not reresentative as smaller values of coefficient of variation were obtained in the user-interactive measurements than manual measurements. It is the remaining cases

Table [5.7] RR intervals obtained by manual (upper), user-interactive (lower) and automatic measurements (ms)

	Observer										Mean RR Interval Measured by 10 Doctors $M(RR)$ (ms)	Std. Dev. of RR Intervals Measured by 10 Doctors $\sigma(RR)$ (ms)	Coeff. of Var. of RR Intervals Measured by 10 Doctors $V(RR) = \frac{\sigma(RR)}{M(RR)} \times 100\%$	RR intervals measured by the automatic algorithm (ms)
Waveforms	**1**	**2**	**3**	**4**	**5**	**6**	**7**	**8**	**9**	**10**				
B 1	1050	1060	1060	1060	1060	1040	1040	1040	1050	1070	1053.0	10.6	1.0	1050
	1053	1046	1046	1053	1057	1046	1046	1053	1050	1046	1049.6	4.1	0.4	
B 2	1100	1100	1100	1100	1110	1090	1100	1110	1100	1100	1101.0	5.7	0.5	1118
	1111	1118	1114	1118	1104	1114	1114	1111	1114	1114	1113.2	4.0	0.4	
G1	1100	1100	1100	1100	1110	1090	1090	1090	1100	1110	1099.0	7.4	0.7	1097
	1097	1101	1091	1101	1097	1094	1097	1097	1101	1094	1097.0	3.4	0.3	
G 2	1060	1080	1080	1060	1070	1060	1060	1060	1110	1070	1071.0	16.0	1.5	1060
	1063	1060	1060	1063	1063	1060	1060	1060	1063	1060	1061.2	1.5	0.1	
E 1	1100	1110	1100	1100	1100	1090	1090	1090	1100	1100	1098.0	6.3	0.6	1094
	1094	1097	1091	1091	1094	1097	1097	1094	1097	1094	1094.6	2.4	0.2	
E 2	1070	1060	1060	1080	1070	1060	1060	1060	1060	1060	1064.0	7.0	0.7	1060
	1060	1060	1063	1057	1057	1060	1060	1060	1063	1060	1060.0	2.0	0.2	
P 1	960	940	980	960	960	950	950	950	950	960	956.0	10.7	1.1	952
	955	952	965	989	952	952	952	948	958	952	957.0	12.0	1.3	
P 2	1020	1060	1020	1020	1040	1030	1020	1020	1030	1020	1028.0	13.2	1.3	1029
	1033	1033	1030	1033	1033	1033	1033	1030	1033	1033	1032.4	1.3	0.1	

Table [5.8] QT intervals obtained by manual (upper), user-interactive (lower) and automatic measurements (ms)

	Observer										Mean QT Interval Measured by 10 Doctors $M(QT)$ (ms)	Std. Dev. of QT Intervals Measured by 10 Doctors $\sigma(QT)$ (ms)	Coeff. of Var. of QT Intervals Measured by 10 Doctors $V(QT) = \frac{\sigma(QT)}{M(QT)} \times 100\%$	QT intervals measured by the automatic algorithm (ms)
Waveforms	1	2	3	4	5	6	7	8	9	10				
B 1	480	500	460	490	500	480	550	480	500	510	495.0	24.2	4.9	505
	501	552	505	491	471	488	464	515	478	467	493.2	26.7	5.4	
B 2	470	580	480	490	490	480	560	490	500	500	504.0	36.3	7.2	511
	518	589	528	515	488	501	562	535	505	481	522.2	33.2	6.4	
G1	460	500	460	450	440	440	440	440	460	460	455.0	18.4	4.0	464
	457	545	491	481	494	464	471	471	471	488	483.3	24.8	5.1	
G 2	460	460	460	450	420	440	430	420	450	450	444.0	15.8	3.6	440
	433	433	430	430	430	433	433	433	437	433	432.5	2.1	0.5	
E 1	460	510	460	470	450	450	480	440	460	450	463.0	20.0	4.3	454
	491	457	484	478	461	450	464	478	491	478	473.2	14.4	3.0	
E 2	480	460	460	460	450	440	440	440	460	440	453.0	13.4	3.0	461
	457	440	457	457	457	454	457	457	461	454	455.1	5.6	1.2	
P 1	420	430	420	420	420	420	420	410	410	410	418.0	6.3	1.5	433
	400	494	423	406	423	393	427	410	417	420	421.3	27.8	6.6	
P 2	430	520	500	460	420	480	510	470	520	510	482.0	36.5	7.6	437
	464	478	366	464	437	467	474	478	444	566	463.8	49.0	10.6	

Figure [5.14] Plot of QT intervals measured from 2 Biphasic (B1,B2), Good (G1,G2), Excellent (E1,E2) and Poor (P1,P2) quality waveforms

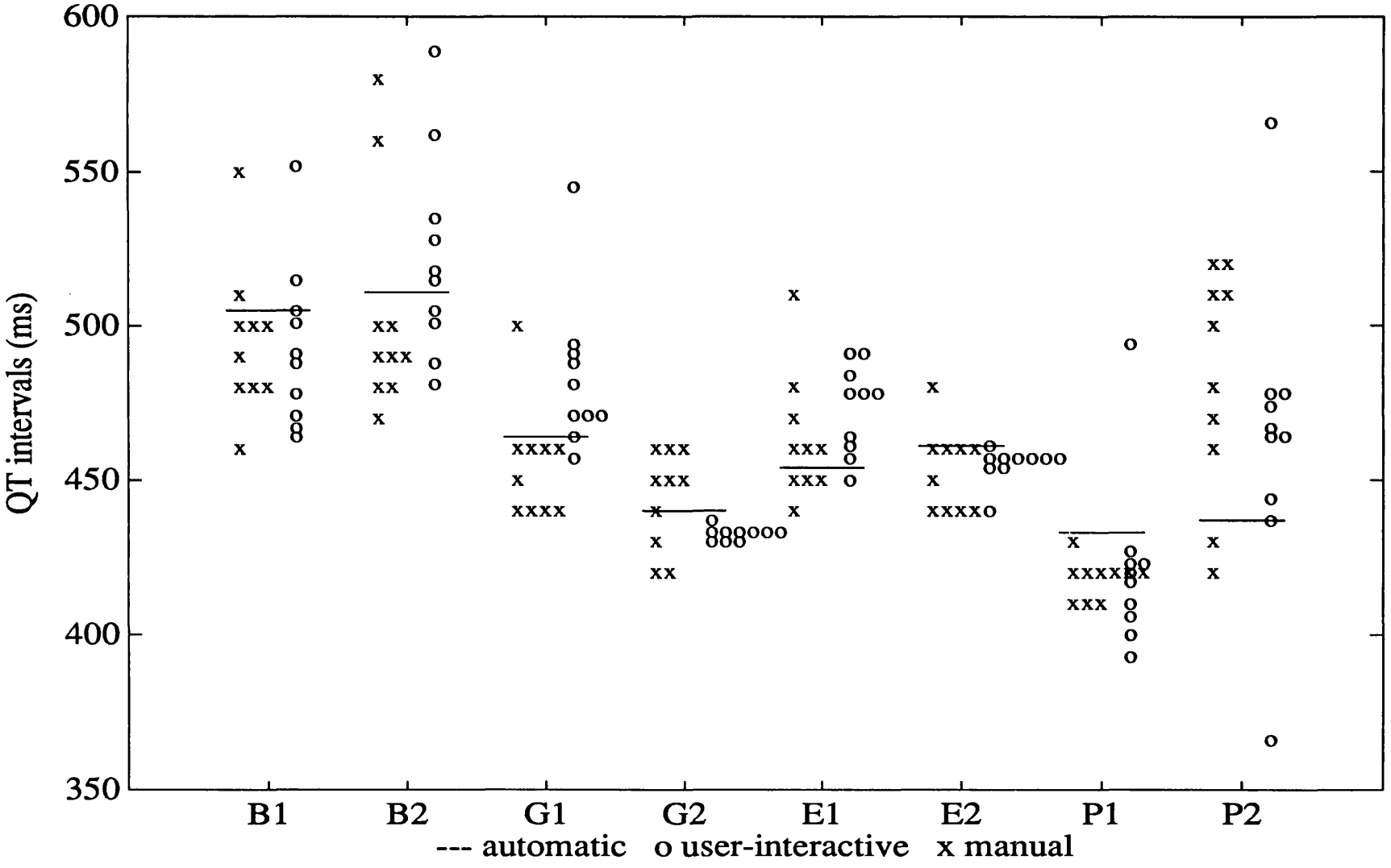

Figure [5.15] Plot of RR intervals measured from 2 Biphasic (B1,B2), Good (G1,G2), Excellent (E1,E2) and Poor (P1,P2) quality waveforms

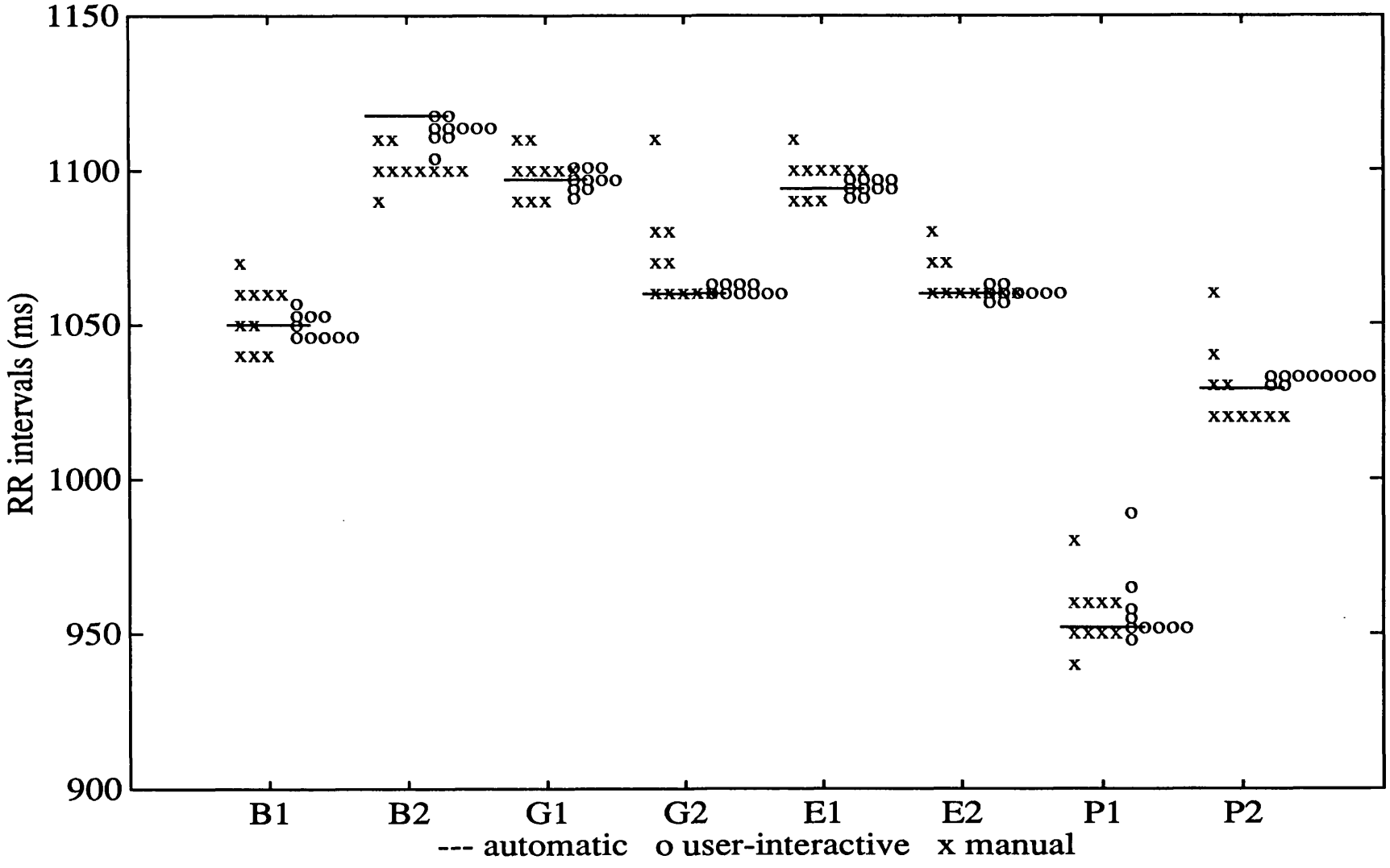

(especially P1 and P2) which reversed this trend and gave the net mean coefficient of variation as shown. This illustrates clearly the subjectivity element when the QT interval, which is a more subjective parameter, is measured by the user-interactive system which is also more sensitive.

5.6 Intra-Observer Variability Assessment

How consistent is any single Cardiologist when he/she makes the same measurements repeatedly? What factors affect this repeatibility?

5.6.1 Test 6

To test if there were any differences (in a single user) when he/she was presented a set of waveforms repeated randomly (unknown to them), a cardiologist was asked to perform such a test, making QT and RR measurements, using the user-interactive system. He was not aware of the nature of the tests.

5.6.2 Results (Test 6)

Table 5.9 and 5.10 show the results obtained for QT and RR intervals respectively. The mean and standard deviation of QT and RR measurements by the cardiologist using 9 different waveforms is calculated. The coefficient of variation which is a normalised value of the standard deviation is also calculated and expressed as a percentage.

Table 5.9 Study of Intra-observer Variability using QT Measurements performed by a Cardiologist

Waveforms	QT Interval Instance 1 (ms)	QT Interval Instance 2 (ms)	QT Interval Instance 3 (ms)	Mean QT Interval $M_{(QT)}$ (ms)	Std. Dev. of QT Intervals $\alpha_{(QT)}$ (ms)	Coeff. of Var. of QT Intervals ($\alpha_{(QT)}$ / $M_{(QT)}$ x 100 %)
Case_01A I_1	471	444	461	458.6	13.7	3.0
Case_02A I_1	454	450	454	452.6	2.3	0.5
Case_03A I_1	474	478	471	474.3	3.5	0.7
Case_04A I_1	396	400	389	395.0	5.6	1.4
Case_01N I_1	342	349	349	346.6	4.0	1.2
Case_02N I_1	332	352	356	346.6	12.9	3.7
Case_03N I_1	430	427	427	428.0	1.7	0.4
Case_07N I_1	342	342	349	344.3	4.0	1.2
Case_06N I_1	383	417	410	403.3	18.0	4.5

Table 5.10 Study of Intra-observer Variability using RR Measurements performed by a Cardiologist

Waveforms	RR Interval Instance 1 (ms)	RR Interval Instance 2 (ms)	RR Interval Instance 3 (ms)	Mean RR Interval $M_{(RR)}$ (ms)	Std. Dev. of RR Intervals $\alpha_{(RR)}$ (ms)	Coeff. of Var. of RR Intervals ($\alpha_{(RR)}$ / $M_{(RR)}$ x 100 %)
Case_01A I_1	1006	1009	1009	1008.0	1.7	0.2
Case_02A I_1	840	840	840	840.0	0.0	0.0
Case_03A I_1	901	908	908	905.6	4.0	0.5
Case_04A I_1	759	759	759	759.0	0.0	0.0
Case_01N I_1	826	826	826	826.0	0.0	0.0
Case_02N I_1	681	681	677	679.6	2.3	0.3
Case_03N I_1	870	870	870	870.0	0.0	0.0
Case_07N I_1	630	630	627	629.0	1.7	0.3
Case_06N I_1	874	874	874	874.0	0.0	0.0

5.6.3 Discussion (Test 6)

The range of standard deviation values obtained for the repeated measurements of QT intervals in the different waveforms ranged from 1.7 to 18.0 ms. In the worst case therefore, the range of intra-observer variability is given by 18 ms. For RR intervals this range was smaller at 0 to 4 ms, i.e. the cardiologist produced very repeatable measurements. This value corresponds to a single sampling interval. The mean coefficient of variation for the repeated measurements of RR and QT interval by a single cardiologist was 0.14% and 1.84% respectively.

Chapter 6 Clinical Investigation and Results

6.1 Introduction

Chapter 1 presented the strong clinical support for the hypothesis that QT intervals recorded on the 12 leads of a standard electrocardiogram contain important information pertaining to irregular and inhomogenous conditions in the pattern of ventricular repolarisation. This hypothesis is supported by studies on patients who show the congenital long QT syndrome, post-infarction patients and patients who die suddenly. This chapter describes a clinical study whose aim was first to find and validate a suitable parameter which would describe QT dispersion. A graphical interface was then developed to calculate and illustrate visully the risk parameter to describe QT dispersion. The second aim of the study was to use this parameter to examine a group of controls and a group of patients with known susceptibility to ventricular arrhythmias in order to examine the importance of QT dispersion and thus shed light on the above hypothesis. Some conclusions are then drawn on the importance of QT dispersion.

6.2 A parameter for risk assessment

The development of a new parameter to assess risk or susceptibility to particular conditions like ventricular arrhythmias, sudden death etc. should be based on certain assumptions and constraints described in this section and should be statistically reliable.

C.Day et al. 1991 defined a parameter known as the *adjusted QT dispersion* to indicate susceptibility of patients to lethal arrhythmias. This is defined as *the result of the maximum rate-corrected QT interval in any of the measurable leads minus the minimum rate-corrected QT interval in any of the measurable leads divided by the square root of the number of leads in which the QT intervals are measurable.* A good quality 12 lead electrocardiogram would normally allow QT interval measurements in each lead. Typically there are two to three waveforms in each lead. Generally, waveforms that are synchronously recorded are studied. Most studies on QT dispersion use a single QT measurement from each lead. This would yield 12 QT intervals in total.

However there are many reasons why the QT intervals may not be measurable in all leads. For example the T wave in a particular lead may be apparently iso-electric or excessive noise may prevent any accurate determination of the Q wave onset or T wave end.

In order to draw conclusions about the homogeneity of repolarisation in the heart, a minimum number of leads from which the QT and RR intervals are measured should be stipulated to make the assessment believable. In the study carried out by C.Day et al. 1990, 1991, the minimum number of leads used was 5. This comprised less than half of the 12 lead data set that can normally be used to make inferences on QT dispersion. Furthermore, their definition of *adjusted QT dispersion* employs extreme values of the rate-corrected QT intervals, i.e. the maximum and minimum. As only half the leads may have been used to make an assessment, there is a high probability that the true maximum or minimum may have occurred in the 6 leads that were not considered. Even if a higher number of leads were considered, the calculation of *adjusted QT dispersion* only uses the 2 extreme values of the 12 QT intervals available. This ignores data from the 10 remaining leads which may be important. Finally the *adjusted QT dispersion* is not standardised to account for naturally occurring differences in QT interval measurements in different people. It depends on absolute measurements which do not lend themselves easily to comparisons. Some drugs have also been known to affect the duration of the QT interval, for example the drug amiodarone is known to prolong QT intervals in all leads. If relative rather than absolute measurements were used to characterise QT dispersion, such an effect can be disregarded. However in absolute measurements of the QT intervals, such an effect can lead to erroneous results of QT dispersion.

In their definition of *adjusted QT dispersion*, C.Day et al. 1991, used QT intervals that were corrected for heart rate using Bazett's formula (H.C.Bazett, 1920). This is the most common measurement that is used to represent the QT interval in all leads of the electrocardiogram. As has been shown in Chapter 1, many researchers starting with Bazett in 1920 felt that the QT interval varied in a distinctive manner with heart rate (represented as the inverse of the RR interval). Bazett proposed that the QT interval varied as the square-root of the heart rate i.e. it varied as the inverse square root of the

preceding RR interval. He proposed that the QT interval corrected for this variation may be a more useful measure of the depolarisation-repolarisation interval of the ventricles. His definition of the corrected QT interval has been adopted world-wide and is given by:

$$QT_C = \frac{QT}{\sqrt{RR}} \quad \ldots\ldots\ldots\ldots\ldots\ldots\ldots\ldots\ldots\ldots\ldots\ldots \quad (6.1)$$

Many other researchers have proposed alternative equations for the correction of the QT interval, some also taking into account QT variation with sex and age. Recent studies (G.R.Pai and J.M.Rawles, 1989) have shown that whilst QT correction using Bazett's formula may be popular, it is inaccurate when dealing with beat-to-beat changes in heart rate, for example, as presented by patients with arrhythmias.

In the study proposed, it was decided that the normal resting 12 lead electrocardiograms showing regular heart rates would be used. The QT intervals recorded would be rate-corrected using Bazett's formula, as the 12 leads were not recorded synchronously, and as this was the most widely accepted and used correction.

In this study, an investigation is made for a suitable new parameter to describe QT dispersion. This is compared to Day et al.'s *adjusted QT dispersion.* It should meet the following requirements:

- (i) It should be based on parameters or variables that are descriptive of the distribution of the population of data, in this case the 12 lead rate-corrected QT intervals.
- (ii) It should attempt to use the maximum quantity of data available.
- (iii) It should yield a relative measure of dispersion, standardised across different groups of patients, so comparisons can be made.

6.3 Design of Experimental Investigation

The first step to finding a parameter that would describe QT dispersion well was to investigate whether a particular distribution with its characteristic parameters could represent across different patient groups, the rate-corrected QT intervals measured from each of the leads. As the normal distribution and its characteristic parameters of mean and standard deviation are well understood and easy to calculate, it was decided that

comparisons between rate-corrected QT values from different patient populations and the normal distribution would be suitable. The *Chi-squared goodness of fit test* was used to perform this comparison.

To enable this test to be performed QT and RR intervals from hard-copy standard 12 lead electrocardiograms of 15 patients with previously documented sustained monomorphic ventricular tachycardia attending an arrhythmia clinic (hence referred to as 'arrhythmogenic patients') and 15 control patients were digitised and measured using the automatic algorithm (as this was thought to be the most objective). The latter were consecutive attendees at an electrocardiography clinic who were not known to have suffered any arrhythmia. Further patient details are given in section 6.4. All patients were in sinus rhythm at the time the electrocardiograms were recorded.

Note that a subsequent electrophysiological study on patient number 10 in the arrhythmogenic group revealed that the original arrhythmia was in fact supraventricular tachycardia with left bundle branch block (ECG in sinus rhythm also showed left bundle branch block). Data from this patient are included in the subsequent tables for interest (i.e. Tables 6.4 - 6.6) but have not been included in any tests or graphs (Figures 6.1 - 6.12).

6.3.1 The generalized χ^2 test for goodness-of-fit

The χ^2 test can be used to assess the goodness of fit of a sample of data to any hypothesized distribution of a population. It performs this in the following way.

Samples of data can be expressed in terms of their occurrence or observed frequencies in the interval of the variate x. Let the hypothesized distribution be denoted by p.d.f. $f(x)$, where it is assumed for the moment that all parameters are specified (simple hypothesis). If the entire range of x is divided into n intervals $k = 1,.....n$ then the probability of observing x in the interval k is

$$p_k = Pr(x \in k) = \int_k f(x)\,dx \quad \ldots\ldots\ldots\ldots\ldots\ldots\ldots\ldots \quad (6.2)$$

Since each observation must fall into *some interval,*

$$\sum_{k=1}^{n} p_k = 1 \quad \ldots\ldots\ldots\ldots\ldots\ldots\ldots\ldots\ldots\ldots \quad (6.3)$$

If the total number of points in the sample is N and if we denote f_k = number (frequency) of sample observations in the kth interval, then

$$N = \sum_{k=1}^{n} f_k \quad \ldots\ldots\ldots\ldots\ldots\ldots\ldots\ldots\ldots\ldots \quad (6.4)$$

From the hypothesized p.d.f. $f(x)$ we would expect to find Np_k in the kth interval.

The *generalised chi-squared statistic is defined as:*

$$X^2 = \sum_{k=1}^{n} \frac{(f_k - Np_k)^2}{Np_k} = \left(\frac{1}{N} \sum_{k=1}^{n} \frac{f_k^2}{p_k} \right) - N \quad \ldots\ldots\ldots\ldots\ldots \quad (6.5)$$

and is used to measure the deviation of the observed sample frequency distribution ($f1$,.....,fn) from that expected from the hypothetical distribution.

As N becomes large, the statistic X^2 becomes (asymptotically) χ^2- distributed with $(n\text{-}1)$ degrees of freedom (eg. S.L.Meyer, 1975):

$$X^2 \rightarrow \chi^2 (n-1) \quad as \quad N \rightarrow \infty \quad \ldots\ldots\ldots\ldots\ldots\ldots\ldots \quad (6.6)$$

If the number of constraints is r where r refers to the number of characteristic parameters of a distribution, then the number of degrees of freedom is reduced by r, and X^2 is asymptotically $\chi^2 (n-r-1)$:

$$X^2 \rightarrow \chi^2 (n-r-1) \quad as \quad N \rightarrow \infty \quad \ldots\ldots\ldots\ldots\ldots\ldots\ldots \quad (6.7)$$

Therefore to perform the χ^2 goodness of fit test :

N observations of data x are divided or binned into n intervals, each containing f_k points. As the asymptotic distribution of the quantity (6.5) is the feature of interest, intervals must be selected to contain at least 4 or 5 data points so that (6.7) is satisfied approximately. The intervals need not be of the same size, and in fact, intervals containing rare occurrence should be summed together to obtain the minimum numbers of 4 or 5. Conversely, the greater the number of intervals the more that can be learned about the shape of the distribution.

p_k is then calculated and X^2 computed using (6.5). A level of significance α is selected and the table of cumulative χ^2 for $(n-r-1)$ degrees of freedom is used to compare X^2 with $\chi^2(n-r-1, 1-\alpha)$. If $X^2 > \chi^2(n-r-1, 1-\alpha)$ the hypothesized $f(x)$ is *rejected* at the significance level α, that is, the fit is not good at significance level α. Otherwise the fit (i.e., $f(x)$) is accepted as being consistent with the data.

6.3.2 Standardisation of QT_c before the Chi-squared test

The Chi-squared goodness of fit test was used to compare (separately) the rate-corrected QT interval distributions of both controls and arrhythmogenics to the normal distribution. QT and RR intervals were measured from 15 controls and 14 arrhythmogenic patients using the automatic algorithm. Rate-corrected QT intervals were calculated in all the leads in which QT and RR intervals were measurable for both groups of patients. As each patient displayed different rate-corrected QT intervals even within the control and arrhythmogenic groups, and as we were interested in comparing *only* the *shape* of the distributions, the rate-corrected QT intervals for each patient were standardised to yield a mean rate-corrected QT interval of 0 and a rate-corrected QT standard deviation of 1. This was performed on each of the measurable leads of a patient using the following equation:

$$(QT_{c_{std}})_i = \frac{(QT_c)_i - \overline{QT_c}}{\sigma(QT_c)} \quad \ldots\ldots\ldots\ldots\ldots\ldots\ldots\ldots\ldots\ldots \quad (6.8)$$

where $(QT_c)_i$ refers to the rate-corrected QT interval in the lead i where i can be any lead: I,II,...V5,V6 of a patient. $\overline{QT_c}$ refers to the mean rate-corrected QT interval calculated from all the measurable leads in a patient and $\sigma(QT_c)$ refers to the standard deviation of the rate-corrected QT intervals also calculated from all the measurable leads in a patient.

Table 6.1a and b describe an example using data from patient number 1 in the control group:

Table 6.1a Creating standardised QT_c for patient number 1 in the Control Group

Lead Name	QT interval /secs	RR interval /secs	$QT_c = \frac{QT}{\sqrt{RR}}\ secs^{1/2}$	$QT_{c_{std}} = \frac{QT_c - \overline{QT_c}}{\sigma(QT_c)}$
I	0.345	0.826	0.380	-0.552
II	0.352	0.830	0.386	0.107
III	0.362	0.826	0.398	1.270
AVR	0.349	0.792	0.392	0.671
AVL	0.328	0.796	0.368	-1.718
AVF	0.342	0.799	0.383	-0.260
V1	0.342	0.789	0.385	-0.024
V2	0.342	0.792	0.384	-0.095
V3	0.359	0.792	0.403	1.766
V4	0.352	0.806	0.392	0.664
V5	0.342	0.809	0.380	-0.491
V6	0.335	0.813	0.372	-1.338

Table 6.1b Mean and Standard Deviation of standardised and non-standardised rate-corrected QT intervals from patient number 1 in the Control Group

Mean QT_c: $\overline{QT_c}$ /secs $^{1/2}$	Standard deviation of QT_c : $\sigma(QT_c)$ /secs $^{1/2}$	Mean $QT_{c_{std}}$: $\overline{QT_{c_{std}}}$	Standard deviation of $QT_{c_{std}}$: $\sigma(QT_{c_{std}})$
0.385	0.010	0.0	1.00

The second and third columns of Table 6.1a show the uncorrected QT intervals and RR intervals expressed in seconds. The fourth column shows the rate-corrected QT intervals and the final column shows the standardised rate-corrected QT intervals calculated using equation (6.8). The mean and standard deviation of both these non-standardised and standardised rate-corrected QT intervals are shown in Table 6.1b. For the latter, the mean obtained is 0 and the standard-deviation is 1.

This process of standardisation is repeated for all the rate-corrected QT intervals for each patient in each group. For each patient there were at least 10 leads in which the QT and RR intervals were measurable. The total number of standardised rate-corrected QT values obtained for the control group was 172 whilst that for the arrhythmogenic group was 153. These rate-corrected standardised values were then used in the Chi-squared goodness of fit test to compare (separately) the distributions of both controls and arrhythmogenics to the normal distribution.

6.3.3 The Chi-squared test and results for Controls and Arrhythmogenics

For the *control group* the distribution of 172 rate-corrected standardised QT intervals is compared to the normal distribution whilst for the *arrhythmogenic group* the distribution of 153 rate-corrected standardised QT intervals is compared to the normal distribution. Using the notation developed in section 6.3.1:

- The number of observations N is 172 for controls and 153 for arrhythmogenics
- k comprises a series of intervals of standardised rate-corrected QT interval ranging from -2.70 to 2.70 in steps of 0.300
- f_k is the actual number of occurrences of standardised rate-corrected QT values in the k^{th} interval
- p_k is the probability of observing standardised rate-corrected QT values in the interval k and for the normal distribution is given by *the area under the normal probability density function curve in the interval k:*

$$p_k = \int_k f(x)\, d(x) = \int_k \frac{1}{\sigma\sqrt{2\pi}} e^{-(x-\bar{x})^2/2\sigma^2}\, d(x) \quad \ldots\ldots\ldots\ldots\ldots (6.9)$$

where $\bar{x}$ is the mean and σ is the standard deviation of the standardised rate-corrected QT intervals calculated from all the leads of the patients in the control group or all the leads of the patients in the arrhythmogenic group.

To calculate the area under the curve the following approximation is used:
Each interval k is sub-divided into 300 intervals of 0.001 and the values of $f(x)$ at each of these sub-intervals is calculated. Using the approximation that the area under each sub-interval of 0.001 is given by the rectangular area $0.001 \times f(x)$ then:

$$p_k = \sum_{s=0}^{s=300} f(x) \times 0.001 \text{ where } x = k + 0.001(s) \quad \ldots\ldots\ldots\ldots (6.10)$$

- Np_k is the predicted number of occurrences of standardised, rate-corrected QT values occurring in the k^{th} interval based on the normal distribution.

Table 6.2 Results from the Chi-squared test for the Control Group

k	f_k		p_k	Np_k		$\frac{(f_k - Np_k)^2}{Np_k}$
-2.7 to < -2.4	0		0.0037	0.6403		
-2.4 to < -2.1	0	⇒ 4	0.0081	1.3938	⇒ 4.787	0.1294
-2.1 to < -1.8	4		0.0160	2.7529		
-1.8 to < -1.5	6		0.0287	4.9333		0.2307
-1.5 to < -1.2	11		0.0466	8.0215		1.1059
-1.2 to < -0.9	15		0.0688	11.8346		0.8467
-0.9 to < -0.6	12		0.0921	15.8425		0.9320
-0.6 to < -0.3	18		0.1119	19.2429		0.0803
0.3 to < 0.0	21		0.1233	21.2077		0.0020
0.0 to < 0.3	16		0.1233	21.2077		1.2788
0.3 to < 0.6	22		0.1119	19.2429		0.3950
0.6 to < 0.9	13		0.0921	15.8425		0.5100
0.9 to < 1.2	15		0.0688	11.8346		0.8467
1.2 to < 1.5	7		0.0466	8.0215		0.1301
1.5 to < 1.8	10		0.0287	4.9333		
1.8 to < 2.1	1	⇒ 12	0.0160	2.7529	⇒ 9.7203	0.5347
2.1 to < 2.4	1		0.0081	1.3938		
2.4 to < 2.7	0		0.0037	0.6403		

Table 6.2 gives the results from the calculations of the Chi-squared test for the group of controls. Testing for the hypothesis:

$$H0 : p_k = \int_k f(x)\, d(x) = \int_k \frac{1}{\sigma\sqrt{2\pi}} e^{-(x-\bar{x})^2/2\sigma^2}\, d(x) \quad \text{for } \textit{the Controls} \quad . \; . \; (6.11)$$

i.e. that the shape of the standardised rate-corrected QT intervals of the control group follows that of the normal distribution, we obtain values of f_k, p_k and Np_k. As can be seen in column two, in the first two intervals of k: k = -2.7 to <-2.4, k = -2.4 to <-2.1, and in the last three intervals of k: k = 1.8 to <2.1, k = 2.1 to <2.4, k = 2.4 to <2.7, each contains fewer than four events. Accordingly, the first three intervals and the last four intervals are each summed to obtain the minimum number of events, four. Np_k is now calculated for the 13 intervals :

k = -2.7 to < -1.8, k = -1.8 to <-1.5, k = -1.5 to <-1.2, k = -1.2 to < -0.9,

k = -0.9 to <-0.6, k = -0.6 to <-0.3, k = -0.3 to < 0.0, k = 0.0 to <0.3,

k = 0.3 to <0.6, k = 0.6 to < 0.9, k = 0.9 to <1.2, k = 1.2 to <1.5, k = 1.5 to <2.7

and the corresponding deviation of the observed sample frequency distribution from that of the hypothetical are computed (last column). For the 13 intervals of k above, the Chi-squared statistic X^2 is given by 0.1294 + 0.2307 + 1.1059 + 0.8467 + 0.9320 + 0.0803 + 0.0020 + 1.2788 + 0.3950 + 0.5100 + 0.8467 + 0.1301 + 0.5347 = 7.02

There are two constraints on the sum firstly due to $\sum p_k = 1$ and secondly due to the number of characteristic parameters of the normal distribution, $r = 2$. There are $n = 13$ data intervals; hence the number of degrees of freedom is $\chi^2(13\text{-}2\text{-}1) = \chi^2(10)$. For more details refer to A.K.Bahn, 1972. Suppose we choose a significance level $\alpha = 0.05$, i.e there is a probability of 0.05 that the true hypothesis H_o will be incorrectly rejected through chance alone. For $\chi^2(10)$, the $\alpha = 0.05$ level corresponds to $\chi^2(10) = 18.31$ (refer to Chi-squared tables in S.L.Meyer, 1972) i.e. 5% of the time random sampling will cause $\chi^2(10)$ to be greater than 18.31. This choice of α means that the choice of fit will be rejected if $X^2 \geq 18.32$. The observed value 7.02 is clearly acceptable and H_o is consistent with the data. Suppose we chose a higher level of significance eg. $\alpha = 0.70$, i.e there is a probability of 0.70 that the true hypothesis H_o will be rejected. For $\chi^2(10)$, the $\alpha = 0.70$ level corresponds to $\chi^2(10) = 7.27$, i.e. 70% of the time random sampling will cause $\chi^2(10)$ to be greater than 7.27. As the X^2 value obtained is even lower than this, i.e. 7.02, this implies that the observed distribution of the data obtained from the group of controls fits the hypothesized normal distribution very well.

Table 6.3 Results from the Chi-squared test for the Arrhythmogenic Group

k	f_k		p_k	Np_k		$\frac{(f_k - Np_k)^2}{Np_k}$
-2.7 to < -2.4	0		0.0037	0.5628		
-2.4 to < -2.1	2	⇒ 6	0.0080	1.2289	⇒ 8.5968	0.7844
-2.1 to < -1.8	1		0.0159	2.4337		
-1.8 to < -1.5	3		0.0286	4.3714		
-1.5 to < -1.2	9		0.0465	7.1217		0.4594
-1.2 to < -0.9	14		0.0688	10.5232		1.1487
-0.9 to < -0.6	16		0.0922	14.1033		0.2551
-0.6 to < -0.3	17		0.1121	17.1437		0.0012
0.3 to < 0.0	17		0.1235	18.9014		0.1913
0.0 to < 0.3	14		0.1235	18.9014		1.2710
0.3 to < 0.6	24		0.1121	17.1437		2.7421
0.6 to < 0.9	8		0.0922	14.1033		2.6413
0.9 to < 1.2	9		0.0688	10.5232		0.2205
1.2 to < 1.5	6		0.0465	7.1217		0.1767
1.5 to < 1.8	7		0.0286	4.3714		1.5805
1.8 to < 2.1	3		0.0159	2.4337		
2.1 to < 2.4	3	⇒ 6	0.0080	1.2289	⇒ 4.2254	0.7453
2.4 to < 2.7	0		0.0037	0.5628		

Table 6.3 gives the results from the calculations of the Chi-squared test for the group of *arrhythmogenics*. Using the same technique as above, the chi-squared statistic X^2 is found to be 12.25.

As there are n = 13 data intervals, the number of degrees of freedom is $\chi^2(13\text{-}2\text{-}1) = \chi^2(10)$. Suppose we choose a significance level $\alpha = 0.05$, i.e there is a probability of 0.05 that the true hypothesis H_o will be rejected. For $\chi^2(10)$, the $\alpha = 0.05$ level corresponds to $\chi^2(10) = 18.31$, (refer to Chi-squared tables in S.L.Meyer, 1972) i.e. 5% of the time random sampling will cause $\chi^2(10)$ to be greater than 18.31. This choice of α means that the choice of fit will be rejected if $X^2 \geq 18.32$. The observed value 12.25 is clearly acceptable and H_o is consistent with the data. Suppose we chose a higher level of significance eg. $\alpha = 0.25$, i.e there is a probability of 0.25 that the true hypothesis H_o will be rejected. For $\chi^2(10)$, the $\alpha = 0.25$ level corresponds to $\chi^2(10) = 12.55$, i.e. 25% of the time random sampling will cause $\chi^2(10)$ to be greater than 12.55. As the X^2 value obtained is even lower than this, i.e. 12.25, this implies that the observed distribution of the data fits the hypothesized normal distribution very well.

6.3.4 Discussion

Both the distributions of the control and arrhythmogenic groups show a very good fit to the normal distribution. This is confirmed by Figures 6.1 and 6.2 which show histograms of the standardised, rate-corrected QT intervals of both groups respectively with normalised 'normal or Gaussian distribution' curves superimposed. The total area is normalised to NI where N is the number of data values and I is the width of a histogram interval.

As the distributions of the standardised rate-corrected QT intervals of both groups follow a normal distribution, a risk parameter to characterise QT dispersion in a patient can be derived from the characteristic parameters of the normal distribution. A parameter known as the *coefficient of variation*, V, is proposed (M.H.Reiger, R.N.Mohapatra, S.N.Mohapatra, 1975). It is a relative measure of dispersion, allowing comparisons across groups with varying magnitudes of data. It also utilises all possible leads of data in a patient, thereby meeting all the requirements outlined in section 6.1. In a patient whose QT intervals were to be studied, the *coefficient of variation* of QT intervals (hence referred to as *QT coefficient of variation*) would give a measure of their dispersion i.e. how much they varied relative to the mean. For each patient it can be calculated using:

$$V_{QT_c} = \frac{\sigma_{QT_c}}{\overline{QT_c}} \times 100\ \% \quad \ldots\ldots\ldots\ldots\ldots\ldots\ldots\ldots\ldots\ldots\ldots (6.13)$$

The mean $\overline{QT_c}$, and standard deviation σ, of the rate-corrected QT interval is calculated from all the leads in which the QT intervals are measurable in a patient. The *QT coefficient of variation* expressed as a percentage is then defined as the standard deviation divided by the mean and multiplied by 100.

Figure [6.1] A histogram of 172 standardised rate-corrected QT intervals from a group of Controls with normalised Gaussian curves superimposed

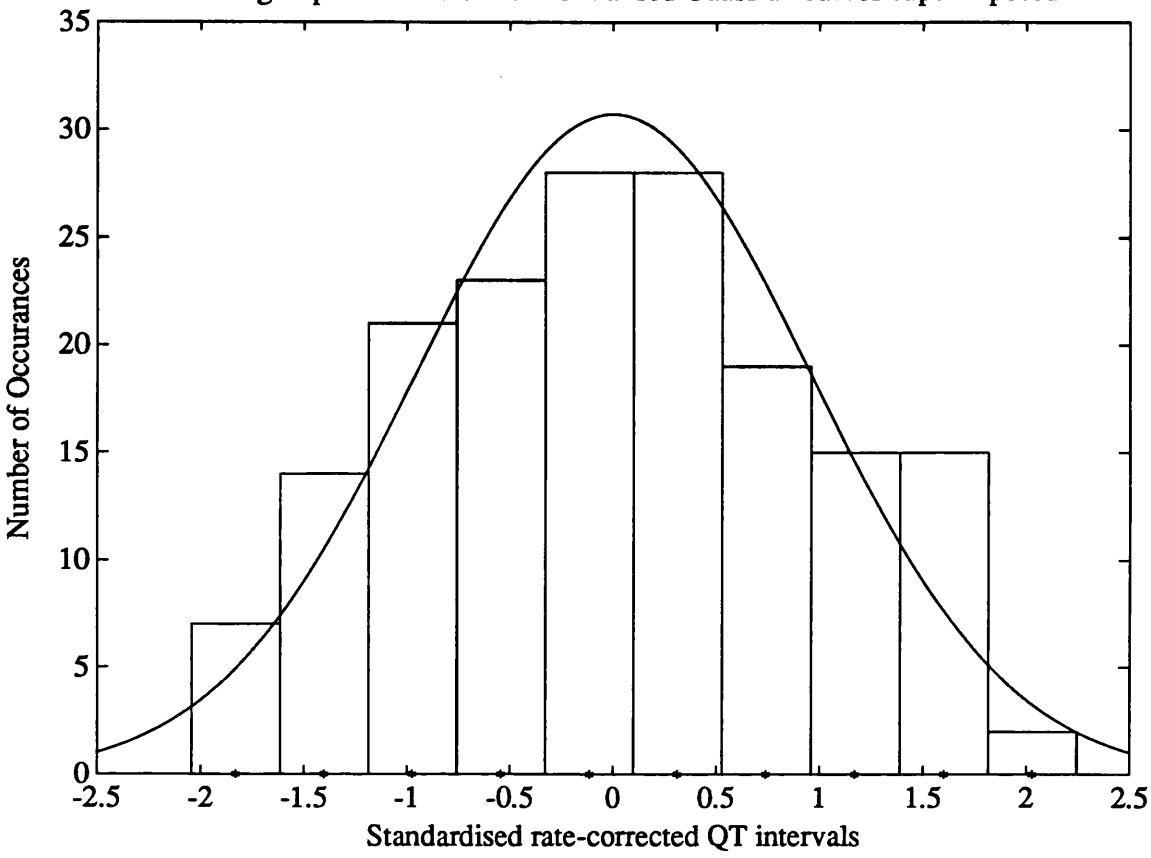

Figure [6.2] A histogram of 153 standardised rate-corrected QT intervals from a group of Arrhythmogenics with normalised Gaussian curves superimposed

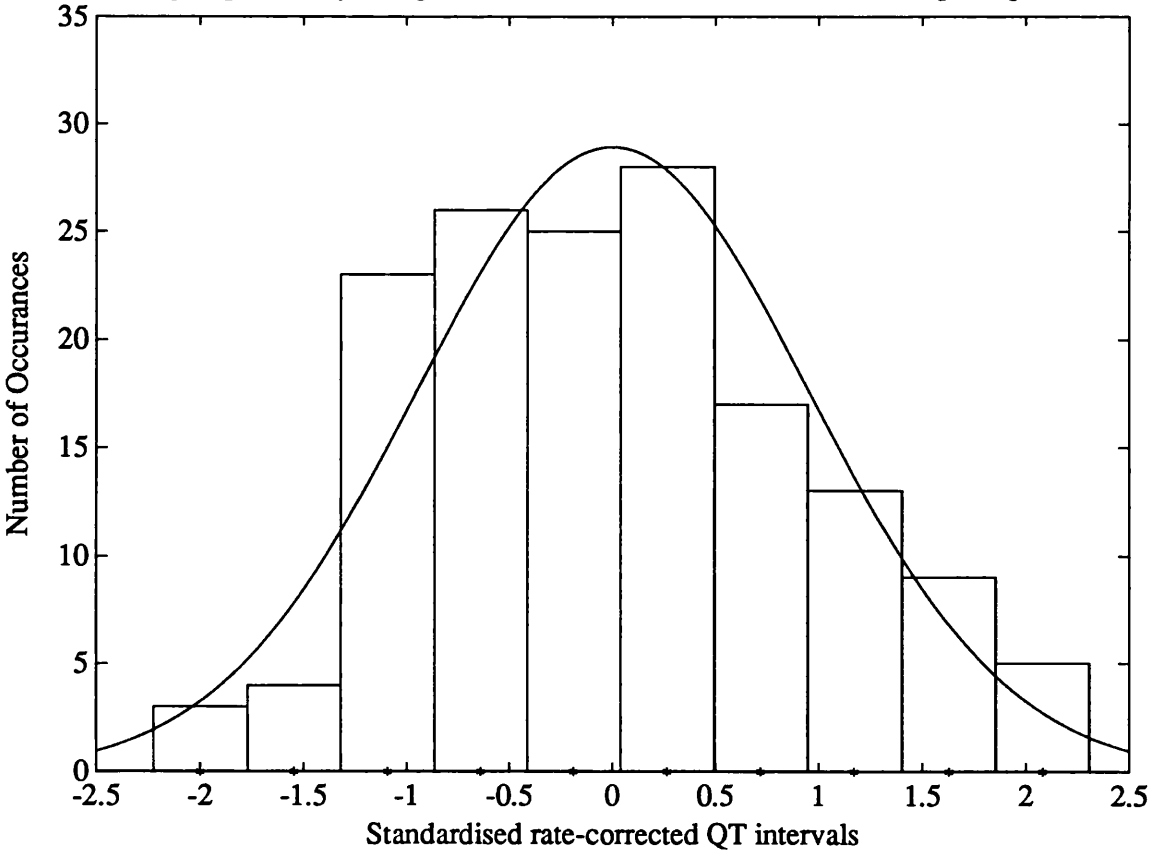

6.4 Clinical Study of Dispersion

From the previous section, the *coefficient of variation, V,* has been established as a suitable risk parameter to assess dispersion of rate-corrected QT intervals in different patients. A clinical study of this parameter in the 2 groups previously mentioned, 15 controls and 15 arrhythmogenics i.e. patients with previously documented sustained monomorphic ventricular tachycardia attending an arrhythmia clinic, can be made to assess its importance as an indicator of risk to ventricular arrhythmias. The QT and RR measurements above were performed by the *automatic* algorithm. In addition to this, measurements were also made on the same data by a cardiologist (not aware of the purpose of the study) using the *user-interactive* algorithm. The *coefficient of variation V,* of rate-corrected QT intervals was calculated for each patient in both the control and arrhythmogenic groups separately, using data obtained from the user-interactive and automatic algorithms. For completeness and to facilitate comparisons, the measure of dispersion as proposed by C.Day et al., 1991 i.e. the *adjusted QT dispersion* was also calculated similarly using rate-corrected QT intervals.

All patients were on treatment and in sinus rhythm at the time the electrocardiograms were recorded. Patient details are given in Tables 6.4a and b. As mentioned previously, a minimum of 10 leads were used per patient. If this requirement could not be met in a particular patient due to the poor quality of their ECG tracings, this patient would be disregarded and another selected for the same group.

Tables 6.5 and 6.6 give the *adjusted QT dispersion* and *QT coefficient of variation* of rate-corrected QT intervals for the 15 controls and 15 arrhythmogenics respectively. These were calculated using QT and RR intervals from the user-interactive and automatic algorithm.

Table 6.4a Clinical details of Control Patients

Patient no :	Age / Gender	Diagnosis	Treatment
1	40M	Angina	Nitrates
2	53M	Hypertension	Nifedipine
3	69M	Angina / Hypertension	Nifedipine
4	47M	Chest pain	Nitrates
5	44F	Chest pain	Nil
6	50M	Hypertension / Atrial fibrillation	Digoxin
7	41M	Supraventricular tachycardia	Mianserin
8	76M	Angina / previous infarct	Metoprolol
9	30F	Chest pain	Nil
10	46M	Hypertension	Enalapril
11	61M	Angina	Nitrates
12	40M	Chest pain	Nil
13	42M	Hypertension / Angina	Metoprolol
14	51M	Angina	Nil
15	36M	Hypertension	Diuretic

Table 6.4b Clinical details of Arrhythmogenic Patients

Patient no :	Age / Gender	Diagnosis	Treatment
1	52M	IHD Ventricular tachycardia	Sotalol
2	72M	IHD Ventricular tachycardia	Amiodarone
3	57M	IHD Ventricular tachycardia	ICD / Amiodarone
4	54M	IHD Ventricular tachycardia	Amiodarone
5	39M	DCM Ventricular tachycardia	Sotalol / Amiodarone
6	42M	DCM Ventricular tachycardia	Mexiletine
7	55M	IHD Ventricular tachycardia	Amiodarone
8	63M	DCM Ventricular tachycardia	Flecainide
9	68M	IHD Ventricular tachycardia	Mexiletine
10	58M	IHD SVT / LBBB*	Atenolol
11	50M	IHD Ventricular tachycardia	Amiodarone
12	47M	IHD Ventricular tachycardia	Sotalol
13	55M	IHD Nonsustained VT	Amiodarone
14	62M	IHD Ventricular tachycardia	ICD
15	57M	IHD Ventricular tachycardia	ICD / Amiodarone

IHD = ischaemic heart disease, DCM = dilated cardiomyopathy

VT = ventricular tachycardia, ICD = implantable defibrillator

* This patient with complete left bundle branch block was originally thought to have ventricular tachycardia. Subsequent electrophysiological study revealed supra ventricular tachycardia only.

Table 6.5 Adjusted QT Dispersion and QT Coefficient of Variation calculated (using both the User-interactive and Automatic algorithms) from Rate-Corrected QT intervals of 15 Control Patients

Controls	Adjusted QT Dispersion (ms) $\frac{QT_c\,(max) - QT_c\,(min)}{\sqrt{No\ of\ leads\ considered}}$		QT Coefficient of Variation V_{QT_c} (%) $\frac{\sigma_{QT_c}}{QT_c} \times 100$	
	User-interactive algorithm	Automatic algorithm	User-interactive algorithm	Automatic algorithm
1	17.6	10.3	4.6	2.7
2	23.3	13.8	5.3	3.6
3	22.9	14.4	5.1	3.3
4	7.8	11.1	2.3	3.2
5	18.5	24.9	5.3	6.3
6	14.9	11.9	3.5	3.4
7	26.7	20.3	5.5	4.8
8	16.5	12.9	3.9	3.6
9	22.1	13.8	5.6	3.7
10	34.9	14.0	8.2	3.1
11	13.1	13.1	3.0	3.6
12	15.2	19.0	4.2	5.1
13	10.9	14.6	2.9	4.5
14	12.4	14.0	3.4	3.1
15	12.2	11.9	3.0	3.3

Table 6.6 Adjusted QT Dispersion and QT Coefficient of Variation calculated (using both the User-interactive and Automatic algorithms) from Rate-Corrected QT intervals of 15 Arrhythmogenic Patients

Arrhythmogenics	Adjusted QT Dispersion (ms) $\frac{QT_c\,(max) - QT_c\,(min)}{\sqrt{No\ of\ leads\ considered}}$		QT Coefficient of Variation V_{QT_c} (%) $\frac{\sigma_{QT_c}}{QT_c} \times 100$	
	User-interactive algorithm	Automatic algorithm	User-interactive algorithm	Automatic algorithm
1	28.5	28.4	6.3	6.2
2	43.9	38.4	8.8	7.9
3	77.2	44.4	14.2	9.2
4	26.1	22.8	5.6	4.4
5	63.0	22.5	13.1	4.9
6	80.9	58.1	14.8	12.4
7	92.5	34.3	18.0	7.8
8	36.8	42.2	8.5	8.8
9	44.6	42.8	13.5	12.4
10	14.9	8.7	3.0	1.9
11	36.0	31.9	9.1	8.0
12	94.8	35.7	16.7	8.8
13	35.4	26.8	7.7	6.6
14	62.8	45.5	12.7	9.3
15	51.9	46.1	11.5	9.7

6.4.1 Analysis of Dispersion using two different risk parameters and two different measurement methods

Using the results from Tables 6.5 and 6.6 of both *adjusted QT dispersion* and *QT coefficient of variation* calculated from QT and RR measurements by the user-interactive algorithm and the automatic algorithm, comparisons can be made between the group of controls and arrhythmogenics (patient number 10 in the arrhythmogenic group is excluded).

In order to establish if rate-corrected QT dispersion as reflected by either the *adjusted QT dispersion* or *QT coefficient of variation* can differentiate between the controls and arrhythmogenics, a good test is one while making no assumptions on the underlying distribution of the data, allows the comparison of the location of their samples. The null hypothesis is that both samples come from the same population, where the samples may be the *adjusted QT dispersion* of the group of controls and arrhythmogenics or they may be the *QT coefficient of variation* of the group of controls and arrhythmogenics. The alternative hypothesis is that the samples are from populations differing in location only. Then, if the samples reflect a difference in location, the appropriate parameter, the *adjusted QT dispersion* or the *QT coefficient of variation* can be said to distinguish between the group of controls and arrhythmogenics. A suitable and powerful test to check for the location of two independent samples is the Wilcoxon-Mann-Whitney test (eg. P.Sprent, 1989).

Wilcoxon-Mann-Whitney Test

A joint ranking of observations from two samples of size m and n are first made, and the sum of the ranks associated with one sample is calculated, S_m or S_n. It does not matter which, but generally speaking, it is easier to calculate either the sum from the sample that tend to involve the smaller ranks, or that for the smaller number of observations if m,n differ substantially. If both samples come from the same population, a fair mix of low-, medium- or high-ranking observations can be expected in each sample.

If the alternative to the null hypothesis of identical populations is that the samples come from populations differing only in location, it might be expected that lower ranks may dominate one sample and higher ranks the other. This concept of a 'shift in location' is important as it epitomises a measure of additive treatment effect. To establish a critical region, the probability of each rank sum for all possible association of ranks with samples of a given size is calculated. Tied ranks are averaged. The null hypothesis is rejected if the results falls in a set that has a low probability under the null hypothesis, but is more likely under the alternative. For samples of size m, n tables exist for critical values at the 5% and 1% levels for both the rank sums S_m, S_n (conveniently labelled the Wilcoxon statistics) and for the closely related (Mann-Whitney) statistics U_m and U_n that are given below.

$$U_m = S_m - \frac{1}{2}m\,(m+1) \quad \ldots\ldots\ldots\ldots\ldots\ldots\ldots\ldots\ldots\ldots \quad (6.14)$$

and

$$U_n = S_n - \frac{1}{2}n\,(n+1) \quad \ldots\ldots\ldots\ldots\ldots\ldots\ldots\ldots\ldots\ldots \quad (6.15)$$

Since S_m+S_n is the sum of all ranks from *1* to m, i.e. $\frac{1}{2}(m+n)(m+n+1)$, it is easily verified that:

$$U_m = mn - U_n \quad \ldots\ldots\ldots\ldots\ldots\ldots\ldots\ldots\ldots\ldots\ldots\ldots \quad (6.16)$$

so that only one of U_m, U_n need to be calculated to determine the other.

Using the Wilcoxon-Mann-Whitney test, we now check the hypothesis H_o *: the samples are from the same population,* indicating that the two parameters, the *adjusted QT dispersion* and *QT coefficient of variation do not* distinguish between the group of controls and arrhythmogenics against H_1 *: the samples are from populations differing in location only,* indicating that the two parameters, the *adjusted QT dispersion* and *QT coefficient of variation, do* distinguish between the group of controls and arrhythmogenics. A two-tail test is appropriate.

Table 6.7 Combined ranks of *adjusted QT dispersion* calculated for 2 samples: Controls and Arrhythmogenics using *User-interactive algorithm*

Value	7.8	10.9	12.2	12.4	13.1	14.9	15.2	16.5	17.6	18.5
Rank	1	2	3	4	5	6	7	8	9	10
Value	22.1	22.9	23.3	26.1	26.7	28.5	34.9	35.4	36.0	36.8
Rank	11	12	13	14	15	16	17	18	19	20
Value	43.9	44.6	51.9	62.8	63.0	77.2	80.9	92.5	94.8,	
Rank	21	22	23	24	25	26	27	28	29,	

Table 6.7 contains all the *adjusted QT dispersion* values in ascending order and their associated ranks. For ease of identification *adjusted QT dispersion* values and ranks for the first sample are underlined.

Here $m = 15$ and $n = 14$.

$S_m = 1 + 2 + 3 + 4 + 5 + 6 + 7 + 8 + 9 + 10 + 11 + 12 + 13 + 15 + 17 = 123$,

whence

$U_m = 123 - \frac{1}{2} \times 15 \times 16 = 3$ from equation (6.14) and

$U_n = (15 \times 14) - 3 = 207$ from equation (6.16)

Using a table of critical values (P.Sprent, 1989), it can be seen that using a two-tail test at the 5% level, the critical value of U_m is 59. Our observed $U_m = 3$ is much, much less than the critical value, hence, the hypothesis that the samples come from the same population, H_o is rejected, and the alternative hypothesis that the samples come from populations differing in location H_1 is accepted. Hence, the *adjusted QT dispersion* calculated using the *user-interactive algorithm* distinguishes well between the 2 samples, controls and arrhythmogenics.

Table 6.8 Combined ranks of *adjusted QT dispersion* calculated for 2 samples: Controls and Arrhythmogenics using *Automatic algorithm*

Value	10.3	11.1	11.9	11.9	12.9	13.1	13.8	13.8	14.0	14.0
Rank	1	2	3.5	3.5	5	6	7.5	7.5	9.5	9.5
Value	14.4	14.6	19.0	20.3	22.5	22.8	24.9	26.8	28.4	31.9
Rank	11	12	13	14	15	16	17	18	19	20
Value	34.3	35.7	38.4	42.2	42.8	44.4	45.5	46.1	58.1,	
Rank	21	22	23	24	25	26	27	28	29,	

Table 6.8 contains all the *adjusted QT dispersion* values in ascending order and their associated ranks. As before, the first sample is underlined.

Using the same analysis as before, $m = 15$ and $n = 14$

$S_m = 1 + 2 + 3.5 + 3.5 + 5 + 6 + 7.5 + 7.5 + 9.5 + 9.5 + 11 + 12 + 13 + 14 + 17 = 122$

$U_m = 122 - \frac{1}{2} \times 15 \times 16 = 2$ and $U_n = (15 \times 14) - 2 = 208$

The observed value $U_m = 2$ is again, very much less than the critical value, 59. The hypothesis that the samples come from the same population, H_o is rejected, and the alternative hypothesis that the samples come from populations differing in location, H_1 is accepted. Hence, the *adjusted QT dispersion* calculated using the *automatic algorithm* is also a good distinguisher between the 2 samples, controls and arrhythmogenics.

Table 6.9 Combined ranks of *QT coefficient of variation* calculated for 2 samples: Controls and Arrhythmogenics using *User-interactive algorithm*

Value	2.3	2.9	3.0	3.0	3.4	3.5	3.9	4.2	4.6	5.1
Rank	1	2	3.5	3.5	5	6	7	8	9	10
Value	5.3	5.3	5.5	5.6	5.6	6.3	7.7	8.2	8.5	8.8
Rank	11.5	11.5	13	14.5	14.5	16	17	18	19	20
Value	9.1	11.5	12.7	13.1	13.5	14.2	14.8	16.7	18.0,	
Rank	21	22	23	24	25	26	27	28	29,	

Table 6.9 contains all the *QT coefficient of variation* values in ascending order and their associated ranks. As before, the first sample is underlined.

$m = 15$ and $n = 14$

$S_m = 1 + 2 + 3.5 + 3.5 + 5 + 6 + 7 + 8 + 9 + 10 + 11.5 + 11.5 + 13 + 14.5 + 18$

$= 123.5$

$U_m = 123.5 - \frac{1}{2} \times 15 \times 16 = 3.5$ and $U_n = (15 \times 14) - 3.5 = 206.5$

Again, as previously, the observed value $U_m = 3.5$ is very much less than the critical value, 59. The hypothesis that the samples come from the same population, H_o is rejected, and the alternative hypothesis that the samples come from populations differing in location H_1 is accepted. Hence, the *QT coefficient of variation* calculated using the *user-interactive algorithm* distinguishes well between the 2 samples, controls and arrhythmogenics.

Table 6.10 Combined ranks of *QT coefficient of variation* calculated for 2 samples: Controls and Arrhythmogenics using *Automatic algorithm*

Value	2.7	3.1	3.1	3.2	3.3	3.3	3.4	3.6	3.6	3.6
Rank	1	2.5	2.5	4	5.5	5.5	7	9	9	9
Value	3.7	4.4	4.5	4.8	4.9	5.1	6.2	6.3	6.6	7.8
Rank	11	12	13	14	15	16	17	18	19	20
Value	7.9	8.0	8.8	8.8	9.2	9.3	9.7	12.4	12.4	
Rank	21	22	23.5	23.5	25	26	27	28.5	28.5	

Table 6.10 contains all the *QT coefficient of variation* values in ascending order and their associated ranks. As before the first sample is underlined.

$m = 15$ and $n = 14$

$S_m = 1 + 2.5 + 2.5 + 4 + 5.5 + 5.5 + 7 + 9 + 9 + 9 + 11 + 13 + 14 + 16 + 18 = 127$

$U_m = 127 - \frac{1}{2} \times 15 \times 16 = 7$ and $U_n = (15 \times 14) - 7 = 203$

Again, we can see that the observed value $U_m = 7$ is much less than the critical value, 59. Therefore the hypothesis that the samples come from the same population, H_o is rejected, and the alternative hypothesis that the samples come from populations differing in location H_1 is accepted again. The *QT coefficient of variation* calculated using the *automatic algorithm* is a good distinguisher of the 2 samples, controls and arrhythmogenics.

6.4.2 Discussion

In each of the above four instances, the appropriate risk parameter, i.e. the *adjusted QT dispersion* or *QT coefficient of variation* each distinguished between the group of controls and arrhythmogenics in both instances of using data from the user-interactive and automatic algorithms.

Figures 6.3 and 6.4 illustrate the results obtained for each risk parameter, the *adjusted QT dispersion* and *QT coefficient of variation* respectively, for both groups of controls and arrhythmogenics, using both methods of measurement, the user-interactive method denoted by 'U.I.' and the automatic algorithm denoted by 'A'. The dashed and solid lines in each of the four groups denotes the mean value of the risk parameter obtained for that group.

Tables 6.11 and 6.12 give the values of mean and standard deviation of *adjusted QT dispersion* and *QT coefficient of variation* respectively for each of the four groups. From Figure 6.3 and Table 6.11, it can be noted that the results of *adjusted QT dispersion* (using the user-interactive algorithm) in the control group are notably different from the arrhythmogenic group. Mean *adjusted QT dispersion* for controls is 17.93 ms, arrhythmogenics 55.31ms. The former are also more closely clustered whilst the latter are more dispersed. Standard deviation for controls is 7.04ms, arrhythmogenics 23.42ms. From Figure 6.4 and Table 6.12, we can see that this is similarly true for user-interactive results of *QT coefficient of variation.* Mean *QT coefficient of variation* for controls is 4.39%, arrhythmogenics 11.46%. As before, the former are also more closely clustered (standard deviation 1.51%) whilst the latter are more dispersed (standard deviation 3.86%).

The above points are also true of the *adjusted QT dispersion* and *QT coefficient of variation* using the automatic algorithm. The results of *adjusted QT dispersion* in the control group are notably different from the arrhythmogenic group. Mean *adjusted QT dispersion* for controls is 14.67 ms, arrhythmogenics 37.14ms. As before the former are more closely clustered than the latter. The standard deviation of the former is 3.88ms, former 10.16ms). For the *QT coefficient of variation*, the mean of the controls is 3.82%,

Figure [6.3] Adjusted QT Dispersion in 15 Controls ('o') and 14 Arrhythmogenics ('+')

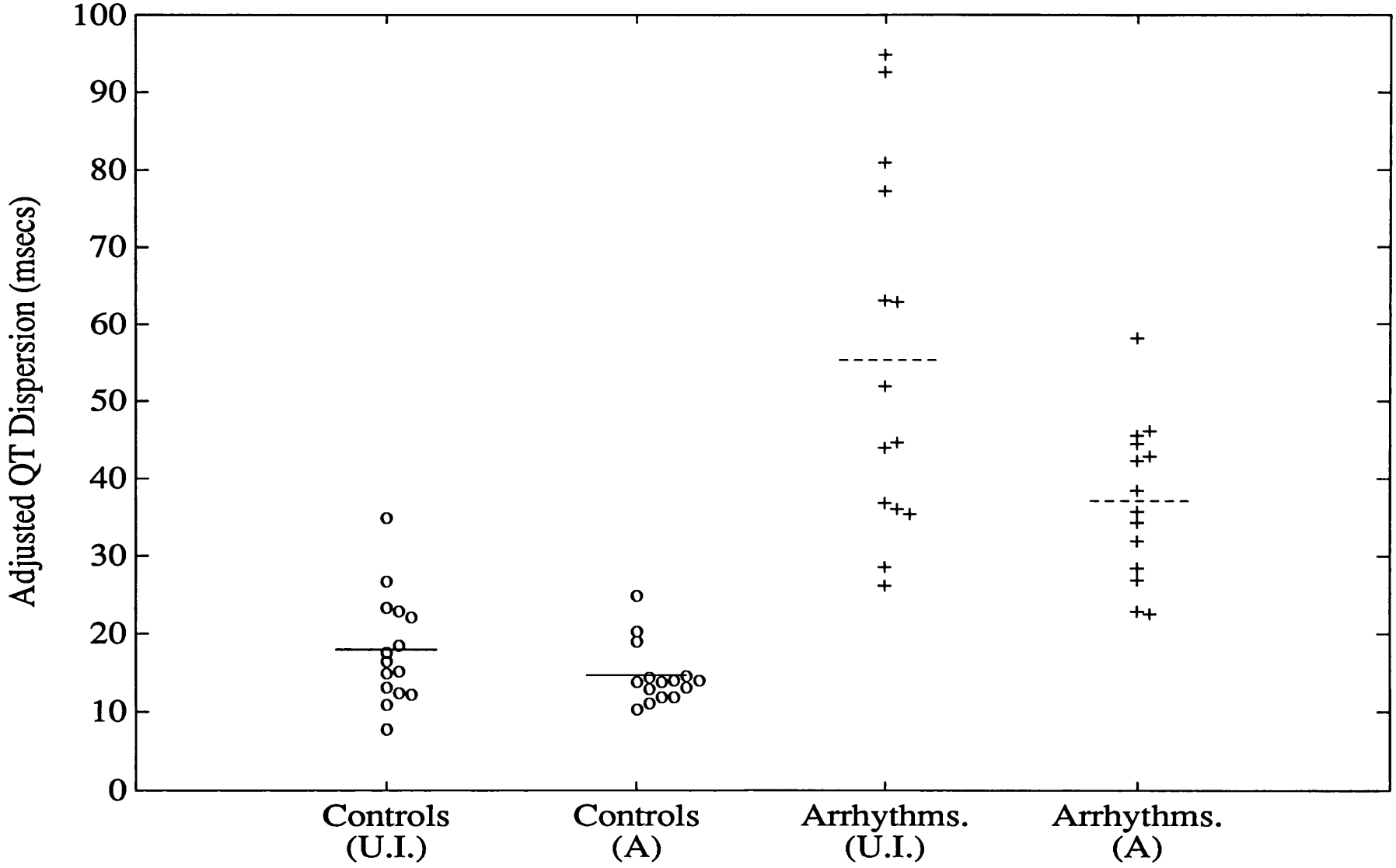

Figure [6.4] QT Coefficient of Variation in 15 Controls ('o') and 14 Arrhythmogenics ('+')

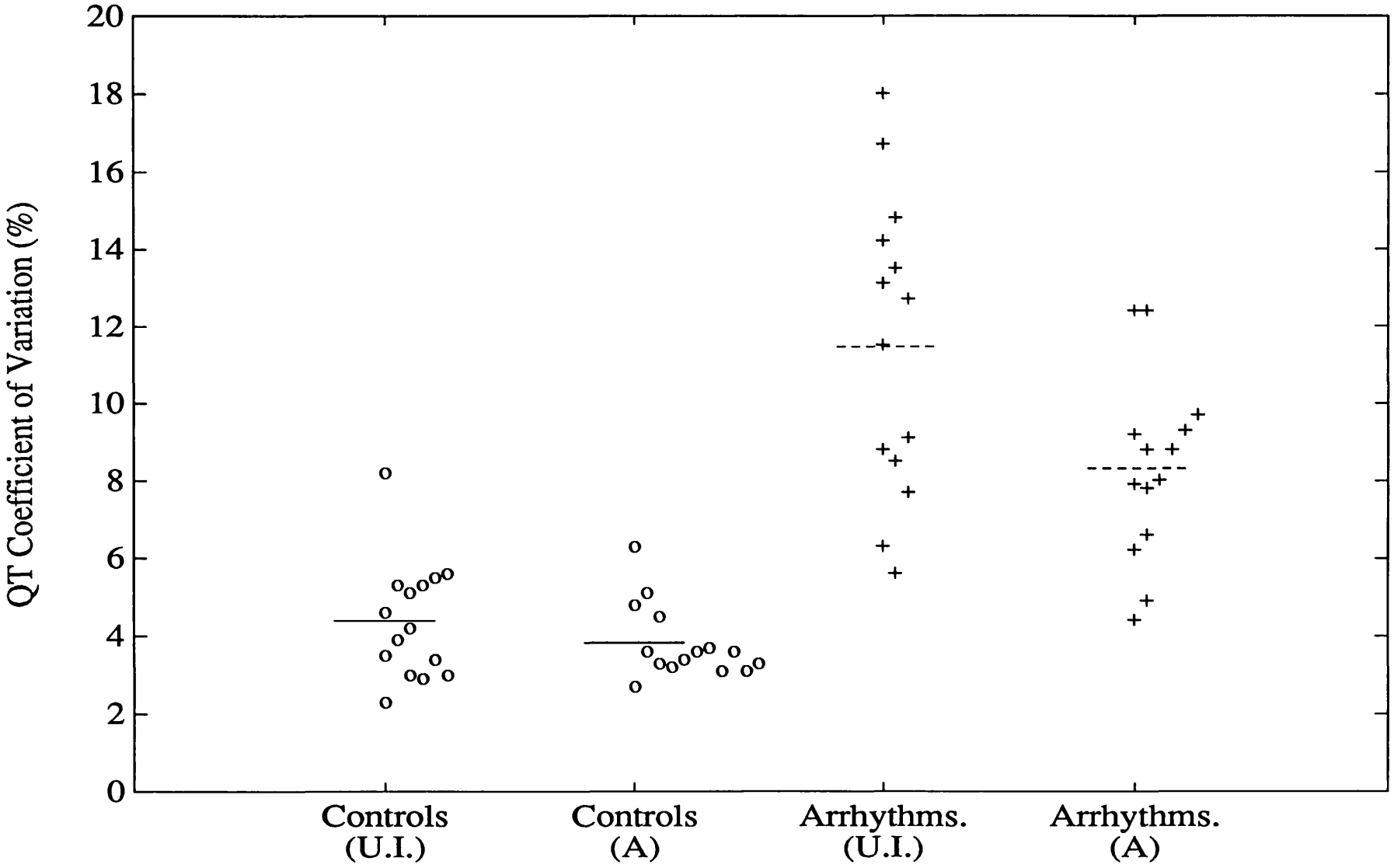

Table 6.11 Mean and Standard deviation of Adjusted QT Dispersion (ms)

Groups	Mean (ms)	Standard deviation (ms)
Controls (User-interactive)	17.93	7.04
Controls (Automatic)	14.67	3.88
Arrhythmogenics (User-interactive)	55.31	23.42
Arrhythmogenics (Automatic)	37.14	10.16

Table 6.12 Mean and Standard deviation of QT Coefficient of Variation (%)

Groups	Mean (%)	Standard deviation (%)
Controls (User-interactive)	4.39	1.51
Controls (Automatic)	3.82	0.95
Arrhythmogenics (User-interactive)	11.46	3.86
Arrhythmogenics (Automatic)	8.31	2.36

whilst that of the arrhythmogenics is 8.31%. Similarly, the standard deviation, giving a measure of how dispersed the values of *QT coefficient of variation* are is 0.95% for the controls and 2.36% for the arrhythmogenics.

It is interesting to note that if we compared the values of *adjusted QT dispersion* in the control group by the two different measurement methods, the user-interactive and the automatic, the former shows a larger mean and spread of values than the latter (standard deviation of the former is 7.04ms, mean 17.93ms; standard deviation of the latter is 3.88ms, mean 14.67ms).

For the arrhythmogenic group, the mean and spread is again greater in the user-interactive algorithm (standard deviation 23.42ms, mean 55.31ms) compared to the automatic algorithm (standard deviation 10.16ms, mean 37.14ms).

Similar inferences can be drawn for the *QT coefficient of variation.* In each case for a particular risk parameter, the automatic algorithm gives a lesser mean and standard deviation than its user-interactive counterpart. However, for both risk parameters, it still manages to discriminate between the group of controls and arrhythmogenics. This is significant, as in any investigation, it is always desirable that the method used should be discriminating, but leaning towards the conservative.

6.4.3 Discrimination of controls and arrhythmogenics using two different risk parameters and two different measurement methods

To investigate if for a particular risk parameter, the user-interactive or automatic algorithms show better power of discrimination between the groups of controls and arrhythmogenics, the following analysis is proposed.

From our previous discussion, it is clear that the distributions of both the *adjusted QT dispersion* and *QT coefficient of variation* for the controls shows a smaller mean and standard deviation than for the group arrhythmogenics, i.e. there is not just a difference in locations as revealed by the Wilcoxon-Mann-Whitney test, but also a difference in spreads.

For 15 values of *adjusted QT dispersion* or *QT coefficient of variation* from the controls and 14 values of the same from the arrhythmogenics, it is difficult to ascertain the true distribution of these values. As the normal distribution is widely understood, and as for this number of values, the normal or Gaussian distribution is as good a fit as any, let us assume that both the distributions of controls and arrhythmogenics for each risk parameter, *adjusted QT dispersion* and *QT coefficient of variation*, and for each measurement method, follow a normal distribution as denoted by:

$$f(x) = \frac{1}{\sigma\sqrt{2\pi}} e^{-(x-\bar{x})^2/2\sigma^2} \quad \ldots\ldots\ldots\ldots\ldots\ldots \quad (6.17)$$

Figure 6.5 shows two histograms of *adjusted QT dispersion* for the group of controls (narrow blocks) and arrhythmogenics (broad blocks), with their normalised Gaussian curves superimposed. This Gaussian curve is calculated by substituting the correct values of mean, $\bar{x}$ and standard deviation, σ of the *adjusted QT dispersion* over the range of values of *adjusted QT dispersion* to be considered. The data used in this case came from the user-interactive algorithm. These histograms and their superimposed, normalised Gaussian curves are repeated for *adjusted QT dispersion* using results from the automatic algorithm in Figure 6.7, *QT coefficient of variation* using the user-interactive algorithm (Figure 6.9) and *QT coefficient of variation* using the automatic algorithm (Figure 6.11).

Figure [6.5] Two histograms of Adjusted QT Dispersion with normalised Gaussian curves superimposed. Controls: narrow Arrhythmogenics: broad (data from the User-interactive algorithm)

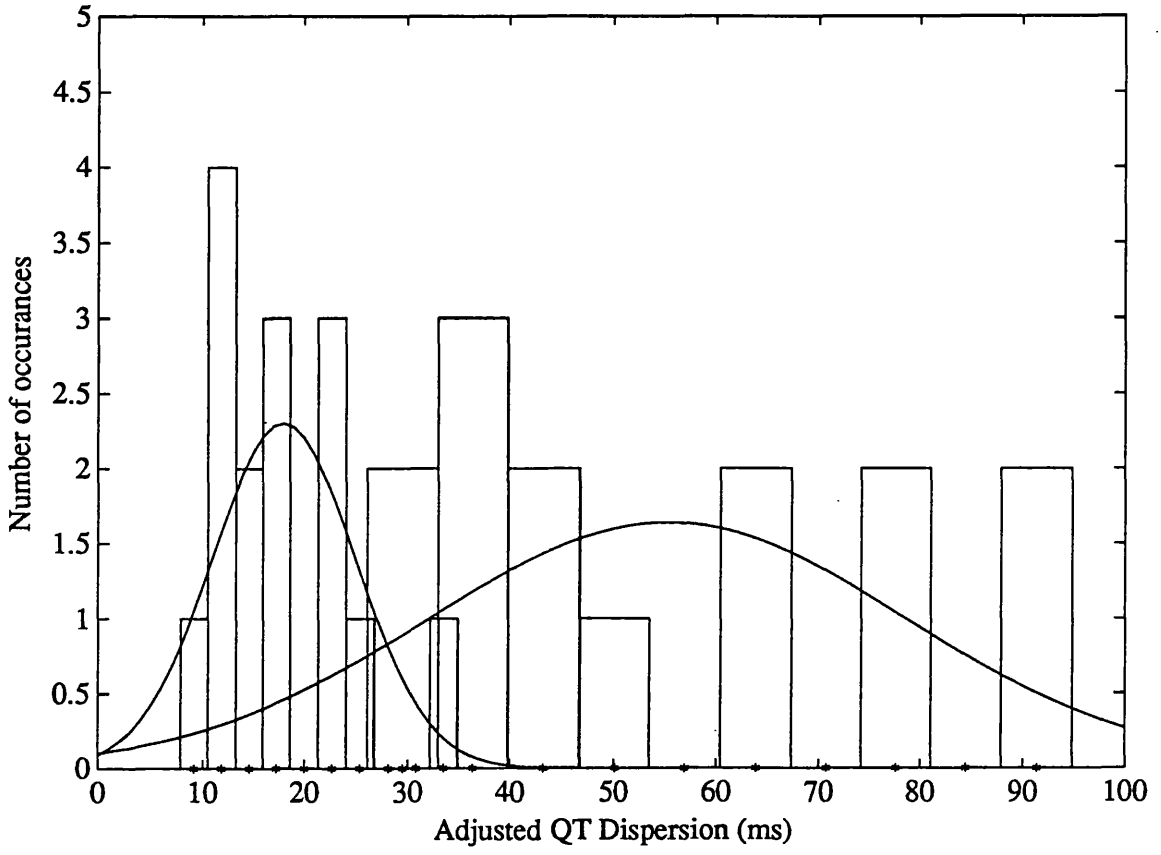

Figure [6.6] The estimated probability that values of Adjusted QT Dispersion lie in the population of Controls: solid line Arrhythmogenics: dashed line (data from the User-interactive algorithm)

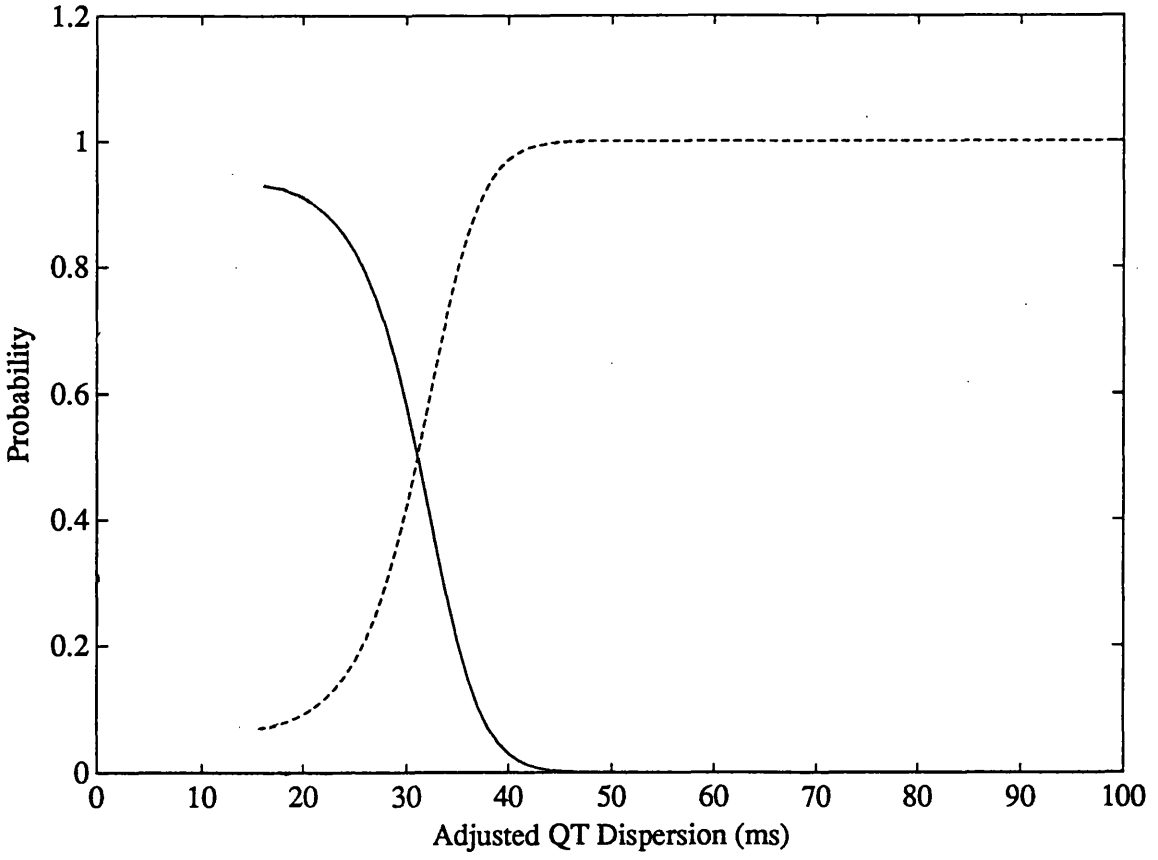

Figure [6.7] Two histograms of Adjusted QT Dispersion with normalised Gaussian curves superimposed. Controls: narrow Arrhythmogenics: broad (data from the Automatic algorithm)

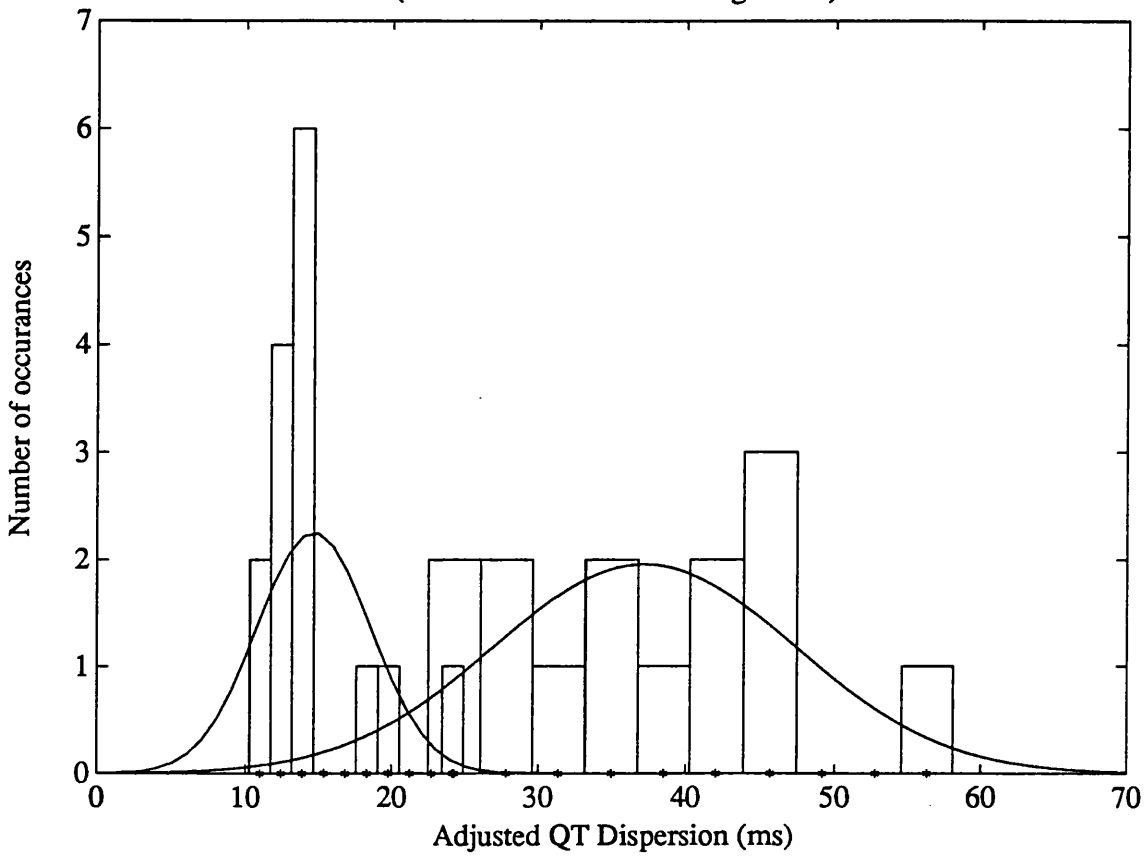

Figure [6.8] The estimated probability that values of Adjusted QT Dispersion lie in the population of Controls: solid line Arrhythmogenics: dashed line (data from the Automatic algorithm)

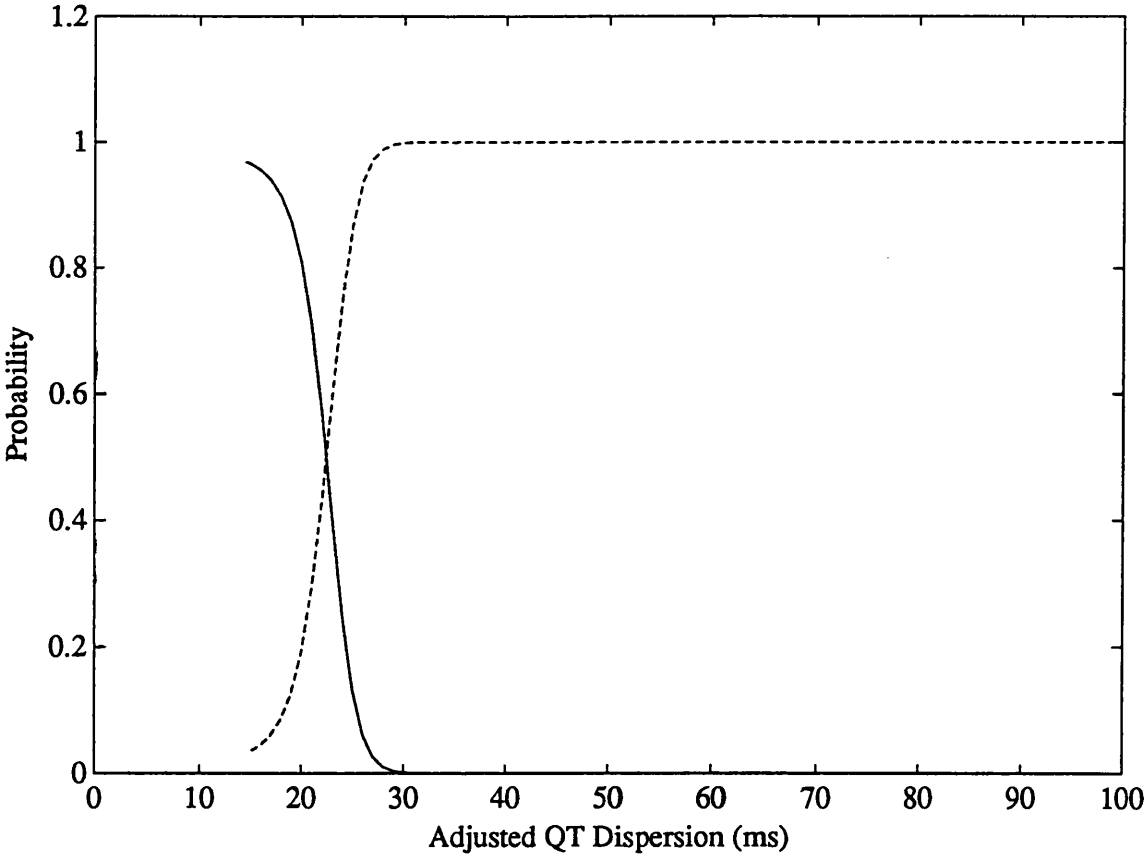

Figure [6.9] Two histograms of QT Coefficient of Variation with normalised Gaussian curves superimposed. Controls: narrow Arrhythmogenics: broad (data from the User-interactive algorithm)

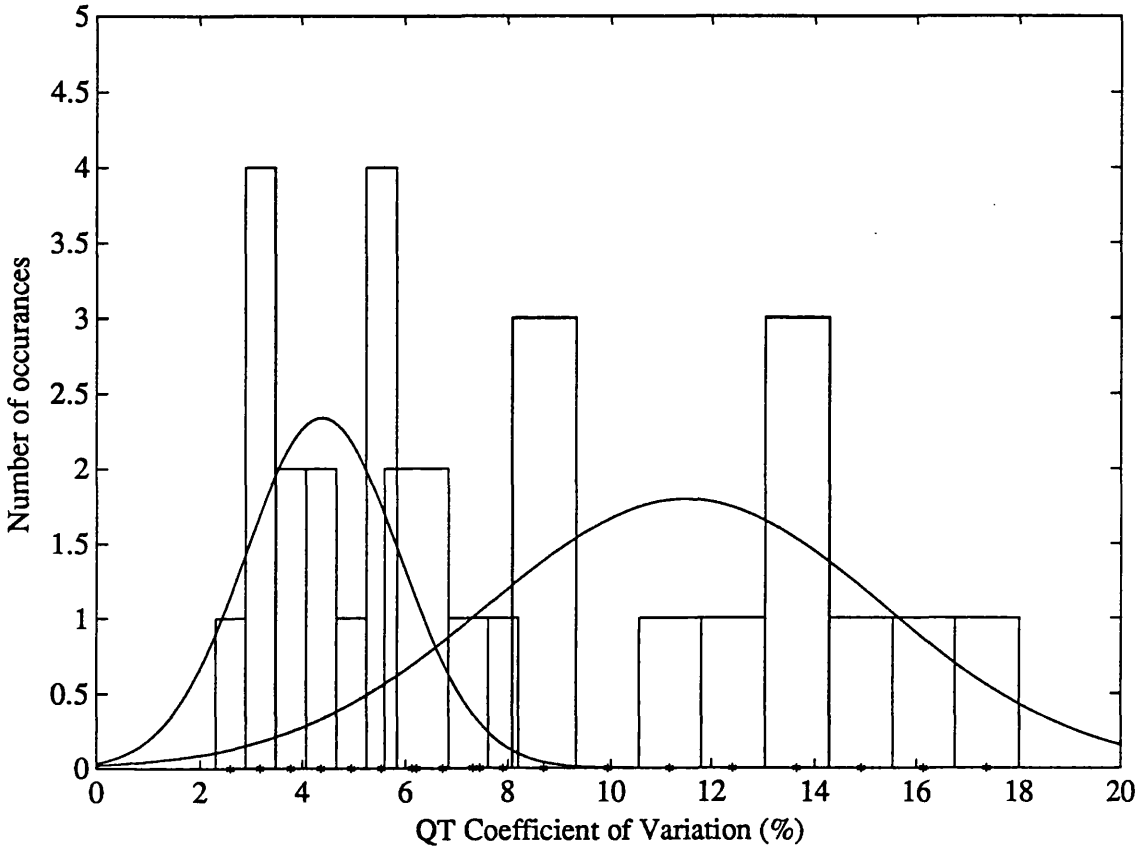

Figure [6.10] The estimated probability that values of QT Coefficient of Variation lie in the population of Controls: solid line Arrhythmogenics: dashed line (data from the User-interactive algorithm)

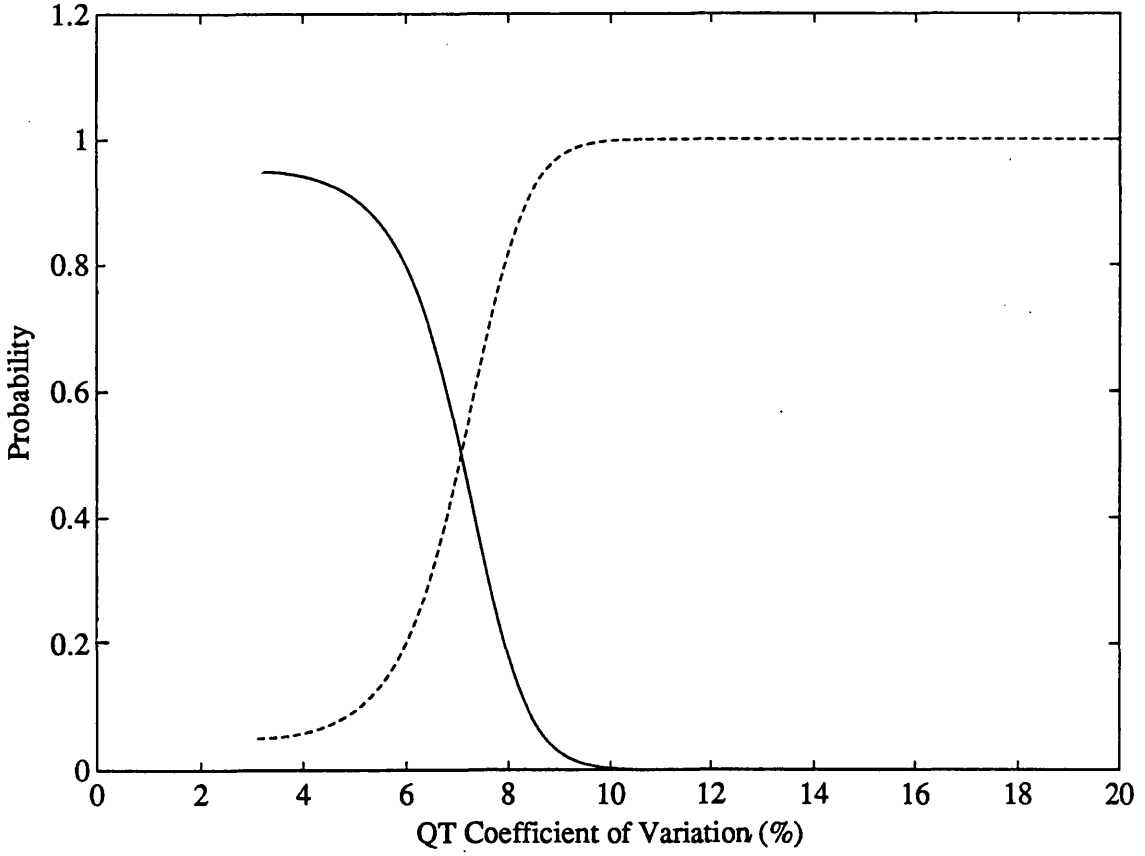

Figure [6.11] Two histograms of QT Coefficient of Variation with normalised Gaussian curves superimposed. Controls: narrow Arrhythmogenics: broad (data from the Automatic algorithm)

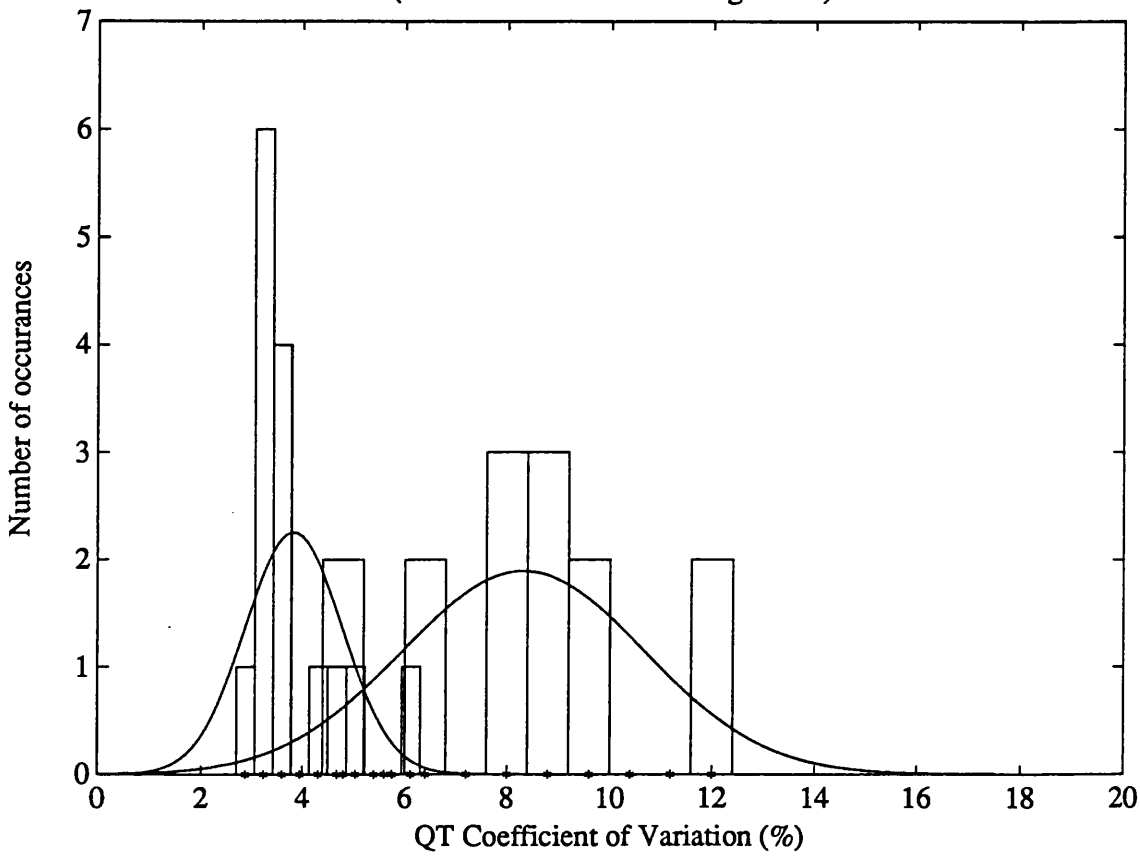

Figure [6.12] The estimated probability that values of QT Coefficient of Variation lie in the population of Controls: solid line Arrhythmogenics: dashed line (data from the Automatic algorithm)

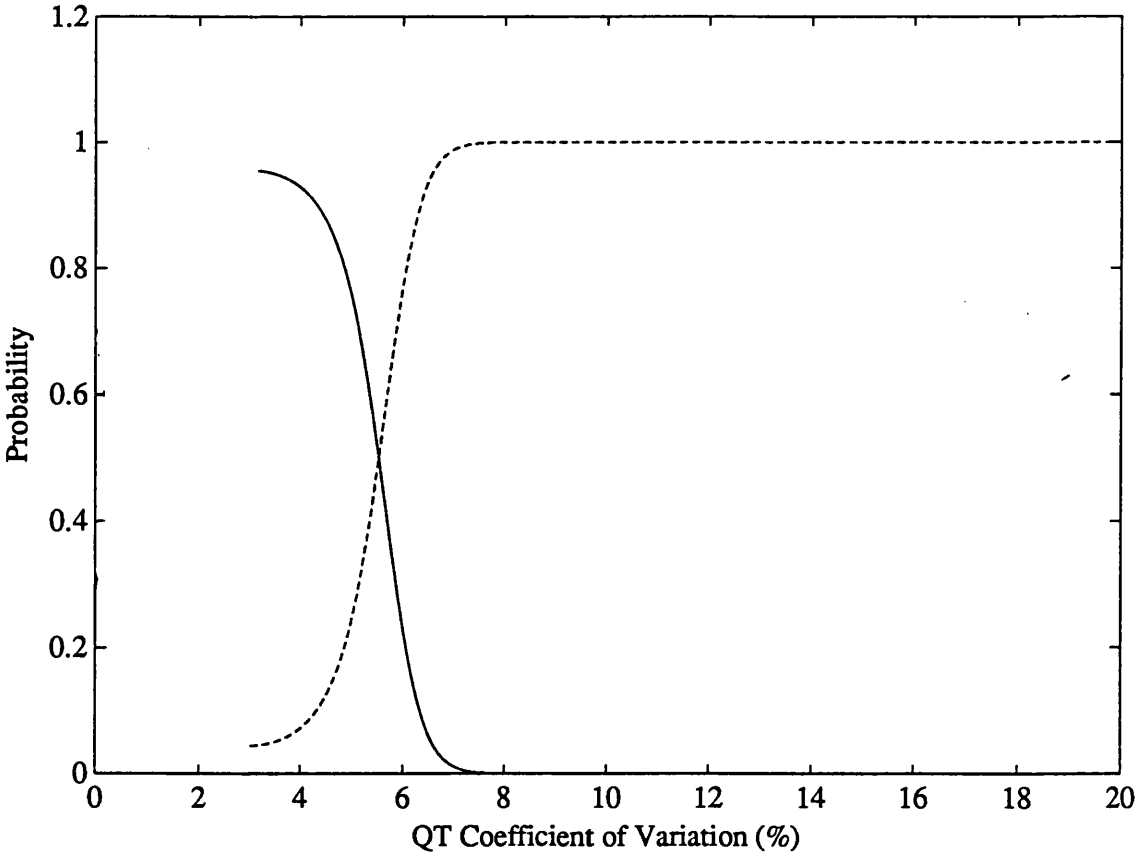

6.4.4 Discussion

It can be seen from each of the above figures, that the distributions of the group of controls and arrhythmogenics are different, but that they possess some degree of overlap in each case. This degree of overlap if interpreted correctly, can lead to better understanding of the discriminating power of a particular method of measurement, using a particular risk parameter.

For example, consider a patient A who was randomly selected from our mixture of controls and arrhythmogenics, and whose adjusted QT dispersion was calculated from the data measured using the user-interactive algorithm. Based on the hypothesis that A must fall in either of these categories, if A displayed an adjusted QT dispersion value of 20ms, what is the probability that A will lie in the population of controls and what is the probability that A will lie in the population of arrhythmogenics?

From Figure 6.5, let us denote the normalised distribution curve of the controls as *a* and that for the arrhythmogenic group as *b*. Using equation 6.17 and the values of $\bar{x}$ and σ denoting the mean and standard deviation of *adjusted QT dispersion* for data from the user-interactive algorithm (Table 6.11),

$$f\,(20,a) = \frac{1}{7.04\sqrt{2\pi}}\, e^{-(20-17.93)^2/2\times 7.04^2} = 0.0543$$

and

$$f\,(20,b) = \frac{1}{23.42\sqrt{2\pi}}\, e^{-(20-55.31)^2/2\times 23.42^2} = 0.00547$$

The probability that A lies in the population of *controls* is given by:

$$P(controls) = \frac{f\,(20,a)}{f\,(20,a) + f\,(20,b)} = \frac{0.0543}{0.0543 + 0.00547} = 0.91$$

and

the probability that A lies in the population of *arrhythmogenics* is given by:

$$P(arrhythmogenics) = \frac{f\,(20,b)}{f\,(20,b) + f\,(20,a)} = \frac{0.00547}{0.00547 + 0.0543} = 0.09$$

Using this method, it can be seen that patient A has a very high probability of lying in the population of controls (0.91) and a lower probability of lying in the population of arrhythmogenics (0.09).

Figure 6.6 illustrates this result graphically via two curves which give the estimated probability that a value of *adjusted QT dispersion* would lie in the group of controls and arrhythmogenics. The solid line gives the values of P(controls) for a range of values of *adjusted QT dispersion*, whilst the dashed line gives the values of P(arrhythmogenics). The two curves of Figure 6.6 confirm the result of P(controls) for an adjusted QT dispersion value of 20ms as 0.91 and P(arrhythmogenics) for the same as 0.09.

These estimated probability curves are repeated for *adjusted QT dispersion* using results from the automatic algorithm in Figure 6.8, *QT coefficient of variation* using the user-interactive algorithm (Figure 6.10) and *QT coefficient of variation* using the automatic algorithm (Figure 6.12).

To understand better the power of discrimination of the two methods of measurement for the group of controls and arrhythmogenics, for each of the above four sets of measurements, values of P(controls) and P(arrhythmogenics) are generated for the 93% probability levels (as this was a value that could be met by all groups) of the relevant risk parameter measured using a particular method of measurement. These values are tabulated in Tables 6.13 - 6.16.

From Table 6.13 we can see that for *adjusted QT dispersion*, the automatic algorithm starts discriminating the group of arrhythmogenics at the lower value of 26ms with a probability higher than 93%, i.e. for values of *adjusted QT dispersion* greater than or equal to 26ms recorded using the automatic algorithm, there is a greater than 93% probability that they lie in the group of arrhythmogenics. For the same value of *adjusted QT dispersion* recorded using the user-interactive algorithm, there is only a 20.94% probability that they lie in the group of arrhythmogenics. There is a higher probability that this value occurs in the group of controls (79.06). The 100% probability level for a value of *adjusted QT dispersion* measured by the automatic algorithm to lie in the group of arrhythmogenics is 37ms. The automatic algorithm reaches this level of greater than 93% probability in a range of *adjusted QT dispersion* of 37ms - 26ms = 11ms.

The 93% probability level that an *adjusted QT dispersion* value recorded using the user-interactive algorithm lies in the group of arrhythmogenics, occurs much later at 38ms and reaches a probability of 100% at 58ms, i.e. a range of 58ms - 38ms = 20ms. This illustrates clearly that although the automatic algorithm gives more conservative

estimates of *adjusted QT dispersion* it is nevertheless more powerful than the user-interactive algorithm when using this risk parameter to discriminate between the controls and arrhythmogenics. This is confirmed by studying the slopes of the dashed line in Figures 6.6 and 6.8.

For *QT coefficient of variation* (Table 6.14), the automatic algorithm starts discriminating the group of arrhythmogenics at the lower value of 6.5% with a probability higher than 93%, i.e. for values of *QT coefficient of variation* greater than or equal to 6.5% recorded using the automatic algorithm, there is a greater than 93% probability that they lie in the group of arrhythmogenics. For the same value of *QT coefficient of variation* recorded using the user-interactive algorithm, there is only a 31.3% probability that they lie in the group of arrhythmogenics. There is a higher probability that this value occurs in the group of controls (68.7%). The 100% probability level for a value of *QT coefficient of variation* measured by the automatic algorithm to lie in the group of arrhythmogenics is 9.2% The automatic algorithm reaches this level of greater than 93% probability in a range of *QT coefficient of variation* of 9.2% - 6.5% = 2.7%.

The 93% probability level that a *QT coefficient of variation* value recorded using the user-interactive algorithm lies in the group of arrhythmogenics, occurs much later at 8.6% and reaches a probability of 100% at 12.8%, i.e. a range of 12.8% - 8.6% = 4.2%. This again illustrates clearly that the automatic algorithm is more powerful than the user-interactive algorithm when using this risk parameter to discriminate between the controls and arrhythmogenics. This is confirmed by studying the slopes of the dashed line in Figures 6.10 and 6.12.

Tables 6.15 and 6.16 gives the less than 93% probability values of *adjusted QT dispersion* and *QT coefficient of variation* for the group of controls. Using similar analysis to above, it can be seen that again, the automatic algorithm is a better discriminator of the group of controls for both risk parameters, than the user-interactive algorithm.

For completeness, Figure 6.13a and b have been included. They illustrate the graphical interface developed to calculate the *adjusted QT dispersion* and *QT coefficient of variation* for each patient and illustrate this information visually. Figure 6.13a shows

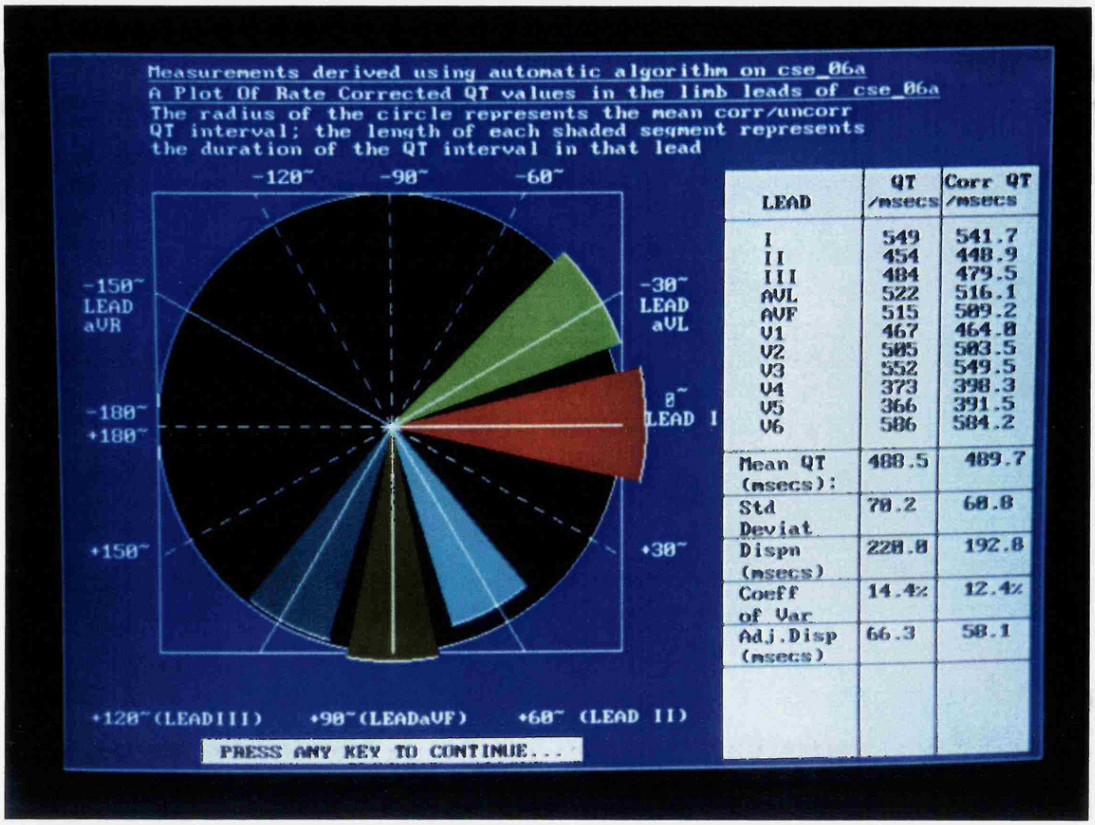

Figure [6.13a] Display of rate-corrected QT intervals recorded in the limb leads using the graphical interface developed

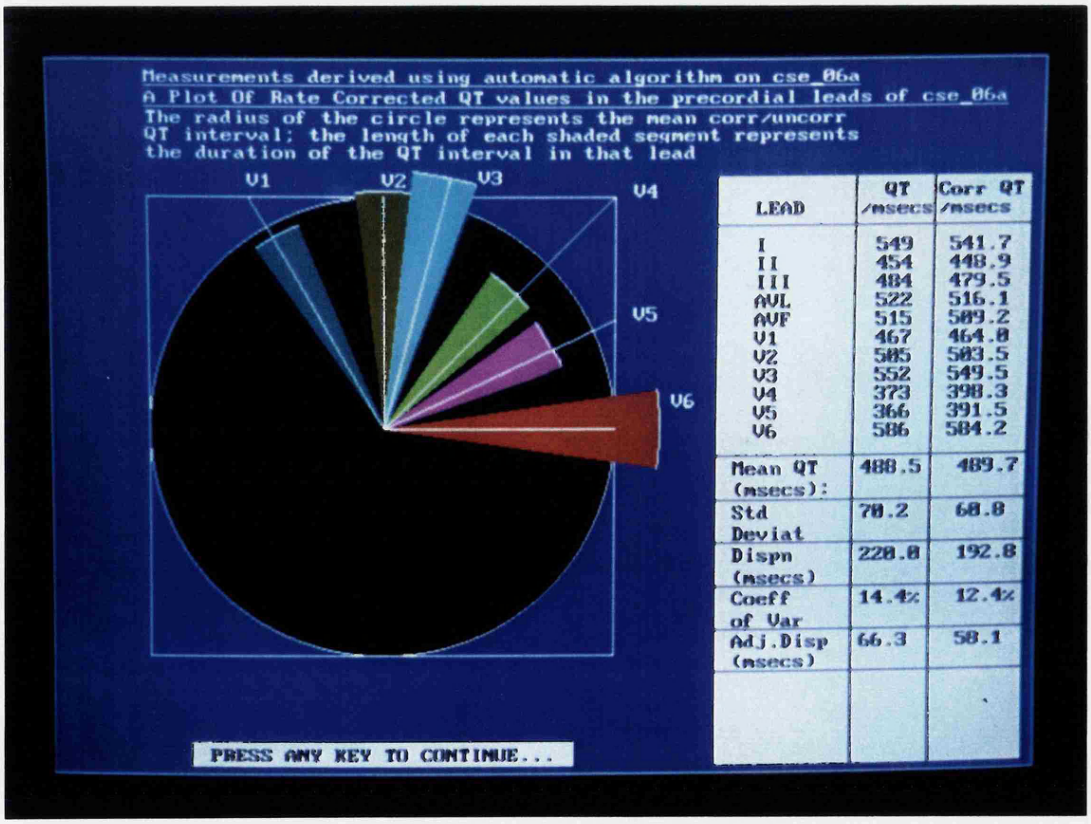

Figure [6.13b] Display of rate-corrected QT intervals recorded in the precordial leads using the graphical interface developed

graphically the QT intervals recorded in each of the limb leads of patient number 6 from the arrhythmogenic group using the automatic algorithm. The QT interval in each lead is expressed by a coloured slice. The length of the slice measured from the the centre of the circle is expressed as a fraction of the mean rate-corrected QT interval (calculated from all the leads in which the QT intervals were measurable) which is given by the radius of the circle. The mean frontal plane electrical axis has been superimposed to illustrate the approximate angles from which each lead records activity. Figure 6.13b displays similar information but for the precordial leads.

Finally, as a point of interest, let us look at the results of the *adjusted QT dispersion* and *QT coefficient of variation* of patient number 10, who was not considered in this study as a subsequent electrophysiological revealed that the original arrhythmia he had was in fact supraventricular tachycardia with left bundle branch block and not a ventricular arrhythmia. From Table 6.6, his *adjusted QT dispersion* value measured using data from the user-interactive algorithm was 14.9ms, whilst that for data from the automatic algorithm was 8.7ms. Similarly his *QT coefficient of variation* using the user-interactive algorithm was 3.0%, whilst that using the automatic algorithm was 1.9%. Clearly, from our discussion and from Tables 6.15 and 6.16, these values have a higher probability of occurring in the control group.

6.5 Conclusion

Both the above discussion and results from the Wilcoxon-Mann-Whitney test confirm that both the risk parameters, *adjusted QT dispersion* and *QT coefficient of variation* distinguish well between the groups of controls and arrhythmogenics. As the arrhythmogenic patients in this study were selected on the basis that they each had documented ventricular arrhythmia, there is clearly an association between either of the parameters, *adjusted QT dispersion* or *QT coefficient of variation* and ventricular arrhythmia. However we have not proved a causitive relationship. Certainly these results seem to support the hypothesis that QT intervals recorded on the 12 leads of a standard electrocardiogram reflect the regional patterns of ventricular repolarisation in the heart as proposed by C.Day et al., 1990,1991,1992.

Similarly, we cannot exclude the possibility that there may exist a group of patients with arrhythmias in whom the distribution of QT intervals is far from Gaussian and in whom the *adjusted QT dispersion* may be a better discriminator than the *QT coefficient of variation*, although these findings have not been seen in our studies. Only wider ranging studies on different patient populations can confirm this.

If QT dispersion (as measured by either parameter) is subsequently proven to be a new an important indicator of susceptibility to lethal ventricular arrhythmias, this would call for a major rethink of the validity of the numerous studies which relied on a single absolute measurement of QT interval as a risk parameter.

Table 6.13
Probability values: P(arrhythms.) for a range of values of Adjusted QT Dispersion using the User-interactive and Automatic algorithms

Adjusted QT Dispersion (ms)	P(arrhythms.) User-interactive	P(arrhythms.) Automatic
25	0.177146	0.867161
26	0.209365	**0.937598**
27	0.249112	**0.973409**
28	0.297425	**0.989518**
29	0.354924	**0.996135**
30	0.421411	**0.998659**
31	0.495464	**0.999561**
32	0.574212	**0.999864**
33	0.653535	**0.99996**
34	0.728797	**0.999989**
35	0.79589	**0.999997**
36	0.852134	**0.999999**
37	0.896639	**1**
38	**0.930071**	1
39	**0.954064**	1
40	**0.970618**	1
41	**0.981657**	1
42	**0.988802**	1
43	**0.993307**	1
44	**0.996079**	1
45	**0.997747**	1
46	**0.99873**	1
47	**0.999297**	1
48	**0.999618**	1
49	**0.999797**	1
50	**0.999894**	1
51	**0.999945**	1
52	**0.999972**	1
53	**0.999986**	1
54	**0.999993**	1
55	**0.999997**	1
56	**0.999999**	1
57	**0.999999**	1
58	**1**	1

Table 6.14
Probability values: P(arrhythms.) for a range of values of QT Coefficient of Variation using the User-interactive and Automatic algorithms

QT Coefficient of Variation (%)	P(arrhythms.) User-interactive	P(arrhythms.) Automatic
6.4	0.28698	0.918078
6.5	0.313037	**0.939257**
6.6	0.341167	**0.955618**
6.7	0.371327	**0.968009**
6.8	0.403419	**0.977229**
6.9	0.437273	**0.983981**
7	0.472648	**0.988856**
7.1	0.509229	**0.992329**
7.2	0.546631	**0.994773**
7.3	0.584417	**0.996474**
7.4	0.62211	**0.997644**
7.5	0.659218	**0.998441**
7.6	0.695259	**0.998978**
7.7	0.729789	**0.999336**
7.8	0.76242	**0.999573**
7.9	0.792844	**0.999728**
8	0.820837	**0.999828**
8.1	0.846267	**0.999892**
8.2	0.869088	**0.999933**
8.3	0.889333	**0.999959**
8.4	0.907096	**0.999975**
8.5	0.922523	**0.999985**
8.6	**0.935794**	**0.999991**
8.7	**0.947109**	**0.999995**
8.8	**0.956677**	**0.999997**
8.9	**0.964705**	**0.999998**
9	**0.971394**	**0.999999**
9.1	**0.97693**	**0.999999**
9.2	**0.981482**	**1**
9.3	**0.985204**	1
.	.	.
.	.	.
.	.	.
12.8	**1**	1

Table 6.15
Probability values: P(controls) for a range of values of Adjusted QT Dispersion using the User-interactive and Automatic algorithms

Adjusted QT Dispersion (ms)	P(controls) User-interactive	P(controls) Automatic
16	**0.92911**	0.955542
17	**0.926306**	**0.93968**
18	**0.922091**	**0.914288**
19	**0.916258**	**0.873423**
20	**0.908517**	**0.808318**
21	**0.898477**	**0.70885**
.	.	.
.	.	.
.	.	.
37	**0.103361**	**0**
.	.	.
.	.	.
58	**0**	0

Table 6.16
Probability values: P(controls) for a range of values of QT Coefficient of Variation using the User-interactive and Automatic algorithms

QT Coefficient of Variation (%)	P(controls) User-interactive	P(controls) Automatic
3.1	0.948941	0.955212
3.2	0.948867	0.954385
3.3	0.948612	0.953135
3.4	0.948173	0.95143
3.5	0.947547	0.949227
3.6	0.946726	0.946466
3.7	0.945703	0.943073
3.8	0.944467	**0.938955**
3.9	0.943004	**0.933997**
4	0.941301	**0.928057**
4.1	**0.939339**	**0.920961**
4.2	**0.937097**	**0.912501**
4.3	**0.934551**	**0.902427**
4.4	**0.931673**	**0.890438**
4.5	**0.928431**	**0.876186**
.	.	.
.	.	.
.	.	.
9.2	**0.18518**	**0**
.	.	.
.	.	.
12.8	**0**	0

CHAPTER 7 Conclusions and Future Work

7.1 Conclusions

The research work undertaken in this thesis has resulted in several new image and signal processing techniques being applied for the digital recovery and analysis of hard-copy ECG waveforms stored on paper.

New heuristic techniques have been developed for pre-processing the scanned images of each of the 12 lead ECG waveforms, for the removal of small clusters of random noise superimposed on the image and for the filling in of small gaps caused by missing pixels (which cause the image to take on a jagged rather than smooth form). A new application of the image processing technique of 'thinning' patterns in binary regions has been found. This technique was used to overcome the effects of the spread of ink of the recording pen on the original hard-copy recording, by recovering the lineal or 'skeletonised' structure of the scanned ECG waveform. Digital values were extracted from the skeletonised image, taking into account the spread effect of the recording pen on the peaks of the waveforms in the original record.

Simple digital filtering algorithms have been designed to remove d.c. offset in the extracted ECG values and to smooth these values to remove the effects of quantisation introduced by the scanning process. All the above algorithms comprise the DISPERSE system.

A graphical display system called the *user-interactive system* has been developed, to allow the user to display the digitised waveforms and perform measurements on them using a cursor. The user-interactive system incorporates a data-base of each patient's bio-data.

Tests validating the digitising algorithms calculated the root-mean-square error between a waveform whose digital values were known and one in which they were recovered using the DISPERSE system. The root-mean-square error was found to be 1 pixel. This indicates the high level of accuracy of the digitising algorithms or DISPERSE system.

An *automatic algorithm* has also been developed which uses new and simple signal processing techniques for the removal of baseline wander, automatic detection of QRS activity, R wave points, QRS onset points and T wave peak and end points. This information is used to calculate QT and RR intervals. In some cases, the automatic algorithm may not be able to recognise all the characteristic points in the ECGs. To give some indication of the performance of the automatic algorithm, it can be said that of the 337 cases analysed, the automatic algorithm showed a success rate in detecting *all* of the characteristic points in more than 92% of the cases.

The overall system has been validated via a series of statistical tests. The user-interactive and automatic methods of measurement have been found to be more accurate than the conventional method of *manual* measurement. The automatic algorithm was also found to be consistent and relatively unbiased. Inter-observer variability was reduced when using the user-interactive system compared to the manual method of measurement especially when the measurement parameter was clearly defined, as for example, the RR intervals are. Intra-observer variability of a cardiologist using the user-interactive algorithm was assessed. For QT intervals the dispersion of repeated measurements obtained in the worst case was 18 ms, whilst in the best case, it was 1.7 ms. For RR intervals the dispersion of repeated measurements obtained in the worst case was 4 ms (approximately 1 sampling point), whilst in the best case, it was <0.1ms, i.e. identical results were obtained each time.

Comparisons were also made between the user-interactive and automatic measurements. These showed that the two measurement methods produced virtually identical results when comparing parameters which were well defined like the RR interval, and a 5 ms approximate bias when comparing the QT interval. The bias between measurements was found to be less between the automatic and user-interactive methods of measurement compared to the automatic and manual methods of measurement.

A new risk parameter to represent *QT dispersion* has been statistically validated. It is known as the *QT coefficient of variation.* An interesting point to note is that the *QT Coefficient of Variation* may be used without correcting for heart-rate if the 12 lead ECGs are recorded simultaneously; it therefore has the advantage that no assumptions

regarding heart rate correction need to be made. Using both this parameter and Day et al.'s *adjusted QT dispersion*, a group comprising patients with documented history of ventricular arrhythmias and a control group were studied to assess the value of *QT dispersion* (as represented by these parameters) in distinguishing the two groups, and hence shed light on the hypothesis that QT intervals recorded on the 12 leads of a standard electrocardiogram reflect the regional patterns of ventricular repolarisation in the heart as proposed by C.Day et al., 1990,1991,1992 and P.D.Higham et al., 1991,1992.

The results obtained showed that both measures of dispersion, the *QT coefficient of variation* and the *adjusted QT dispersion* distinguished well between the arrhythmogenic and control groups. These tests were carried out using data from the user-interactive and automatic algorithm. Whilst both sets of data distinguished well between the two groups, the data obtained from the automatic algorithm was found to be slightly more effective than its user-interactive counterpart. The results of QT dispersion obtained were found to support the hypothesis above. A graphical interface which takes in measurements made manually, using the user-interactive and automatic algorithms, calculates *QT dispersion* using the parameters above, and provides a graphical display of the QT intervals in the different leads for each patient, was developed successfully.

There are many benefits that can be gained from using the system developed:

- (a) The digitising algorithms provide a means of recovering waveform data that is only conventionally available in hard-copy form. This data can be stored permanently and a data-base created of different morphological 12 lead ECGs. Large archives of data, for example, from patients who have undergone clinical trials and for whom the subsequent outcomes have become known, can be studied. Furthermore, digital procedural algorithms that can only be applied to digital data can also be implemented. Parameters of importance in the digitised waveforms can be automatically analysed hence overcoming problems due to user-bias. These techniques are also general enough to be used to recover *any* waveforms recorded on paper. In the area of geology research, seismological data is often stored on paper. Similarly, these techniques can also be used in an industrial environment where processes are continuously monitored for faults and signals representing these faults are stored on paper.

- (b) The user-interactive algorithm allows the doctor to interactively make measurements of QT and RR intervals, using a cursor. The cursor is controlled by a mouse. As the cursor is made to follow the outline of the waveform, it is very sensitive to the movement of the mouse and hence accurate measurements can be made. Note that although in this case, the user-interactive algorithm is used to display data recovered from standard 12 lead hard-copy records, it can also be used to display data recorded digitally. The graphics capabilities incorporated in the user-interactive system enable the doctor to adjust the effective resolution of the graphical display and therefore allow features of the waveform to be accentuated if necessary. The software incorporates the storage and display of each patient's bio-data. Useful information like the number of samples in the ECG waveform, the sampling rate used, etc. are all displayed. The software also incorporates help menus.
- (c) The automatic algorithm allows the automatic measurements of the QT and RR intervals. The doctor can select a patient lead and the automatic algorithm will detect the characteristic points of the ECG waveform in the signal. The results of the algorithm are then displayed to the user, and if necessary, they can be amended. The main advantage of the algorithm is that it is consistent and relatively unbiased. Note that although in this instance the automatic algorithm is used to display data recovered from standard 12 lead hard-copy sheets, it can also be used to analyse data recorded digitally.

Ultimately the test of any systems success is whether it is actually used. The system developed has been found to be easy to use by various doctors. It is already being used at the Leicester University Cardiology Department at Glenfield Hospital, in the recovery and automatic analysis of the 12 lead ECG waveforms stored on paper.

7.2 Future work

There are two directions in which future work related to this system can be undertaken: in the field of engineering and in the field of cardiology. From the engineering point of view, there are specific as well as general areas of work that can be addressed. The following sections outline these areas.

7.2.1 Specific areas of Work (Engineering based)

(i) One of the reasons the system was developed was to facilitate the retrospective study of the 12 lead ECG of patients who may have subsequently died. It is the case that the quality of the 12 lead ECGs of these patients, are not always very good. In some cases these records are very old and in other cases only photocopies of the original ECG waveforms exist. (In our studies to date, only original hard-copy recordings have been used). When scanning photocopies of the standard 12 lead ECGs, strong grid lines get incorporated. This problem cannot be removed by optical filter paper, as it is caused by apparently black waveforms on a black grid. To this end algorithms can be developed which will firstly remove the grid lines on the image and secondly, fill in the gaps in the ECG waveforms caused by the grid removal.

(ii) A second and useful feature that can be incorporated into the *automatic* determination of the T wave end is a confidence measure indicating the T wave end reliability or quality. Thus if the T wave end was thought to be of poor quality, a flag could be set which could alert the user who can check this result.

(iii) At the moment the segmentation procedure of the automatic algorithm uses the R wave (or Q or S wave if the R wave is not present) to determine the RR interval and segment each lead into its constituent waveforms. This method relies on the QRS wave being repeatable in all the waveforms in each lead. In all but one of the cases considered, the QRS wave shapes were found to be repeatable. A method which studies the 'active segments' (A.Gerber and R.Struder, 1984) of the ECG waveforms in a lead for segmentation may be appropriate to overcome this problem.

(iv) The system software developed currently runs on an IBM compatible DELL 286 PC machine (with maths co-processor) under the MS-DOS operating system. The reason a personal computer was chosen for the project was because of its portability within a hospital and relative inexpense. However the problems with using a personal computer system is that the image processing and automatic routines are limited by the speed and memory capacity of the machine. The length of the ECG waveforms that can be analysed at any one time by the program is restricted by the memory capacity of the machine and the MS-DOS operating system (six hundred and forty kilobytes).

Overall, the system takes quite a long time to analyse the 12 lead ECG waveforms of each patient starting from the process of scanning and ending with the result of their *QT dispersion*. For each patient, if the analysis comprised 2 or 3 waveforms per lead and 12 leads were analysed, the whole analysis would take approximately 1 hour and 40 minutes.(This may however be done by a technician rather than a cardiologist). The algorithms in the DISPERSE system have been written in C. However, the automatic algorithm has been implemented in MATLAB, a high level computing language/ package written in C. Using Matlab causes the execution time of the automatic algorithm to be slow. Therefore, to enable quicker processing, the automatic algorithm can be translated into C. This will halve the time it takes to run the program.

Currently, an operator is required to initiate each process of the analysis: the scanning, segmentation using a graphics editor etc., execution of the user-interactive and automatic algorithms, calculation and graphics display of *QT dispersion*. The reason for this is that with current hardware limitations, it is quicker and more efficient for the user to initiate each stage of the analysis. The hardware cannot cope with multi-tasking or even sequential processing of each of these stages independently, due to memory limitations and lack of parallel processing power.

However with the current development of more powerful operating systems and computer processors, these problems can be solved. The powerful OS/2 operating system or UNIX operating system which runs on SUN workstations can be used to allow for more computing power and parallel processing. The computer could also use a digital signal processing (DSP) board (for example the Texas Instruments TMS320C25 DSP board) working in parallel with the main processor to perform tasks such as filtering and numerical analysis routines. This would dramatically increase the speed of the program and overcome memory problems. Using these more powerful machines and systems, an expert system can be developed to control and schedule each stage of the analysis so that the need for an operator can be overcome.

7.2.2 General areas of Work (Engineering-based)

In a more general sense the algorithms in the system developed can be used in three different areas which all link into each other:

(i) As mentioned briefly before, the system can be used in the development of a large scale data-base of standard 12 lead ECGs that are conventionally stored on paper. New electrocardiograph machines now use digital techniques to record and store the standard 12 lead ECG. These 12 lead ECGs (which are of high quality) can be stored in the data-base. Standard 12 lead ECGs from different clinical trials comprising different patient groups, can be digitised and stored. This would provide a data-base of ECGs containing different morphological information. Such a data-base would be highly advantageous as it would allow the permanent archiving and storage of such data as well as the sharing of information via the distribution of such data.

(ii) Another way to expand the usefulness of the overall system developed is via the inclusion of a neural network. A neural network is a processor of information consisting of simple processing elements connected together. Each processing element is a very simple model of a neuron in the brain (J.Bishop and R.Mitchell, 1991). Each element stores experimental knowledge after a process of learning from task examples (I.Aleksander and H.Morton, 1990).

The neural network can be trained to recognise different types of normal and diseased ECGs by using a training set of the different features of the P, QRS and T wave amplitude and duration characteristics which correspond to the different normal and diseased states of the heart. For example, using the *data* from the standard 12 lead ECG database mentioned above, morphological characteristics of the ECG corresponding to cardiac problems such as hypertrophy, bundle branch block and infarction can be used to train a neural network for the classification of different cardiac disease.

At the moment the automatic algorithm yields characteristic features of the standard ECG which relate to the QRS and T wave activity only. This algorithm can be extended further to extract P wave activity, and other amplitude and duration measurements. All this information can then be fed into a neural network with other clinical measurements. The neural network would then make a clinical diagnosis based on the information available.

Neural networks are powerful tools in the field of decision making because they have the potential for performance improvement as they acquire more knowledge about the domain over time; they are able to handle fuzzy data, that is they are able to learn

and then recognize certain data patterns and those which are similar; they are also inherently parallel in their operation and therefore have the ability to operate much faster than conventional computer programs (J.Bishop and R.Mitchell, 1991).

(iii) The algorithms developed can also be incorporated into a large expert system such as the one developed at the Leicester University Engineering Department for electromyographical signals (EMG) analysis. The expert system would manage several loosely coupled tasks, for example signal processing, interpretation of results, management of the consultation and presentation of results to the user. Such an expert system would use a blackboard architecture rather than a rule based model because the blackboard architecture provides the modularity, dynamic control and efficiency needed. The blackboard system architecture contains a set of knowledge sources, a hierarchically organised blackboard and scheduling control mechanisms.

During a clinical assessment of the ECG the expert system could incrementally construct a picture of the current status of the patient from available measurements, different analysis methods performed, and clinical observations, until a clinical diagnosis can be made. The 12-lead ECG data-base which can have data constantly added to it could be the first knowledge source; a *QT dispersion* parameter could be incorporated as another knowledge source which could be used to predict patients at risk from lethal ventricular arrhythmias. Similarly the output of the neural networks developed for the classification of cardiac disease could also be treated as a series of knowledge sources. Figure [7.1] shows a block diagram of the architecture of the blackboard system (taken from A.S.Sehmi et al., 1991).

7.2.3 Specific areas of Work (Cardiology based)

From the clinical point of view, the overall system which has been validated, can now be used to undertake different clinical studies. Two different types of studies can be made. The first is one in which the value of *QT dispersion* is studied in different patient groups as a risk predictor, for example of ventricular arrhythmias. The second study is the analysis of *QT dispersion changes* over a course of treatment or time, in different patient groups. Such a study will allow a greater understanding of the electrophysiological mechanisms that cause QT dispersion.

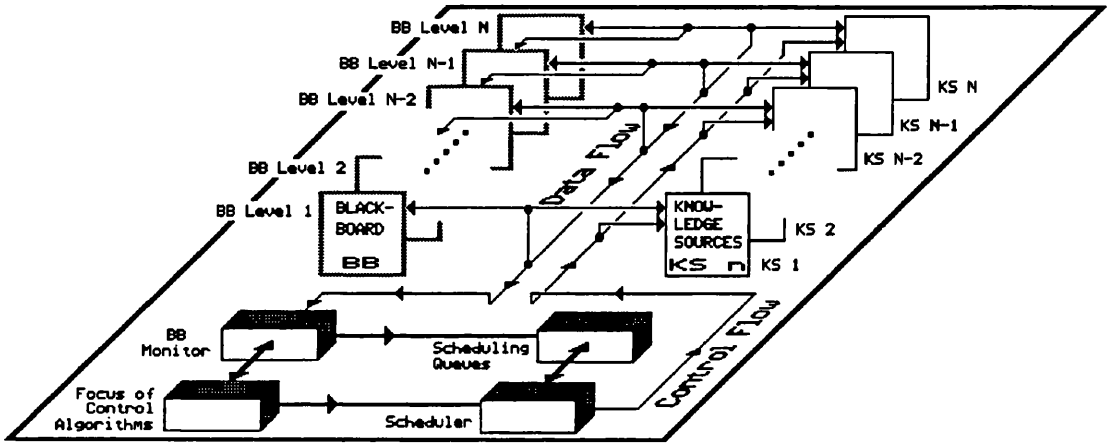

Figure [7.1] An example of the architecture of of a black-board system (extracted from A.Sehmi et al., 1991)

REFERENCES

J.A.Abildskov, G.M.Vincent, K.Evans, M.J.Burgess (1981): Distribution of body surface ECG potentials in familial QT interval prolongation [Abstract]. American Journal Cardiology. Vol.47, pp.480.

J.A.Abildskov (1975). The sequence of normal recovery of excitability in the dog heart. Circulation. Vol.52, pp.442-446.

S.Ahnve, L.Erhardt, T.Lundman, N.Rehnqvist, A.Sjogren (1980): Effect of metoprolol on QT intervals after acute MI. Acta Med. Scand. Vol.208, pp.223-228.

S.Ahnve, C.Helmers, T.Lundman (1980): QT(corrected) Intervals at Discharge after Acute Myocardial Infarction and Long-Term Prognosis. Acta Med. Scand. Vol.208, pp.55-60.

S.Ahnve, C.Helmers, T.Lundman, N.Rehnqvist, A.Sjogren (1980): QT intervals in acute MI: First year prognostic implications. Clinical Cardiology. Vol.3, pp.303.

S.Ahnve,M.D. (1985): Correction of the QT interval for heart rate: Review of different formulas and the use of Bazett's formula in myocardial infarction. American Heart Journal. Vol.109, pp.568-574.

I.Aleksander, H.Morton (1990): An Introduction to Neural Computing. Chapman and Hall Ltd.

A.Algra, H.Le Brun, C.Zeelenberg (1987): An algorithm for computer measurements of QT intervals in the 24 hour ECG. Computers in Cardiology. IEEE Computer Society Press, pp.117-119.

Richard Ashman (1942): The normal duration of the QT interval. American Heart Journal. Vol.23, pp.522-534.

A.K.Bahn (1972): Basic Medical Statistics. Grune and Stratton Inc. Chapter 6.

H.C.Bazett (1920): An analysis of the time relations of electrocardiograms. Heart. Vol.7, pp.353-70.

J.Bishop, R.Mitchell (1991): Neural Networks - An Introduction. IEE Colloquium, Neural Networks for systems: Principles and applications, Digest No: 1991/019, pp.1/1-1/3.

J.M.Bland and D.G.Altman (1986): Statistical Methods for Assessing Agreement between Two Methods of Clinical Measurement. The Lancet (i), pp.307-310.

H.Blum (1967): A Transformation for Extracting New Descriptors of Shape. Models for the Perception of Speech and Visual Form, Wathen-Dunn, MIT Press, Cambridge, Mass..

P.J.Bourdillon,M.R.C.P. (1979): Prolonged QT interval to Predict Sudden Death. Circulation. Vol.59, pp.1079-1080.

W.W.Brooks, R.L.Verrier, B.Lown (1978): Influence of vagal tone on Stellectomy induced changes in ventricular electrical stability. American Journal of Physiology, pp.234:503.

K.F.Browne, D.P.Zipes, J.J.Herger, E.N.Prystowsky (1982): Influence of the autonomic nervous system on the QT interval in man. American Journal of Cardiology. Vol.50, pp.1099.

K.F.Browne, E.Prystowsky, J.J.Herger, D.A.Chilson, D.P.Zipes (1983): Arrhythmias and Conduction Disturbances: Prolongation of the QT interval in Man during Sleep. American Journal of Cardiology. Vol.52, pp.55-59.

M.J.Burgess, L.S.Green, K.Millar, R.Wyatt, J.A.Abildskov (1972): The sequence of normal ventricular recovery. American Heart Journal. Vol.84, pp.660-669.

C.Cabo, C.Hernandez, M.A.Gonzalez de Mingo, J.Marquez, J.L.Castillo-Olivares (1989): Digital filtering for electrogram signal processing: Computers in Cardiology, IEEE pp.541-544.

R.W.F.Campbell, P.Gardiner, P.A.Amos, D.Chadwick, R.S.Jordan (1985): Measurement of the QT interval. European Heart Journal. Vol:6 (Suppl D). pp.81-85.

J.C.Cowan, C.J.Hilton, C.J.Griffiths, S.Tansuphaswadikul, J.P.Bourke, A.Murray, R.W.F.Campbell (1988): Sequence of epicardial repolarisation and configuration of the T wave. British Heart Journal. Vol.60, pp.424-33.

J.C.Cowan, K.Yusoff, M.Moore, P.Amos, A.Gold, J.Bourke, S.Tansuphaswadikul, R.W.F.Campbell (1988): Importance of lead selection in QT interval measurenment. American Journal of Cardiology. Vol.61, pp.83-87.

P.H.Coumel, Rosengarten, J.F.Leclercq, P.Attuel (1982): Role of sympathetic nervous system in non-ischemic ventricular arrhythmias. British Heart Journal. Vol.47, pp.137.

G.Critelli, F.Marciano, M.Mazzarella, M.L.Migaux (1982): QT Interval Measurements of Long Term ECG Recordings. Application of an Automatic Holter Analysis System. Computers in Cardiology, IEEE Computer Society Press, pp.481-484.

C.P.Day, J.M.McComb, R.W.F.Campbell (1990): QT dispersion: an indication of arrhythmia risk in patients with long QT intervals. British Heart Journal. Vol.63, pp.342-344.

C.P.Day, J.M.McComb, J.Matthews, R.W.F.Campbell (1991): Reduction in QT dispersion by sotalol following myocardial infarction. European Heart Journal. Vol.12, pp.423-427.

C.P.Day, J.M.McComb, R.W.F.Campbell (1992): QT dispersion in sinus beats and ventricular extrasystoles in normal hearts. British Heart Journal. Vol.67, pp.39-41.

J.P.M de Sa (1982): Digital FIR Filtering for removal of ECG Baseline wander. Journal of Clinical Engineering. Vol.7, No 3, pp.235-240.

Lars Edenbrandt and Olle Pahlm (1988): Comparison of various Methods for Synthesizing Frank-like Vectorcardiograms from the Conventional 12 Lead ECG. Computers in Cardiology, IEEE Computer Society Press, pp.71-74.

W.Einthoven, G.Fahr, A.deWart (1950): On the direction and manifest size of the variations of potential in the human heart and on the influence of the position of the heart on the form of the Electrocardiogram. [Translated by HE Hoff and P Sekeli] American Heart Journal. Vol.40, pp.163.

The .EXE Magazine (May 1989): The .PCX and .PCC File Formats. Vol.3, Issue 11.

G.Forssell, E.Orinius (1981): QT prolongation and ventricular fibrillation in acute MI. Acta Med. Scand. Vol.210, pp.309.

E.Frank (1956): An accurate clinically practical system for spatial vectorcardiography. Circulation. Vol.13, pp.737-749.

M.R.Franz, K.Bargheer, W.Rafflenbeul, A.Haverich, P.R.Lichtlen (1987): Monophasic action potential mapping in human subjects with normal electrocardiograms: direct evidence for the genesis of the T wave. Circulation. Vol.75, pp.379-86.

A.Gerber, R.Studer (1984): A new framework and computer program for Quantitative EMG signal analysis. IEEE Trans. on BME. Vol.31, pp.857-863.

R.C.Gonzalez, P.Wintz (1987): Digital Image Processing. Addison Wesley Publishing Company.

M.J.Goldman (1982): Principles of Clinical Electrocardiography. Lange Medical Publications.

F.Gritzali, G.Frangakis, G.Papakonstantinou (1988): A Method for the detection of the P and T waves. Computers in Cardiology, IEEE Computer Society Press, pp.79-82.

W.G.Guntheroth, M.D. (1982): The QT interval and Sudden Infant Death Syndrome. Circulation. Vol.66, pp.502-504.

S.Haenel (1982): Automated Computer Input of Paperwritten ECG Records by Image Analysis. First IEEE Computer Society International Symposium on Medical Imaging and Image Interpretation. pp.248-259.

P.Hamilton, W.Tompkins (1986): Quantitative Investigation of QRS Detection Rules using the MIT/BIH Arrhythmia Database. IEEE Trans. on BME. Vol.33, No.12, pp.1157-1165.

J.R. Hampton (1986): The ECG made easy. Churchill Livingston. Medical Division of Longman Group UK Limited.

J.Han, B.G.Goel (1972): Electrophysiologic precursors of ventricular tachyarrhythmias. Arch. Intern. Med. Vol.129, pp.749-755.

J.Han, G.K. Moe (1964): Non-uniform recovery of excitability in ventricular muscle. Circulation Research. Vol.14, pp.44-60.

R.E.Haynes, A.P.Hallstrom, L.A.Cobb (1978): Repolarisation abnormalities in survivors of out of hospital ventricular fibrillation. Circulation. Vol 57, pp.654.

P.D.Higham, S.S.Furniss, J.P.Bourke, R.W.F.Campbell (1991): Dynamic changes in QT dispersion during the early phase of acute myocardial infarction: relevance for ventricular fibrillation. [Abstract].Proceedings of Annual British Cardiac Society Meeting, pp.167.

P.D.Higham, R.W.F.Campbell (1992): QT Dispersion in Ischemia and Infarction. European Heart Journal. Volume 13, Abstract Supplement, pp.448. (Proceedings of the XIVth Congress of the European Society of Cardiology, Barcelona, Spain)

P.D.Higham, D.S.Reid, R.W.F.Campbell, S.S.Furniss (1992): Reperfusion and QT Dispersion. European Heart Journal. Volume 13, Abstract Supplement, pp.448. (Proceedings of the XIVth Congress of the European Society of Cardiology, Barcelona, Spain)

P.G.Hoel (1971): Introduction to mathematical statistics. Fourth edition. Wiley International Ltd. Chapter 12.

H.Inoue, I.Toda, A.Nozaki, H.Matsuo, T.Sugimoto (1985): Effects of bretylium tosylate on inhomogeneity of refractoriness and ventricular fibrillation threshold in canine hearts with quinidine-induced long QT interval. Cardiovascular Research. Vol.19, pp.655-660.

A.M.Katz (1977): Physiology of the Heart. Raven Press Books Ltd., New York, pp.257-268.

R.E.Kleiger, J.P.Miller, J.T.Bigger, A.J.Moss (1987): Decreased heart rate variability and its association with increased mortality after acute myocardial infarction. American Journal of Cardiology. Vol.59, pp.256.

C.S.Kuo, K.Munakata, C.P.Reddy, B.Surawitz (1983): Characteristics and possible mechanisms of ventricular arrhythmia dependent on the dispersion of action potential durations. Circulation. Vol.67, pp.1356-67.

P.Laguna, N.V.Thakor, P.Caminal, R.Jane, H.R.Yoon, A.B de Luna, V.Marti, J.Guindo (1990): New algorithm for QT interval analysis in 24-hour Holter ECG: performance and applications. Med. and Biol. Eng. and Comp. Vol.28, pp.67-73.

E.Lepeschkin, B.Surawitz (1952): The measurement of the QT interval of the electrocardiogram. Circulation. Vol.6, pp.378-88.

Ch.L.Levkov (1987): Orthogonal Electrocardiogram derived from the Limb and Chest electrodes of the conventional 12-Lead system. Med. & Biol. Eng. and Comp. Vol.25, pp.155-164.

P.A.Lynn (1971): Recursive digital filters for biological signals. Med and Biol Eng and Comp. Vol.9, pp.37-43.

P.A.Lynn (1977): Online digital signals for biological signals: some fast designs for a small computer. Med. and Biol. Eng. and Comp. Vol.15, pp.534-540.

V.Marti, A.Bayes de Luna, J.Arriola, V.Songa, J.Guindo, J.D de Rozas, J.Marrugat, F.Sanz, with the collaboration of N.Thakor, Y.Min, P.Caminal, P.Laguna (1988): Value of Dynamic QT(corrected) in Arrhythmology. 8th International Congress 'The New Frontiers of Arrhythmias' Marilleva, Italy, January 31-February 6, pp.683-691.

S.L.Meyer (1975): Data analysis for scientists and engineers. John Wiley and Sons, Inc., Chapter 31, Appendix vii.

D.M.Mirvis (1985): Spatial Variation of QT intervals in Normal Persons and Patients With Myocardial Infarction. American College of Cardiology. Vol.5, No.3, pp.625-631.

M.Moller (1981): QT interval In Relation to Ventricular Arrhythmias and Sudden Death in postmyocardial Infarction Patients. Acta Med. Scand. Vol.210, pp.73-77.

G.Nyberg, A.Vedin, C.Wilhelmsson (1979): QT time in patients treated with alprenolol or placebo after MI. British Heart Journal. Vol.41, pp.452-455.

J.O'Donnell, S.B.Knoebel, D.E.Lovelace, P.L.McHenry (1981): Computer Quantitation of Q-T and terminal T wave (aT-eT) Intervals during Exercise: Methodology and Results in Normal Men. American Journal of Cardiology. Vol.47, pp.1168-1172.

G.R. Pai, J.M.Rawles (1989): The QT interval in atrial fibrillation. British Heart Journal. Vol.61, pp.510-513.

J.Pan, W.J.Tompkins (1985): A Real-Time QRS Detection Algorithm. IEEE Trans on BME. Vol.32, No.3, pp.230-236.

T.Pavlidis (1990): Algorithms for Graphics and Image Processing. Computer Science Press.

E.Pisani, E.Pellegrini, G.Ansuini, G.Di Noto, C.Rimatori, P.Russo (1985): Performance evaluation of algorithms for QT interval measurements in ambulatory ECG monitoring. Computers in Cardiology, IEEE Computer Society Press, pp.459-462.

S.Pohjola-Sintonen, P.Siltanen, J.Haapakoski (1986): Usefulness of QT(corrected) interval on the discharge electrocardiogram for predicting survival after acute myocardial infarction. American Journal of Cardiology. Vol.57, pp.1066.

S.J.Poppl (1979): Methods in One-and Two Dimensional Signal Processing. Biomedical Pattern Recognition and Image Processing, eds. K.S.Fu and T.Pavlidis, pp.69-110. Berlin: Dahlem Konferenzen. Verlag Chemie GmbH, D-6940, Weinheim.

P.E.Puddu, R.Jouve, J.Torresani, A.Jouve (1981): QT interval and primary ventricular fibrillation in acute MI. American Heart Journal. Vol.101, pp.118.

P.E.Puddu, M.G.Bourassa (1986): Prediction of sudden death from QT(corrected) interval prolongation in patients with chronic ischemic heart disease. Journal of Electrocardiology. Vol.19, pp.203.

M.H.Reiger, R.N.Mohapatra, S.N.Mohapatra (1982): Biomedical Statistics with Computing. John Wiley and Sons. Chapter 4.

D.J.Rowlands (1980): Understanding the Electrocardiogram - A new approach. Section 1: The Normal ECG. Imperial Chemical Industries Limited.

I.Schlamowitz,M.C. (1946): An analysis of the time relationships within the cardiac cycle of normal men. American Heart Journal. Vol.31, pp.329-342.

P.J.Schwartz,M.D., Stewart Wolf,M.D. (1978): QT interval Prolongation as a Predictor of Sudden Death in Patients with Myocardial Infarction. Circulation. Vol.57, pp.1074-1077.

P.J.Schwartz, M.Montermerlo, M.Facchini, P.Salice, D.Rosti, D.Poggio, R.Giorgetti (1982): The QT interval throughout the first six months of life : A prospective study. Circulation. Vol.66, pp.496.

W.A. Seed, M.Noble, P.Oldershaw, R.B.Wanless, A.J.Drake, D.Redwood, S.Pugh, C.Mills (1987): Relation of human cardiac action potential duration to the interval between beats : Implications for the validity of rate corrected QT interval. British Heart Journal. Vol.57, pp.32-37.

A.S.Sehmi, G.H.Loudon, N.B.Jones, S.Kabay (1991): Knowledge-based systems in neuroelectric signal processing and interpretation. IEE Proceedings, Part A physical Science, Measurement and Instrumentation, Management and Education (submitted for publication).

Mansour Shoaleh-var, T.Lundman, S.Ahnve (1978): Relation between QT interval and ventricular arrhythmias in acute MI. British Heart Journal. Vol.40, pp.439.

E.Simonson,M.D., Lee.D.Cady,M.D., M.Woodbury (1962): The normal QT interval. American Heart Journal. Vol.63, pp.747-753.

P.Sprent (1989): Applied Nonparametric Statistical Methods. Chapman and Hall Ltd. Chapter 5.

J.L.Talmon, J.H.van Bemmel (1983): Template Waveform Recognition Revisited. Results for the CSE data base. Computers in Cardiology, IEEE Computer Society Press, pp.249-252.

G.J.Taylor, R.S.Crampton, R.S.Gibson, P.T.Stebbins, M.T.G.Waldman, G.A.Beller (1981): Prolonged QT interval at onset of acute MI in predicting early phase ventricular tachycardia. American Heart Journal. Vol.102, pp.16.

H.Toyoshima, R.L.Lux, R.Wyatt, M.J.Burgess, J.A.Abildskov (1981). Sequences of early and late phases of repolarisation of dog ventricular epicardium. Journal of Electrocardiology. Vol.14, pp.143-152.

P.Trahanias, E.Skordalakis (1988): Delineation of the boundaries of the ECG complexes. Computers in Cardiology, IEEE Computer Society Press, pp.501-504.

S.Usui, I.Amidror (1982): Digital Low-Pass Differentiation for Biological Signal Processing. IEEE Trans. on BME. Vol.29, No 10, pp.686-693.

J.A.van Alste and T.S.Schilder (1985): Removal of Base-Line Wander and Power-Line Interference from the ECG by an Efficient FIR Filter with a Reduced Number of Taps. IEEE Trans. on BME. Vol.32, No.12 pp.1052-1060.

J.H.van Bemmel, J.L.Talmon, J.S.Duisterhout, S.J.Hengeveld (1973): Template Waveform Recognition Applied ECG/VCG Analysis. Computers and Biomedical Research. Vol 6, pp.430-441.

E.M.Vaughan Williams (1980): Antiarrhythmic action, the puzzle of perhexiline, London, Academic Press: pp.26-30.

R.Wariar, C.Eswaran (1991): Integer Coefficient band-pass filter for the simultaneous removal of baseline wander, 50 and 100Hz interference from the ECG. Med and Biol Eng and Comp. Vol.29, pp.333-336.

J.Wartak (1970): Computers in Electrocardiography. Charles C.Thomas, Springfield, Ill.

L.E.Widman, G.L.Freeman (1989): A-to-D Conversion from Paper Records with a Desktop Scanner and a Microcomputer. Computers and Biomedical Research. Vol.22, pp.393-404.

K.Wheelan, J.Mukharji, R.E.Rude, W.Poole, N.Gustafson, L.Thomas, H.Strauss, A.Jaffe, J.Muller, R.Roberts, C.Croft, E.Passamani, J.Willerson, Milis study group (1986): Sudden death and its relation to QT interval prolongation after acute myocardial infarction: Two year follow up. American Journal of Cardiology. Vol.57, pp.745-50.

T.Y.Zhang, C.Y.Suen (1984): A Fast Parallel Algorithm for Thinning Digital Patterns. Communications of the ACM. Vol.27, Number 3, pp.236-239.

Appendix A

H.K.Bhullar, D.P.de Bono, J.C.Fothergill, N.B. Jones (Sept. 1991):A Computer Based System for the Study of QT intervals. Proceedings, Computers in Cardiology, Venice, IEEE Press, Los Alamitos, USA, 533-536.

A Computer Based System for the Study of QT Intervals

H.K.Bhullar
Dept. of Engineering
Univ. of Leicester
Leicester, U.K.

D.P.de Bono
Dept. of Cardiology
Univ. of Leicester
Leicester, U.K.

J.C.Fothergill
Dept.of Engineering
Univ. of Leicester
Leicester, U.K.

N.B.Jones
Dept.of Engineering
Univ. of Leicester
Leicester, U.K.

Abstract

Recent research suggests that the dispersion of QT intervals across 12 leads of the standard electrocardiogram (ECG) is a clinically important indicator of the susceptibility of patients to serious ventricular arrhythmias. This hypothesis can be further tested by measuring ECGs from large clinical trials in which outcome is known for each patient. These ECGs are stored on paper. We have developed a system which scans ECG waveforms stored on paper, and converts them to digital data stored on computer. The system which incorporates a user-interface, enables quick and reliable measurements of QT intervals, thereby replacing the tedious and potentially insensitive method of hand measurements. Preliminary results of comparison between hand and user-interactive measurements are presented to show the accuracy and characteristics of the system.

1 Introduction

The prognostic value of a single prolonged QT interval has for a long time been the subject of debate and discussion. It is believed to be an indicator of delayed or asynchronous ventricular repolarisation. This increase in the degree of dispersion of repolarisation could predispose a patient to the occurrence of malignant ventricular arrhythmias and sudden death [1,2]. Recent research [3,4,5,6] indicates strong evidence that regional differences in repolarisation is reflected by the differences in the QT interval measured in the 12 different leads. In his study of QT intervals involving 150 torso electrodes, Mirvis has shown that normal patients and patients with myocardial infarction show different and distinctive spatial distributions that are consistent with known myocardial physiology. Further evidence in this direction comes from Campbell's group who suggest that QT variation across 12 leads reflect spatial differences in myocardial recovery time. In patients with prolonged QT intervals, the group found that QT dispersion across 12 leads distinguished between those with ventricular arrhythmias and those without. By far the most common form of data storage is still on paper. Larger numbers of twelve lead scalar ECGs are already available from clinical trials where the eventual outcome of these patients is known. In most studies involving the measurement of QT intervals, hand measurements are still popular. Digitising pads have also been used. Whilst being adequate, these methods do not provide for further analysis via transformations of the waveform data. The following sections describe the system that has been designed to overcome these problems by allowing data stored on paper to be converted to digital data stored on computer. A user-friendly interface has also been developed to allow the cardiologist to perform measurements of QT and RR intervals.

2 Scanning ECG images

A flatbed black and white Hewlett Packard ScanJet Plus scanner is used to capture 12 lead ECG records, at 300 dots per inch (d.p.i). The 12 lead image is stored as an image file in the 'PCX' format. A graphics editor is then used to segment the image into 12 sets of individual lead data, each stored as a 'PCX' file.

3 Interpretation of files

For each lead image file, a two dimensional array comprising 1's and 0's is created. This is done by interpreting each 'PCX' file. The background or white pixels are denoted by 0's; the black pixels forming the waveforms are denoted by 1's.

4 Error considerations

Many different sorts of errors are introduced in the scanning process. The square sampling grid used by the scanner introduces sharp edges in the waveform images. These correspond to the introduction of high frequencies

in the image. Such 'aliasing' problems can cause the loss of gaps or random scatter of pixels in the image, resulting in shape distortion. These problems would be encountered even at high sampling frequencies [8]. Different paper granularities and different recording pen thickness can also contribute to these problems. In the system developed, pre-processing of the entire data array is carried out before any digital values are extracted.

5 Pre-processing the ECG waveform

Figure 1(a) shows a 5x5 window that is used to traverse column by column, for all rows, each element of the two-dimensional data array. As this window traverses the array, each element of the array is in turn assigned to be p1 and the relationship between itself and its 8 and 16 neighbours is studied. A set of heuristic rules studying these relationships is then used to make a decision on where random noise exists in the image. Once the entire array has been traversed, these points are deleted (changed from 1 to 0). The rules then check for gaps or disconnectedness in the image, and again when the entire array has been traversed, points relating to the gaps are then filled (changed from 0 to 1).

Figure 1(b) shows a segment of ECG data derived from a relatively straight area of ECG waveform. P1 is an example of a pixel point that has been detected as random noise. The rules that detect this, and which decide its

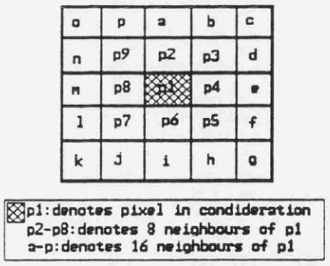

Fig. 1(a)

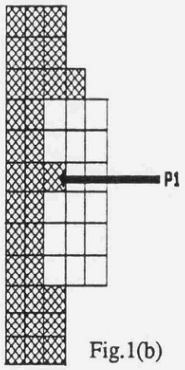

Fig.1(b)

subsequent removal are given here: i) p1=1 and ii) the logical 'or' of p2, p3, p4, p5, p6, a, b, c, d, e, f, g, h, i is 0 and iii) the logical 'and' of p7, p8, p9, j, p is 1.

These rules are implemented taking into account that the pixel data can be oriented in any four directions (right, left, up or down). A 5x5 window was selected as in our experience, random noise would not be distributed in groups larger than this and that most missing pixels causing gaps in the image occur within such an area.

Figures 2(a) and 2(b) show the elimination of random noise and the filling in of gaps of a peak in an ECG waveform. This was performed by the pre-processing stage.

6 Thinning the ECG waveform

The main consideration in the reconstruction of ECG waveforms is the preservation of shape information, so that digital data can be recovered accurately. Because of this consideration, a scanner sampling rate of 300 d.p.i. was used. This would further ensure that no lines would be broken in the reconstructed image. As can be seen in Figure 2(a), this causes a width of more than 2 pixels to be used to form the reconstructed image. An important

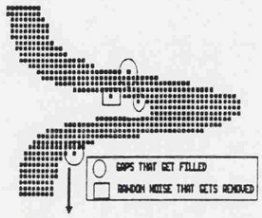

Fig. 2(a) Unthinned and Unprocessed Image

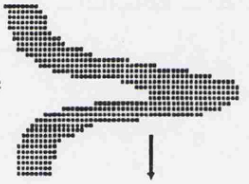

Fig. 2(b) Pre-processed Image

Fig. 2(c) Skeleton of an ECG Waveform Peak.

approach for recapturing the lineal structure of data without destroying its connectivity is a procedure called thinning [7,8,9]. Thinning is often used on binary images to obtain their 'skeleton'. Because of its suitability, it has been used here to recover ECG waveform shape. An algorithm developed by Zhang & Suen [1984] has been adopted for this procedure. Figure 2(c) shows the recovery of the thinned image or skeleton. As can be seen in Figure 2(a), thinning has yielded the lineal structure of the ECG waveform.

7 Recovery of digital data

Digital data values are extracted from the skeleton of the ECG waveform by taking the mid-point offset of the start and end pixel in each row of the array containing the skeleton. This gives a data file with amplitude values for each data point. Based on the relationship between the scanner sampling rate used and the time and amplitude relationships on the actual data records (on paper), an appropriate time value and amplitude can be assigned to each data point. This set of data points is then high-pass and low-pass filtered at cut-off frequencies of 0.12Hz and 75Hz respectively.

8 User-interactive system

A user-interactive system was designed to allow the display of each patient's retrieved ECG waveform. The system was designed to allow for user-interactive measurements using cursors. In the following section, the terms "user-interactive technique" will be used to denote measurements performed using this system.

9 Preliminary tests

Preliminary tests were carried out on the system with data from three patients giving reliable ECG waveforms from a total of 35 leads. The data was analysed by both the conventional "by hand" technique and by using our "user-interactive" technique described above. Since the system was designed by an engineer but measurements are usually made by a cardiologist, these analyses were carried out by both the system designer (observer1) and an independent cardiologist (observer2). As the QT interval is not always well defined (for example the T wave end is often unclearly delimited), it was decided to also make measurements of the RR' interval. As this is generally the most clearly defined interval of the ECG waveform this would give an indication of the "best" performance of the system in comparison to the conventional hand measurements.

Bland and Altman [10] have discussed techniques for assessing the agreement between measurement methods. They have shown that the use of the Pearson's product-moment correlation coefficient ("r") may be misleading since it is an indicator of correlation and not necessarily of agreement. We have therefore adopted a similar procedure to them.

Figure 3 shows, for each lead, the difference between user-interactive and hand measurements of the RR' interval as a function of the mean RR' interval. Data is taken from both observers. The mean of the differences, which is indicative of a consistent bias, was -0.26%

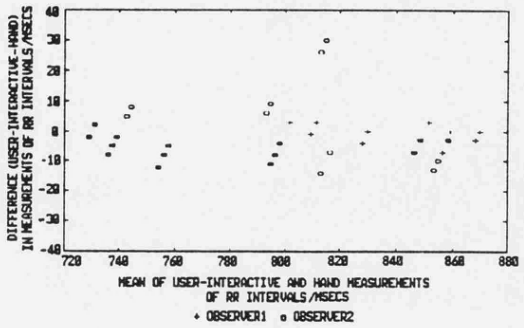

Fig. 3

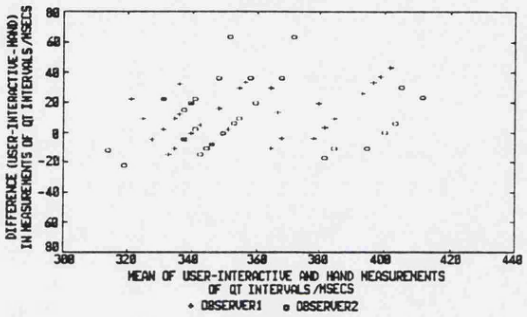

Fig. 4

(-2.1msecs) and the standard deviation of the differences, which is an indicator of the confidence of the agreement of the two methods, was 1.5% (12 msecs). The bias may be considered negligible since it is much smaller than the standard deviation; it can therefore be concluded that the reconstruction of the waveform image is likely to be accurate. Since the RR' intervals are the best defined, ±1.5% is a representation of the likely accuracy of the system (for this number of waveforms).

Figure 4 shows the results of similar measurements but using QT intervals. The mean of the differences in this case was 2.4% (9 msecs) with a standard deviation of 7.5% (28 msecs). Again the bias represented by the mean is small, but the standard deviation is much greater than for the RR' interval, thereby representing a decrease in agreement. This cannot be accounted for in terms of a malfunction of the user-interactive technique (since there was good agreement of RR' intervals) but must be because the QT intervals themselves are less clearly defined, i.e. the lack of agreement is due to inconsistencies in the way the observers have interpreted the QT intervals.

It is interesting to consider whether inter-observer variability is decreased when the user-interactive system is employed. Figure 5 shows, for each lead, the difference between the observer's measurements of the RR' interval.

The figure shows measurements made using both techniques. The mean of the differences (bias) is negligible in both cases (0.51% hand and 0.002% user-interactive) and the standard deviation, indicative of inter-observer variability, is decreased from 1.4% to 0.3%. The user-interactive technique appears successful in this respect. For the QT intervals, (Figure 6), the bias is again negligible (3.2% hand and 2.1% user-interactive) but inter-observer variability is only slightly reduced from 5.3% to 4.1%. Again this is thought to be due to inconsistencies in the way observers interpret QT intervals.

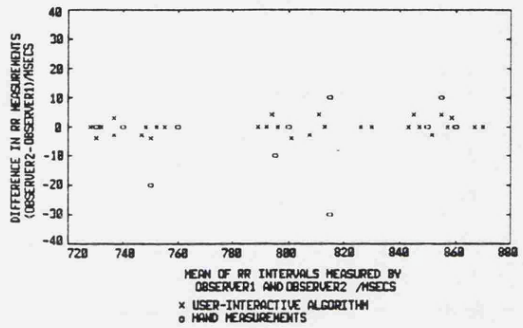

Fig. 5

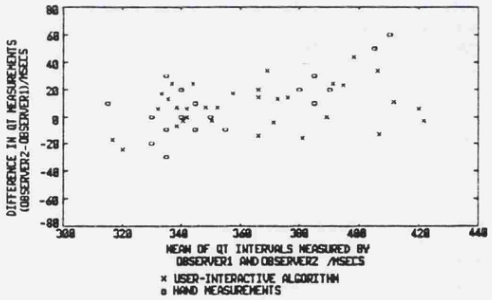

Fig. 6

10 Conclusions

These preliminary tests have indicated that the system reconstructs the waveforms in a computer-compatible format accurately. The user-interactive system was easily used by a cardiologist who had not used the system before. Typical agreement between the user-interactive and hand techniques is better than 3% as indicated by RR' interval measurements; this may be representative of an increase in the absolute accuracy of measurement when using the user-interactive technique. Inter-observer variability is decreased when the waveforms are clearly delineated.

Acknowledgements

Many thanks are due to Dr. Trevor Johnson of the Cardiology Dept., Glenfield Hospital, Leicester for his help in performing relevant measurements. Thanks are also due to Dr. G.H.Loudon, Mr. J.T.Wang and Mr. T.Tran of the Engineering Dept., Leicester University for their kind support and advice.

References

[1] Schwartz P.J, Wolf S.,"QT interval prolongation as predictor of sudden death in patients with myocardial infarction", *Circulation*, Vol. 57, pp.1074-7,1978.

[2] Han J, Moe G.K."Non-uniform recovery of excitability in ventricular muscle", *Circulation Res* Vol. 14, pp.44-60, 1964.

[3] C.P.Day, J.M.McComb, R.W.F.Campbell, "QT dispersion: an indication of arrhythmia risk in patients with long QT intervals", *British Heart Journal*, Vol. 63, pp. 342-344, 1990.

[4] C.P.Day, J.M.McComb, J.Matthews, R.W.F.Campbell, "Reduction in QT dispersion by sotalol following myocardial infarction", *European Heart Journal*, Vol. 12 , pp.423-427, 1991.

[5] P.D.Higham, S.S.Furniss, J.P.Bourke, R.W.F.Campbell, "Dynamic changes in QT dispersion during the early phase of acute myocardial infarction: relevance for ventricular fibrillation", *Proceedings of Annual British Cardiac Society Meeting*, pp.167, April/May 1991.

[6] D.M.Mirvis, "Spatial Variation of QT intervals in Normal Persons and Patients With Myocardial Infarction", *American College of Cardiology*, Vol.5, No.3, pp.625-631, March 1985.

[7] R.C.Gonzalez & P.Wintz, *Digital Image Processing*, Addison Wesley Publishing Company, Nov. 1987.

[8] T.Pavlidis, *Algorithms for Graphics and Image Processing*, Computer Science Press, 1990.

[9] T.Y.Zhang & C.Y.Suen, "A Fast Parallel Algorithm for Thinning Digital Patterns", *Communications of the ACM*, Vol. 27, Number 3, pp.236-239, March 1984.

[10] J.M.Bland & D.G.Altman, "Statistical Methods for Assessing Agreement between Two Methods of Clinical Measurement", *The Lancet*, pp.307-310, February 8, 1986.

Appendix B

H.K.Bhullar, J.C.Fothergill, D.P.de Bono (March 1992): Computer-based techniques for the optimal extraction of medical data from graphical paper records. IEE Colloquim on Medical Imaging - Image Processing and Analysis, Digest Number : 1992/051.

COMPUTER-BASED TECHNIQUES FOR THE OPTIMAL EXTRACTION OF MEDICAL DATA FROM GRAPHICAL PAPER RECORDS

***H.K.Bhullar, *J.C.Fothergill, **D.P.de Bono**

Abstract

In the medical environment, important waveform data are often stored as paper records produced by chart recorders etc. Typical data stored include electromyograms (EMG), electrocardiograms (ECG) and electroencephalograms (EEG). Many such paper records exist in hospital archives and are very useful for retrospective studies of patients where the eventual outcomes are known. In order to enable computer-based processing of such data, it is necessary to extract the waveform data automatically in such a way that problems such as random noise and thick line widths are overcome. A system is described which uses a new technique for the conversion of two dimensional waveforms conventionally stored on paper to a one dimensional array of data values.

Paper records containing the waveform data are first scanned using a high resolution, flatbed, black and white scanner. The two dimensional pixel based images that are captured are stored as image files in the computer. Three digital image processing techniques are applied to these stored images. The first is a heuristic method for the automatic removal of random noise and the filling in of gaps in the captured image which are errors introduced during the scanning process. The second technique involves thinning each pixel based waveform to derive its skeleton. This is an important and necessary stage as it attempts to overcome the effects associated with the thickness of the pen recorder lines, on the original image. In the final part of the processing, data values are extracted from the thinned waveforms. These values are then filtered to eliminate quantisation errors introduced in the scanning process.

Results using ECG waveforms are presented. In order to demonstrate the accuracy of the techniques, computer-based measurements of the recovered waveforms are shown to compare well with manual measurements made by cardiologists on the original waveforms stored on paper.

1 Introduction

As a result of advances in digital technology, many hospitals now utilise advanced computers to record Electrocardiographic (ECG), Electromyographic (EMG) and Electroencephalographic (EEG) data on line via an A-to-D card or onto magnetic tape, which can then be played back and digitised. There are many advantages to analysing data digitally. Useful transformations can be applied to the data and measurements of useful parameters can be automated, thus reducing overall errors in data analysis.

In many cases, these data are often stored as graphical paper records printed by a chart recorder. Indeed, in the area of ECG analysis, the most common mode, of storing the standard 12 lead ECG of each patient is as a paper record. In the area of ECG analysis, recent research has shown that important diagnostic information is reflected in simple ECG recordings stored on paper [1]. Figure 1(a) shows an example of a standard 12 lead ECG stored on paper. Many of the hospital archives containo paper records of unique waveform shapes relating to rare conditions that if their digital values could be extracted, would be of great use as references.

A new method for the recovery of digital data is described in this paper. The following sections describe the new technique for data recovery that involves 'pre-processing', 'thinning' and extracting data values.

***Department of Engineering**
**** Department of Cardiology**
University of Leicester, Leicester LE1 7RH.

2 Scanning Medical Images

A flatbed black and white Hewlett Packard ScanJet Plus scanner connected to an IBM compatible AT machine, via an appropriate interface is used to scan medical waveforms. The scanner sampling rate is 300 dots per inch (d.p.i.). This is an equivalent sampling rate of 295 Hz (3.4 msecs/pixel) for data recorded at 25mm/sec. It must be ensured that the images to be scanned must be oriented in a straight line vertically to ensure that the waveforms detected are not rotated, as this may introduce a relative offset when digital values are extracted. Appropriate colour filters are used to eliminate any background grid lines. These waveform images are first stored as one image file in the '.PCX' format which is compatible with most software programs and which can be easily interpreted so that the way in which the data representing the image is organised can be understood easily. This would allow for further manipulation of the image waveforms. Furthermore data storage with the .PCX format is quicker than for the TIFF format and occupies less space. A graphics editor is then used to segment the single .PCX image into rectangles, each containing a single waveforms, and each stored as a '.PCX' file.

3 Interpretation of files

For each lead image file, a two dimensional array comprising 1's and 0's is created by interpreting each '.PCX' file [2]. The background or white pixels are denoted by 0's; the black pixels forming the waveforms are denoted by 1's.

4 Error Considerations

Many different sorts of errors are introduced in the scanning process. The square sampling grid used by the scanner introduces sharp edges in the waveform images. These correspond to the introduction of high frequencies in the image. Such 'aliasing' problems can cause the loss of gaps and random scatter of pixels in the image, resulting in shape distortion and random marks on the original image. These problems may also arise due to the different scanner sensitivity to different pen recordings. These factors would be encountered even at high sampling frequencies. Different paper granularities, different recording pen thicknessess and irregularities of the pen tracing also contribute to this problem. In the system developed, pre-processing of the entire data array is carried out before any digital values are extracted.

5 Pre-processing Medical Waveforms

Figure 2(a) shows a 5x5 window that is used to traverse column by column, for all rows, each element of the two-dimensional data array. As this window traverses the array, each element of the array is in turn assigned to be 'p1' and the relationship between itself and its 8 and 16 neighbours is studied. A set of heuristic rules studying these relationships are then used to make a decision on where there exists random noise in the image. Once the entire array has been traversed, these points are deleted (changed from 1 to 0). The rules then check for gaps or disconnectedness in the image, and again when the entire array has been traversed, points relating to the gaps are changed from 0 to 1.

Figure 2(c) shows an unthinned and unprocessed image of a typical ECG waveform. The point marked (a)* (and described by the corresponding 'rule diagram' Rule(a) in Figure 2(b)) describes an example of a point that has been detected as random noise and which should be deleted. Points (b)*,(c)*,(d)*,(e)* and (f)* on Figure 2(c) have been tagged as gaps in the image waveform that need to be filled, and these points are similarly described by their corresponding 'rule-diagrams' in Figure 2(b). Some of the rules that describe the orientation of the pixels in the 8 and 16 neighbourhood, which decide whether the pixel point under consideration should be removed or filled are given below:

Rules for the removal of randomly distributed pixels

Rule (a)

If:

i) p1 is 1

ii) the logical '*or*' of p4,p5,p6,p7,p8,e,f,g,h,i,j,k,l,m is 0

iii) the logical '*and*' of p9,p2,p3,n,d is 1

then store the coordinates of p1 in a file for later removal

Rules for the filling in of gaps and removal of disconnectedness

Rule (b)

If:

i) p1 is 0

ii) the logical '*or*' of p7,p8,p9,j,p is 0

iii) the logical '*and*' of p3,p4,p5,b,h is 1

iv) the logical '*and*' of p6,p2 is 1

then store the coordinates of p1 in a file for later conversion to a value of 1

Rule (c)

If:

i) p1 is 0

ii) the logical '*or*' of p3,p4,p5,b,h is 0

iii) the logical '*and*' of p7,p8,p9,j,p is 1

iv) the logical '*and*' of p2,p6 is 1

then store the coordinates of p1 in a file for later conversion to a value of 1

Rule (d)

If:

i) p1 is 0

ii) the logical '*or*' of l,p7 is 1 and the logical '*or*' of p5,p6,f is 0

iii) the logical '*and*' of p9,p2,p3,n,d is 1

iv) the logical '*and*' of p4,p8 is 1

then store the coordinates of p1 in a file for later conversion to a value of 1

Rule (e)

If:

i) p1 is 0

ii) the logical '*or*' of f,p5 is 1 and the logical '*or*' of p6,p7,l is 0

iii) the logical '*and*' of p9,p2,p3,n,d is 1

iv) the logical '*and*' of p4,p8 is 1

then store the coordinates of p1 in a file for later conversion to a value of 1

Rule (f)

If:

i) p1 is 0

ii) the logical '*or*' of p9,p2,p3,n,d is 0

iii) the logical '*and*' of p5,p6,p7,f,l is 1

iv) the logical '*and*' of p8,p4 is 1

then store the coordinates of p1 in a file for later conversion to a value of 1

These rules are implemented taking into account that the data can be oriented in any four directions (right, left, up or down; compare points b* and c* in Figure 2(c)). A 5x5 window was selected as in our experience, random noise would not be distributed in groups larger than this and that most missing pixels causing gaps in the image occur within such an area.

Figure 2(d) shows the elimination of random noise and the filling in of gaps of the ECG waveform. This was performed by the pre-processing stage.

6 Thinning Medical waveforms

The main consideration in the reconstruction of medical waveforms is the preservation of shape information, so that digital data can be recovered accurately. Because of this consideration, a scanner sampling rate of 300 dots per inch was used. This would further ensure that no lines would be broken in the reconstructed image. As can be seen in Figure 2(c), this causes a width of more than 2 pixels to be used to form the reconstructed image. An important approach for recapturing the lineal structure of data without destroying its connectivity is a procedure called 'thinning' [3],[4],[5].

Thinning is often used on binary images to obtain their skeleton, where the skeleton of a region may be defined by the medial axis transform (MAT) proposed by Blum (1967) [6]. The MAT of a region R with border B is defined as follows. For each point p in R, its closest neighbour in B is found. If more than one such neighbour exists for p, it is said to belong to the medial axis (skeleton) of R. The concept of 'closest' depends on the definition of a distance and therefore the MAT will be influenced by the choice of a given distance measure. Because of its suitability, it has been used here to recover different medical waveform shapes. An algorithm developed by Zhang & Suen [1984] for thinning binary regions has been adopted for this procedure. Three main constraints are generally applicable to thinning algorithms. The algorithms that iteratively delete edge points of a region should not remove end points, break connectedness or cause excessive erosion of the region. Figure 2(e) shows the recovery of the thinned image or skeleton. As can be seen in Figure 2(d), thinning has yielded the lineal structure of the ECG waveform.

7 Recovery of digital data

Digital data values are extracted from the skeleton of a waveform by taking the mid-point offset of the start and end pixel in each row of the array containing the skeleton. This gives a data file with amplitude values for each data point. Based on the relationship between the scanner sampling rate used and the time and amplitude relationships on the actual data records (on paper), appropriate time and amplitude values can be assigned to each data point. This data can then be low-pass filtered ie. smoothed to reduce the effects of quantisation introduced in the scanning process.

8 User-interactive system

A user-interactive system was designed to allow the display of each patient's medical waveforms. The system was designed amongst other things, to allow for user-interactive measurements using cursors to be performed on these waveforms. An advantage of the system is that the 'arrow' cursor used to make user-interactive measurements is made to follow the data values in the signal, and this allows for greater sensitivity in measurements as random human error associated with positioning of the cursor is reduced.

9 Validation of System Accuracy

To test the accuracy with which the new technique recovered graphical data stored on paper, it was decided that 116 ECG waveforms comprising data from ten patients would be scanned and processed (compare with previous study, Bhullar et al, 1991). Conventional 'QT interval' and 'RR interval' measurements (Figure 1(b)) were performed by both the conventional "by hand" technique which involved the observer making these measurements on the ECG waveforms stored on paper using a ruler and calipers and by using the "user-interactive" technique described in this paper, which involves making cursor-interactive measurements on the recovered data stored on computer. Since the system was designed by an engineer but measurements are usually made by a cardiologist, these analyses were carried out by both the system designer (observer1) and an independent cardiologist (observer2). Since the QT interval is not always well defined (for example the T wave end is often unclearly delimited), it was decided to also make measurements of the RR' interval. As this is generally the most clearly defined interval of the ECG waveform this would give an indication of the "best" performance of the system in comparison to the conventional hand measurements.

Bland and Altman [8] have discussed techniques for assessing the agreement between measurement methods. They have shown that the use of the Pearson's product-moment correlation coefficient ("r") may be misleading since it is an indicator of correlation and not necessarily of agreement. We have therefore adopted a similar procedure to them.

Figure 3 shows, for each lead, the difference between user-interactive and hand measurements of the RR' interval as a function of the mean RR' interval. Data is taken from both observers. The mean of the difference of observer1 is -0.2%, whilst that of observer2 is 0.5%. The combined mean of the differences of both observers, which is indicative of a consistent bias, was 0.15% (1.3 msecs) and the standard deviation of the differences, which is an indicator of the confidence of the agreement of the two methods, was 1.2% (10 msecs). The bias may be considered negligible since it is much smaller than the standard deviation; it can therefore be concluded that the reconstruction of the waveform image is likely to be accurate. Since the RR' intervals are the best defined, +/- 10 msecs is a good representation of the likely accuracy of the system.

Figure 4 shows the results of similar measurements but using QT intervals. The mean of the difference of observer1 was 3.4%, whilst that of observer2 was 4.8%. The combined mean of the differences of both observers in this case was 4.1% (14.3 msecs) with a standard deviation of 8.0% (28 msecs). Both the bias represented by the mean and the standard deviation of the differences are much greater than for the RR' interval. This apparent increase in bias and the decrease in agreement cannot be accounted for in terms of a malfunction of the user-interactive technique (since there was good agreement of RR' intervals) but must be because the QT intervals themselves are much worse defined, i.e. the lack of agreement is due to inconsistencies in the way the observers have interpreted the QT intervals.

It is interesting to consider whether accuracy in measurements is increased when the user-interactive system is employed. Figure 5 shows, for each lead, the difference between the observer's measurements of the RR' interval. The figure shows measurements made using both techniques. The mean of the differences (bias) is negligible in both cases (0.76% hand and 0.05% user-interactive) and the standard deviation, indicative of inter-observer variability, is decreased from 1.1% to 0.4%. For the QT intervals, (Figure 6), the bias is again negligible (2.4% hand and 0.99% user-interactive). However inter-observer variability is increased from 3.8% to 6.4%. As inter-observer variability with RR interval measurements improved with the user-interactive system, and as RR intervals are well defined as conventionally sharp peaks in the ECG, the apparent increase in inter-observer variability reflected with QT interval measurements may represent the greater accuracy of the user-interactive system as well as the greater subjectivity involved in the measurements of QT intervals.

10 Review of Techniques

There are three popular techniques that are used in the extraction of data values from graphical records. The use of digitising pads is one such technique. Because it depends on the user for the selection of points, only certain points of interest in a signal are generally recorded. Digitising whole sets of signals is time consuming,and prone to errors due to user selection of data points.

Haenel [1982] [9] employs the second technique which involves the use of a high resolution TV camera to scan ECG records. The experimental resolution achieved by Haenel was 260 d.p.i. and full chart length was processed by ten frames scanned in particular overlay and connected after curve extraction by a fast correlation method. Again, this is time consuming and the choice of a high resolution TV camera should be balanced against the hardware costs and the quality of the original recording. The main advantage of cameras compared to expensive optical scanners is that they can be used directly with non-printed images.

The final technique that has been proposed for the recovery of digital data from graphical records is by the use of a flatbed optical scanner. Widman and Freeman [1989] [10] have developed a computer program that stores and processes image data in the Tagged Image File Format (TIFF). The typical time it takes to store a TIFF file that is 8.5 inches by 11 inches is 2.5 minutes if the image is uncompressed and 1.3 minutes if the image is compressed. The storage space required for an uncompressed TIFF file of the above dimensions is approximately 1.06 Megabytes, whilst that for a compressed TIFF file is approximately 25 Kilobytes. The method proposed in this paper employs the '.PCX' file storage format, which is easy to interpret and for the above dimensions, occupies 40 Kilobytes and takes 10 seconds to store.

The method proposed by Widman and Freeman firstly identifies the line representing the signal in the image using a line following algorithm. As the line representing the signal is a few pixels in width, two methods are then proposed for the extraction of data values relating to the value of the signal: the mid-point method and the slope following method.

The former method, as mentioned by the authors, filters high frequencies in the signal which may be significant. Taking the mid-point of a segment to represent the true data point also distorts rapidly changing signals, and makes it more prone to noise artefacts.

The latter method accepts the data point at the top of the line segment if the signal line is rising rapidly and at the bottom of the line segment when the line is falling rapidly, and in regions of the image where the slope is not above or below the established threshold, the value of the line is considered to be the mid-point of the segment. Whilst this method is intuitively pleasing, at low frequencies the signal is still prone to noise due to the mid-point of the segment being selected as the data point.

11 Discussion

The technique proposed in this paper does not require a search for the line representing the signal. Like Widman and Freeman, only one signal waveform is stored per file to be interpreted. A pre-processing stage has been incorporated to eliminate random noise and fill in the gaps in the image. Unlike Widman and Freeman, the new method proposes 'thinning' as a means of recovering the lineal structure of the waveforms recorded, before data values are extracted. The extraction of data values employs the mid-point method but operates on the skeleton of the image, not the original image as proposed by Widman and Freeman. The skeleton of an image gives a reliable representation of the basic structure of the image when it is not distorted by pen thickness.

12 Conclusions

These preliminary validation tests have indicated that the system reconstructs the waveforms in a computer-compatible format accurately. It makes use of technology that is available and affordable. The user-interactive system is easily used by a cardiologist who has not used the system before. Typical agreement between the user-interactive and hand techniques is better than 2.4% as indicated by RR' interval measurements; this may be representative of an increase in the absolute accuracy of measurement when using the user-interactive technique. Inter-observer variability is decreased when the waveforms are clearly delineated. This system is already being used at the Leicester University Cardiology Department in the recovery of the standard 12 lead ECG waveforms stored on paper. It replaces the method of tedious hand measurements, and has proven to be as reliable and possibly more accurate than hand measurements.

13 Acknowledgements

Many thanks are due to Dr.William Goddart of the Cardiology Dept, Glenfield Hospital, for his help in performing large numbers of tedious measurements.

14 References

[1] C.P.Day, J.M.McComb, R.W.F.Campbell, "QT dispersion: an indication of arrhythmia risk in patients with long QT intervals", British Heart Journal, Vol. 63, pp. 342-344, 1990.

[2] "The .PCX and .PCC File Formats", .EXE Magazine, Vol. 3, Issue 11, May 1989.

[3] R.C.Gonzalez & P.Wintz, "Digital Image Processing", Addison Wesley Publishing Company, November 1987.

[4] T.Pavlidis, "Algorithms for Graphics and Image Processing", Computer Science Press, 1990.

[5] T.Y.Zhang & C.Y.Suen, "A Fast Parallel Algorithm for Thinning Digital Patterns", Communications of the ACM, Vol. 27, Number 3, pp.236-239, March 1984.

[6] H.Blum, "A Transformation for Extracting New Descriptors of Shape", Models for the Perception of Speech and Visual Form, Wathen-Dunn, MIT Press, Cambridge, Mass., 1967.

[7] H.K.Bhullar, D.P.de Bono, J.C.Fothergill, N.B.Jones,"A Computer Based System for the Study of QT Intervals", Annual Conference on Computers in Cardiology, September 23-26, 1991, Venice.

[8] J.M.Bland & D.G.Altman, "Statistical Methods for Assessing Agreement between Two Methods of Clinical Measurement", The Lancet, pp.307-310, February 8, 1986.

[9] S.Haenel, "Automated Computer Input of Paperwritten ECG Records by Image Analysis", First IEEE Computer Society International Symposium on Medical Imaging and Image Interpretation, pp.248-259, October 26-28, 1982.

[10] L.E.Widman & G.L.Freeman,"A-to-D Conversion from Paper Records with a Desktop Scanner and a Microcomputer",Computers and Biomedical Research, Vol. 22, pp.393-404, 1989.

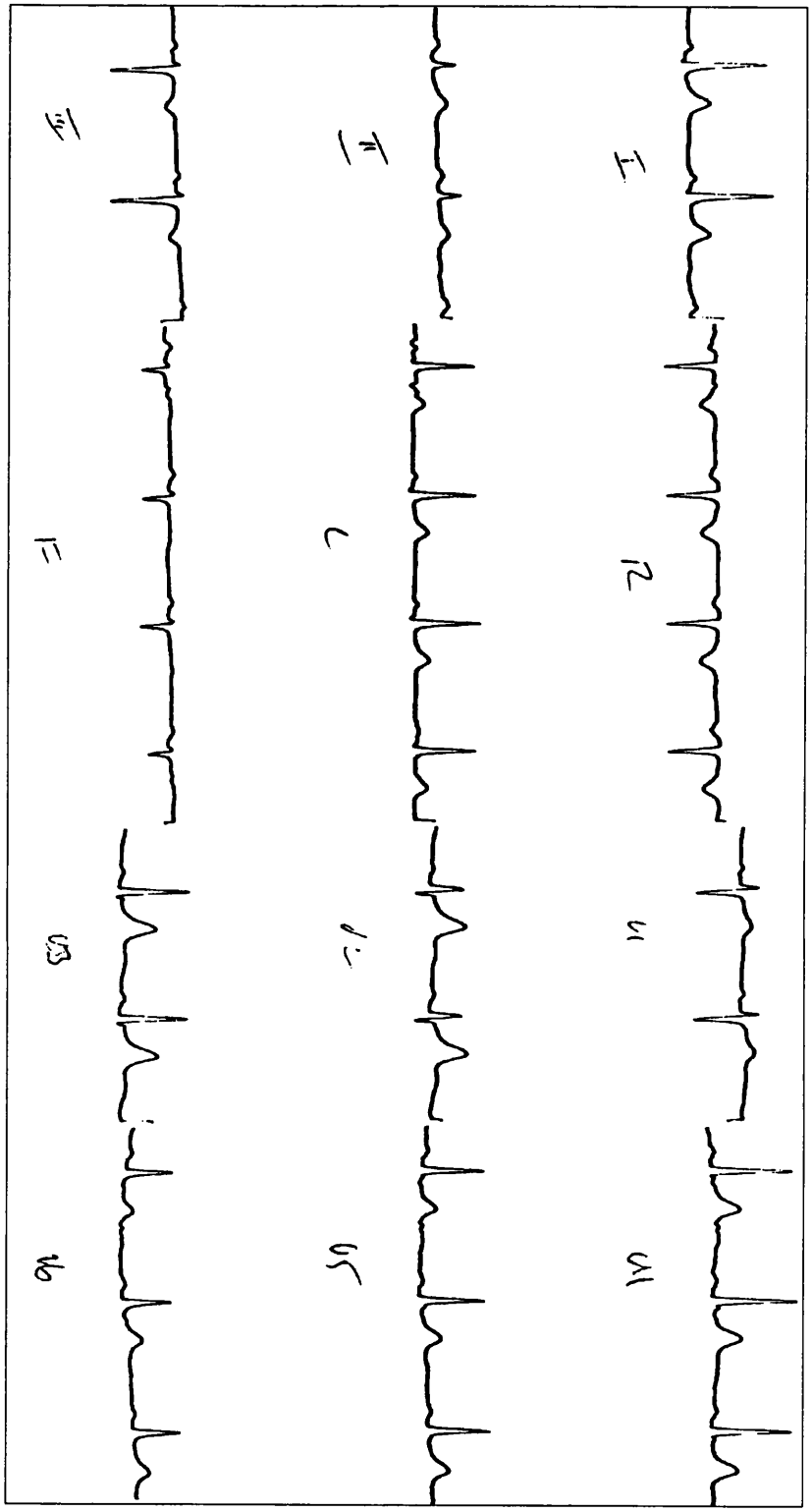

Figure 1(a)

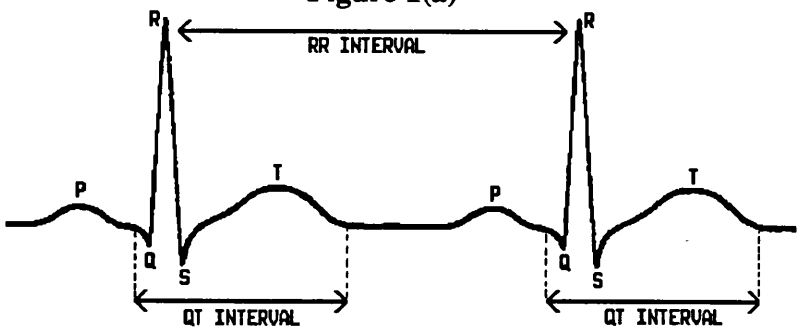

Figure 1(b)

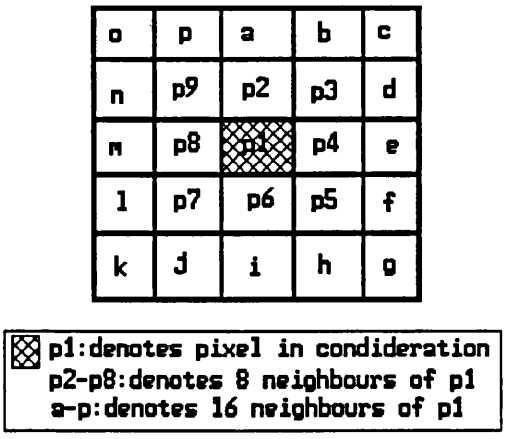

Figure 2(a)

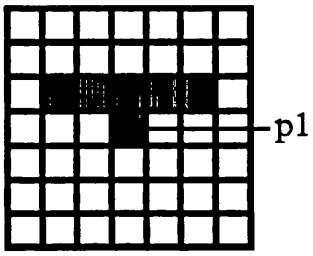

Rule (a)

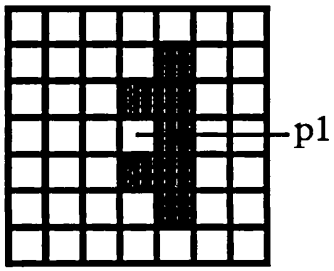

Rule (b)

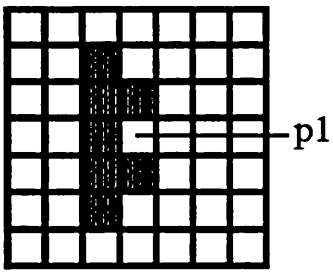

Rule (c)

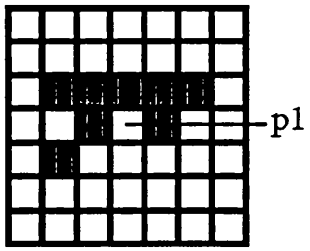

Rule (d)

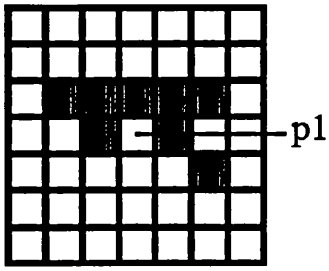

Rule (e)

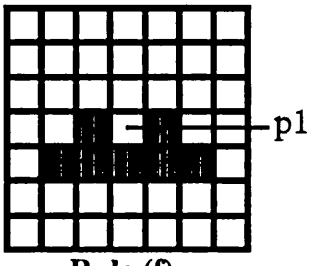

Rule (f)

Figure 2(b)

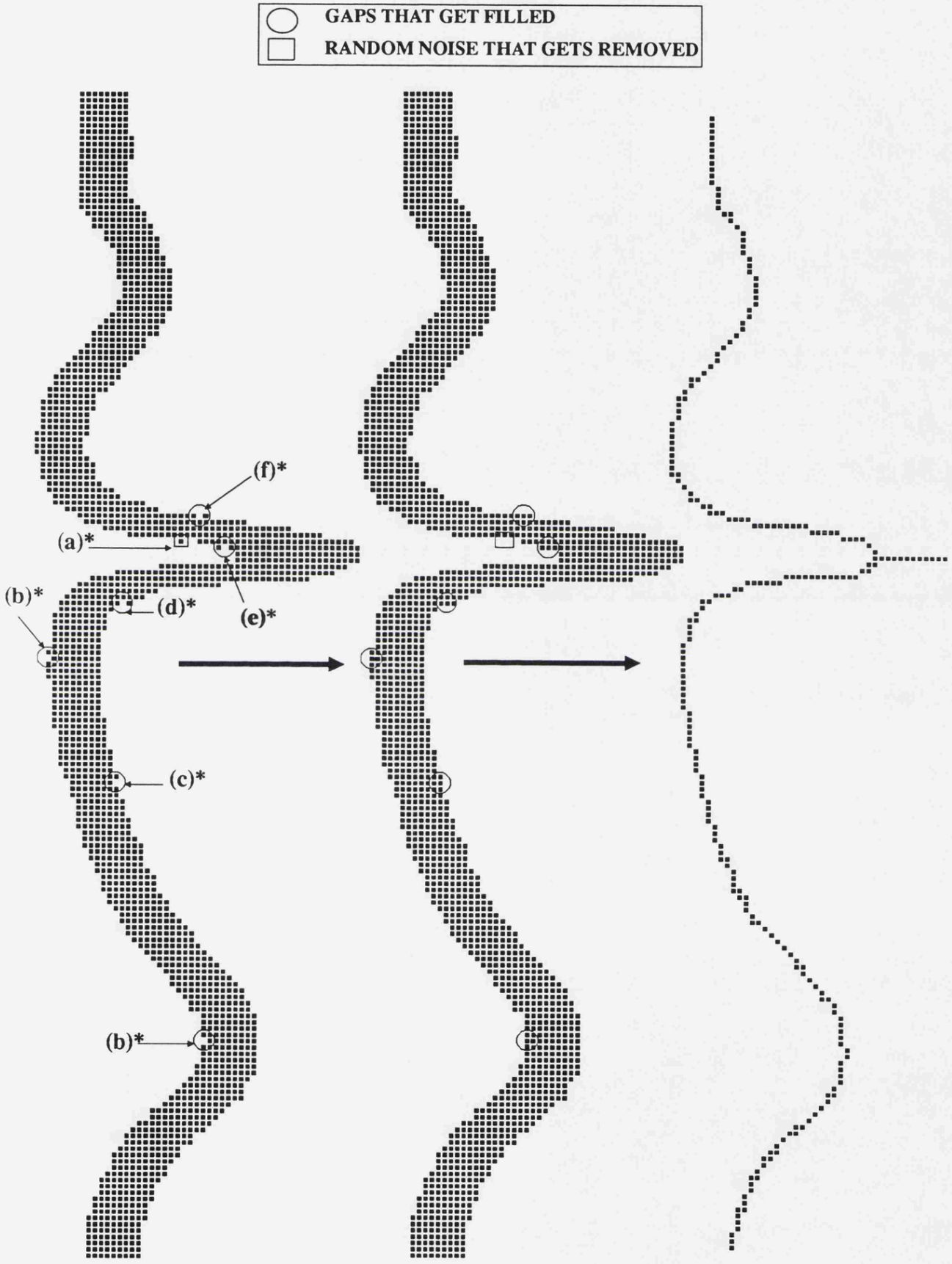

Figure 2(c) Unthinned and Unprocessed Image

Figure 2(d) Pre-processed Image

Figure 2(e) Skeleton of an ECG Waveform

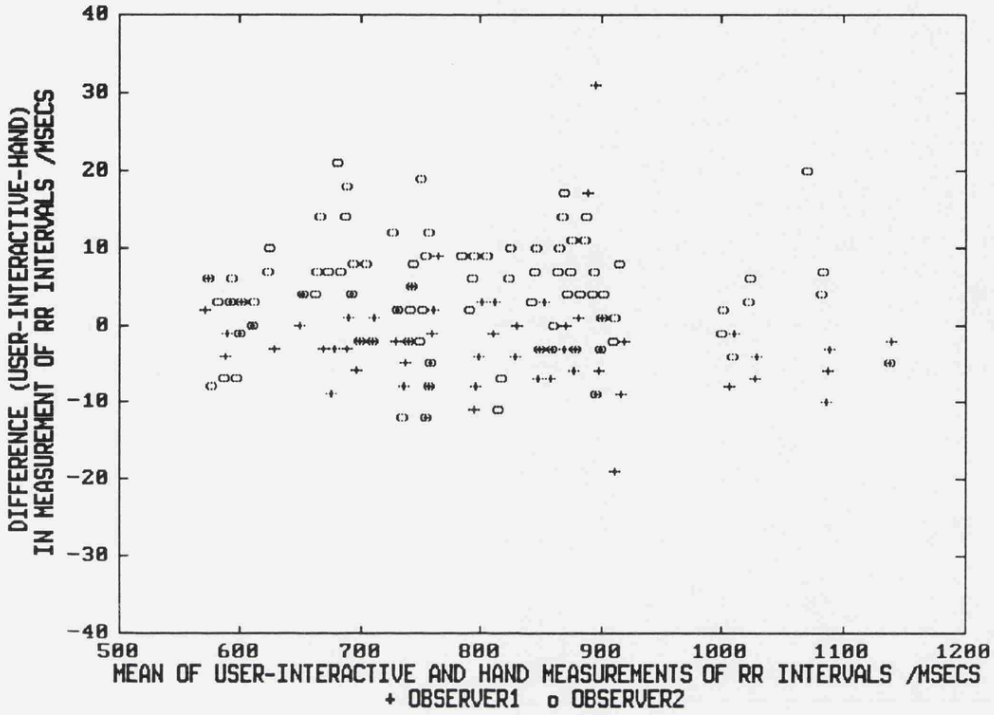

Figure 3

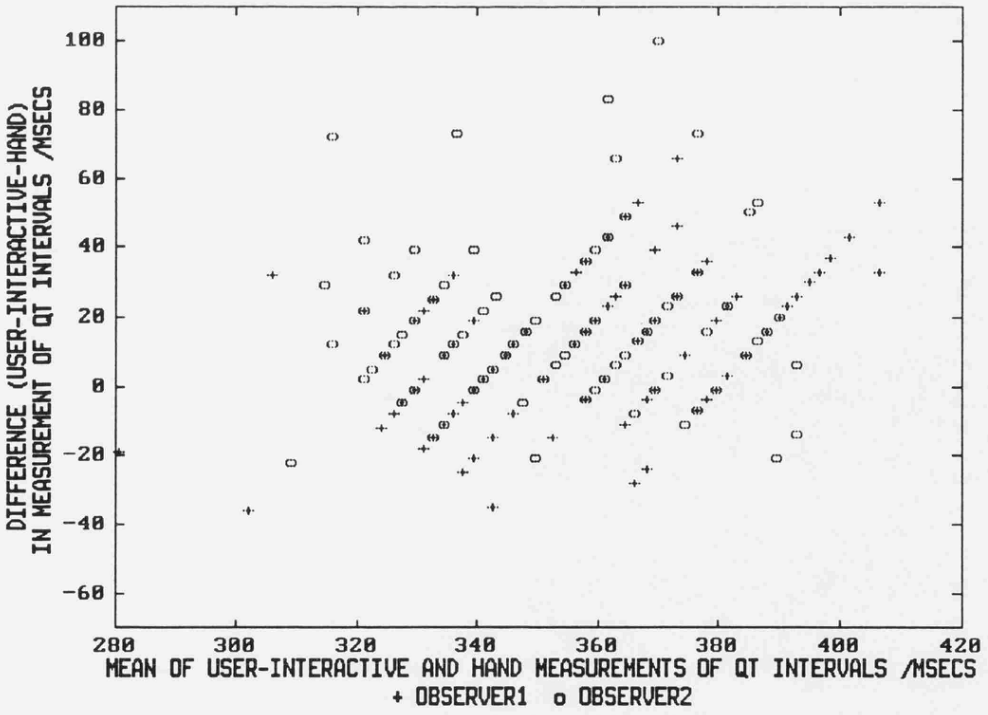

Figure 4

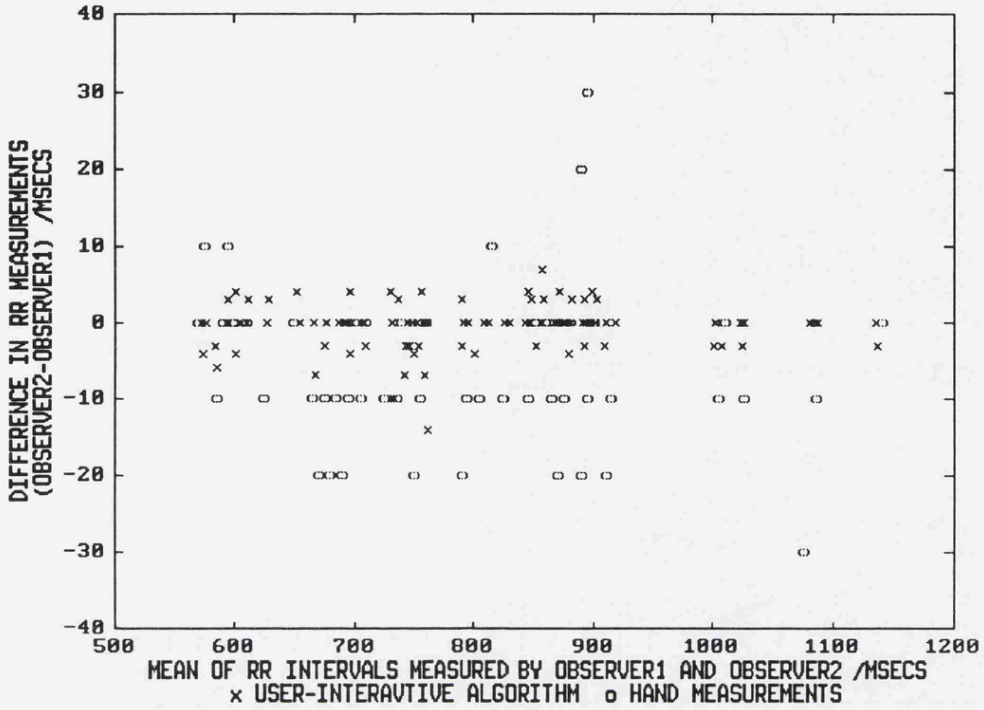

Figure 5

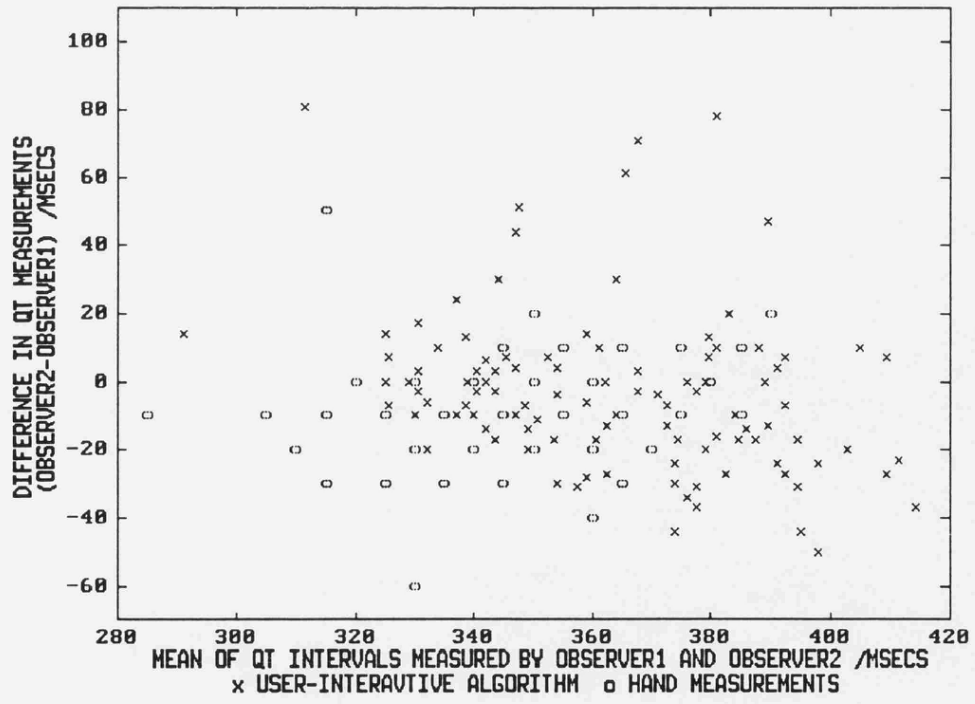

Figure 6

Appendix C

D.P.de Bono, H.K.Bhullar, Goddard WP, J.C.Fothergill (August, 1992): Automated measurement of QT dispersion identifies patients at risk from ventricular tachycardia. European Heart Journal, Volume 13, Abstract Supplement, pp 369. (Proceedings of the XIVth Congress of the European Society of Cardiology, Barelona, Spain)

Automated measurement of QT dispersion identifies patients at risk from ventricular tachycardia.

D.P.de Bono, *H.K.Bhullar, W.P.Goddard, *J.C.Fothergill

(September, 1992 : XIVth Congress of the European Society of Cardiology, Barcelona, Spain.)

Abstract

Variation in the apparent QT interval of the electrocardiogram (ECG) measured in different leads (QT dispersion) may reflect heterogeneity of ventricular repolarisation and thus predisposition to ventricular arrhythmia (Day, McComb, Campbell, Br Heart J 1992:67:39). We have developed an automated, personal computer based system for measuring multilead QT intervals from a hard copy ECG, and calculating adjusted QT dispersion (QTmax-QTmin/square root of the number of leads) and adjusted coefficient of variation. The system is both more rapid and more reproducible than manual measurement. QT intervals are measured in 10 patients confirmed at electrophysiological study to be at risk from ventricular tachycardia (VT) and in 10 age matched hospital controls. Mean adjusted QT dispersion for controls was 20.5 milliseconds, (95% CI 6.5 to 34.5; mean adjusted coefficient of variation was 1.46%, 95% CI 0.52 to 2.4. VT patients had larger and more variable adjusted dispersions (median 53.45, range 14.9 - 175 milliseconds) and adjusted coefficients of variation (median 3.4%, range 0.9 to 11%). Both were significantly greater than the control values (p=0.004, p=008, Mann Whitney test). Automated measurement of QT dispersion may be useful in the rapid identification of patients at risk from ventricular arrhythmias.

Departments of Cardiology and *Engineering,
University of Leicester,
Leicester LE1 7RH,
U.Kingdom

Appendix D

H.K.Bhullar, J.C.Fothergill, D.P.de Bono: Automated measurement of QT interval dispersion from hard-copy electrocardiograms for the prediction of arrhythmia risk. Submitted for publication to the Journal of Electrocardiology (Sept. 1992).

Automated measurement of QT interval dispersion from hard-copy electrocardiograms for the prediction of arrhythmia risk

Harsangeet K Bhullar BSc, John C. Fothergill*, William P. Goddard MRCP(UK), David P. de Bono MD, Departments of Cardiology and *Engineering, University of Leicester.

Correspondence to Professor DP de Bono, Dept of Cardiology, Clinical Science Wing, Glenfield General Hospital Leicester LE3 9QP, U.K. tel. (44)533 871471 ext.3021, Fax (44)533 875792.

This work was supported by the British Heart Foundation, London, England.

Structured Abstract

Objectives: The objective of the present study was to develop and validate a personal-computer based technique for i) converting hard-copy electrocardiograms to digital records ii) automatically measuring QT interval dispersion from the digitised records.

Background: Increased "dispersion" of the QT interval of the electrocardiogram has been proposed as a marker for an increased risk of cardiac arrhythmias. Hand measurement of QT dispersion is slow and potentially prone to observer error. Further validation of the usefulness of QT dispersion as an aid to risk stratification, and its realistic use in clinical practice, would be facilitated by a rapid and reproducible automatic technique.

Methods: High quality hard copy simultaneously recorded 12 lead electrocardiograms were scanned by a flat-bed scanner interfaced with a personal computer which used specially written software to convert analog traces to skeletonised and smoothed digital data which were then analysed by a user-interactive cursor system or by an automatic analysis algorithm. The system was validated by comparing measurements on the original electrocardiogram with user interactive and automatic measurements on the digitised traces by a panel of 10 observers on 8 recordings chosen to represent differences in recording quality. QT dispersion measurements were made on 12 lead electrocardiograms from 14 patients with documented ventricular arrhythmias and 15 control patients using both user-interactive and automatic modes.

Results: There was excellent correlation between hand and user interactive measurements by the same observer. Coefficients of inter-observer variation were 0.925% (manual, RR), 0.375% (semiautomatic, RR), 4.5% (manual, QT) 4.85% (semiautomatic, QT). Automated measurements were observer independent and extremely repeatable (coefficient of variation for repeat measurements 0.137% RR, 0.370% QT).

In the automatic mode, median adjusted QT dispersion was 34.8msec range 22.5-58.1 for arrhythmia patients, 13.8msec, range 10.3-24.9, for controls ($p<0.001$). Median coefficient of interlead QT variation was 8.8% range 4.4 to 12.4% for arrhythmia patients, 3.6% range 2.7 - 6.3% for controls ($p<0.001$). The automatic measurements were more conservative and less likely to give spuriously large values for QT dispersion than user interactive measurements.

Conclusions: Automated QT dispersion measurements are a useful and practicable addition to present methods for predicting the risk of ventricular arrhythmias.

Condensed Abstract

A personal-computer based system is described for converting hard-copy electrocardiograms to digital data and automatically determining QT interval dispersion. Adjusted QT dispersion and coefficient of interlead QT interval variation were both significantly greater in a group of 14 patients with ventricular arrhythmias than in a control group. Automated QT dispersion measurement was more consistent and reliable than observer measurement.

Introduction:

Ventricular arrhythmias are an important cause of sudden cardiac death. The initiation of a ventricular arrhythmia frequently involves an immediate stimulus such as an extrasystole acting against a background of increased arrhythmogenicity. The latter depends partly on variable factors such as autonomic tone, and partly on more enduring abnormalities in ventricular structure and metabolism. Inhomogeneity in conduction velocity and/or repolarisation rate in different parts of the ventricles could provide a substrate for tachycardia reentry circuits, and the resulting tachycardia might decay into ventricular fibrillation. The QT interval of the electrocardiogram has long been regarded

as a measure of ventricular repolarisation (1). If the heart acted as a single perfect electrical dipole, the QT interval measured in each of the conventional electrocardiographic leads would be identical. In practice, the heart behaves more like an array of dipoles, and different leads will tend to reflect predominantly the events in the nearest part of the left ventricular muscle mass. Several publications have now demonstrated that QT intervals as actually measured in different leads do indeed vary, and the concept of QT dispersion as an index of repolarisation heterogeneity and a possible marker of arrhythmia risk is increasingly accepted (2-4).

Manual measurement of QT interval is time consuming and requires experience and attention to detail. The onset of the QRS complex is usually easily identified, but the end of the T wave, with its more gradual return to baseline, can be hard to localise. In some leads the end of the T wave may be impossible to determine, and to allow for this the concept of "adjusted" QT dispersion, in which the difference between maximum and minimum QT interval is divided by the square root of the number of leads in which the QT interval is measurable, has been adopted (4). Digitisation of the QT interval measurement using a digitising pad or graticule attached to a computer has been widely used for resarch purposes; it helps both to speed calculation and to reduce operator bias. The measurement however is still time consuming, and this is perhaps reflected in the limited number of patients reported in many studies.

On-line digitisation of the signal is a feature of many modern electrocardiographs, and a number of algorithms have been developed for automatic measurement of the QT interval. Most commercial cardiographs do not however offer QT interval measurements on every lead, nor do they calculate QT dispersion. Moreover the majority of electrocardiograms, including those recorded in large scale trials of, for example, thrombolytic therapy, are preserved as hard-copy analogue paper records. We have therefore sought to develop a simple and robust technique which would (i) convert ECG waveforms recorded on paper to digital data suitable for computer processing. (ii) analyse these waveforms in terms of individual lead QT intervals and QT dispersion. In this paper we describe such a method, assess its reproducibility in comparison with

manual measurements, and describe the results obtained in a series of patients with "normal" electrocardiograms and in patients with a documented predisposition to ventricular arrhythmias.

Materials and Methods:

Simultaneous 12-lead electrocardiograms were routinely recorded on paper at 25mm/second using Nihon-Cohden Model ECG-6353/D/F/L electrocardiographs. The analysis system consisted of a flat-bed scanner (Hewlett Packard ScanJet Plus) interfaced with a personal computer (Dell 286 + maths coprocessor). The electrocardiogram, covered with an appropriately coloured filter to mask the background grid, was passed through the scanner to produce a pictorial image file at 300 d.p.i resolution (ScanGal, Hewlett Packard) . A graphics editor was used to divide the image into subfiles corresponding to individual leads. Specially designed algorithms were then used to skeletonise and smooth the image to compensate for finite line width in the original recording (5). The resulting digital data can be displayed on the computer screen at known magnifications (figure 1) for user- interactive measurements using a cursor, or used for automated measurement of RR or QT intervals. The automated analysis program used in this study was designed to allow visual monitoring of each stage in the analysis program, and to identify as unanalysable waveforms with excessive interference or completely isoelectric QT segments. QT intervals were rate- corrected and QT dispersion presented either as "adjusted QT dispersion" ((QTmax-QTmin)/square root of number of leads used for measurement) or as a coefficient of interlead QT interval variation (Standard deviation of QT intervals/mean QT interval). At least 10 leads were used in these calculations.

QT and RR interval measurements on digitised tracings using user interactive and fully automatic modes were compared with manual measurements on the original electrocardiogram by a panel of ten physicians. 8 ECG leads were chosen to encompass a spectrum from "excellent" to "poor" in terms of recording quality, and incorporating both mono- and biphasic T wave patterns. Reproducibility of user-interactive measurements by a single operator was assessed using three measurements each of nine leads presented in random order.

QT dispersion measurements were made using automatic and user interactive techniques on 15 patients with previously documented sustained monomorphic ventricular tachycardia attending an arrhythmia clinic and on 15 controls (consecutive attendees at an electrocardiography clinic) not known to have suffered any arrythmia. Brief patient details are given in table 1. All patients were on treatment and in sinus rhythm at the time the electrocardiograms were recorded. A subsequent repeat electrophysiological study on one patient (#10) suggested that the original arrhythmia was in fact supraventricular tachycardia with left bundle branch block (ECG in sinus rhythm also showed left bundle branch block). Data from this patient are included in tables, but have been excluded from the figures and the intergroup comparisons

Statistical methods

Coefficients of variation were calculated as (standard deviation x 100 /mean). Manual and user-interactive measurements were compared using the technique of Bland and Altman (6). QT dispersion measurements on arrhythmia patients and controls were compared using the Mann Witney U test and two-sample t test.

Results:

All ten physicians found the system easy to use after about 20 minutes instruction. Comparison between manual and user interactive measurements showed good correlation for both RR interval and QT interval. There was no detectable bias for RR interval measurements and 95% confidence intervals were $\pm$ 5 milliseconds, for QT measurements mean bias (user interactive - hand measurement) was 11 milliseconds, 95% confidence intervals 8-14 milliseconds. Coefficients of inter- observer variation were 0.925% (manual, RR), 0.375% (semiautomatic, RR), 4.5% (manual, QT) 4.85% (semiautomatic, QT). As expected, the inter-observer variation for RR interval measurement was less than for QT interval measurement. Mean coefficients of variation for repeated user-interactive measurement of RR and QT interval by the same observer were 0.11% and 1.71% respectively.

The relationship between manual, user interactive and automated measurements on the same ECG waveform is shown in Table 2 and figure 2. The automated measurements were extremely repeatable (coefficient of variation for repeat measurements 0.137% RR, 0.370% QT).

The adjusted QT dispersions and coefficients of QT interval variation for arrhythmia and control patients using the user-interactive and automatic modes are shown in figures 3 and 4 and tables 3 and 4.

With the user-interactive system the median adjusted QT dispersion for arrhythmia patients was 44.6 msec range 26.1 - 92.5msec. For controls, median adjusted QT dispersion was 19.4msec, range 7.8 -33.2msec. The median coefficient of (interlead) QT variation was 12.7%, range 5.6 - 36.5% for arrhythmia patients and median 5%, range 2.3-7.8% for controls.

Using the automatic system median adjusted QT dispersion was 34.8msec range 22.5-58.1 for arrhythmia patients, 13.8msec, range 10.3 - 24.9, for controls. Median coefficient of interlead QT variation was 8.8% range 4.4 to 12.4% for arrhythmia patients, 3.6% range 2.7 - 6.3% for controls. The patient and control distributions were significantly different at $p<0.001$ level for either parameter (Mann Whitney U test/two sample t-test), irrespective of whether the user-interactive or automatic system was used.

Whilst there was good agreement for control patients, there was a clear tendency for the user interactive mode to give greater values, particularly for adjusted QT dispersion, in the arrhythmia patient group ($p<0.035$ for adjusted QT dispersion, $p<0.04$ for QT coefficient of variation). Direct comparison of individual lead measurements for the four patients showing the greatest discrepancy indicated that in each case the discrepancy was due to a different interpretation of the point of QT offset in a single lead. An example is shown in figure 5.

Discussion:

The technical problems involved in the accurate measurement of QT intervals have been discussed by several authors (7-9). Basically they can be divided into problems of bias, where results are consciously or subconsciously "rounded" up or down, problems

of precision, where, particularly, T wave offset is difficult to define as the wave gradually approaches the baseline, and problems of interpretation, especially where the T wave is biphasic or followed by a U wave.

Evidence of rounding bias is apparent in the non- uniform distribution of manual QT measurements in figure 2, and it is clear that this is reduced in the user- interactive computer measurements. The precision of the user-interactive computer measurement is enhanced by magnification of the trace, and the movement of the cursor makes it easier to appreciate inflections. The precision of any system which attempts to analyse previously recorded analogue data will of course be limited by the fidelity of the original data; if leads are not recorded simultaneously factors such as variation in recording speed and spontaneous beat to beat QT variation may become important. The use of a scanning speed of 300 dots per inch in itself imposes a limit of resolution of approximately 4msec on traces recorded at 25mm per second. The small but consistent mean difference between manual and user-interactive measurement of the QT interval (but not the RR interval) probably reflects the effect of different line thickness on assessment of the QT offset point.

The fully-automated system is both unbiased and, within these limitations, precise, but is potentially prone to problems of interpretation. In figure 2 the automatic measurement is consistent, but does not necessarily correlate with the mean value of manual or user-interactive measurements. There are various strategies which can be used to cope with this situation: we have chosen to use a series of algorithms designed to cope with different configurations of T wave, to display the points chosen for onset and offset, and to reject waveforms with excessive interference or isoelectric T waves. Despite these potential limitations, when user-interactive and automatic modes are compared on a population of patients with previously documented ventricular arrhythmias, there is a definite tendency for the automatic mode to be more conservative, i.e. to show less QT dispersion than the user-interactive system. From our basic hypotheses concerning the origin of QT dispersion, it seems inherently unlikely that a single QT measurement will differ strikingly from measurements in adjacent leads; it is on this basis that we believe the more conservative automatic

measurement is likely to be the right one. Our programme provides a display of individual QT intervals along the conventional ECG lead vectors which enables a rapid visual check for this problem. Many arrhythmia or post infarct patients have electrocardiograms which are qualitatively abnormal on visual inspection, and it is also possible that this introduces an unconscious observer bias in QT interval measurement.

Whether the increased QT dispersion identified in the "arrhythmia group" patients was fundamental to their arrhythmia susceptibility, or the result of some other factor such as medication or the extent of ventricular damage, is beyond the scope of this paper. Day and colleagues proposed an (unadjusted) QT dispersion of 100msec as distinguishing between normal and arrhythmogenic patients (3). This corresponds to an adjusted dispersion of 28.9msec, a value exceeded by none of our control patients but 10 of our 15 arrhythmogenic patients The definitive identification of increased QT dispersion as an independent risk marker for ventricular arrhythmias and sudden death will depend on prospective studies involving large numbers of patients; it is to facilitate the rapid analysis of large numbers of electrocardiograms for such a study, which is now in progress, that the present system was developed.

Software developed for this application will be made available to bona-fide researchers in return for a nominal donation to the British Heart Foundation and acknowledgement in subsequent publications.

Acknowledgements: This work was supported by the British Heart Foundation. We are grateful to Drs Underwood, Johnson, Brack, Glancy, More, McCance, Muzulu, Bharaj and Lall for manual and user-interactive ECG measurements, to Dr JD Skehan for allowing us access to patients under his care, and to Mrs J Thomas and Mrs V Knott for ECG tracings.

Legend to illustrations:

Figure 1: Photograph of hard-copy electrocardiogram compared with its digitised, skeletonised and smoothed image.

Figure 2: Plot of manual (x), user interactive (o) and fully automated (-) QT and RR interval measurements from 8 electrocardiogram leads. Pairs were chosen to represent excellent (E), good (G), poor (P) and biphasic (B) T wave recordings. Manual and user interactive measurements were made by a panel of 10 physicians presented with leads in random order.

Figure 3: Plots of adjusted QT dispersion in 14 patients with documented ventricular arrhythmia and 15 control patients.

UI = user interactive, A = automatic

Figure 4: Plots of coefficient of interlead QT interval variation in 14 patients with documented ventricular arrhythmia and 15 control patients.

UI = user interactive, A = automatic

Figure 5: Example of a waveform (arrhythmogenic patient #3, lead V3) with widely differing QT measurements by automatic (502 msec) and user-interactive (646msec)techniques. QT intervals for adjacent leads were V2 496, V4 495 msec (automatic). It is clear that the automatic algorithm has correctly selected the nadir between T and U wave, whilst the observer has opted for the end of the U wave.

Table 1: Details of patients and controls.

Table 2: Comparison between manual, user interactive and automatic measurements of RR and QT intervals for 8 selected ECG leads examined by 10 physicians.

Table 3. Table of adjusted QT dispersion and coefficient of QT interval variation (user-interactive measurement) in 14 patients with documented ventricular arrhythmia, one with suspected ventricular arrhythmia subsequently shown to be supraventricular (#10) and 15 control patients.

Table 4. Table of adjusted QT dispersion and coefficient of QT interval variation (automatic measurement) in 14 patients with documented ventricular arrhythmia, one with suspected ventricular arrhythmia subsequently shown to be supraventricular (#10) and 15 control patients.

References:

1. Waller AD. A demonstration on man of electromotive changes accompanying the heart's beat. J. Physics 1887; 8:229

2. Mirvis DM Spatial variation of QT intervals in normal persons and patients with acute myocardial infarction. J Am Coll Cardiol 1985; 5:625-31

3. Day CP. McComb JM, Campbell RWF. QT dispersion : an indication of arrhythmia risk in patients with long QT intervals. Br Heart J. 1990; 63:342-4

4. Day CP, McComb JM, Campbell RWF. QT dispersion in sinus beats and ventricular extrasystoles in normal hearts. Br Heart J 1992; 67:39-41

5. Bhullar HK, de Bono DP, Fothergill JC, Jones NB. A computer based system for the study of QT intervals. Proceedings, Computers in Cardiology, Venice 1991, IEEE Press, Los Alamitos, USA, 533-536

6. Bland JM, Altman DG. Statistical method for assessing agreement between two methods of clinical assessment. Lancet 1986;i: 307-310

7. Lepeschkin E, Surawicz B. The measurement of the QT interval of the electrocardiogram. Circulation 1952; 6: 378-87

8. Cowan JC, Yusoff K, Moore M et al. Importance of lead selection in QT interval measurement. Am J Cardiol 1988; 61:83-7

9. Cowan JC, Hilton CJ, Griffith CJ et al. Sequence of epicardial repolarisation and configuration of the T wave. Br Heart J 1988; 60:424-33

TABLE 1

CLINICAL DETAILS OF PATIENTS

CONTROL GROUP:

Number	Age/gender	Diagnosis	Treatment
1	40M	Angina	Nitrates
2	53M	Hypertension	Nifedipine
3	69M	Angina/Hypertension	Nifedipine
4	47M	Chest pain	Nitrates
5	44F	Chest pain	Nil
6	50M	Hypertension/Atrial fibrillation	Digoxin
7	41M	Supraventricular tachycardia	Mianserin
8	76M	Angina/previous infarct	Metoprolol
9	30F	Chest pain	Nil
10	46M	Hypertension	Enalapril
11	61M	Angina	Nitrates
12	40M	Chest pain	Nil
13	42M	Hypertension/angina	Metoprolol
14	51M	Angina	Nil
15	36M	Hypertension	Diuretic

ARRHYTHMIA GROUP

1	52M	IHD	Ventricular tachycardia	Sotalol
2	72M	IHD	Ventricular tachycardia	Amiodarone
3	57M	IHD	Ventricular tachycardia	ICD/amiodarone
4	54M	IHD	Ventricular tachycardia	Amiodarone
5	39M	DCM	Ventricular tachycardia	Sotalol/amiodarone
6	42M	DCM	Ventricular tachycardia	Mexilitine
7	55M	IHD	Ventricular tachycardia	Amiodarone
8	63M	DCM	Ventricular tachycardia	Flecainide
9	68M	IHD	Ventricular tachycardia	Mexiletine
10	58M	IHD	SVT/LBBB*	Atenolol
11	50M	IHD	Ventricular tachycardia	Amiodarone
12	47M	IHD	Ventricular tachycardia	Sotalol
13	55M	IHD	Nonsustained VT	Amiodarone
14	62M	IHD	Ventricular tachycardia	ICD
15	57M	IHD	Ventricular tachycardia	ICD/amiodarone

IHD = ischaemic heart disease, DCM = dilated cardiomyopathy
VT = ventricular tachycardia ICD = implantable defibrillator
* This patient with complete left bundle branch block was originally thought to have ventricuar tachycardia. Subsequent electrophysiological study revealed supraventricular tachycardia only.

Bhullar Photocopy of Figure 1

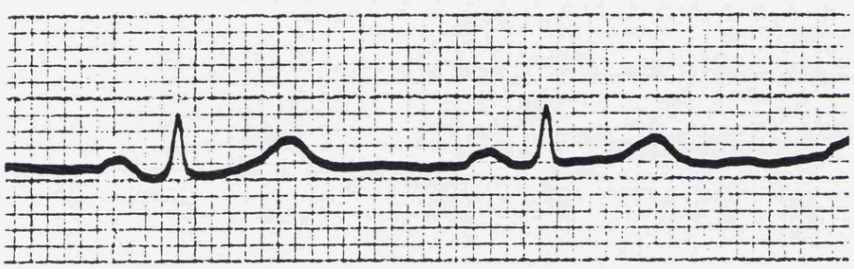

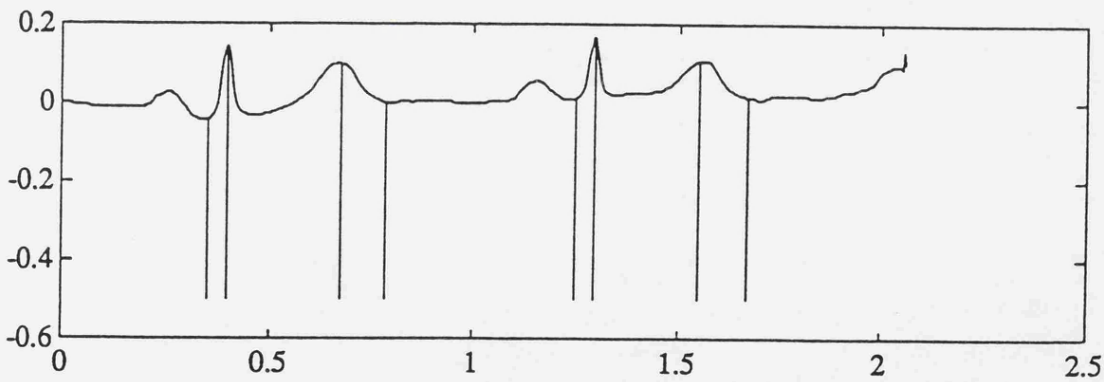

PLOT SHOWING QRS ONSET, R WAVE PEAK, T WAVE PEAK AND END

Bhullar Photocopy of Figure 2

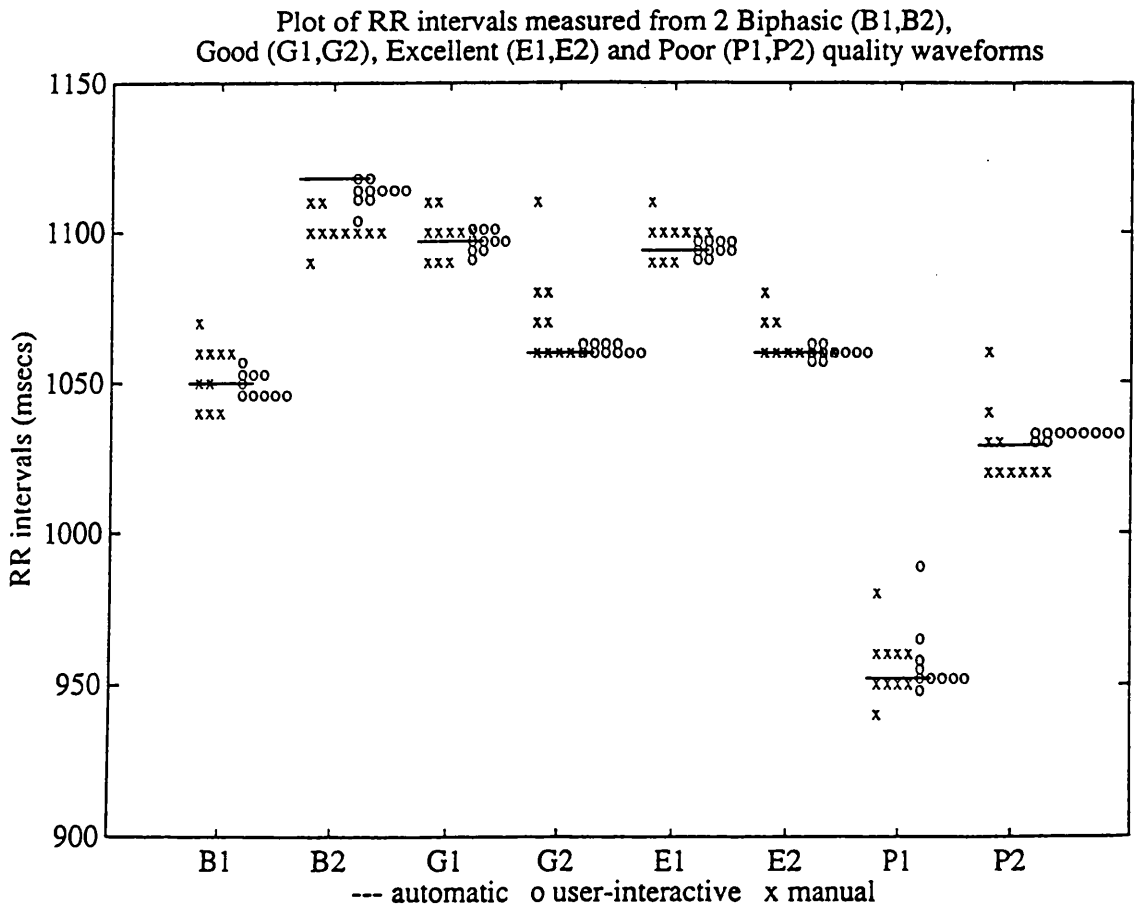

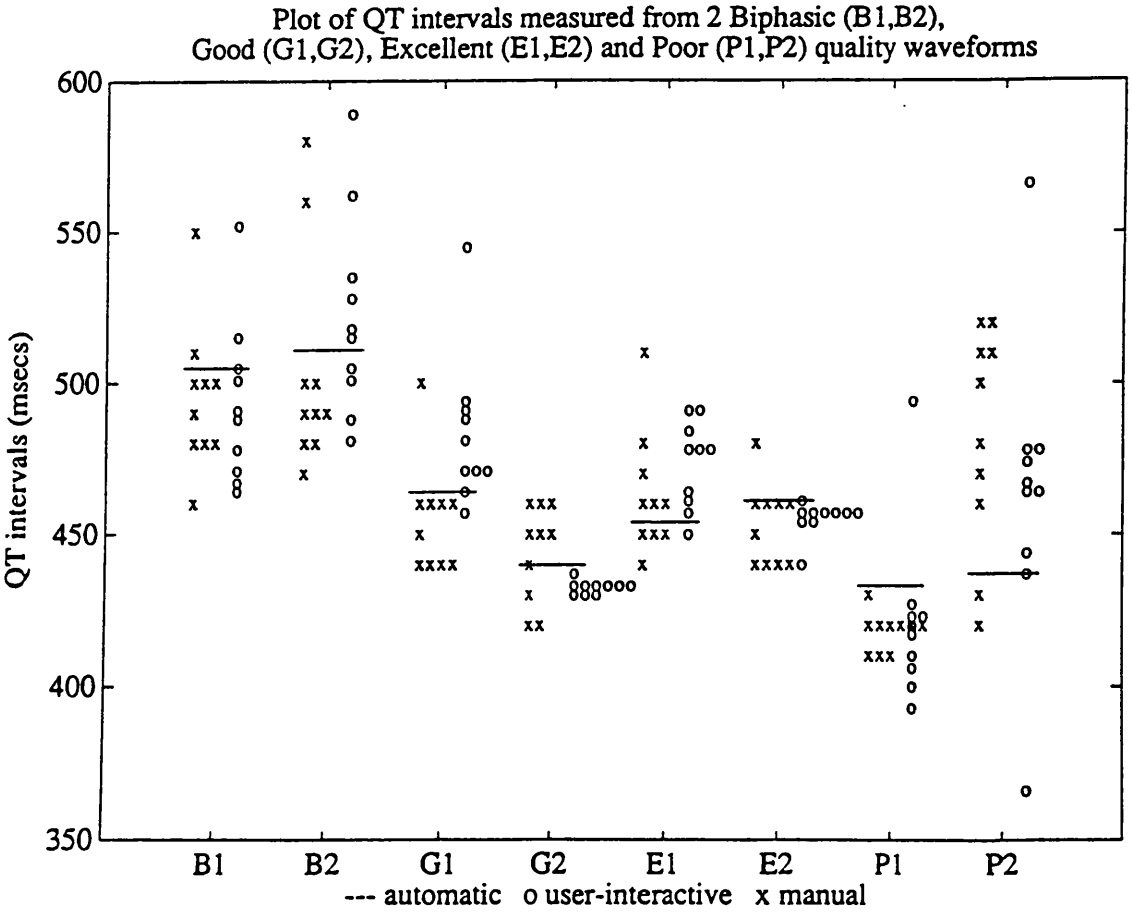

Bhullar Photocopies of Figures 3 and 4

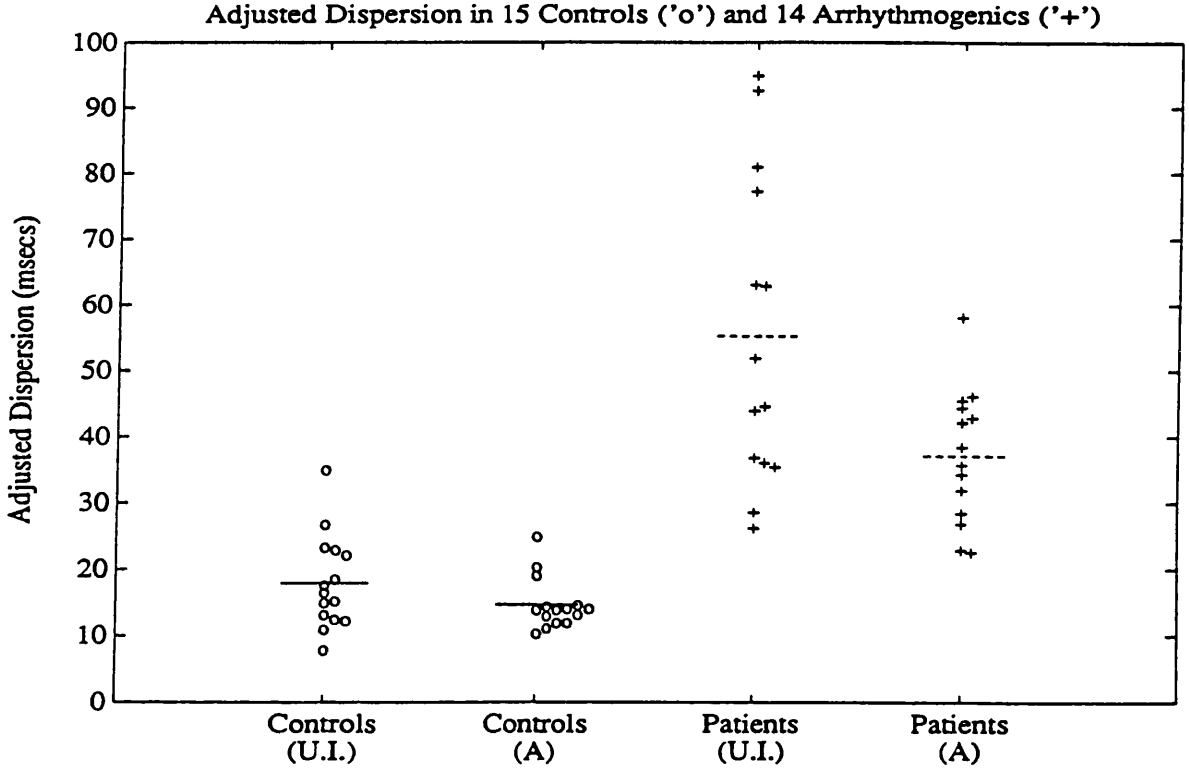

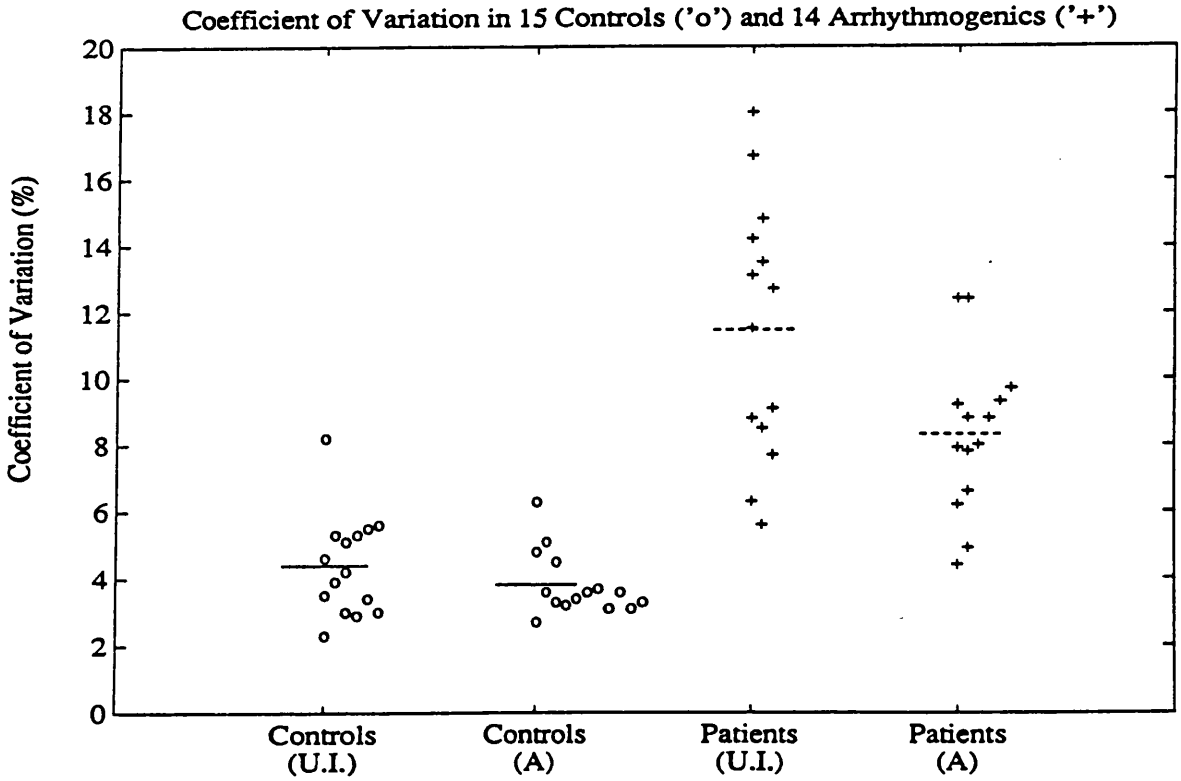

Bhullar Photocopy of Figure 5

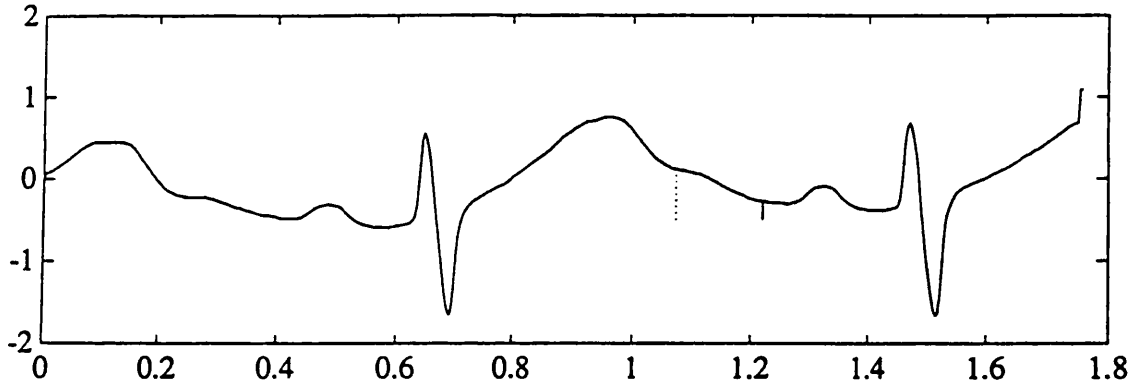

Table 2

QT intervals obtained by manual (upper), user-interactive (lower) and automatic measurement (msecs)

	Observer										Mean QT Interval Measured by 10 Doctors $Mdoc_{(QT)}$ (msecs)	Std. Dev. of QT Intervals Measured by 10 Doctors $\alpha doc_{(QT)}$ (msecs)	Coeff. of Var. of QT Intervals Measured by 10 Doctors ($\alpha doc_{(QT)}$ / $Mdoc_{(QT)}$ x 100 %)	QT intervals measured by the automatic algorithm (msecs)
Waveforms	1	2	3	4	5	6	7	8	9	10				
B 1	480	500	460	490	500	480	550	480	500	510	495.0	24.2	4.9	505
	501	552	505	491	471	488	464	515	478	467	493.2	26.7	5.4	
B 2	470	580	480	490	490	480	560	490	500	500	504.0	36.3	7.2	511
	518	589	528	515	488	501	562	535	505	481	522.2	33.2	6.4	
G1	460	500	460	450	440	440	440	440	460	460	455.0	18.4	4.0	464
	457	545	491	481	494	464	471	471	471	488	483.3	24.8	5.1	
G 2	460	460	460	450	420	440	430	420	450	450	444.0	15.8	3.6	440
	433	433	430	430	430	433	433	433	437	433	432.5	2.1	0.5	
E 1	460	510	460	470	450	450	480	440	460	450	463.0	20.0	4.3	454
	491	457	484	478	461	450	464	478	491	478	473.2	14.4	3.0	
E 2	480	460	460	460	450	440	440	440	460	440	453.0	13.4	3.0	461
	457	440	457	457	457	454	457	457	461	454	455.1	5.6	1.2	
P 1	420	430	420	420	420	420	420	410	410	410	418.0	6.3	1.5	433
	400	494	423	406	423	393	427	410	417	420	421.3	27.8	6.6	
P 2	430	520	500	460	420	480	510	470	520	510	482.0	36.5	7.6	437
	464	478	366	464	437	467	474	478	444	566	463.8	49.0	10.6	

Table 3

Adjusted Dispersion and Coefficient of Variation calculated using Rate-Corrected QT intervals from 15 Controls

Controls	Adjusted Dispersion (msecs) $\frac{QT_c\,(max) - QT_c\,(min)}{\sqrt{No\ of\ leads\ considered}}$	Coefficient of Variation (%) $\frac{Std\ deviation(QT_c)}{Mean(QT_c)} \times 100$
1	17.6	4.6
2	23.3	5.3
3	22.9	5.1
4	7.8	2.3
5	18.5	5.3
6	14.9	3.5
7	26.7	5.5
8	16.5	3.9
9	22.1	5.6
10	34.9	8.2
11	13.1	3.0
12	15.2	4.2
13	10.9	2.9
14	12.4	3.4
15	12.2	3.0

Adjusted Dispersion and Coefficient of Variation calculated using Rate-Corrected QT intervals from 15 Arrhythmogenic Patients

Patient	Adjusted Dispersion (msecs) $\frac{QT_c\,(max) - QT_c\,(min)}{\sqrt{No\ of\ leads\ considered}}$	Coefficient of Variation (%) $\frac{Std\ deviation(QT_c)}{Mean(QT_c)} \times 100$
1	28.5	6.3
2	43.9	8.8
3	77.2	14.2
4	26.1	5.6
5	63.0	13.1
6	80.9	14.8
7	92.5	18.0
8	36.8	8.5
9	44.6	13.5
10	14.9	3.0
11	36.0	9.1
12	94.8	16.7
13	35.4	7.7
14	62.8	12.7
15	51.9	11.5

Table 4

Adjusted Dispersion and Coefficient of Variation calculated using Rate-Corrected QT intervals from 15 Controls

Controls	Adjusted Dispersion (msecs) $\frac{QT_c\,(max) - QT_c\,(min)}{\sqrt{No\ of\ leads\ considered}}$	Coefficient of Variation (%) $\frac{Std\ deviation(QT_c)}{Mean(QT_c)} \times 100$
1	10.3	2.7
2	13.8	3.6
3	14.4	3.3
4	11.1	3.2
5	24.9	6.3
6	11.9	3.4
7	20.3	4.8
8	12.9	3.6
9	13.8	3.7
10	14.0	3.1
11	13.1	3.6
12	19.0	5.1
13	14.6	4.5
14	14.0	3.1
15	11.9	3.3

Adjusted Dispersion and Coefficient of Variation calculated using Rate-Corrected QT intervals from 15 Arrhythmogenic Patients

Patient	Adjusted Dispersion (msecs) $\frac{QT_c\,(max) - QT_c\,(min)}{\sqrt{No\ of\ leads\ considered}}$	Coefficient of Variation (%) $\frac{Std\ deviation(QT_c)}{Mean(QT_c)} \times 100$
1	28.4	6.2
2	38.4	7.9
3	44.4	9.2
4	22.8	4.4
5	22.5	4.9
6	58.1	12.4
7	34.3	7.8
8	42.2	8.8
9	42.8	12.4
10	8.7	1.9
11	31.9	8.0
12	35.7	8.8
13	26.8	6.6
14	45.5	9.3
15	46.1	9.7

Appendix E

Heuristic rules for the removal of random noise and the filling in of gaps in the scanned image

Rules for the removal of random noise

Rule (1)
If:
i) p1 is 1
ii) the logical *'or'* of p2,p3,p4,p5,p6,p7,p8,p9 is 0
then store the coordinates of p1 in a file for later removal

Rule (2a)
If:
i) p1 is 1
ii) the logical *'or'* of p2,p3,p4,p5,p6,a,b,c,d,e,f,g,h,i is 0
iii) the logical *'and'* of p7,p8,p9,j,p is 1
then store the coordinates of p1 in a file for later removal

Rule (2b)
If:
i) p1 is 1
ii) the logical *'or'* of (p2,p3,p4,p8,p9,a,b,c,d,e,m,n,o,p is 0
iii) the logical *'and'* of p5,p6,p7,f,l is 1
then store the coordinates of p1 in a file for later removal

Rule (2c)
If:
i) p1 is 1
ii) the logical *'or'* of (p2,p6,p7,p8,p9,a,j,k,l,m,n,o,p,i is 0
iii) the logical *'and'* of p3,p4,p5,b,h is 1
then store the coordinates of p1 in a file for later removal

Rule (2d)
If:
i) p1 is 1
ii) the logical *'or'* of (p4,p5,p6,p7,p8,e,f,g,h,i,j,k,l,m is 0
iii) the logical *'and'* of p9,p2,p3,n,d is 1
then store the coordinates of p1 in a file for later removal

Rule (3)
If:
i) p1 is 1
ii) the logical *'or'* of m,p8,p4,e is 0
iii) the logical *'and'* of n,o,p9,p,p2,a,p3,b,d,c,l,k,p7,j,p6,i,p5,h,f,g is 1
then store the coordinates of p1 in a file for later removal

Rules for the filling in of gaps

Rule (4)
If:
i) p1 is 0
ii) the logical *'and'* of p2,p3,p4,p5,p6,p7,p8,p9 is 1
then store the coordinates of p1 in a file for later conversion to a value of 1

Rule (5a)
If:
i) p1 is 0
ii) the logical *'or'* of p3,p4,p5,b,h is 0
iii) the logical *and* of p7,p8,p9,j,p is 1
iv) the logical *and* of p2,p6 is 1 **or** p2 is 1 and p6 is 0 and i is 1 **or**
p6 is 1 and p2 is 0 and a is 1
then store the coordinates of p1 in a file for later conversion to a value of 1

Rule (5b)
If:
i) p1 is 0
ii) the logical *'or'* of p7,p8,p9,j,p is 0
iii) the logical *and* of p3,p4,p5,b,h is 1
iv) the logical *and* of p6,p2 is 1 **or** p6 is 1 and p2 is 0 and a is 1 **or**
p2 is 1 and p6 is 0 and i is 1
then store the coordinates of p1 in a file for later conversion to a value of 1

Rule (6a)
If:
i) p1 is 0
ii) the logical *'or'* of p9,p2,p3,n,d is 0 **or**
the logical *'or'* of p9,n is 1 and the logical 'or' of p2,p3,d is 0 **or**
the logical *'or'* of p3,d is 1 and the logical 'or' of n,p9,p2 is 0
iii) the logical *'and'* of p5,p6,p7,f,l is 1
iv) the logical *and* of p8,p4 is 1 **or** p8 is 1 and p4 is 0 and e is 1 **or**
p4 is 1 and p8 is 0 and m is 1
then store the coordinates of p1 in a file for later conversion to a value of 1

Rule (6b)
If:
i) p1 is 0
ii) the logical *'or'* of p5,p6,p7,f,l is 0 **or**
the logical *'or'* of f,p5 is 1 and the logical *'or'* of p6,p7,l is 0 **or**
the logical *'or'* of l,p7 is 1 and the logical 'or' of p6,p5,f is 0
iii) the logical *'and'* of p9,p2,p3,n,d is 1
iv) the logical *and* of p4,p8 is 1 **or**
p4 is 1 and p8 is 0 and m is 1 **or** p8 is 1 and p4 is 0 and e is 1
then store the coordinates of p1 in a file for later conversion to a value of 1

Appendix F

The top level structure diagrams for the atomatic algorithm

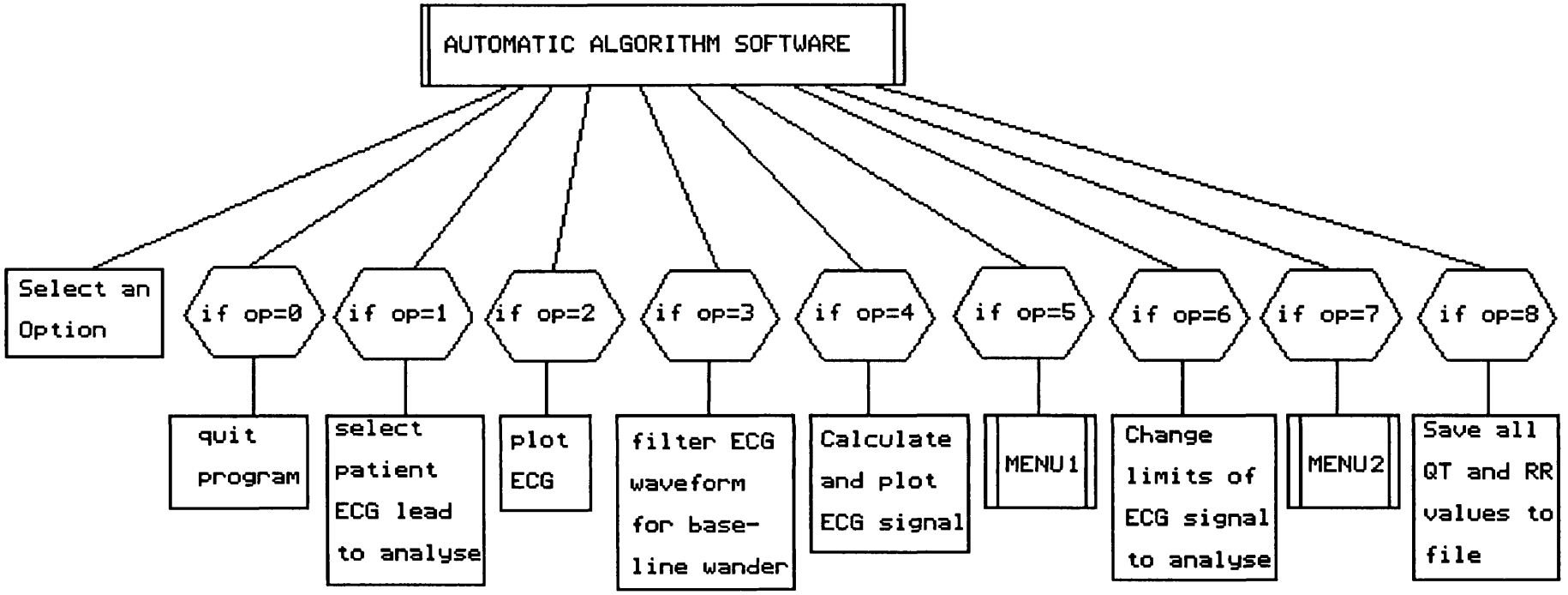
AUTOMATIC ALGORITHM SOFTWARE
Select an Option
if op=0
if op=1
if op=2
if op=3
if op=4
if op=5
if op=6
if op=7
if op=8
quit program
select patient ECG lead to analyse
plot ECG
filter ECG waveform for base-line wander
Calculate and plot ECG signal
MENU1
Change limits of ECG signal to analyse
MENU2
Save all QT and RR values to file

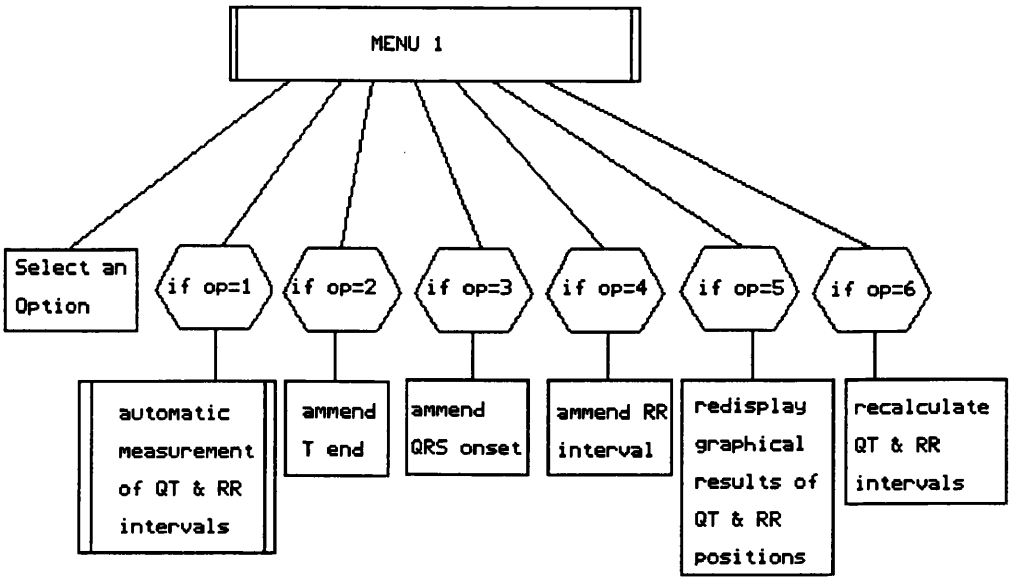
MENU 1
Select an Option
if op=1
if op=2
if op=3
if op=4
if op=5
if op=6
automatic measurement of QT & RR intervals
ammend T end
ammend QRS onset
ammend RR interval
redisplay graphical results of QT & RR positions
recalculate QT & RR intervals

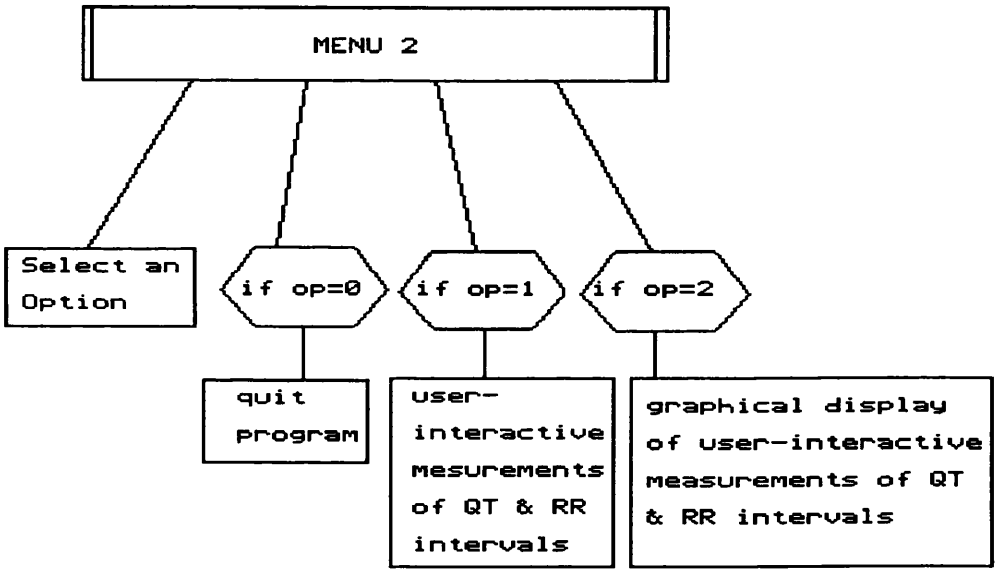
MENU 2
Select an Option
if op=0
if op=1
if op=2
quit program
user-interactive mesurements of QT & RR intervals
graphical display of user-interactive measurements of QT & RR intervals

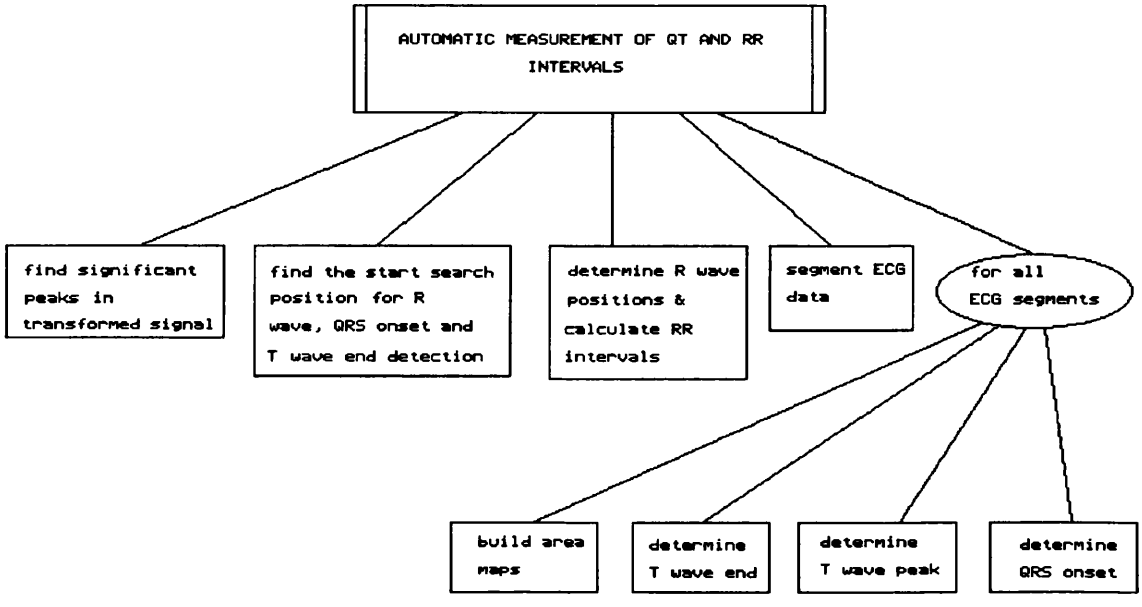
AUTOMATIC MEASUREMENT OF QT AND RR INTERVALS
find significant peaks in transformed signal
find the start search position for R wave, QRS onset and T wave end detection
determine R wave positions & calculate RR intervals
segment ECG data
for all ECG segments
build area maps
determine T wave end
determine T wave peak
determine QRS onset

Appendix G

H.K.Bhullar, J.C.Fothergill, D.P.de Bono: How Should QT Variation be Measured: Adjusted Dispersion, Coefficient of Variation, or Both? Submitted for publication to the European Heart Journal (Nov. 1992).

HOW SHOULD QT DISPERSION BE MEASURED: ADJUSTED DISPERSION, COEFFICIENT OF VARIATION, OR BOTH?

Harsangeet K. Bhullar, John C. Fothergill* and David P de Bono

Departments of Cardiology and *Engineering, University of Leicester, UK

Correspondance: Prof D.P. de Bono, Department of Cardiology, Clinical Science Wing, Glenfield General Hospital, Leicester LE3 9QP tel 0533 871471 ext 3038, fax 0533 875792

Summary

Electrocardiographic QT interval dispersion is a measure of heterogeneity of ventricular repolarisation which may identify patients at risk from arrhythmias. In the course of developing an automated technique for measuring QT dispersion from the standard 12 lead electrocardiogram, we studied the spatial distribution of QT variation and compared adjusted QT dispersion with coefficient of interlead QT variation in 14 patients with documented arrhythmias and 15 control patients. QT intervals were normally distributed in either population, but both adjusted QT dispersion and coefficient of interlead QT variation were significantly greater in the arrhythmia patients. Spatial distribution of QT variation reflected structural abnormalities such as previous infarction.

Coefficient of variation is more conservative, uses information from more leads, and is less susceptible to problems over the interpretation of a single lead. Adjusted QT dispersion is marginally easier to calculate and may, in theory, be more sensitive to an arrhythmogenic abnormality. The two measurements provide complementary information, and where possible both should be used.

Key Words: Electrocardiography, QT interval, arrhythmia prediction

Introduction

The association of a prolonged electrocardiographic QT interval with susceptibility to cardiac arrhythmias and sudden death in the congenital long QT syndromes (1) has long been recognised. Schwartz and Wolf (2) identified a prolonged QT interval as an independent predictor of mortality after myocardial infarction, and their observations have been confirmed by Algra (3). Mirvis(4), and more recently Day and colleagues (5-7) have pointed out that if the mechanism of the increased susceptibility to arrhythmias identified by a long QT interval is an increased heterogeneity of ventricular repolarisation times, then QT dispersion, i.e. the difference in QT interval as measured in different ECG leads, may be a more informative measurement. Day and colleagues (5) have introduced the concept of "adjusted QT dispersion" , defined as the result of the maximum rate corrected QT interval in any of the measurable leads minus the minimum rate corrected QT interval in any of the measurable leads divided by the square root of the number of leads in which QT intervals are measurable. The latter term acknowledges the fact that the T wave may be isoelectric or otherwise unmeasurable in a number of leads, and applies a correction factor for the possibility that the true dispersion will be underestimated if fewer than 12 leads are measured.

This approach, though elegant, has conceptual and practical limitations. First, because it concentrates on extreme values, it deliberately ignores information in up to ten of the twelve leads of the conventional electrocardiogram. Second, for the

same reasons, it is sensitive to observer errors in measuring the two extreme intervals. Third, because it is an absolute rather than a relative measurement, it will tend to be affected by factors which affect the mean QT interval, even when these do not necessarily reflect changes in repolarisation homogeneity. For example, drug-induced QT prolongation without an increase in adjusted QT dispersion (7) actually indicates an increase in homogeneity. The Adjusted QT dispersion also intrinsically depends on Bazett's assumption that QT interval is proportional to the square root of the RR interval.

We became increasingly aware of these problems while developing an automatic computerised technique for measuring QT dispersion (8,9). We have therefore compared computer-derived measurements of adjusted QT dispersion with another measure of QT heterogeneity, coefficient of interlead QT variation, in 14 patients with documented arrhythmias and 15 control patients, and in the present paper we discuss the advantages and disadvantages of these two ways of expressing dispersion.

Patients and Methods

QT dispersion measurements were made using automatic and user interactive techniques on 14 patients with previously documented sustained monomorphic ventricular tachycardia attending an arrhythmia clinic and on 15 controls (consecutive attendees at an electrocardiography clinic) not known to have suffered any arrythmia. Brief patient details are given in table 1. All patients were on treatment and in sinus rhythm at the time the electrocardiograms were recorded.

Simultaneous 12-lead electrocardiograms were routinely

recorded on paper at 25mm/second using Hewlett Packard or Siemens electrocardiographs. The electrocardiograms were converted to digital images using a flatbed scanner. Specially designed algorithms were used to derive digital values of the ECG waveforms using skeletonising and filtering techniques (8). The waveforms were analysed using purpose-designed software to detect QRS onset and T wave offset. If U waves were present the algorithm identified the T-U nadir. Leads where T wave offset could not accurately be measured were identified as not analysable. The program allowed for observer monitoring and override if appropriate.

QT intervals were rate-corrected using Bazett's formula (10) to give corrected QT intervals (QTc). QT dispersion was presented either as "adjusted QT dispersion" ((QTcmax-QTcmin)/square root of number of leads used for measurement) or as a coefficient of interlead QT interval variation (Standard deviation of QT intervals/mean QT interval).

QT dispersion measurements on arrhythmia patients and controls were compared using the Mann Witney U test. Rank orders for QT dispersion measurements given by the adjusted QT dispersion and coefficent of interlead variation methods were compared using Spearman's rank correlation coefficient R. The statistical distribution of QT intervals was studied by normalising the rate-corrected QT intervals for each patient to have a mean of 0 and a standard deviation of unity using the formula:

$$(QTstd)i = \frac{(QT)i - \overline{QT}}{\sigma(QT)}$$

where (QT)i refers to the corrected QT interval in any lead i from a given patient, $\overline{QT}$ is the mean rate corrected QT interval for all measurable leads in that patient, and $\sigma(QT)$ refers to the standard deviation of QT intervals in that patient. Note that provided leads are recorded simultaneously the rate correction is represented in numerator and denominator and can be eliminated. There were 172 standardised QT values for the controls, and 153 for the arrhythmia patients. These were used to construct separate frequency histograms which were compared with a standardised Normal (Gaussian) curve using the Chi-squared statistic (appendix)

Results:

Distribution of Standardised QT intervals

Figure 1 shows a histogram of standardised QT intervals for control patients, and figure 2 a histogram of standardised QT intervals for arrhythmia patients. Each bar in the histogram represents the frequency of QT measurements which differ from the mean by the number of standard deviations represented on the x axis. In both cases, a normalised Gaussian curve is superimposed.

Testing for goodness of fit using the Chi squared statistic gives, for the control patients, Chi square = 7.02, with 10 degrees of freedom. The alpha = 0.05 level corresponds to a Chi-square of 18.31, and alpha = 0.70 to a Chi square of 7.27. This implies an excellent fit between the observed distribution of

data and the hypothesised normal distribution. For arrhythmia patients, Chi square is 12.25, degrees of freedom 10, Chi squared for alpha = 0.05 is 18.31 and Chi squared for alpha = 0.25 is 12.51. Again, this shows compatibility with a hypothesised normal distribution.

Spatial Distribution of QT intervals

The computer program was designed so as to be able to give a spatial display of QT intervals corresponding to the conventional orientation of electrocardiographic leads (figure 3). A circle corresponds to the mean QT interval, and radii to the QT intervals in individual leads. In each of the arrhythmia patients studied there was a smooth transition from "short" to "long" QT intervals. In patients with definite ECG evidence of previous infarction, there was a tendency for longer QT intervals to coincide with the infarct site.

Differences between Control and Arrhythmia populations

The distribution of adjusted QT dispersion and coefficient of interlead QT variation for control and arrhythmia populations is shown in figure 4. Median adjusted QT dispersion was 34.8msec range 22.5-58.1 for arrhythmia patients, 13.8msec, range 10.3-24.9, for controls ($p<0.001$). Median coefficient of interlead QT variation was 8.8% range 4.4 to 12.4% for arrhythmia patients, 3.6% range 2.7 - 6.3% for controls ($p<0.001$).

Comparison between Adjusted QT dispersion and Coefficient of Interlead QT variation

Spearman's rank order coefficient R for comparing the rank order of QT dispersion in the arrhythmia patients given by

adjusted QT dispersion and coefficient of interlead QT variation was 0.70, $p < 0.05$.

Discussion

We confirmed the differences in QT dispersion between control and arrhythmia-prone populations described by others (6-8) In control patients, QT interval measurements were normally distributed, as would be expected for chance variation in measurement. In our population of arrhythmia patients, QT intervals still approximated to a normal distribution, and description of QT dispersion as a coefficient of interlead QT variation is thus valid. In theory, the most "arrhythmogenic" situation might result from a localised but severe repolarisation inhomogeneity which might be reflected by QT prolongation in a single lead. In our population this was not seen, other than as an artifact, and both the analysis of pooled standardised QT intervals and inspection of spatial plots indicated that a regional prolongation of QT interval seen in a number of leads was usual, as previously described by Mirvis (4). We cannot exclude the possibility that strictly localised QT prolongation might be seen in another or larger series.

If QT interval measurements are all made accurately and QT distribution is Gaussian then rate-corrected QTmax-QTmin is mathematically related to coefficient of variation and the two measurements would be expected to show a high degree of correlation. In our study a minimum of 10 leads was measured for each patient, and the difference between adjusted dispersion and rate corrected QTmax-QTmin is therefore small. This explains the

good ranking correlation between adjusted dispersion and coefficient of varition we observed. Provided all 12 leads are recorded simultaneously, coefficient of variation should be independent of rate correction, for the same rate correction factor appears in numerator and denominator. Coefficient of variation is less susceptible to interpretation errors in measuring a single lead, and may thus be less dependent on operator experience and bias.

Coefficient of variation is a function of the number of leads measured. We have not introduced an adjustment for "missing" leads, since if QT distribution is approximately normal the error thus introduced is small: one missing lead introduces an error of -4.3%, two leads an error of -8.7% . Conversely, adjusted QT dispersion will give large dispersion values for cardiograms with many isoelectric or indeterminate T waves: these features may themselves indicate an increased arrhythmia risk, but it may be inappropriate to attribute this to increased dispersion. In our present state of understanding of the causes and implications of QT dispersion, and in the context of developing technology for accurate measurement, it may be prudent for the time being to express QT dispersion both as adjusted dispersion and as coefficent of interlead variation.

Acknowledgements

This work was supported by the British Heart Foundation. We are grateful to Mrs J Thomas and Mrs V. Knott for ECG recordings.

References

1. Schwartz PJ, Periti M, Malliani A. The Long QT syndrome. Am Heart J. 1975; 89:378-85

2. Schwartz PJ, Wolf S. QT interval prolongation as a predictor of sudden death in patients with myocardial infarction. Circulation 1978; 57: 1074-77

3. Algra A, Electrocardiographic Risk Factors for Sudden Death. Thesis, Erasmus University, Rotterdam 1990.

4. Mirvis DM Spatial variation of QT intervals in normal persons and patients with acute myocardial infarction. J Am Coll Cardiol 1985; 5:625-31

5. Day CP, McComb JM, Campbell RWF. QT dispersion: an indication of arrhythmia risk in patients with long QT intervals Br Heart J 1990; 63: 342-44

6. Day CP, McComb JM, Campbell RWF. QT dispersion in sinus beats and extrasystoles Br Heart J 1992;67:39-41

7. Day CP, McComb JM, Matthews J, Campbell RWF. Reduction in QT interval by sotalol following myocardial infarction. Eur Heart J. 1991; 12: 423-7

8. Bhullar HC, de Bono DP, Fothergill JC, Jones NB. A computer based system for the study of QT intervals. Proceedings, Computers in Cardiology, Venice 1991, IEEE Press, Los Alamitos, USA, 533-536

9. de Bono DP, Bhullar HK, Goddard WP, Fothergill JC. Automated measurement of QT dispersion identifies patients at risk from ventricular tachycardia. Eur Heart J 1992; 13:369 (abstr)

10. Bazett HC An analysis of the time relations of electrocardiograms. Heart 1920; 7: 353-70

Legend:

Figure 1 Histogram of 172 standardised rate corrected QT intervals from control patients with a normalised Gaussian curve superimposed. Each bar in the histogram represents the frequency of QT measurements which differ from the mean by the number of standard deviations represented on the x axis.

Figure 2 Histogram of 153 standardised rate corrected QT intervals from patients with ventricular arrhythmia with a normalised Gaussian curve superimposed.

Figure 3. Horizontal plane vector diagram indicating QT intervals in leads V1 through V6 in a patient with previous anteroseptal infarction. The radius of the circle indicates the mean QT interval measured from all 12 leads. There is QT prolongation in leads V1-V3 and corresponding relative shortening in leads V4-V6.

Figure 4. Distribution of (a) adjusted QT dispersion and (b) coefficient of interlead QT variation in control and arrhythmia patients.

Appendix:

The observed frequencies of individual lead QT measurements lying a specified number of standard deviations from the mean are shown in figures 1 and 2. For the purposes of this study standardised QT measurements were divided into 13 intervals. The predicted frequencies implied by a Gaussian distribution can be calculated from the area under the normal probability density function curve:

$$p(t_1-t_2) = \int_{t_1}^{t_2} \frac{1}{\sqrt{2\pi}} e^{-\frac{t^2}{2}}$$

Where p(t1-t2) is the probability of observing QT interval measurements lying between t1 and t2 standard deviations from the mean.

X^2 is calculated as

$$X^2 = \left[\frac{1}{N}\sum_{k=1}^{k=n}\frac{fk^2}{pk}\right] - N$$

where N is the total number of points in the sample, divided into 13 intervals, fk is the observed, and pk the predicted, number of observations in the kth interval. If N is sufficiently large,

$$X^2 \longrightarrow \chi^2_{(n-r-1)}$$

and the Chi-squared distribution tables can be entered with (13-r-1) degrees of freedom, where r is the number of parameters used to describe the theoretical distribution: r = 2 in the case of a Gaussian curve, hence 10 degrees of freedom.

Figure [1] A histogram of 172 standardised rate-corrected QT intervals from a group of Controls with normalised Gaussian curves superimposed

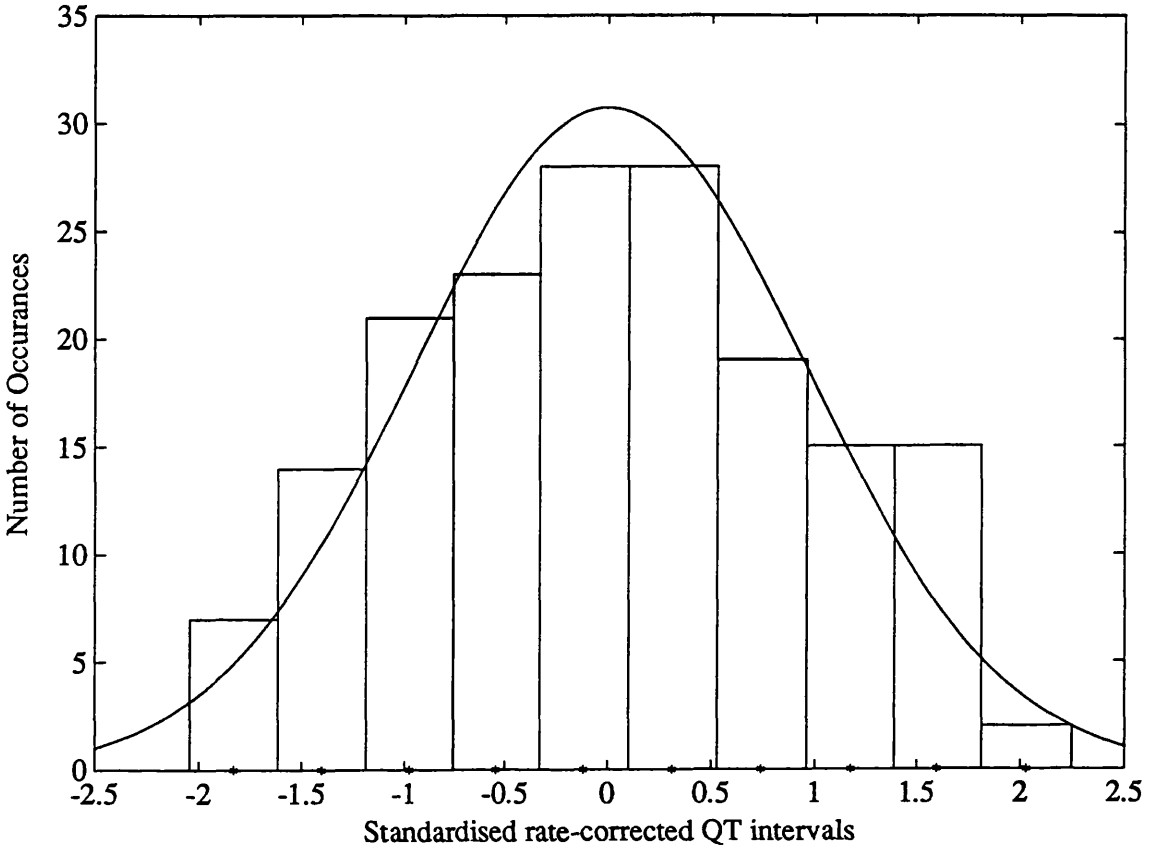

Figure [2] A histogram of 153 standardised rate-corrected QT intervals from a group of Arrhythmogenics with normalised Gaussian curves superimposed

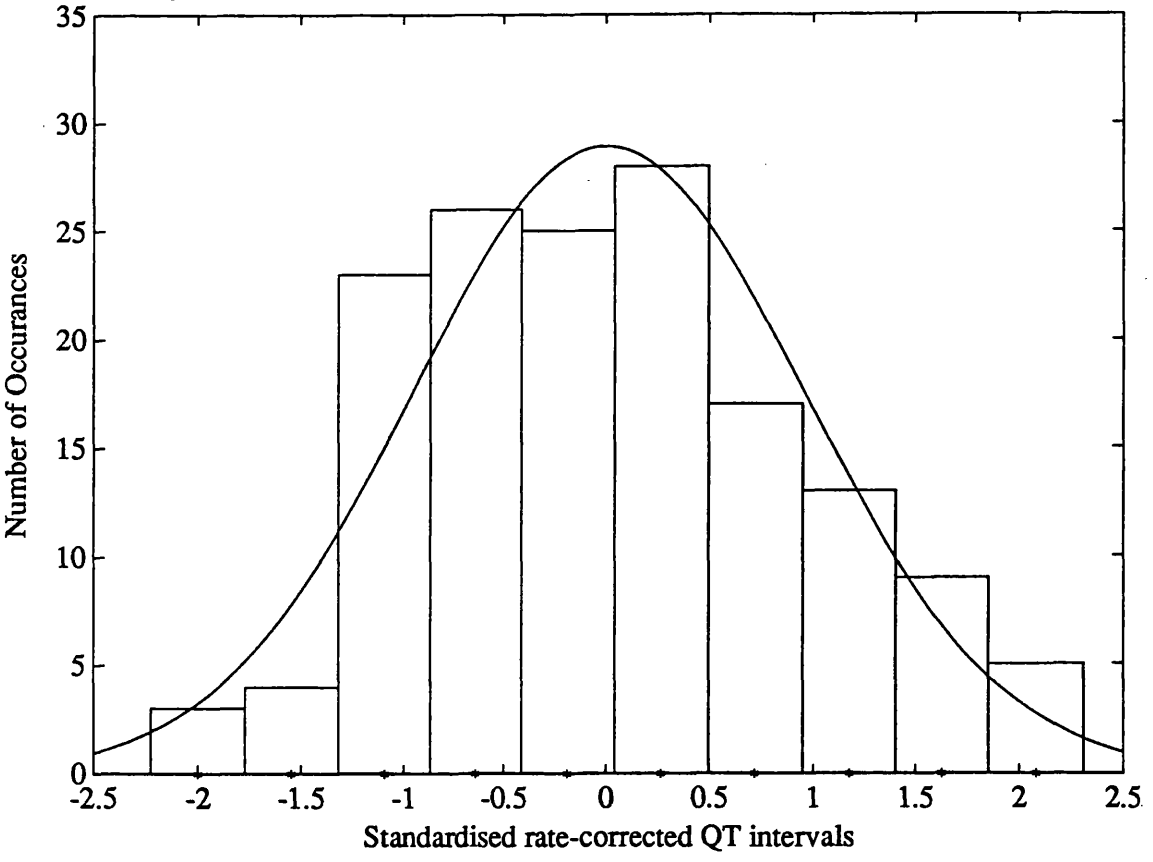

Figure 3a

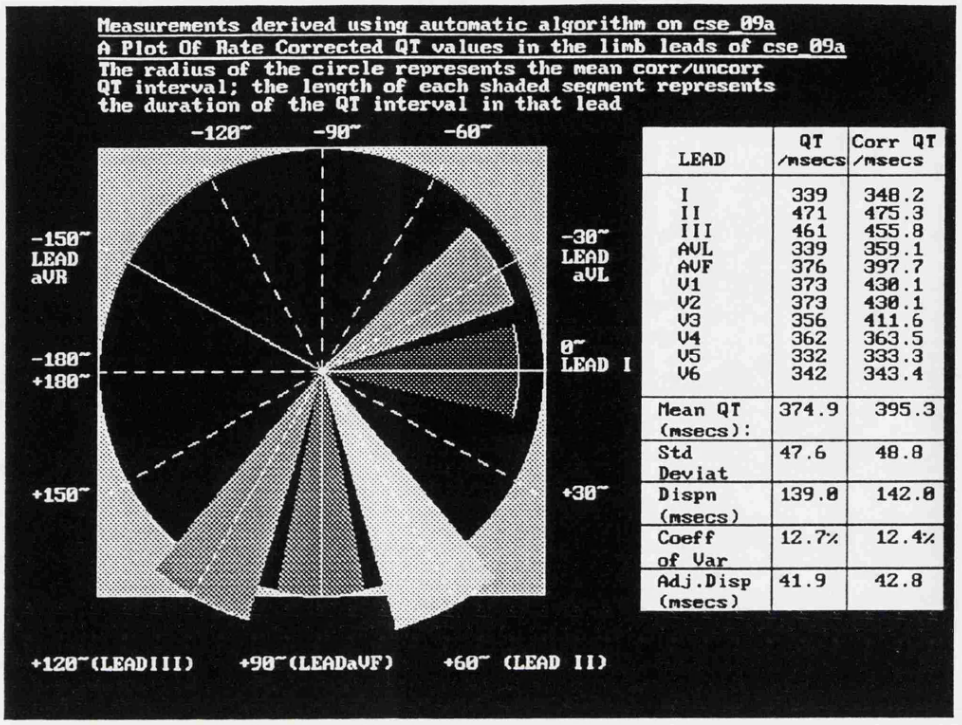

LEAD	QT /msecs	Corr QT /msecs
I	339	348.2
II	471	475.3
III	461	455.8
AVL	339	359.1
AVF	376	397.7
V1	373	430.1
V2	373	430.1
V3	356	411.6
V4	362	363.5
V5	332	333.3
V6	342	343.4
Mean QT (msecs):	374.9	395.3
Std Deviat	47.6	48.8
Dispn (msecs)	139.0	142.0
Coeff of Var	12.7%	12.4%
Adj.Disp (msecs)	41.9	42.8

Figure 3b

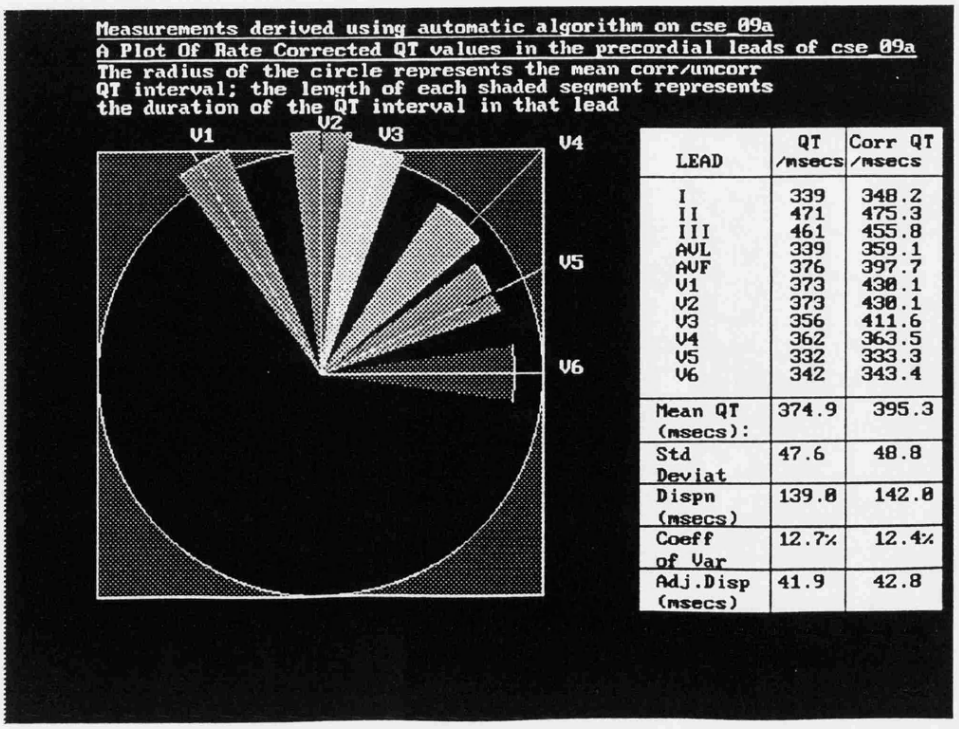

LEAD	QT /msecs	Corr QT /msecs
I	339	348.2
II	471	475.3
III	461	455.8
AVL	339	359.1
AVF	376	397.7
V1	373	430.1
V2	373	430.1
V3	356	411.6
V4	362	363.5
V5	332	333.3
V6	342	343.4
Mean QT (msecs):	374.9	395.3
Std Deviat	47.6	48.8
Dispn (msecs)	139.0	142.0
Coeff of Var	12.7%	12.4%
Adj.Disp (msecs)	41.9	42.8

Figure [4a] Adjusted Dispersion in 15 Controls ('o') and 14 Arrhythmogenics ('+')

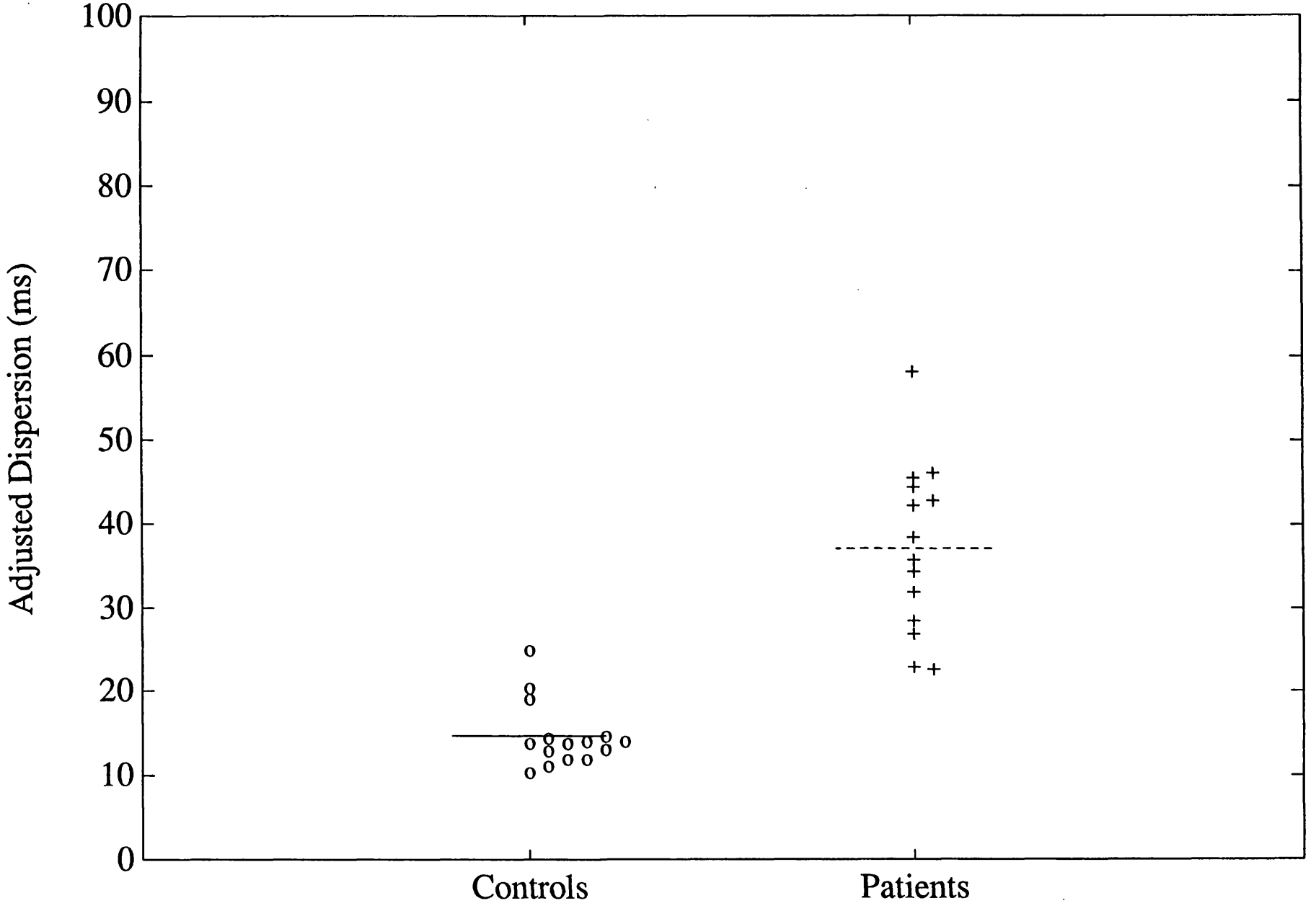

Figure [4b] Coefficient of Variation in 15 Controls ('o') and 14 Arrhythmogenics ('+')